

Determination of the denitrification capacity of
unconsolidated rock aquifers using ^{15}N tracer experiments at
groundwater monitoring wells - development of a new method
to assess actual and future denitrification in aquifers

Dissertation

zur Erlangung des Doktorgrades
der Fakultät für Forstwissenschaften und Waldökologie
der Georg-August-Universität Göttingen

vorgelegt von

Diplom Geologe Wolfram Eschenbach

geboren in Burg

Göttingen, 2014

1. Gutachter: Prof. Dr. Heinz Flessa
2. Gutachter: Prof. Dr. Jürgen Böttcher

Tag der mündlichen Prüfung: 28.01.2014

"Ich bin mir jedenfalls bewusst, dass ich keine Weisheit besitze, weder groß noch klein."

Sokrates

Table of contents

Figures	V
Tables	VI
Danksagung	VII
Abstract	IX
Kurzfassung	XI
Preface and Outline	XIII
1 General Introduction	1
1.1 Nitrate pollution of groundwater	1
1.2 The nitrogen cycle	3
1.3 Denitrification in groundwater	6
1.4 Objectives of this thesis	9
2 Online measurement of denitrification rates in aquifer samples by an approach coupling an automated sampling and calibration unit to a membrane inlet mass spectrometry system	11
Abstract.....	11
2.1 Introduction.....	12
2.2 Experimental	15
2.2.1 Study site	15
2.2.2 Set-up	16
2.2.2.1 Incubation of aquifer mesocosms and sampling procedures.....	16
2.2.3 On- and offline measurement and analysis of dissolved gases	17
2.2.4 Automated online analysis using ASCU-MIMS	18
2.2.4.1 Principle of online dissolved gas analysis with MIMS	19
2.2.4.2 Sampling procedure and analysis.....	19
2.2.5 Manual offline approach with GC-IRMS	21
2.2.5.1 Sampling and offline analysis of NO_3^- , SO_4^{2-} and denitrification gases.....	22
2.3 Calculations.....	23
2.3.1 ^{15}N abundance of denitrified NO_3^-	23
2.3.2 Mathematical approaches to determine the contribution of labelled denitrification gases in a mixture of N_2 and N_2O gases	23
2.3.2.1 Method I – Mulvaney	24
2.3.2.2 Method II – isotope pairing method.....	25
2.3.2.3 Method III – Spott and Stange	26
2.3.3 Precision and limit of detection	26

2.3.4 Estimating potential bias from in situ degassing	27
2.4 Results and Discussion	28
2.4.1 Comparison between ASCU-MIMS and GC-IRMS gas Analysis	28
2.4.2 Comparison of three different mathematical ¹⁵ N approaches	30
2.4.3 Denitrification rates and influence of the experimental set-up on the measured time pattern of denitrified (N ₂ +N ₂ O)	36
2.4.4 Comparison of ASCU-MIMS with previous methods	40
2.5 Conclusions	41
3 Predicting the denitrification capacity of sandy aquifers from shorter-term incubation experiments and sediment properties	43
Abstract	43
3.1 Introduction	44
3.2 Materials and methods	47
3.2.1 Study sites	47
3.2.2 Sampling procedures	48
3.2.3 Laboratory incubations	48
3.2.3.1 Standard treatment	48
3.2.3.2 Intensive treatment	49
3.2.4 Analytical techniques	50
3.2.5 Calculated parameters	52
3.2.6 Statistical analysis and modelling	53
3.2.7 Basic assumption and methodical limitations of the presented approach	54
3.3 Results	55
3.3.1 Incubations and independent variables: grouping of aquifer material	55
3.3.2 Time course of denitrification products, denitrification rates and cumulative denitrification at the end of incubations	55
3.3.3 Sediment parameters	57
3.3.4 The stock of reactive compounds and its availability for denitrification during incubation	59
3.3.4.1 Standard treatment	59
3.3.4.2 Intensive treatment	61
3.3.5 Relationship between the cumulative denitrification and sediment parameters	61
3.3.6 Regression models to predict $D_{cum}(365)$	63
3.3.6.1 Predicting $D_{cum}(365)$ from initial denitrification rates	63
3.3.6.2 Predicting $D_{cum}(365)$ from sediment parameters	64
3.3.7 Predicting the stock of reduced compounds (SRC) from $D_{cum}(365)$ and estimation of the minimal lifetime of denitrification (emLoD)	66
3.4 Discussion	68
3.4.1 Groundwater redox state and sample origin	68
3.4.2 Predicting $D_{cum}(365)$ from initial denitrification rates and time course of denitrification ...	68
3.4.3 Predicting $D_{cum}(365)$ of aquifer sediments, correlation analysis and regression models	73

3.4.3.1	Sediment parameters and their relation to $D_{cum}(365)$	73
3.4.3.2	Predicting $D_{cum}(365)$ from sediment variables	75
3.4.4	From $D_{cum}(365)$ and SRC to the assessment of the lifetime of denitrification within the investigated aquifers.....	77
3.4.5	Are laboratory incubation studies suitable for predicting in situ processes?.....	80
3.4.5.1	Limitations of the $^{15}\text{NO}_3^-$ labelling approach.....	80
3.4.5.2	Are the NO_3^- concentrations during incubation comparable to those in situ and what is their influence on the measured denitrification rates?	80
3.4.5.3	Is one year incubation suitable to predict the denitrification capacity over many decades in an aquifer?	81
3.4.5.4	Did laboratory incubation studies really indicate what happens in situ?	82
3.5	Conclusions	83
3.6	Supplement to chapter 3:	85
4	Predicting the denitrification capacity of sandy aquifers from in situ measurements using push-pull ^{15}N tracer tests.....	97
	Abstract.....	97
4.1	Introduction.....	99
4.2	Materials and methods	102
4.2.1	Study sites.....	102
4.2.2	Single well push-pull ^{15}N tracer tests.....	103
4.2.4	Pre-conditioning of wells in the NO_3^- -free zone of the FFA.....	106
4.2.3	Incubation of parallels of aquifer material.....	107
4.2.5	Analytical techniques	107
4.2.5.1	Analysis of dissolved ^{15}N labelled denitrified N_2 and N_2O	107
4.2.5.2	Analysis of NO_3^- , SO_4^{2-} and Br^-	109
4.2.6	Calculations of denitrification rates	109
4.2.7	Detection limit and precision of denitrification derived ($\text{N}_2+\text{N}_2\text{O}$) measurements.....	110
4.2.8	Statistical analysis and modelling.....	110
4.2.9	Estimating sediment properties using regression functions with $D_r(\text{in situ})$	111
4.3	Results	112
4.3.1	Grouping of push-pull test measuring points	112
4.3.2	In situ denitrification rates and time courses of denitrification products	113
4.3.3	Relationship between $D_r(\text{in situ})$, $D_{cum}(365)$ and aquifer parameters	115
4.3.3.1	Comparison of $D_r(\text{in situ})$ and $D_{cum}(365)$	115
4.3.3.2	Regression models to predict $D_{cum}(365)$, SRC and denitrification relevant aquifer parameters from $D_r(\text{in situ})$	117
4.4	Discussion.....	121
4.4.1	Time courses of denitrification products and $D_r(\text{in situ})$ compared with $D_r(365)$	121
4.4.2	Interpretation of observed time courses of produced ($\text{N}_2+\text{N}_2\text{O}$).....	124
4.4.3	Predicting $D_{cum}(365)$ and SRC of aquifer sediments from $D_r(\text{in situ})$	126
4.4.4	Possible confounding factors and uncertainties	128

4.5 Conclusions	129
4.6 Supplement to chapter 4:	131
5 Synthesis and general conclusions.....	135
5.1 Methodical Part	135
5.2 Experimental part	138
5.2.1 Prediction of the denitrification capacity of sandy aquifers from shorter-term incubations	139
5.2.2 Predicting the denitrification capacity of sandy aquifers from in situ measurements using push-pull ¹⁵ N tracer tests.....	142
5.3 Future research and perspectives and methodical improvements.....	146
5.3.1 Methodical improvements	146
5.3.2 Future research perspectives	147
References	151
Appendix	165

Figures

Fig. 1.1: The nitrogen cycle.	4
Fig. 2.1: Set-up of the automated measuring and calibration unit in combination with a membrane-inlet mass spectrometer.	17
Fig. 2.2: Concentration courses of denitrified (N_2+N_2O) (B_c) in the pore water of the aquifer material from the sulphidic (S) and non-sulphidic mesocosms (nS)	29
Fig. 2.3: Theoretical and measured overestimation of denitrified N_2 in liquid samples due to the use of Eqn. for B from Mulvaney (1984) in the case of high B/A ratios in the sample.	32
Fig. 2.4: Susceptibility of the three investigated mathematical approaches to errors in ^{15}N abundance of denitrified NO_3^- . X is the ^{15}N fraction in the denitrified NO_3^-	35
Fig. 2.5: Measured concentration courses of denitrification derived (N_2+N_2O) in the pore water of the sulphidic material compared with calculated concentrations with and without degassing of labelled denitrification gases.	38
Fig. 3.1: Time courses of denitrification products (N_2+N_2O) (average of 3 to 4 replicas per depth) from different groups of aquifer material during standard (a–c) and intensive treatment (d).	56
Fig. 3.2: FFA, GKA, nS, S and tZ indicate Fuhrberger Feld, Großenkneten, non-sulphidic, sulphidic and transition zone aquifer material, respectively.	60
Fig. 3.3: Relation between denitrification rates determined during 7 ($D_r(7)$), 84 ($D_r(84)$) and 365 ($D_r(365)$) days of incubation.	63
Fig. 4.1: Schematic of push-pull ^{15}N tracer tests at groundwater monitoring and multilevel wells.	105
Fig. 4.2: Time courses of denitrification derived (N_2+N_2O) and dissolved O_2 during ^{15}N push-pull tests in the FFA (A and C) and GKA (B and D).	112
Fig. 4.3: Relation between in situ denitrification rates determined by ^{15}N push-pull tracer tests and average denitrification rates during one year of incubation	115
Fig. 4.4: Time courses of denitrification derived (N_2+N_2O) during push-pull tests without pre-conditioning (A) (grey diamonds) and with pre-conditioning B (black diamonds) at multilevel well B4 in the FFA.	119
Fig. 4.5: D_r (in situ) after 5 weeks of pre-conditioning of aquifer material (black diamonds) in comparison to D_r (in situ) without pre-conditioning.	119

Supplement to chapter 3:

Fig. S3.1: Sampling locations within the Fuhrberger Feld and Großenkneten catchment in Lower Saxony (Germany).	93
Fig. S3.2: Distribution of different sediment parameters in the aquifer material from the Fuhrberger Feld aquifer (FFA) and the Großenkneten aquifer (GKA)	94
Fig. S3.3: Measured NO_3^- consumption during incubations. (The NO_3^- concentrations at the last sampling date of intensive incubations were not measured.)	95

Tables

Table 2.1:	Instrumental precision of the 29/28 molecular ion mass ratio estimated from the coefficient of variation (CV) of six repeated measurements of a standard	30
Table 3.1:	Sediment parameters of the incubated aquifer material (medians with ranges in brackets).....	58
Table 3.2:	Initial denitrification rates, cumulative denitrification during one year, stock of reduced compounds, sulphate formation capacity and estimated minimal lifetime of denitrification (medians with ranges in brackets).	59
Table 3.3:	Spearman rank correlation coefficients between $D_{cum}(365)$ and sediment parameters for the whole data set and partial data sets.....	62
Table 3.4:	Simple linear regressions between $D_{cum}(365)$ and $D_r(t)$, $f^{B-C}(D_{cum}(365)) = A+B \times f^{B-C}(D_r(t))$	62
Table 3.5:	Results of multiple linear regression analysis between $D_{cum}(365)$ and various selections of sediment parameters.	65
Table 3.6:	Simple regression between $D_{cum}(365)$ and SRC, $f^{B-C}(SRC) = A+B \times f^{B-C}(D_{cum}(365))$. $D_{cum}(365)$ is the mean of 3 to 4 replications per aquifer sample.	67
Table 4.1:	Overview of the conducted push-pull ^{15}N tracer tests in both aquifers and depth position of their filter screens.	103
Table 4.2:	Background conditions of groundwater at the locations of push-pull ^{15}N tracer tests.....	113
Table 4.3:	In situ denitrification rates (D_r (in situ)) and minimum and maximum values of D_r (in situ) in dependence of the range of estimated effective porosities (0.2 to 0.4). .	116
Table 4.4:	Means, standard deviation and ranges of D_r (in situ) of the data sets.	118
Table 4.5:	Simple regressions between D_r (in situ) and $D_{cum}(365)$ and SRC from anaerobic incubations with corresponding aquifer material. $f^{B-C}(X) = A + B \times f^{B-C}(D_r$ (in situ)).....	120

Supplement to chapter 3:

Table S3.1:	Sediment parameters and basic properties of all incubated samples.	89
Table S3.2:	Denitrification rates, cumulative denitrification, stock of reduced compounds, sulphate formation capacity and estimated minimal lifetime of denitrification of all incubated samples.	90
Table S3.3:	Simple regression between $D_{cum}(365)$ and sediment parameters (X), $f^{B-C}(D_{cum}(365)) = A + B \times f^{B-C}(X)$	91
Table S3.4:	Ratios of modelled $D_{cum}(365)$ vs measured $D_{cum}(365)$ for samples with high (> 20 mg N kg ⁻¹) and low $D_{cum}(365)$ (< 20 mg N kg ⁻¹).....	92
Table S3.5:	Lambda values of the Box-Cox transformed sediment parameters.....	92

Supplement to chapter 4:

Table S4.1:	Denitrification rates, cumulative denitrification, stock of reduced compounds, sulphate formation capacity and estimated minimal lifetime of denitrification	132
Table S4.2:	Lambda values of the Box-Cox transformed D_r (in situ) and variables measured during anaerobic incubation.	133
Table S4.3:	Simple regressions between D_r (in situ) and individual sediment parameters from aquifer parallels. $f^{B-C}(X) = A + B \times f^{B-C}(D_r$ (in situ)).	133
Table S4.4:	Lambda values of the Box-Cox transformed sediment parameters.....	134
Table S4.5:	Lambda values of the Box-Cox transformed variables.....	134

Danksagung

Mein Dank gilt allen die mich bei dieser Arbeit unterstützt haben, für ihre Hilfe und ihre Geduld.

Im Besonderen möchte ich mich bei PD Dr. Reinhard Well für die Initiierung dieses Projektes sowie für die engagierte Betreuung bedanken. Seine wissenschaftliche Begleitung und die geführten Diskussionen waren für diese Arbeit sehr fruchtbar.

Herrn Prof. Dr. Heinz Flessa danke ich für die Übernahme des ersten Gutachtens und der Betreuung dieses Projektes. Für die Übernahme des Koreferats danke ich sehr herzlich Herr Prof. Dr. Jürgen Böttcher.

Mein Dank für Rat, Unterstützung und zahlreiche Diskussionen gilt im besonderen Herrn Prof. Dr. em. Wolfgang Walther, weiterhin möchte ich mich für die gute Zusammenarbeit bei Markus Penning und Egon Harms bedanken. Darüber hinaus danke ich Prof. Dr. Wilhelmus Duijnsveld, Prof. Dr. Rudolf Liedel, Dr. Michael Dietze, Werner Raue und Rolf Hoppe für die unkomplizierte technische und personelle Unterstützung bei den zahlreichen Tracerversuchen im Gelände. Dr. Michael Brudel bin ich sehr zu Dank verpflichtet für Rat und Hilfe bei der Inbetriebnahme des MIMS-Massenspektrometers. Dr. Jürgen Prenzel möchte ich für fruchtbare Diskussionen und Anregungen im Bereich Isotopenrechnungen danken. Herrn Dr. Holger Wurl danke ich für die Begleitung des Projekts von Seiten der DBU.

Ganz besonders herzlichen bedanken möchte ich mich bei den Mitarbeitern der Abteilung Agrarpädologie des Departments für Nutzpflanzenwissenschaften der Universität Göttingen, ohne deren bereitwillige, weitreichende und fortwährende Unterstützung diese Arbeit nicht möglich gewesen wäre. Das gute Arbeitsklima und die Kollegialität in dieser Abteilung habe ich sehr zu schätzen gelernt. Daher möchte ich mich ausdrücklich bei Dr. Christian Ahl für die Unterstützung die mir seine Abteilung gewährte bedanken. Im Besonderen bin ich Ingrid Ostermeyer und Karin Schmidt zu Dank verpflichtet, die bei Laborarbeiten mit ihrem Engagement eine unverzichtbare Hilfe waren. Genauso möchte ich Dr. Peter Gernandt, Susann Enzmann und Gerhard Benseler danken, die mich an verschiedenen Stellen unterstützt haben.

Dr. Jens Dyckmans dem Leiter des Kompetenzzentrums Stabile Isotope und Reinhard Langel möchte ich für die vielen Isotopenanalysen danken die im Rahmen dieser Arbeit anfielen. Dem technischen Personal der Ökopedologie der gemäßigten Zonen danke ich für die zahlreichen durchgeführten Analysen. Für weitere Hilfe im Gelände und Labor bedanke ich mich bei Ingo Haase, Marlen Gritschke und Joanna Ziomkowska.

Schließlich möchte ich sehr meinen Eltern für ihre fortdauernde Unterstützung und Ermutigung danken. Mein Dank gilt ebenso meinen Freunden, sowie denen die ein Stück meines Lebenswegs mit mir teilten und mir auf die eine oder andere Art nach wie vor am Herzen liegen.

Abstract

The nitrogen cycle is one of the most important nutrient cycles in terrestrial ecosystems and has been dramatically altered by increasing anthropogenic inputs of reactive nitrogen (Nr) to terrestrial ecosystems. Nitrate (NO_3^-) emissions from the agricultural sector are the dominant source of Nr fluxes to aquatic systems like aquifers and NO_3^- pollution of groundwater is a problem due to eutrophication of surface waters receiving polluted groundwater, possible indirect emissions of nitrous oxide (N_2O) and increasing costs for keeping the standard for NO_3^- in drinking water. Denitrification is the most important process of NO_3^- attenuation in groundwater and is accompanied by an irreversible loss of reduced compounds, which leads to an inevitable reduction of the denitrification capacity of aquifers.

Denitrification is difficult to measure and to predict on aquifer or river catchment scale. Therefore, knowledge about the denitrification capacity of aquifers is important for the designation of nitrate vulnerable zones. Against this background, the main objective of this thesis is to improve methods to measure denitrification in situ as well as in the laboratory and to develop an approach to estimate the denitrification capacity of aquifers.

All investigations were conducted within two Pleistocene sandy aquifers in Lower Saxony, Germany, the Fuhrberger Feld aquifer, situated NE of the city of Hannover, and the Großenkneten aquifer SW of the city of Bremen. Both aquifers receive considerable NO_3^- inputs via seepage waters from agricultural fields and intense denitrification is known to take place within both aquifers.

To improve laboratory measurements of denitrification, an automatic sampling and calibration unit coupled to a membrane inlet mass spectrometer (ASCU-MIMS) suitable for online measurement of denitrification (chapter 2) was developed and tested during a ^{15}N tracer experiment with incubation of aquifer material from the Fuhrberger Feld aquifer. It was shown that online analysis of denitrification rates measured with ASCU-MIMS was in good agreement with the well established offline isotope analysis by GC-IRMS. From 3 investigated ^{15}N aided mathematical approaches the approach given by Spott and Stange (2007) was found to be most suitable for the determination of denitrification from ASCU-MIMS raw data. The approach given by Mulvaney (1984) can be used under certain circumstances (chapter 2). The latter approach has the advantage that it is not necessary to analyse molecular ion mass 30, which is often biased.

To estimate denitrification capacity of aquifers it was tested if the stocks of reduced compounds (SRC) of the investigated aquifer samples from both aquifers could be estimated from the measured cumulative denitrification during one year of anaerobic incubation

($D_{\text{cum}}(365)$) (chapter 3). $D_{\text{cum}}(365)$ showed good linear regressions with the SRC of aquifer material from the reduced zone of both aquifers. From this finding it is concluded that $D_{\text{cum}}(365)$ is a useful indicator for the denitrification capacity of aquifer material. Overall, median SRC (1.3 g N kg^{-1}) and $D_{\text{cum}}(365)$ ($15.6 \text{ mg N kg}^{-1} \text{ yr}^{-1}$) of sulphidic aquifer samples was 5 respectively 10 times higher than the one of non-sulphidic samples.

Initial denitrification rates measured at the beginning of incubations were poorly related to predict $D_{\text{cum}}(365)$, indicating that short-term incubations are not suitable to predict the SRC. Among the tested sediment parameters total organic carbon (C_{org}) and KMnO_4 -labile organic carbon (C_1) yielded the best predictions of $D_{\text{cum}}(365)$ for the whole data-set of aquifer material from both aquifers. Regression analysis revealed that for non-sulphidic and sulphidic aquifer material different sediment parameters yielded the best regressions with $D_{\text{cum}}(365)$ and the SRC. The kinetics of denitrification during the conducted incubations could be described with zero-order kinetics, suggesting that the NO_3^- concentration during the experiments was not limiting the measured denitrification activity (chapter 3). Denitrification in the non-sulphidic samples, where only organotrophic denitrification occurred, was kinetically much slower than in the sulphidic samples.

Push-pull ^{15}N tracer tests for the measurement of in situ denitrification rates ($D_r(\text{in situ})$) were tested in the aquifers as an approach to estimate SRC without the need to collect and analyse aquifer material. These tests were carried out in groundwater monitoring wells at the same position and with filter screens in the same depths as the origin of the incubated aquifer samples. $D_r(\text{in situ})$ ranged from 0.0 to $51.5 \mu\text{g N kg}^{-1} \text{ d}^{-1}$ and were lower than average laboratory rates ($D_r(365)$), especially for in situ measuring points in the NO_3^- -free groundwater zone of both aquifers where sulphides are mostly present. After pre-conditioning of one multilevel well by the repeated injection of NO_3^- containing groundwater in the zone of NO_3^- free groundwater to stimulate denitrifying bacteria, $D_r(\text{in situ})$ increased strongly which resulted in much better agreement of $D_r(\text{in situ})$ and laboratory $D_r(365)$. From these results it is concluded that the deeper NO_3^- -free groundwater zones of aquifers require pre-conditioning prior to $D_r(\text{in situ})$ measurements to obtain potential in situ denitrification rates reflecting SRC. It is assumed that this is due to the slow response of the microbial community to the initial input of NO_3^- .

Kurzfassung

Der Stickstoffkreislauf ist einer der wichtigsten Nährstoffkreisläufe im Bereich terrestrischer Ökosysteme und wird dramatisch von steigenden anthropogenen Einträgen an reaktivem Stickstoff (Nr) beeinflusst. Nitrat (NO_3^-) Emissionen von Agrarflächen sind die dominante Quelle von Nr Einträgen in Systemkompartimente wie Aquifere. NO_3^- Verschmutzung von Grundwässern führt zu steigenden Kosten für die Trinkwasserversorgung und kann die Eutrophierung von Oberflächengewässern begünstigen, wenn diese erhöhte NO_3^- Einträge beispielsweise über Grundwässer erhalten. Erhöhte NO_3^- Konzentrationen im Grundwasser können über diesen Weg auch zu steigenden indirekten Emissionen des Klimarelevanten Gases Lachgas (N_2O) führen.

Denitrifikation ist der wichtigste Prozess bei der Reduktion von NO_3^- Konzentrationen im Grundwasser und führt zum Verbrauch des Stoffvorrats an reduzierten Verbindungen, d.h. zur Verringerung der Denitrifikationskapazität von Aquiferen. Die Denitrifikation ist auf der Skala von Aquiferen und Flusseinzugsgebieten nur schwer mess- und modellierbar. Somit ist Wissen über die Verteilung der Denitrifikationskapazität in Aquiferen wichtig für die effektive Ausweisung von Zonen in denen eine Minderung von NO_3^- Emissionen aus der Landwirtschaft angezeigt ist.

Vor diesem Hintergrund ist das zentrale Ziel dieser Arbeit: Methoden zur in situ und Labormessung der Denitrifikation zu verbessern und Methoden für die Abschätzung der Denitrifikationskapazität von Aquiferen zu testen.

Alle Untersuchungen wurden in zwei pleistozänen, sandigen Aquiferen in Niedersachsen durchgeführt. Dies waren das Fuhrberger Feld nordöstlich von Hannover und das Grundwassereinzugsgebiet bei Großenkneten. Beide Aquifere weisen hohe NO_3^- Einträge ins Grundwasser über die Grundwasserneubildung unter landwirtschaftlichen Nutzflächen auf. In beiden Aquifere läuft eine intensive Denitrifikation ab.

Um die Messung der Denitrifikation im Labor zu verbessern wurde eine automatische Probenahme- und Kalibriereinheit gekoppelt mit einem Membraneinlass-Massenspektrometer entwickelt (ASCU-MIMS) und während eines ^{15}N -Tracer Experiments mit Inkubation von Aquifermaterial aus dem Fuhrberger Feld getestet. Es konnte gezeigt werden, dass die online Messungen mit ASCU-MIMS in guter Übereinstimmung mit offline GC-IRMS Analysen waren. Weiterhin wurden 3 mathematische Ansätze auf ihre Eignung zur Berechnung der Denitrifikation aus ASCU-MIMS Rohdaten geprüft. Der mathematische Ansatz von Spott und Stange (2007) stellte sich dabei als der geeignetste Ansatz dar. Der Ansatz von Mulvaney (1984) kann unter gewissen Randbedingungen (Kapitel 2) genutzt werden und hat den

Vorteil, dass das Masse-zu-Ladungsverhältnis 30, welches meist spektrale Interferenzen unerwünschter Ionen aufweist, nicht ausgewertet werden muss.

Um die Denitrifikationskapazität von Aquiferen abzuschätzen, wurden ein Jahr andauernde anaerobe Inkubationen durchgeführt. Es wurde getestet ob der Gehalt an reduzierten Verbindungen (SRC) im untersuchten Aquifermaterial aus der gemessenen kumulativen Denitrifikation ($D_{\text{cum}}(365)$) abgeschätzt werden kann (Kapitel 3). Die Höhe von $D_{\text{cum}}(365)$ zeigte gute lineare Beziehungen mit dem Gehalt an reduzierten Verbindungen in den untersuchten Aquiferproben, auf Grundlage dieser Ergebnisse wird daher davon ausgegangen, dass $D_{\text{cum}}(365)$ ein Indikator für die Denitrifikationskapazität von Aquifermaterial darstellt. Insgesamt waren die medianen SRC (1.3 g N kg^{-1}) und $D_{\text{cum}}(365)$ ($15,6 \text{ mg N kg}^{-1} \text{ a}^{-1}$) Werte der sulfidischen Aquiferproben 5 bzw. 10 mal höher als die der nicht-sulfidischen Aquiferproben.

Die initialen Denitrifikationsraten am Beginn der Inkubationen waren nicht geeignet $D_{\text{cum}}(365)$ vorherzusagen, was zeigte das Kurzzeit-Inkubationen nicht geeignet sind um den SRC abzuschätzen. Von den untersuchten Sedimentparametern zeigten der total organische Kohlenstoffgehalt (C_{org}) und der KMnO_4 -labile C_{org} die besten Abschätzungen von $D_{\text{cum}}(365)$ für den gesamten Datensatz mit Proben aus beiden Aquiferen. Regressionsanalysen zeigten, dass für nicht-sulfidisches und sulfidisches Aquifermaterial verschiedene Sedimentparameter die besten Regressionen mit $D_{\text{cum}}(365)$ und dem SRC aufwiesen. Die Kinetik der Denitrifikation während den Inkubationen konnte mit einer Reaktion nullter-Ordnung beschrieben werden, was andeutet, dass die Konzentration von NO_3^- während der Inkubationen eine mindere Bedeutung für die Höhe von $D_{\text{cum}}(365)$ aufwies (Kapitel 3).

Es wurde getestet ob Push-pull ^{15}N -Tracer Tests in Grundwassermessstellen zur Messung von in situ Denitrifikationsraten ($D_{\text{r}}(\text{in situ})$) geeignet sind um die Gehalte an reduzierten Verbindungen im Aquifermaterial um die Messstelle abzuschätzen, ohne das Aquiferproben gewonnen und analysiert werden müssen. Die gemessenen $D_{\text{r}}(\text{in situ})$ Werte reichten von 0.0 bis $51.5 \mu\text{g N kg}^{-1} \text{ d}^{-1}$ und waren niedriger als im Labor gemessene Denitrifikationsraten ($D_{\text{r}}(365)$). Dies zeigte sich besonders bei Messpunkten in der NO_3^- -freien Grundwasserzone beider Aquifere. Nach pre-conditioning, mittels wiederholter Injektionen von Nitrat haltigem Grundwasser in NO_3^- freie Tiefen einer Multilevelmessstelle, stiegen die $D_{\text{r}}(\text{in situ})$ stark an. Auch die Übereinstimmung von $D_{\text{r}}(\text{in situ})$ und $D_{\text{r}}(365)$ verbesserte sich nach pre-conditioning. Von diesen Ergebnissen ausgehend, wird angenommen, dass pre-conditioning im Bereich von NO_3^- -freiem Grundwasser nötig ist für die Messungen aussagekräftiger Denitrifikationsraten bzw. der Ableitung von SRC Gehalten aus in situ Messungen.

Preface and Outline

This Thesis was worked out at the Soil Science of Temperate and Boreal Ecosystems of the University of Göttingen within the project “Determination of the long-term denitrification capacity of loose rock aquifers using ^{15}N tracer experiments at groundwater wells - Development of a new method for the practice to identify denitrifying areas”. This research was funded by the Deutsche Bundesstiftung Umwelt (DBU). Cooperation partner was the Oldenburgisch-Ostfriesischer Wasserverband (OOWV).

The study sites were two drinking water catchment areas in Lower Saxony, Germany. The Fuhrberger Feld aquifer is situated 30 km NE of the city of Hannover and the Großenkneten aquifer about 30 km SW of the city of Bremen.

This thesis consists of 5 chapters. Chapter 1 gives a general insight into diffuse nitrate emissions from the agricultural field into groundwater, the nitrogen cycle and denitrification in aquifers, which is considered to be the most important process for nitrate attenuation in groundwater. In chapter 2 introduces a novel automated sampling and calibration unit coupled to a membrane inlet mass spectrometry system (ASCU-MIMS) for online analysis of denitrification during ^{15}N tracer experiments, which was developed during this thesis. This chapter focuses on the online measurement of denitrification, suitable ^{15}N mathematical approaches for evaluation of experimental data and possible confounding factors during the conducted incubation experiment. Chapter 3 provides a simple framework for the prediction of denitrification capacity of aquifers based on regression analysis of experimental data obtained from anaerobic incubation of aquifer material and the measurement of several sediment parameters. In chapter 4 it is evaluated if the denitrification capacity of aquifers can be predicted from in situ measurements of denitrification rates using push-pull ^{15}N tracer tests at groundwater wells. This chapter examines also the influence of pre-conditioning of aquifer material prior to subsequent push-pull ^{15}N tracer tests material on measured in situ denitrification rates. At the end of this chapter a theoretical interpretation of the observed time courses of denitrification during in situ measurements is provided. General conclusions from the results of this thesis and future research perspectives are given in the synthesis at the end of this work (chapter 5).

Results of chapter 2 and 3 are published in:

Eschenbach, W. and Well, R.: Online measurement of denitrification rates in aquifer samples by an approach coupling an automated sampling and calibration unit to a spectrometry system, *Rapid Commun. Mass Spectrom.*, 25, 1993 membrane inlet mass -2006, 10.1002/rcm.5066, 2011.

Eschenbach, W., and Well, R.: Predicting the denitrification capacity of sandy aquifers from shorter-term incubation experiments and sediment properties, *Biogeosciences*, 10, 1013-1035, 10.5194/bg-10-1013-2013, 2013.

1 General Introduction

“The largest uncertainties in our understanding of the N budget at most scales are the rates of natural biological nitrogen fixation, the amount of reactive nitrogen storage in most environmental reservoirs, and the production rates of N_2 by denitrification.” (Galloway et al., 2004)

This work tries to contribute to the last of these three problems at the scale of aquifers as an important part of terrestrial ecosystems and methodically in the field of denitrification measurement methods.

1.1 Nitrate pollution of groundwater

The nitrogen cycle is one of the most important nutrient cycles in terrestrial ecosystems (Hayatsu et al., 2008) and includes the four major sub-processes: nitrogen fixation, mineralization, nitrification and denitrification. During this nutrient cycle molecular nitrogen (N_2), which is unavailable for most organisms, is converted to reactive nitrogen (Nr)¹ and back to N_2 (see Sect. 1.2). Since the beginning of industrialisation the nitrogen cycle was dramatically altered by increasing anthropogenic inputs of Nr to terrestrial ecosystems. Since 1860 these inputs of Nr have increased from 262 to 389 Tg N yr⁻¹ (early 1990s) and a further raise to 492 Tg N yr⁻¹ by 2050 is expected (Galloway et al., 2004). The production of Nr via the Haber-Bosch process alone contributed approximately with 100 Tg N yr⁻¹ to the increase until the early 1990s. From this amount about 86 % was used to make fertilisers world-wide (Galloway et al., 2004). The yearly consumption of mineral and organic fertilisers were 12.1 and 9.1 million tons, respectively, in the EU-27 in 2007 (European Commission, 2011). Total fertilizer application in the European Union range from 0 to 977 kg N ha⁻¹ yr⁻¹ and mean values of diffuse Nr emissions (mainly from agriculture) per river sub-basins in the European Union range from 3 to > 30 kg N ha⁻¹ yr⁻¹ with highest values in Northwest Europe (Bouraoui et al., 2009). Diffusive Nr emissions from the agriculture contribute with 51 to over 90 % to total nitrogen load to terrestrial ecosystems in the (Bouraoui et al., 2009). Nr emissions from

¹ The term reactive nitrogen is used in this work in accordance to Galloway et al. (2004) and includes all biologically or chemically active N compounds like reduced forms (e.g., NH_3 , NH_4^+), oxidized forms (e.g., NO_x , HNO_3 , N_2O , NO_3^-) and organic compounds (e.g., urea, amines, proteins...).

the agricultural sector are therefore the dominant source of Nr fluxes to aquatic systems like aquifers, which receive considerable loads of Nr mostly in form of NO_3^- leaching from the agricultural field.

NO_3^- pollution of groundwater is a problem due to eutrophication of surface waters receiving polluted groundwater (Vitousek et al., 1997) and due to potential health risks of NO_3^- in drinking water and the increasing costs for keeping the standard for NO_3^- in drinking water ($< 50 \text{ mg } \Gamma^{-1}$, Drinking Water Directive 98/83/EC) (Dalton and Brand-Hardy, 2003; Defra, 2006). 15 % of the groundwater monitoring wells from the nitrate monitoring network in the EU-27 showed NO_3^- concentrations above $50 \text{ mg } \Gamma^{-1}$ and 34 % of these monitoring stations exhibited increasing NO_3^- concentrations during the period 2004-2007 (European Commission, 2011). Altogether, the share of nitrogen loads to river basins that comes from diffusive agricultural sources remains high in large parts of Europe. 41 % of the area of the EU-27 has been designated as nitrate vulnerable zones and member states of the EU are required to review these zones at least every four years (European Commission, 2011).

Possible side effects of the NO_3^- load to groundwater are the mobilisation of metals or acidification of groundwater. Oxidation of iron sulphides with NO_3^- can mobilise reduced iron (Fe^{2+}) (see Sect. 1.3), this could lead to exceeding the limit for dissolved iron in drinking water ($0.2 \text{ mg Fe } \Gamma^{-1}$). Dissolved Fe^{2+} can be oxidized and precipitate as iron hydroxides in the vicinity of groundwater wells, which can cause expensive repair costs (Hansen, 2005). Uranium, a common contaminant in the subsurface at radioactive waste and nuclear industrial sites (Riley et al., 1992), is also a natural contaminant in phosphate fertilisers (Boukhenfouf and Boucenna, 2011) and can be remobilised from anoxic aquifers by nitrate (Senko et al., 2002).

The most important process of NO_3^- attenuation in groundwater is denitrification (Korom, 1992). Denitrification in groundwater is mainly depending on the amount and microbial availability of reduced compounds in aquifers and is spatially highly variable, ranging from 0 to 100% of the NO_3^- input (Seitzinger et al., 2006). This process is accompanied by the irreversible oxidation of reduced compounds, which leads inevitably to a reduction of the denitrification capacity of aquifers. This raises the questions how rates of denitrification will respond to the increased anthropogenic Nr input (Seitzinger et al., 2006) and where and how long denitrification in aquifers can remediate NO_3^- pollution (Kölle et al., 1985). Knowledge about the denitrification capacity of aquifers is also important for foresighted designation of nitrate vulnerable zones in the EU, what is required by article 10 of the Nitrate Directive (European Commission, 2011).

The investigations during this thesis were conducted in two sandy aquifers (the Fuhrberger Feld aquifer (FFA) and the Großenkneten aquifer (GKA)) in Lower Saxony, Northwest Germany. Both aquifers are Pleistocene unconsolidated rock aquifers, which are typical for Northern Germany, and are located within two drinking water catchments. An intense agricultural land use leads to considerable NO_3^- contamination of shallow groundwater in both aquifers.

1.2 The nitrogen cycle

Denitrification is one of the key processes in the nitrogen (N) cycle (Fig. 1.1). In the following, this cycle will be discussed briefly to draw attention to possible processes of nitrogen turnover in the investigated aquifers. The nitrogen cycle starts with the cleavage of the triple bond in molecular nitrogen (N_2) during biological and / or chemical nitrogen fixation (Haber-Bosch process) (reaction path (RP) 1 in Fig. 1.1). The end product of these two strict anaerobic conversion processes is ammonia (NH_3). In water, dissolved NH_3 reacts to ammonium (NH_4^+) by protonation. Other processes that fix some atmospheric nitrogen by breaking up the triple bond in N_2 are lightning and the combustion of fossil fuels whereby N_2 is converted into nitrogen oxides (NO_x).

Fixed nitrogen in form of ammonium (NH_4^+) or nitrate (NO_3^-) can then be incorporated into the biomass of organisms (R-NH_2) via assimilation (RP 2 and 7). After the death of organisms organic nitrogen (R-NH_2) can again be mineralized to NH_3 by decomposers (RP 3).

Nitrification is performed by ammonia-oxidizing bacteria and ammonia-oxidizing archaea under aerobic conditions. Nitrifiers are able to oxidize NH_3 or NH_4^+ to nitrite (NO_2^-) via the intermediate hydroxylamine (NH_2OH) (RP 4 and 5). Whereas the first reaction (RP 4) requires aerobic conditions, the second oxidation of hydroxylamine (NH_2OH) to NO_2^- (RP 5) requires no additional molecular oxygen (Poth and Focht, 1985). In a second step of nitrification, NO_2^- is further oxidized to NO_3^- (RP 6) under aerobic conditions. It was shown that nitrification can lead to the formation of N_2O under limited O_2 concentrations. Three principal processes of N_2O formation during nitrification have been suggested but are still not totally elucidated (see Khalil et al. (2004) and citations therein): (i) The oxidation of NH_4^+ to NO_2^- (RP 4 and 5) under aerobic conditions and the subsequent diffusion of NO_2^- to anaerobic microsites followed by reduction to N_2O and N_2 via RP 9, 10 and 11. This mechanism is similar if not partly or complete identical to nitrifier-denitrification (see below). (ii) When O_2 concentrations decline, NO_2^- is supposed to be used as an additional electron

acceptor for the oxidation of NH_4^+ via various nitrification intermediates like NH_2OH or other instable intermediates resulting in N_2O formation (Poth and Focht, 1985). (iii) It is supposed that a certain proportion of NH_4^+ is converted during nitrification to N_2O via nitrification intermediates. For example it is hypothesized that N_2O could be a consequence of the short lived intermediate NOH (Ostrom et al., 2000). In the saturated zone of the investigated aquifers (FFA and GKA) nitrification is supposed to be of minor importance (Well et al., 2012).

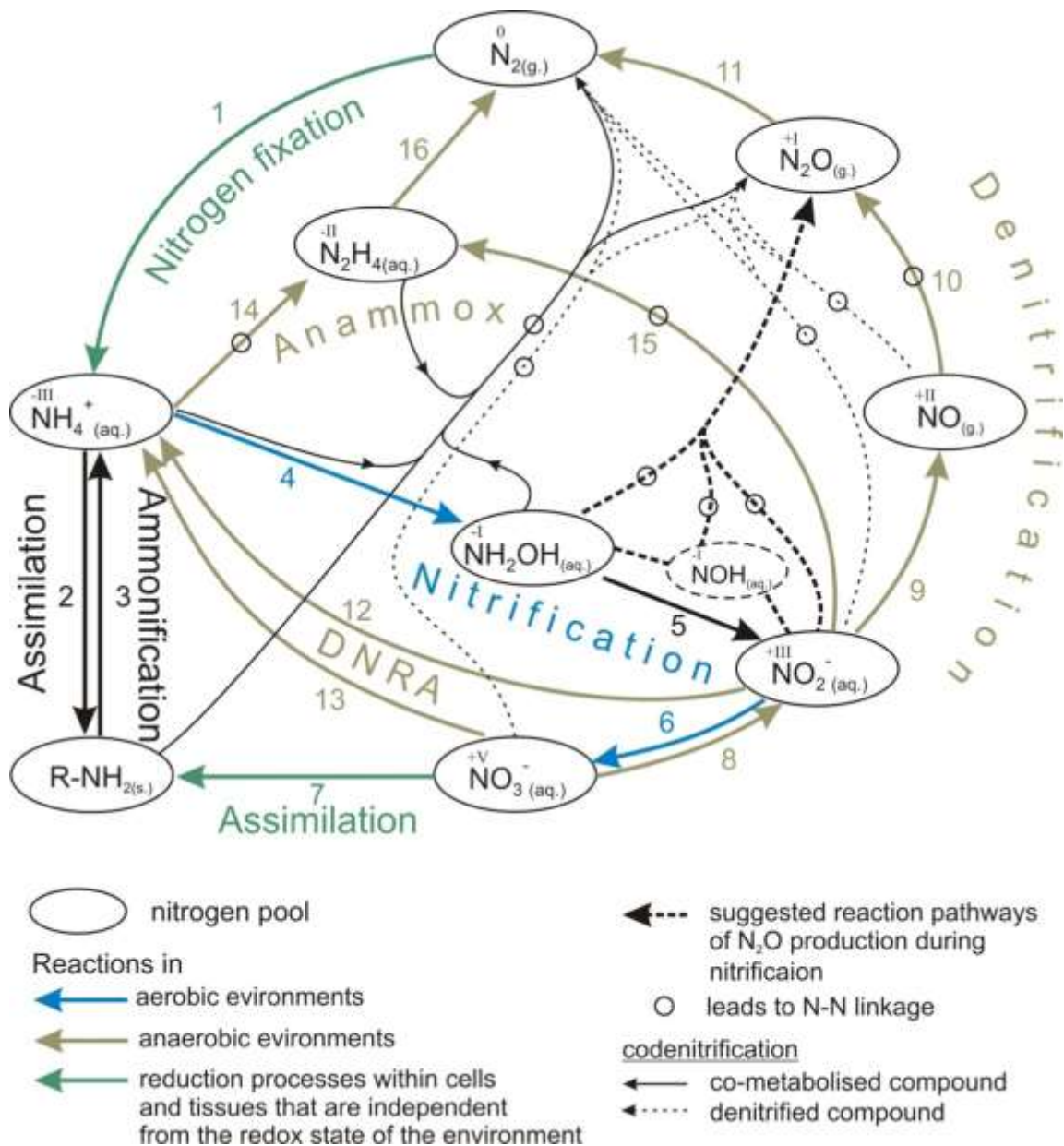


Fig. 1.1: The nitrogen cycle. R-NH₂: pool of organic N-compounds; DNRA: dissimilatory nitrate reduction to ammonium. Aerobic and anaerobic conditions can be considered on the cell-, microsite- or bigger-scales, the blue and yellow arrows refer to the microsite scale.

Denitrification is one of the key processes closing the nitrogen cycle (Fig. 1.1) via the microbial mediated stepwise anaerobic reduction of NO_3^- and NO_2^- through nitric oxide (NO) and nitrous oxide (N_2O) to the ultimate end product N_2 (RP 8 to 11) (Davidson and Seitzinger, 2006). Most denitrifiers are facultative anaerobic organotrophic bacteria using organic carbon for growth and maintenance but some denitrifiers are lithotrophs (Rivett et al., 2008; Korom, 1992) using reduced inorganic compounds like reduced iron (Fe^{2+}) or reduced sulphur (S^- , FeS_2). Beside bacteria also some fungi are able to denitrify (Kumon et al., 2002). Denitrification in aquifers is one of the major sinks for reactive nitrogen, which will be addressed below in more detail.

Nitrifier-denitrification follows the reaction paths 4 to 5 under aerobic and 9 to 11 under anaerobic conditions. In this process nitrifiers stop oxidation of NH_4^+ at NO_2^- when oxygen depletes and switch to denitrification (Wrage et al., 2001). Presumably this process is of minor importance in aquifers compared to soils because changes in the redox state within aquifers are usually much slower than in soils.

Under strict anaerobic conditions, dissimilatory nitrate reduction to ammonium (DNRA) is an alternative pathway for the reduction of NO_3^- . DNRA can remediate NO_3^- concentrations via the reduction of NO_2^- to NH_4^+ (RP 12) (van de Leemput et al., 2011) after preceding reduction of NO_3^- to NO_2^- or directly to NH_4^+ (RP 13) (Robertson et al., 1996). It is thought that DNRA is favoured under NO_3^- limited conditions and in environments rich in labile organic carbon (Burgin and Hamilton, 2007; Rivett et al., 2008; van de Leemput et al., 2011). A chemolithoautotrophic form of DNRA combines the reduction of NO_3^- with sulphur forms (free sulphides or elemental sulphur). Free sulphides are supposed to be able to inhibit denitrification (Burgin and Hamilton, 2007) but metal-bound sulphides may not inhibit but support denitrification (Böttcher et al., 1990; Burgin and Hamilton, 2007; Kölle et al., 1985). At all DNRA is seldom reported to be the dominant process of NO_3^- reduction in groundwater systems (Rivett et al., 2008) and chemical modelling by van de Leemput et al. (2011) suggested that DNRA is rather of importance under low NO_3^- concentrations and high C: NO_3^- ratios. DNRA is not likely an important process during this investigation because the groundwater in both aquifers is NH_4^+ -free, NH_4^+ formation was not observed during the conducted experiments and these experiments were not NO_3^- limited.

In the 1990s, a new chemolithoautotrophic microbial process of anaerobic ammonium oxidation (anammox) was discovered, by which NH_4^+ is combined with NO_2^- to hydrazine (N_2H_4) by a comproportionation reaction (RP 14 and 15). N_2H_4 is then converted into N_2 (RP 16) (Jetten et al., 1998). Contrary to marine environments, where high rates of anammox are

reported, in freshwater systems there is not much evidence for anammox (van de Leemput et al., 2011; Burgin and Hamilton, 2007). There are, to the author's knowledge, no studies about anammox in fresh water aquifers, whereas it is reported to exist in wastewater treatment systems, marine sediments and lakes (Jetten et al., 1998; Schubert et al., 2006; Dalsgaard et al., 2005).

Codenitrification, for the first time reviewed by Spott et al. (2011), is a microbially mediated process in which oxidized nitrogen is reduced (denitrified compound: NO_3^- , NO_2^- , NO) and reduced nitrogen is oxidized (co-metabolised compound: NH_4^+ , R-NH_2 , NH_2OH , N_2H_4). Codenitrification might be based on N-nitrosation reactions (Tanimoto et al., 1992; Weegaerssens et al., 1988) in which N of the denitrified compound forms a N-N linkage with the N of co-metabolised compounds (Spott et al., 2011) resulting in the formation of hybrid N_2O and / or N_2 . Most codenitrifying species are known as normal denitrifiers and found within all three domains (i.e. bacteria, archaea, eucaryota) (Spott et al., 2011). There is no information about the importance of codenitrification during nitrate attenuation in aquifers and this process is not yet considered in reviews about denitrification in aquifers.

1.3 Denitrification in groundwater

Denitrification (Fig. 1.1, RP 8 to 11) is supposed to be the quantitatively most important process of NO_3^- attenuation in groundwater (Korom, 1992) and riparian buffer zones (Burt et al., 1999).

There are 4 requirements for denitrification to take place (Firestone, 1982): (i) anaerobic conditions or low dissolved oxygen availability in reactive sites, (ii) N-oxides as electron acceptor, (iii) availability of electron donors and (iv) the existence of a microbial community able to denitrify. (i) Anaerobic conditions are considered to be one prerequisite for a microbial community to switch from O_2 to NO_3^- respiration. Denitrification presumably occurs at dissolved O_2 concentrations in groundwater below 1-2 $\text{mg O}_2 \text{ l}^{-1}$ (Rivett et al., 2008). A groundwater sample is usually a mixture of groundwater from well and poorly drained zones within the pore space of the aquifer material at the sampling point. Because of this the reported O_2 limit is probably an apparent limit for denitrification, since denitrification can take place in isolated microsites or bio-films with lower O_2 concentrations in the water than in the surrounding groundwater. (ii) Complete denitrification leads to the total consumption of NO_3^- in groundwater because there is no minimal concentration required for denitrification. On the other hand, Wall et al. (2005) showed that above a threshold of 0.88 $\text{mg NO}_3^- \text{-N l}^{-1}$

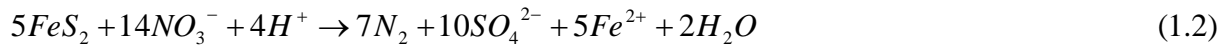
NO_3^- was no longer limiting for denitrification in river sediments. Some studies also reported a zero order kinetic of denitrification at NO_3^- concentrations $> 1 \text{ mg NO}_3^- \text{-N } \Gamma^{-1}$ (Morris et al., 1988; Korom et al., 2005), i.e. that denitrification rates were apparently independent of nitrate concentrations. (iii) Important electron donors in aquifers are organic carbon (Korom, 1992; Rivett et al., 2008), reduced sulphides and reduced iron (Fe^{2+}) (Korom, 1992). Organic carbon in aquifers is usually only partly available for microbial denitrification (Konrad, 2007). Iron sulphides like pyrite (FeS_2) are regularly reported to be available electron donors in anoxic parts of aquifers (Kölle et al., 1983; Böttcher et al., 1991; Korom, 1992). The reactivity and / or availability of pyrite depends on its microcrystalline structure (Kölle et al., 1985). In some aquifers, availability of pyrite to denitrification has been shown to be larger compared to organic carbon (Konrad, 2007; Weymann et al., 2010; Böttcher et al., 1991). Beside reduced compounds in the solid phase of aquifers, also dissolved organic carbon (DOC) or dissolved Fe^{2+} can reduce NO_3^- . Korom (1992) stated that groundwater containing Fe^{2+} normally show only low or no detectable NO_3^- concentrations. The importance of DOC for denitrification in groundwater is still an open question. Weymann et al., (2010) did not observe significant consumption of DOC during anaerobic incubations of aquifer material from the FFA. The typical concentrations of bioavailable DOC in groundwater of UK aquifers are relatively low and may not lead to substantial denitrification (Rivett et al., 2007). Nonetheless, rates of denitrification are often related to DOC concentrations in groundwater (Rivett et al., 2008). (iv) A vast variety of microbes are reported to be able to conduct denitrification, they are ubiquitous (Seitzinger et al., 2006) and they are found even at great depths in aquifers (e.g., to 185 m in a limestone (Morris et al., 1988), to 289 m in a clayey sand aquifer (Francis et al., 1989), or even to 450 m depth in a granite aquifer (Nielsen et al., 2006), respectively). When oxygen becomes depleted in groundwater, facultative anaerobes can switch to NO_3^- as electron acceptor and with further decreasing oxygen concentrations obligate denitrifiers begin to consume NO_3^- (Rivett et al., 2008).

Organotrophic and lithotrophic denitrification pathway can be distinguished regarding possible electron donors. During organotrophic denitrification, organic carbon functions as electron donor, while the required electrons during lithotrophic denitrification come from inorganic reduced compounds. Organotrophic denitrification can be described by the following formula (Jorgensen et al., 2004):

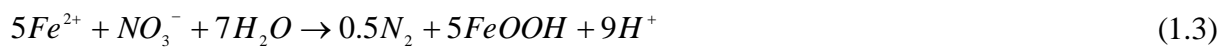


This denitrification pathway is accompanied by the formation of HCO_3^- and CO_2 . Denitrification with the iron sulphide pyrite as electron donor is considered a typical reaction

pathway of lithotrophic denitrification in aquifers (Rivett et al., 2008) and can be described according to Kölle et al. (1983) as:



Beside denitrified N_2 , this reaction releases SO_4^{2-} and reduced iron (Fe^{2+}) as reaction products to the groundwater. This reaction is mediated by the bacteria *Thiobacillus denitrificans* (Kölle et al., 1983) but can also be mediated by many other lithotrophs. Fe^{2+} released during oxidation of iron sulphides (Eqn. 1.2) may then further be oxidised by nitrate or dissolved oxygen and the evolved Fe^{3+} can precipitate as ferric oxide or iron oxyhydroxides after deprotonation, releasing H^+ ions to the groundwater (Eqn. 1.3) (Kölle et al., 1983).



While there are numerous laboratory incubation studies evaluating denitrification rates of aquifer sediments, there are only few studies reporting long-term denitrification capacity and / or the stock of reactive compounds capable to support denitrification in the investigated aquifer sediments (Kölle et al., 1985; Houben, 2000; Mehranfar, 2003; Weymann et al., 2010; Well et al., 2005). Even less investigations tried to predict the denitrification capacity from *in situ* measurement of denitrification rates or develop stochastic models to estimate the denitrification capacity from independent sediment variables (Konrad, 2007; Well et al., 2005).

Denitrification in aquifers is reviewed by Hiscock et al. (1991), Korom (1992), Burgin and Hamilton (2007) and Rivett et al. (2008). Recently, the first review about codenitrification has been published by Spott et al. (2011).

1.4 Objectives of this thesis

Methodical part

As introduced above, denitrification is a key process of the nitrogen cycle, but “Unfortunately, it is a miserable process to measure.” (Groffman et al., 2006). This is mainly because of the high background of N_2 , the dominant end product of denitrification in the environment. Therefore, sensitive and time-saving measuring methods for denitrification are required (Groffman et al., 2006).

Objective I: The first objective of this thesis was to develop an automated sampling and calibration unit coupled to a membrane inlet mass spectrometry system (MIMS) for the online measurement of denitrification, to test its performance and accuracy during a ^{15}N -tracer experiment and examine three different mathematical methods for calculating denitrification rates from MIMS raw data.

Also the influence of *in situ* degassing on the measurement of denitrification rates after ^{15}N -tracer addition was modelled and compared with the observed time course of denitrification products. *In situ* degassing occurred due to the formation of gaseous denitrification products in the pore water during the tracer experiment. The final aim was to develop a measuring system for automated online measurement of denitrification after ^{15}N tracer addition. Results are given in chapter 2.

Experimental part

The following research topics are considered to improve the understanding of denitrification: “Quantification of conditioned denitrification rates: ...that may be scaled from laboratory to field.” and “Quantification of field-scale denitrification: field assessment of denitrification occurrence and rates is challenging; improved field methods are required.” (Rivett et al., 2008).

The objectives two and three of this thesis are dedicated to these research topics and provide a combined approach of long-term anaerobic incubation experiments with aquifer material and *in situ* measurement of denitrification rates at groundwater monitoring wells at the origin of the incubated aquifer samples. The final goal of these two objectives was to predict laboratory measurements from *in situ* measurements of denitrification in the field.

Objective II: The main objective of the laboratory study introduced in chapter 3 was to estimate the denitrification capacity measured during long-term incubation experiments and the stock of reduced compounds of aquifer samples from initial denitrification rates and from chemical properties of the aquifer samples using different regression models.

From the experimental data, the minimal life-time of denitrification in the investigated aquifer material was estimated. During an additional intensive incubation experiment the exhaustibility of the denitrification capacity in aquifers samples was tested.

Objective III: During field experiments (chapter 4) *in situ* denitrification rates were measured using push-pull ^{15}N tracer tests at groundwater monitoring wells. The measured *in situ* denitrification rates were compared to long-term denitrification rates measured in the laboratory and regression models were tested to estimate the denitrification capacity as well as the stock of reduced compounds from *in situ* denitrification rates.

The influence of *in situ* conditioning of monitoring wells within the nitrate-free groundwater zone was evaluated during additional push-pull tests.

2 Online measurement of denitrification rates in aquifer samples by an approach coupling an automated sampling and calibration unit to a membrane inlet mass spectrometry system

Abstract

Aquifers within agricultural catchments are characterised by high spatial heterogeneity of their denitrification potential. Therefore, simple but sophisticated methods for measuring denitrification rates within the groundwater are crucial for predicting and managing N-fluxes within these anthropogenic ecosystems. Here, a newly developed automated online ^{15}N -tracer system is presented for measuring $(\text{N}_2+\text{N}_2\text{O})$ production due to denitrification in aquifer samples. The system consists of a self-developed sampler which automatically supplies sample aliquots to a membrane-inlet mass spectrometer.

The developed system has been evaluated by a ^{15}N -nitrate tracer incubation experiment using samples (sulphidic and non-sulphidic) from the aquifer of the Fuhrberger Feld in Northern Germany. It is shown that the membrane-inlet mass spectrometry (MIMS) system successfully enabled nearly unattended measurement of $(\text{N}_2+\text{N}_2\text{O})$ reduction within a range of 10 to 3300 $\mu\text{g N } \Gamma^{-1}$ over 7 days of incubation. The automated online approach provided results in good agreement with simultaneous measurements obtained with the well-established offline approach using isotope ratio mass spectrometry (IRMS). In addition, three different ^{15}N -aided mathematical approaches have been evaluated for their suitability to analyse the MIMS raw data under the given experimental conditions. Two approaches, which rely on the measurement of $^{28}\text{N}_2$, $^{29}\text{N}_2$ and $^{30}\text{N}_2$, exhibit the best reliability in the case of a clear ^{15}N enrichment of evolved denitrification gases. The third approach, which uses only the ratio of $^{29}\text{N}_2/^{28}\text{N}_2$, overestimates the concentration of labelled denitrification products under these conditions. By contrast, at low ^{15}N enrichments and low fractions of denitrified gas, the latter approach is on a par with the other two approaches. Finally, it can be concluded that the newly developed system represents a comprehensive and simply applicable tool for the determination of denitrification in aquifers.

2.1 Introduction

Denitrification, the reduction of nitrate (NO_3^-) to nitrous oxide (N_2O) and dinitrogen (N_2), is important to primary production, water quality and chemistry at the landscape, regional and global scales (Groffman et al., 2006). NO_3^- loading of near-surface groundwater (Hiscock et al., 1991; Korom, 1992) or riparian zones (Martin et al., 1999; Sanchez-Perez et al., 2003; Kneeshaw et al., 2007) is a well-known problem for the quality of water resources and, because of the growing need for agricultural products worldwide, ever an increasing one. Due to the input of fertilizer-N, agricultural fields have considerable potential for NO_3^- leaching, which can cause eutrophication of water bodies (Vitousek et al., 1997), and for the emission of N_2O , a trace gas contributing to global warming. However, agricultural fields also have great potential for an effective management that can reduce these emissions to aquifers or riparian systems (Seitzinger et al., 2006). Inputs of NO_3^- to aquifers or riparian systems can be minimised by fertiliser management, i.e. by matching application rates with plant demand or integrated plant nutrition systems (Roy et al., 2002). However, identification of aquifer sites with low or high denitrification potential is a prerequisite for being able to mitigate the export of NO_3^- to adjacent ecosystems effectively. Aquifers show a high spatial heterogeneity of denitrification in groundwater, which ranges from 0 to 100% of the N-input, mainly depending on the amount and microbial availability of reduced minerals or organic C in the aquifer, capable of supporting denitrification (Seitzinger et al., 2006). Therefore, information about the denitrification rates within aquifers is important for predicting and managing N-fluxes within agricultural catchments.

To measure denitrification rates in the saturated zone, there are three basic approaches. (1) The rates can be obtained by the indirect derivation of denitrification rates from gradients and mass balances of NO_3^- , sulphate (SO_4^{2-}) and other redox-relevant species (Korom, 1992; Frind et al., 1990). It is difficult and laborious to obtain quantitative estimates of denitrification rates with this method due to the spatial and temporal heterogeneity of these chemical parameters within aquifers and the difficulty of determining groundwater flow paths and groundwater residence times. (2) Denitrification rates can also be obtained from laboratory incubation studies with either undisturbed or disturbed material (Paramasivam et al., 1999; Smith and Duff, 1988; Well et al., 2005; Weymann et al., 2010). Those incubations can be either conducted with the ^{15}N -tracer technique or the acetylene inhibition method, or by measurement of NO_3^- consumption. Laboratory incubations offer the opportunity for

precise measurements of denitrification, but their transferability to in situ conditions is still under debate (Weymann et al., 2010). Another disadvantage is that sampling of deeper aquifer material is difficult and highly expensive. (3) A third method is the in situ measurement of denitrification by single-well push-pull tests. This technique was first applied by Trudell et al. (1986) and consists of a rapid injection of test solution at an existing well ('push phase') and a longer period of recovery of the injected solution ('pull phase'). This method was successfully applied in a variety of studies (Trudell et al., 1986; Istok et al., 1997; Schroth et al., 2001; McGuire et al., 2002; Harris et al., 2006), where denitrification rates were indirectly estimated from the depletion of NO_3^- . To distinguish the consumption of tracer NO_3^- from its dilution with surrounding groundwater, the NO_3^- concentrations in the samples were measured in relation to the concentrations of a conservative tracer (e.g. bromide (Br^-)) added to the injected solution. Smith and Davis (1974) showed that Br^- is a conservative tracer well suited to investigate the movement of NO_3^- in soils and subsoils. Because this approach requires the consumption of significant fractions of the injected NO_3^- within the experimental period, it is only suitable for detecting relatively large denitrification rates. (Weymann et al. (2010) measured initial denitrification rates of 2.7 to 258 $\mu\text{g N kg}^{-1} \text{ day}^{-1}$ after anaerobic incubation of aquifer material from the Fuhrberger Feld aquifer (FFA); from this range only the highest denitrification rates can be evaluated by the measurement of NO_3^- depletion.) A method for the direct determination of gaseous denitrification products and thus offering higher sensitivity was first tested in a laboratory set-up by Well and Myrold (1999). In situ push-pull tests with direct measurement of gaseous denitrification products have been used only in a limited number of studies (Sanchez-Perez et al., 2003; Kneeshaw et al., 2007; Well and Myrold, 2002; Addy et al., 2002; Well et al., 2003; Addy et al., 2005; Kellogg et al., 2005), which is in part due to the effort necessary for the gastight collection of water samples and the laborious analysis of dissolved gases in the laboratory using gas chromatography or mass spectrometry. Single well push-pull tests can be conducted with most types of groundwater monitoring wells (Konrad, 2007). Networks of such wells are often available in catchments and could thus be used for the spatial mapping of denitrification using push-pull tests.

Here a new instrumental set-up is presented, an automated sampling and calibration unit coupled to a membrane inlet mass spectrometry (ASCU-MIMS) system, designed for the in situ analysis of ^{15}N -labelled N_2 and N_2O in groundwater during ^{15}N -tracer experiments. This approach was tested successfully in the field during several ^{15}N -tracer push-pull experiments (unpublished data). This instrumentation should enhance the applicability of in situ as well as

Chapter 2

laboratory measurements of denitrification and denitrification rates in groundwater and thus facilitate the determination of the spatial heterogeneity of denitrification rates.

The objectives of this study are to (i) develop the ASCU-MIMS system, (ii) test its performance and accuracy during a laboratory ^{15}N -tracer experiment, and (iii) examine the suitability of three different methods for calculating denitrification rates from MIMS raw data.

2.2 Experimental

2.2.1 Study site

The FFA is a drinking water catchment area in Northern Germany, about 30 km NE of Hannover, consisting of carbonate-free, highly permeable Quaternary sands of 20 to 40 m thickness. The unconfined aquifer contains unevenly distributed amounts of microbial available sulphides and organic carbon. An intense agricultural use leads to considerable NO_3^- inputs to the groundwater. Detailed information about the FFA has been given by Strebel et al. (1992) and Frind et al. (1990).

Evidence of an intense ongoing denitrification within this aquifer is given by NO_3^- and redox gradients (Böttcher et al., 1992) as well as by excess- N_2 measurements (Weymann et al., 2008). Two different denitrification zones are present in this aquifer: the zone of organotrophic denitrification near the groundwater surface with organic carbon (C_{org}) as electron donor, and a deeper zone of predominantly lithotrophic denitrification with pyrite as electron donor (Böttcher et al., 1992; von der Heide et al., 2008; Böttcher et al., 1991).

The aquifer material used in this ^{15}N -tracer study originates from two depths of the FFA about 30 m south of a measuring field plot used by Weymann et al. (2009). The aquifer material was collected in March 2009 with a hand-operated bailer boring auger set (EIJKELKAMP, Giesbeek, The Netherlands) which consisted of a stainless steel bailer, casing tubes (o.d. of 10 cm) and a tube clamp. The aquifer material was extracted from 3 m and 7 m below the soil surface out of the organotrophic and lithotrophic denitrification zone with non-sulphidic and sulphidic material, respectively. From each depth, approximately 50 l of aquifer material were collected. The extracted aquifer material was directly transferred from the bailer into 16-l plastic buckets. The buckets were filled until the supernatant groundwater overflowed and were then closed airtight. The aquifer material was stored for 5 days at 10°C (approximately the mean groundwater temperature in the FFA).

2.2.2 Set-up

2.2.2.1 Incubation of aquifer mesocosms and sampling procedures

The tracer solution used in this experiment was prepared in 10-l glass bottles by dissolving $K^{15}NO_3$ (60 at % ^{15}N) in deionised water. Two 60-l PVC vessels were each filled with 15 l of the tracer solution. Approximately 45 l of the extracted aquifer material from each depth (3 and 7 m) of the FFA were then separately and carefully transferred from the 16-l plastic buckets into the 60-l PVC vessels, using one vessel for each depth. The water-saturated aquifer material was homogenised within the 60-l PVC vessels to achieve a homogenous distribution of the tracer. Hereby, the tracer solution was diluted with the initial pore water of the aquifer material. The mix of tracer solution and pore water will be referred to as the diluted tracer solution. After the mixing stage, each of the two 60-l PVC vessels contained 45 l of aquifer material saturated with the diluted tracer solution and approximately 15 l of supernatant diluted tracer solution. The aquifer material and diluted tracer solution from the two 60-l PVC vessels were then transferred into six 20-l PVC buckets with a height of 26 cm and i.d. of 32 cm, three buckets for material of each depth level. First, approximately 4 l of the supernatant diluted tracer solution were filled into each bucket and then 15 l of the water saturated aquifer material were slowly transferred. In order to release any trapped air within the aquifer material the buckets were repeatedly shaken. During the transfer from the 60-l PVC vessels the aquifer material was always covered with supernatant diluted tracer solution. The final level of the diluted tracer solution in each of the 20-l PVC buckets was 4 cm above the sediment surface. The total amount of diluted tracer solution in each 20-l PVC bucket was estimated as 9 l which results from the supernatant (4 l) and the pore volume of the aquifer material (5 l), estimated assuming a porosity of 0.35 (Franken et al., 2009). These buckets containing the ^{15}N -labelled aquifer material are referred to as mesocosms. Filter elements were installed 10 cm above the bottom of each mesocosm. The filter elements consisted of PE tubing (6 mm i.d.) with a 70- μ m mesh around the bottom of the tubing. The filter elements were connected with Tygon® tubing (1.6 mm i.d. and 4.8 mm o.d.) to solenoid valves of the automated measuring system described below (Fig. 2.1). The NO_3^- concentrations of the diluted tracer solution were 19.4 ± 0.29 and 12 ± 0.43 mg N Γ^{-1} in the mesocosms with aquifer material from 3 and 7 m depth (i.e. the non-sulphidic and sulphidic mesocosms), respectively. All the mesocosms were incubated for 7 days at room temperature (approx. 20 °C). Online analysis (ASCU-MIMS) of dissolved gases was conducted automatically at 4-h intervals.

Water samples were collected two to four times a day for reference measurements of dissolved gases using offline gas analysis by gas chromatography coupled to isotope ratio mass spectrometry (GC-IRMS) (see Sect. 2.2.4 and 2.2.5).

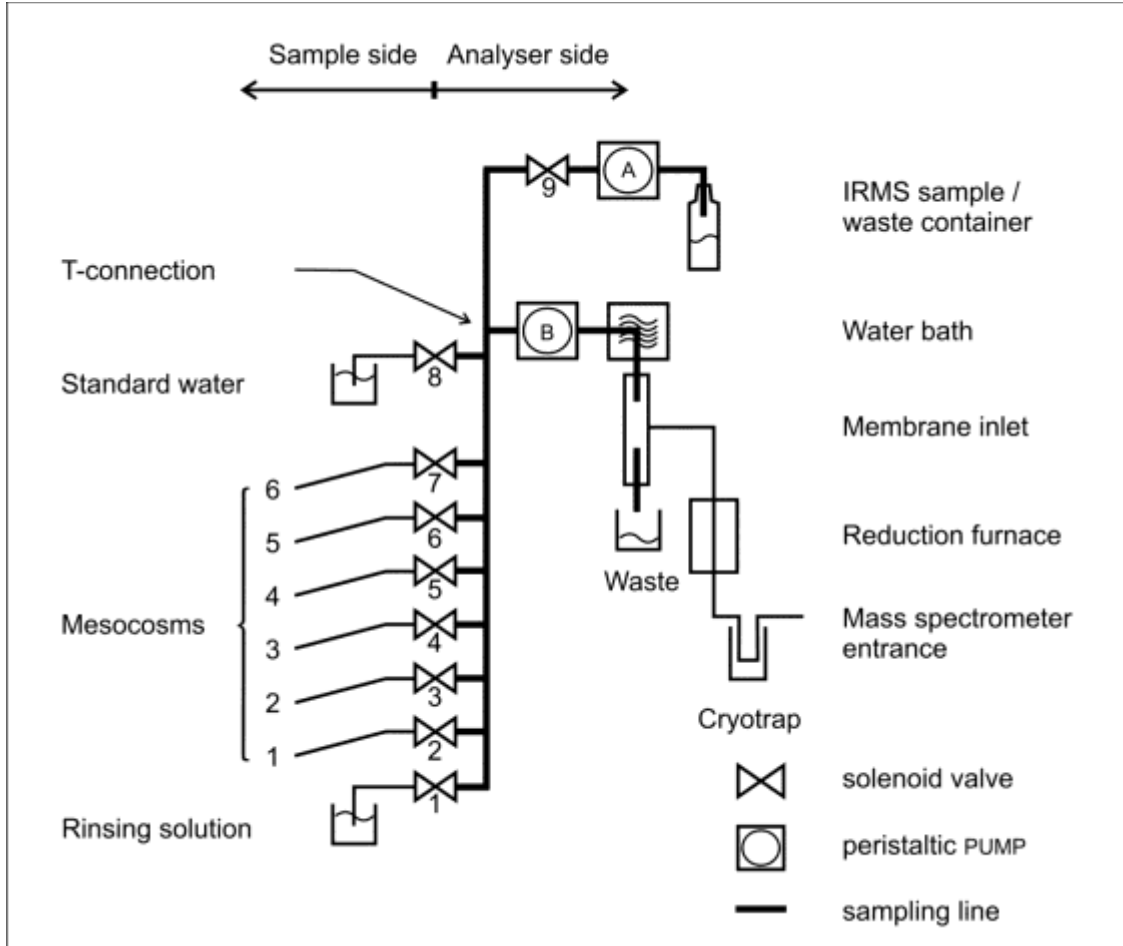


Fig. 2.1: Set-up of the automated measuring and calibration unit in combination with a membrane-inlet mass spectrometer.

2.2.3 On- and offline measurement and analysis of dissolved gases

For the isotopic analysis of ^{15}N -labelled denitrified N_2 and N_2O in this study N_2O was reduced to N_2 in an elemental copper furnace prior to entry into the mass spectrometer for both online analysis by ASCU-MIMS and offline analysis by GC-IRMS. The sum of N_2 and N_2O isotopologues was thus detected as N_2 . Therefore, the phrase ($\text{N}_2+\text{N}_2\text{O}$) was used when the sum of N_2 and N_2O was meant. The N_2O concentrations were measured separately by GC. For the calculation of the dissolved denitrification products from the isotope data, the $\Delta^{28}\text{N}_2$,

$\Delta^{29}\text{N}_2$ and $\Delta^{30}\text{N}_2$ values were calculated as the measured increases on molecular ions at mass 28, 29 und 30 during the laboratory experiment.

2.2.4 Automated online analysis using ASCU-MIMS

For the sampling and online dissolved gas analysis of pore water an automated sampling and calibration unit (ASCU) coupled to a MIMS system (Fig. 2.1) was used, which consisted of a quadrupole mass spectrometer (GAM 200, InProcess, Bremen, Germany) equipped with a membrane inlet. Data acquisition was performed by IPI QuadStar 32-bit software (Inficon AG, Balzers, Lichtenstein).

The ASCU consisted of peristaltic pumps, a cryostatic water bath and a set of nine PC-controlled solenoid valves (Type 6012, Bürkert, Ingelfingen, Germany). On the sample side the valves were connected via tygon tubing to a glass vessel containing the rinsing solution (valve 1), to the mesocosms (valves 2 to 7) and to the air-equilibrated standard water (valve 8) (Fig. 2.1, sample side). The analyser side of the ASCU consisted of the sampling line, the reduction furnace, a water bath and the membrane inlet (Fig. 2.1, analyser side). The solenoid valves on the analyser side were connected with each other to form the sampling line (Fig. 2.1). At the end of the sampling line a peristaltic pump (PUMP A, ISMATEC, BVP-Standard, Wertheim-Mondfeld, Germany) transferred most of the sampled solution from the sample side and through the sampling line to a permanent outlet leading either to a waste container or to a sampling vial to store samples for further analysis (Fig. 2.1, IRMS sample/waste container). A small part of the sampled solution was pumped through a T-connection by a second peristaltic pump (PUMP B, Gilson Model 312, Villiers-le-Bel, France) which was connected via stainless steel tubing to the membrane inlet of the analyser (Fig. 2.1, T-connection, PUMP B). The membrane inlet and stainless steel tubings were placed within a cryostatic water bath (Thermo Haake, HAAKE AG, Karlsruhe, Germany) to ensure constant sample and membrane inlet temperatures during the extraction of dissolved gases from the sample in the membrane inlet. The water bath also contained a flask with air-equilibrated standard water (Fig. 2.1, water bath, membrane inlet). The membrane inlet consisted of a 4 cm long piece of silicone tubing (Silastic Dupont, 0.3 mm i.d. and 0.15 mm wall thickness) connected to in and out flowing stainless steel capillaries. The silicone tubing was placed within a glass tube that was directly connected with the mass spectrometer by a stainless steel capillary. The sample solution flowed inside the silicone tubing, and the outside of the silicone tubing was exposed to the high vacuum of the mass spectrometer. A reduction

furnace consisting of stainless steel tubing (250 mm long, 4 mm i.d.) filled with elemental copper and a cryotrap with liquid nitrogen were placed in the vacuum line prior to entry into the mass spectrometer source in order to reduce N_2O to N_2 and to remove water vapour and CO_2 (Fig. 2.1).

2.2.4.1 Principle of online dissolved gas analysis with MIMS

Using online dissolved gas analysis with MIMS, water samples can be directly introduced into the mass spectrometer via the membrane inlet without any sample preparation. A semi-permeable membrane is the interface between the sample at atmospheric pressure and the high vacuum of the mass spectrometer. The dissolved gases of the measured water sample will diffuse through the membrane into the mass spectrometer. On passing the membrane the water sample is degassed quantitatively. The dissolved gas concentrations can then be calculated from the measured intensities of the recorded molecular ion masses of the dissolved gases.

2.2.4.2 Sampling procedure and analysis

One measuring cycle with ASCU-MIMS consisted of six software-controlled steps in the following order: (i) the recording of the instrumental noise signals on the selected molecular ion masses (blank measurement), (ii) the calibration of the MIMS system by the measurement of the standard water, (iii) the online measurement of pore water within the mesocosms, (iv) repeating the calibration, (v) repeating the blank measurement, and (vi) rinsing the ASCU with pure water.

For the measurement of the instrumental noise signals on the selected molecular ion masses (step (i)) all valves were closed and PUMPS A and B were switched off. The standard water was then pumped for 15 min through the membrane inlet to calibrate the MIMS system (Fig. 2.1, valve 8 open, all other valves closed, PUMP A switched off, PUMP B switched on, step (ii)). After the calibration of the MIMS system, valve 8 was closed and the pore water from the first mesocosm was pumped through the sampling line by PUMP A and to the membrane inlet by PUMP B for 15 min (Fig. 2.1, valves 2 and 9 open, all other valves closed, PUMPS A and B switched on, step (iii) for mesocosm 1). Before the pore water from the next mesocosm was sampled, the whole ASCU was rinsed for 2 min (Fig. 2.1, valves 1 and 9 open,

all other valves closed, PUMP A and PUMP B switched on). The mesocosms 2 to 6 were sampled and analysed in the same way as mesocosm 1. After the sampling and online measurement of the pore water from all the mesocosms, the standard water (step (iv)) and the instrumental noise (step (v)) on the selected molecular ion masses were measured again. Finally, the sampling system was rinsed for 1.5 h (step (vi)). For that purpose, the rinsing solution was pumped through the sampling line and the membrane inlet by PUMPS A and B (Fig. 2.1, valves 1 and 9 open, all other valves closed, PUMPS A and B switched on). Afterwards, the whole measuring process was restarted with the measurement of the instrumental noise and the standard water, as described above. The suction rates of PUMPS A and B were 10 and 0.7 ml min⁻¹, respectively. The duration of each sampling cycle was 4 h, including 1.5 h rinsing.

This 4-h sampling interval for every mesocosm was maintained over 1 week. For the online measurement a total sample volume of 150 ml per measurement was needed to obtain sufficient flushing of the inner volumes of tubings, stainless steel capillaries and solenoid valves of the ASCU. From this sampled volume only 10 ml were pumped to the membrane inlet.

During the experiment the molecular ion masses of N₂, O₂ and Ar were recorded; to measure the N₂ isotopologues of (N₂+N₂O) the reduction furnace to reduce N₂O to N₂ was placed between the membrane inlet and the mass spectrometer entrance (Fig. 2.1).

It was tested if the sum of N₂ and N₂O could be measured simultaneously for different ratios of dissolved N₂ to dissolved N₂O. For that purpose, different amounts of N₂O were injected into serum bottles containing 78 ml pure water and a 40 ml headspace. The concentrations of N₂ and N₂O in the pure water as well as the partial pressures of N₂ and N₂O in the headspace were known. After the injection of different amounts of pure N₂O into the headspace, headspace gases and water were equilibrated by shaking. The deviation between the calculated and measured concentrations of N₂O in pure water after equilibration was between -5.4 and 21.9 %. The deviation between the measured and calculated concentration sum of N₂ and N₂O was always in the range of -4 to 6 %. These results confirmed that N₂O reduction to N₂ was complete and the sum of N₂ and N₂O was thus successfully detected as N₂.

The MIMS system was calibrated against air-equilibrated water of known salinity (Fig. 2.1, standard water), which was maintained at a constant temperature. Because the concentrations of dissolved gases in air-equilibrated water depend on the partial pressures of the individual gases in the air, the barometric pressure was recorded during the incubation experiment (Kana et al., 1994). The molecular ion masses 28, 29, 30, 32, 40 and 44 (²⁸N₂, ²⁹N₂, ³⁰N₂, ³²O₂, ⁴⁰Ar

and $^{44}\text{CO}_2$) were recorded and the dissolved concentrations of Ar and the nitrogen isotopologues were calculated following the same protocol as described by An et al. (2001).

For the measurement of the major atmospheric gases with MIMS, the dependence between signal intensity and dissolved gas concentration in a sample is linear for a wide range of dissolved gas concentrations (Kana et al., 1994; Tortell, 2005; Lapack et al., 1991). This was confirmed for the quadrupole mass spectrometer used in this study, finding linearity for the range of dissolved gas concentrations of Ar and N_2 measured during this experiment (10 to $900 \mu\text{mol l}^{-1}$).

$^{30}\text{N}_2$ was calibrated using the $^{28}\text{N}_2$ (m/z 28) signal and the instrumental response factor (f_{30}) as proposed by Jensen et al. (1996).

Direct calibration of $^{30}\text{N}_2$ with air-equilibrated water was not possible because of the small fraction of $^{30}\text{N}_2$ in atmospheric N_2 and thus a high background-to-sample ratio on molecular ion mass 30. The instrumental noise signal at m/z 30 can be affected by the formation of NO^+ in the ion source if O_2 is present. O_2 was removed in the reduction furnace within the vacuum line of the measuring system (Fig. 2.1, reduction furnace). The signal intensity on m/z 32 was recorded to measure the O_2 background within the mass spectrometer to check for any formation of NO^+ and found that it was always low ($<5\text{E}-11$ A). The instrumental response factor for $^{29}\text{N}_2$ in relation to $^{28}\text{N}_2$ (f_{29}) was derived according to Jensen et al. (1996).

The signal of the molecular ion at mass 44 was measured because CO^+ , a possible fragment ion of CO_2 within the ion source, can interfere the measurement of the molecular ion at mass 28. During the experiment the m/z 44 signal was always $< 4\text{E}-11$ A (i.e. 0.04 % of the signal intensity of the molecular ion at mass 28) showing that the liquid nitrogen trap prior to the entrance of the mass spectrometer effectively trapped CO_2 .

2.2.5 Manual offline approach with GC-IRMS

For the offline analysis of dissolved gases by GC-IRMS, the dissolved gases had to be transferred quantitatively into the gas phase. Briefly, this was achieved by manual filling of serum bottles, sealing them air tight, creating a gas headspace, equilibrating the headspace with the liquid phase and analysing the headspace gases by GC-IRMS.

2.2.5.1 Sampling and offline analysis of NO_3^- , SO_4^{2-} and denitrification gases

Water samples were collected manually 2 to 4 times per day from the permanent outlet of the ASCU-MIMS system (Fig. 2.1, IRMS sample) for the GC-IRMS analysis of ($\text{N}_2+\text{N}_2\text{O}$). Serum bottles (26 ml) were placed at the end of the sampling line to collect pore water of the sampled mesocosm (step (iii), Sampling procedure and analysis; Fig. 2.1, GC-IRMS sample).

The outflow tubing of the sampling line was placed at the bottom of the serum bottles. After an overflow of at least three times the volume of these bottles, the tubing was removed and the bottles were immediately sealed air tight with grey butyl rubber septa (Altmann, Holzkirchen, Germany) and aluminium crimp caps. Afterwards, the samples were adjusted to 25 °C in a temperature-controlled room and a headspace was generated within the serum bottles by the injection of 15 ml of ambient air, replacing the same volume of sample solution. The replaced solution was directly transferred to 20-ml PE vials and frozen for later NO_3^- and SO_4^{2-} analysis. The vials were then agitated for 3 h on a horizontal shaker at constant temperature (25 °C) to equilibrate the dissolved gases with the headspace gas. Finally, 13 ml of the headspace gas were transferred to an evacuated 12-ml Exetainer® (Labco, High Wycombe, UK) with a plastic syringe. The nitrogen-containing gases in the Exetainers were then a mixture of N_2 and N_2O gained from the atmosphere and from denitrification, respectively.

The ^{15}N analysis of ($\text{N}_2+\text{N}_2\text{O}$) by GC-IRMS was performed at the Centre for Stable Isotope Research and Analysis in Göttingen, Germany, within 2 weeks, following the method described in Well et al. (2003). N_2O was measured using a gas chromatograph (Fisons GC 8000, Milan, Italy) equipped with a split-injector and an electron-capture detector and a HP-Plot Q column (50 m length \times 0.32 mm i.d.; Agilent Technologies, Santa Clara, CA, USA) kept at 38 °C. The concentrations of denitrified N_2 and N_2O in the gas samples were calculated as described by Well and Myrold (1999) and Well et al. (2003). The concentration of N_2O in the added atmospheric air was taken into account when calculating the N_2O production. From the obtained molar concentrations in the headspace, the concentrations of dissolved gases were calculated taking into account temperature, headspace pressure, the liquid-to-headspace volume ratio and the solubilities given by Weiss (1970) and Weiss and Price (1980).

The NO_3^- concentrations in the samples were determined photometrically in a continuous flow analyser (Skalar, Erkelenz, Germany).

SO_4^{2-} was analysed by potentiometric back-titration of excess Ba_2^+ ions remaining in the solution after the addition of BaCl_2 . EDTA was used as the titrant. The SO_4^{2-} concentrations in the pore water of the sulphidic material increased from 30.2 ± 0.92 at the beginning to $41.2 \pm 4.29 \text{ mg SO}_4^{2-}\text{-S } \Gamma^{-1}$ at the end of the ^{15}N -tracer test. In the case of the non-sulphidic material, no detectable SO_4^{2-} formation was observed.

2.3 Calculations

2.3.1 ^{15}N abundance of denitrified NO_3^-

The ^{15}N abundance of denitrified NO_3^- was calculated from N_2 isotopologues as follows (Jensen et al., 1996):

$$X = \frac{100}{1 + \frac{\Delta N_2^{29}}{2f_{30}\Delta N_2^{30}}} \quad (2.1)$$

where X is the ^{15}N fraction in the denitrified NO_3^- , assuming a random distribution of N isotopes within the evolved N_2 to form the N_2 isotopologues (Hauck and Bouldin, 1961). X was also estimated from the dilution of ^{15}N -labelled tracer NO_3^- with pore water NO_3^- of natural ^{15}N abundance in order to check the value of X derived from the N_2 isotopologues.

2.3.2 Mathematical approaches to determine the contribution of labelled denitrification gases in a mixture of N_2 and N_2O gases

One objective of this work was to compare the three different ^{15}N -aided mathematical approaches presented below (Methods I to III) with respect to their suitability for MIMS measurements. These methods calculate N_2 from denitrification. However, $(\text{N}_2+\text{N}_2\text{O})$ was analysed, since N_2O was reduced to N_2 prior to entry into the mass spectrometer ion source. Because of this, Eqn. (2.1) and the following cited formulae are only valid to calculate the fraction of denitrified $(\text{N}_2+\text{N}_2\text{O})$ for the presented data if the produced N_2O and N_2 have the same ^{15}N abundances. This is only fulfilled if both species originate from a common denitrification pathway and from the same pool of labelled N. Moreover, the cited formulae

imply that the added ^{15}N -labelled NO_3^- and possible background NO_3^- in the tracer solution is well mixed and that the evolved $^{28}\text{N}_2$, $^{29}\text{N}_2$ and $^{30}\text{N}_2$ follow a binomial distribution, i.e. ^{14}N and ^{15}N are randomly paired.

2.3.2.1 Method I – Mulvaney

To study the N_2 flux from soil, Mulvaney (1984) derived an equation for the calculation of the fraction of tracer-derived labelled N_2 within a mixture of soil-emitted and atmospheric background N_2 . During the incubation of unsaturated soil, the amount of background N_2 is typically large since the gaseous denitrification products are usually accumulated within an air-filled enclosure and the soil pore space is partially filled with air. On the condition that (i) the ^{15}N abundance of the denitrified NO_3^- (X) is known, (ii) denitrification is the sole gaseous nitrogen forming process, and (iii) the amount of N_2 evolved from the labelled NO_3^- pool is small compared with the atmospheric N_2 in the sample, the fraction of denitrified N_2 can be determined by measuring only $^{29}\text{N}_2/^{28}\text{N}_2$ ratios.

Following this approach the fraction of dissolved denitrified ($\text{N}_2+\text{N}_2\text{O}$) (here referred to as B) in a mixture with dissolved ($\text{N}_2+\text{N}_2\text{O}$) gained from the atmosphere was calculated with the equation given in Table 1 in Mulvaney's (1984) paper (equation for triple collector mass spectrometer). This equation will be referred to as 'Eqn. for B ' given by Mulvaney (1984). The concentration of dissolved denitrified ($\text{N}_2+\text{N}_2\text{O}$) in the sample (B_c) is the product of B and the total concentration of ($\text{N}_2+\text{N}_2\text{O}$) originating from the atmosphere and from denitrification (D_c):

$$B_c = D_c \times B \quad (2.2)$$

The calculation for B given by Mulvaney (1984) is an approximation based on the assumption that the fraction of labelled denitrification products within the mixture of atmospheric and labelled denitrified ($\text{N}_2+\text{N}_2\text{O}$) is very small, i.e. it does not significantly increase the amount of ($\text{N}_2+\text{N}_2\text{O}$) in the sample. This prerequisite is not necessarily fulfilled during the MIMS measurement of dissolved denitrification products in liquid samples, because the concentration of dissolved atmospheric N_2 in water is very low compared with that in soil air samples.

The performance of this approach was evaluated at the relatively low background concentrations of natural ($\text{N}_2+\text{N}_2\text{O}$) (A_c) dissolved in the pore water within the aquifer

mesocosms. For that purpose, the theoretical distribution of N_2 isotopologues in modelled mixtures of A_c ($14.42 \text{ mg N } \Gamma^{-1}$) with varying concentrations of denitrified (N_2+N_2O) (B_c) was calculated. The range of A_c and B_c in the modelled mixtures was selected to cover the results of this tracer test. A binomial distribution of N_2 isotopologues according to their ^{15}N abundance was assumed for the labelled (N_2+N_2O) evolved and also for the natural background (N_2+N_2O) in this modelled mixtures. B_c was then calculated using the Eqn. for B given by Mulvaney (1984) and compared with the theoretical B_c .

2.3.2.2 Method II – isotope pairing method

The isotope pairing method (IPM) was developed by Nielsen (1992) and has been successfully applied in a multitude of ^{15}N -tracer studies, mostly in flow-through experiments with estuarine or marine sediments and a supernatant water phase (Eyre et al., 2002; Smith et al., 2006; Bohlke et al., 2004).

The IPM calculates the concentration of denitrification gases from the recorded increases on the signal intensity of the molecular ion masses 29 and 30 ($\Delta^{29}N_2$ and $\Delta^{30}N_2$, respectively) during a tracer experiment under the assumption that only denitrification contributes to the change in the isotope composition of the measured dissolved N_2 in the sample. The concentration of labelled denitrified (N_2+N_2O) was calculated based on Eqns. (1) and (2) given by Nielsen (Nielsen, 1992). The sum of the values given by these two equations is the total concentration of denitrified (N_2+N_2O).

These equations assume constancy of the concentration of non-labelled background N_2 during the analysed time interval, a condition which is generally fulfilled in flow through experiments. However, during push-pull experiments, these predictions can be invalid due to mixing of the tracer solution with ambient pore water. In addition, degassing processes within the pore space of the sediment can cause a decrease in background N_2 . The IPM does not calculate the fraction of ^{15}N -labelled denitrification gases in individual samples. Therefore, two measurements are necessary to calculate the increase in the denitrification gases formed during the investigated time interval (Eyre et al., 2002; Rysgaard et al., 1994) or to subtract a standard with the same amount of N_2 from the measured sample (Nielsen, 1992).

2.3.2.3 Method III – Spott and Stange

Spott and Stange (2007) derived a new mathematical approach, calculating the fraction of ^{15}N -tracer-derived N_2 in a mixture with atmospheric N_2 with respect to possible contributions of several N_2 -forming processes. In this study their simplified approach was used, which assumes that the produced N_2 originates exclusively from the labelled NO_3^- pool, i.e. there is no formation of non-labelled N_2 precursors, e.g. by nitrification. This assumption is appropriate as denitrification has been shown to be the dominating microbial process in the FFA (Böttcher et al., 1992).

The fraction of dissolved denitrified ($\text{N}_2+\text{N}_2\text{O}$) (B) in a mixture with ($\text{N}_2+\text{N}_2\text{O}$) gained from the atmosphere (A) was calculated based on Eqn. (13) from Spott and Stange (2007). The concentration of dissolved denitrified ($\text{N}_2+\text{N}_2\text{O}$) can then be determined with Eqn. (2.2). The mole fractions of $^{29}\text{N}_2$ and $^{30}\text{N}_2$ (i.e. α_{29} and α_{30}) used in Eqn. (13) from Spott and Stange (2007) can be calculated from the MIMS raw data as follows:

$$\alpha_{29} = \frac{{}^{29}\text{N}_2 f_{29}}{{}^{28}\text{N}_2 + {}^{29}\text{N}_2 f_{29} + {}^{30}\text{N}_2 f_{30}} \quad (2.3)$$

$$\alpha_{30} = \frac{{}^{30}\text{N}_2 f_{30}}{{}^{28}\text{N}_2 + {}^{29}\text{N}_2 f_{29} + {}^{30}\text{N}_2 f_{30}} \quad (2.4)$$

where f_{29} and f_{30} are the instrumental response factors (see Experimental set-up, Sampling procedure and analysis) and $^{28}\text{N}_2$, $^{29}\text{N}_2$ and $^{30}\text{N}_2$ are the measured intensities on the ion masses 28, 29 and 30.

The advantages of this mathematical approach over that of Nielsen (1992) are that only one measurement is needed to calculate the fraction of denitrified ($\text{N}_2+\text{N}_2\text{O}$) and, compared with Mulvaney (1984), the equations are valid for any ratio between labelled denitrified ($\text{N}_2+\text{N}_2\text{O}$) and atmospheric ($\text{N}_2+\text{N}_2\text{O}$).

2.3.3 Precision and limit of detection

To compare the instrumental precisions of ASCU-MIMS and GC-IRMS analysis with respect to the fraction of dissolved denitrified ($\text{N}_2+\text{N}_2\text{O}$) (B) and the concentration of dissolved denitrified ($\text{N}_2+\text{N}_2\text{O}$), coefficients of variation (CVs) were calculated by Gaussian error propagation using the partial derivatives of the Eqn. for B given by Mulvaney (1984) and

Eqn. (2.2) above. The detection limit was calculated as the minimum amount of labelled denitrified (N_2+N_2O) in a given background of natural (N_2+N_2O) necessary to increase the measured $^{29}N_2/^{28}N_2$ ratio to fulfil the following equation:

$$r_{sa} - r_{st} \geq 3 \times sdr_{st} \quad (2.5)$$

where r_{sa} and r_{st} are the $^{29}N_2/^{28}N_2$ ratios in sample and standard, respectively, and sdr_{st} is the standard deviation of repeated r_{st} measurements.

2.3.4 Estimating potential bias from in situ degassing

N_2 and N_2O production in aquifers can cause degassing of dissolved N_2 and N_2O which can bias the determination of N_2 and N_2O production in aquifers (Visser et al., 2007; Visser et al., 2009).

This effect was modelled by calculating theoretical time courses in the concentration of denitrified (N_2+N_2O) within the pore water during ongoing denitrification with and without simultaneous in situ degassing of dissolved gas (Fig. 2.5). For these calculations, the closed system equilibration (CE) model proposed by Aeschbach-Hertig et al. (2008) was employed to estimate partitioning of the gas between pore water and gas bubbles. The only extension made to this model was that the concentrations of $^{28}N_2$, $^{29}N_2$ and $^{30}N_2$ were separately calculated, instead of the total N_2 . For all N_2 isotopologues the same Henry constant was used.

The following input parameters for modelling were used. (i) The molar concentrations of the major dissolved gases in the pore water before denitrification had started. (ii) The measured initial denitrification rate leading to increasing molar concentrations of evolved $^{28}N_2$, $^{29}N_2$ and $^{30}N_2$ in the pore water during the experiment. (iii) The maximum total dissolved gas pressure (mTDGP) before gas bubbles will form in the pore space. The mTDGP is equal to the sum of the hydrostatic, atmospheric and capillary pressure. In the calculations, mTDGP was assumed to be 1036 mbar, resulting from 50 mbar hydrostatic and 987 mbar atmospheric pressure. The capillary pressure was assumed to be negligible in the hydraulic active pores of the incubated aquifer material. (iv) The initial trapped air to water volume ratio was set to 0, which means that before in situ degassing took place, there was no trapped gas phase in the pore space of the water-saturated aquifer material. If the calculated actual total dissolved gas pressure (aTDGP) exceeds the sum of the hydrostatic, atmospheric and capillary pressure (mTDGP) (i.e. the pore water is oversaturated in dissolved gases) due to

production of denitrification gases, gas bubbles will form. These trapped gas bubbles will then expand until the aTDGP in the pore water is equal to the mTDGP. The new equilibrium concentrations of the different gases depend on the volume ratio of trapped gas bubbles to pore water and the different Henry constants for the various gases (Aeschbach-Hertig et al., 2008).

2.4 Results and Discussion

2.4.1 Comparison between ASCU-MIMS and GC-IRMS gas Analysis

The concentrations of ^{15}N -labelled denitrified ($\text{N}_2+\text{N}_2\text{O}$) increased in the sampled pore water from the non-sulphidic and sulphidic mesocosms with time, as expected (Fig. 2.2). To compare online measurement using ASCU-MIMS with offline GC-IRMS analysis (as established in the Centre for Stable Isotope Research and Analysis in Göttingen, Germany) raw data obtained with both approaches were calculated with Eqn. for B given by Mulvaney (1984) and Eqn. (2.2). The two analytical methods were in close agreement up to a concentration of denitrified ($\text{N}_2+\text{N}_2\text{O}$) of $1500 \mu\text{g N } \Gamma^{-1}$ (Fig. 2.2(A)). For higher concentrations of denitrified ($\text{N}_2+\text{N}_2\text{O}$), the ASCU-MIMS system increasingly overestimated the concentrations of denitrified ($\text{N}_2+\text{N}_2\text{O}$), as will be discussed later (see Sect. 2.4.2). If the ASCU-MIMS raw data are calculated with the approach given by Spott and Stange (2007), the ASCU-MIMS and GC-IRMS measurements are in good conformity for the whole range of denitrified ($\text{N}_2+\text{N}_2\text{O}$) concentrations (Fig. 2.2(A)).

The ^{15}N enrichment of denitrified NO_3^- calculated from the N_2 isotopologues (Eqn. (2.1)) was 37.4 ± 1.08 and 59.2 ± 0.72 atom % in the non-sulphidic and sulphidic mesocosms, respectively. These data were in good agreement with the values obtained by GC-IRMS, which were 37.17 ± 1.23 and 59.08 ± 0.24 atom % for the non-sulphidic and sulphidic mesocosms, respectively. Both approaches satisfactorily coincided with the ^{15}N abundances of the denitrified NO_3^- calculated from the NO_3^- concentrations before and after mixing of tracer solution and pore water, which were 37.0 ± 0.55 and 60.0 ± 0.82 atom % for the non-sulphidic and sulphidic mesocosms, respectively.

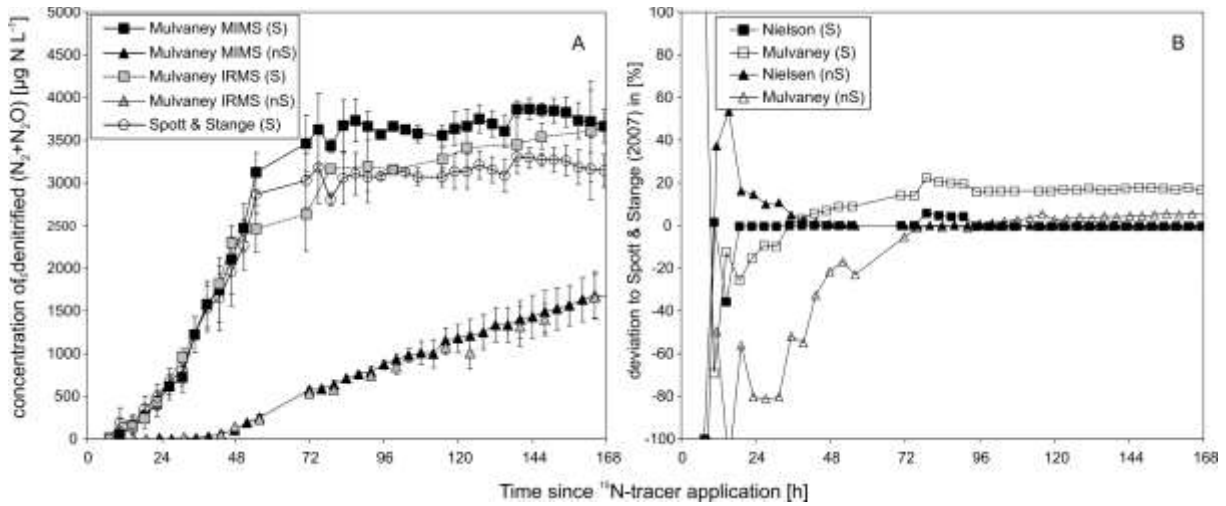


Fig. 2.2: Concentration courses of denitrified (N_2+N_2O) (B_c) in the pore water of the aquifer material from the sulphidic (S) and non-sulphidic mesocosms (nS) during the 7-day laboratory tracer experiment. (A) Comparison of the concentration of denitrified (N_2+N_2O) (B_c) calculated from online ASCU-MIMS and offline GC-IRMS data (Eqn. for B given by Mulvaney) and online analysis with GC (Eqn. (13) given by Spott and Stange (2007)). (B) Percentage deviation of the concentration values of denitrified (N_2+N_2O) calculated from MIMS data with Eqns. (1) and (2) from Nielsen (1992) and Eqn. for B from Mulvaney (1984) compared with values calculated with Eqn. (13) from Spott and Stange (2007).

The detection limit of produced denitrified (N_2+N_2O) for the ASCU-MIMS and GC-IRMS analyses was 1.5 and 2.5 $\mu\text{g N L}^{-1}$, respectively (Table 2.1). Although the precision of the $^{29}\text{N}_2/^{28}\text{N}_2$ ratio measurement with GC-IRMS was almost 7 times better than with ASCU-MIMS, the detection limit for the amount of denitrified (N_2+N_2O) was slightly better with ASCU-MIMS, because the background of natural N_2 dissolved in the pore water (A_c) is much smaller than for the GC-IRMS samples with the large N_2 background in the generated air headspace in the sample vials. The instrumental precision of the fraction of denitrified (N_2+N_2O) (B) was comparable for both methods (Table 2.1) and similar to the precision given for previous measurements of B reported by Well et al. (1998) and Siegel et al. (1982) with CVs [%] of 0.26 and 0.36, respectively. Despite equal instrumental precisions for both methods, the standard deviations between replicate samples were higher with the GC-IRMS method (Fig. 2.2(A)). This can be explained by the error introduced by the sample preparation, i.e. headspace generation and equilibration of headspace gases with dissolved gases, required for GC-IRMS analysis. The analysis of groundwater samples is thus more precise with the MIMS method, which instantaneously detects dissolved gases in water samples during sampling.

Table 2.1: Instrumental precision of the 29/28 molecular ion mass ratio estimated from the coefficient of variation (CV) of six repeated measurements of a standard (air-N₂ equilibrated with water). The CVs for (*B*) and (*B_c*) were calculated by error propagation and the limit of detection of labelled denitrified (N₂+N₂O) was calculated with Eqn. (2.5).

Method	Instrumental precision CV	limit of detection ^a	CV calculated from error propagation ^b	
			<i>B</i>	<i>B_c</i>
	%	µg N l ⁻¹	%	
IRMS	0.020	2.5	0.191	0.963
MIMS	0.133	1.5	0.577	0.931

^aThe limit of detection was calculated after Eqn. (2.5).

^bThe propagation of error was calculated from Eqn. for *B* given by Mulvaney (1984) and Eqn. (2.2).

The good agreement between the two methods (Fig. 2.2) shows that the establishment of the new online ASCU-MIMS approach was successful. This analytical method is thus in principle suitable for the in situ analysis of denitrification using ¹⁵N-tracer tests.

2.4.2 Comparison of three different mathematical ¹⁵N approaches

To optimise the analysis of MIMS raw data, three different ¹⁵N-aided mathematical approaches were investigated. To the best of knowledge the new mathematical approach given by Spott and Stange (2007) was applied in this study for the first time to quantify the formation of denitrification gases during a ¹⁵N-tracer experiment in combination with MIMS. Comparison of these approaches was necessary due to differences in their susceptibility to analytical error and differences in their reaction to the experimental conditions. The following aspects are considered in this comparison. (i) The ASCU-MIMS system can be calibrated with air-equilibrated water for ²⁸N₂ and ²⁹N₂ but not for ³⁰N₂. For this aspect, method I by Mulvaney (1984) is advantageous since it is applicable to measurement of ²⁸N₂ and ²⁹N₂ only. (ii) The sensitivity of the three approaches to the accuracy in determining the ¹⁵N abundance of the denitrified NO₃⁻ (*X*) was investigated. This was necessary because *X* varies with time since the ¹⁵N-labelled NO₃⁻ pool undergoing denitrification can be diluted with natural NO₃⁻ during tracer tests and the determination of *X* can be biased by NO⁺ formation within the mass spectrometer, affecting the molecular ion at mass 30. (iii) The isotope pairing method (IPM)

given by Nielsen (1992) is mostly used in flow-through experiments with the sampling of the supernatant water phase above the denitrifying substrate and the use of highly enriched $^{15}\text{N-NO}_3^-$ as tracer. In this set-up, the background concentration of dissolved natural N_2 is well known and the IPM uses the background concentration of dissolved N_2 to calculate the concentration of evolved denitrification gases. However, in pore water extraction experiments like this study, the background concentration of dissolved N_2 may vary.

The time courses of denitrified ($\text{N}_2+\text{N}_2\text{O}$) concentrations calculated with the approach of Nielsen (1992) and Spott and Stange (2007) are in good agreement after the second day of the tracer test (Fig. 2.2(B)). The relative difference between both methods was $<1.5\%$ except for an initial period of 24 and 44 h after tracer application in the sulphidic and non-sulphidic mesocosms, respectively. The fact that relative deviations were high ($>10\%$) in this initial period may be attributed to the low concentrations of denitrified ($\text{N}_2+\text{N}_2\text{O}$) (B_c) (<15 and $100 \mu\text{g N } \Gamma^{-1}$ in the non-sulphidic and sulphidic mesocosms, respectively) and therefore to a possible error in the calculated ^{15}N abundance of the denitrified NO_3^- (X). This error might be explained by the relatively high background of the molecular ion at mass 30 compared with the measured signal. Moreover, the different sensitivities of these two approaches with respect to error in the determination of X might have contributed to the observed differences (discussed below). During later periods with $B_c >15$ and $100 \mu\text{g N } \Gamma^{-1}$ in the non-sulphidic and sulphidic mesocosms, respectively, the new approach given by Spott and Stange (2007) is in very good conformity to the widely used IPM and is thus fully suitable for MIMS data. During the whole tracer test, the absolute deviation between these two methods never exceeded 1 and $10 \mu\text{g N } \Gamma^{-1}$ for the non-sulphidic and sulphidic mesocosms, respectively. The approach of Mulvaney (1984) is only in relatively good agreement with the two other approaches (within $<10\%$ deviation) for samples with a concentration of denitrified ($\text{N}_2+\text{N}_2\text{O}$) below $1500 \mu\text{g N } \Gamma^{-1}$. Above this threshold, the Mulvaney approach leads to an overestimation which increases in parallel with the concentration of denitrified ($\text{N}_2+\text{N}_2\text{O}$) (Figs. 2.2(A) and 2.3).

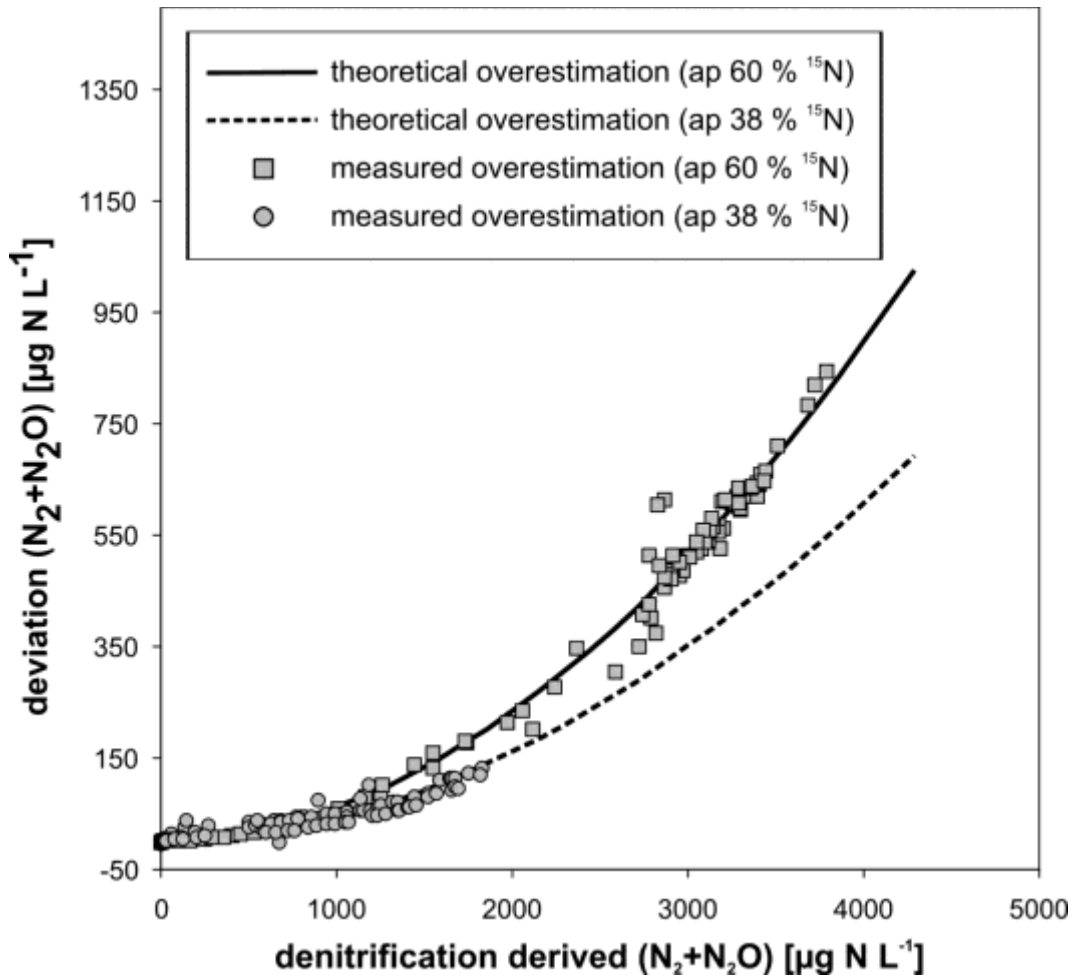


Fig. 2.3: Theoretical and measured overestimation of denitrified N_2 in liquid samples due to the use of Eqn. for B from Mulvaney (1984) in the case of high B/A ratios in the sample. For the theoretical curves the following parameters were set in accordance with the experimental conditions: ^{15}N abundance of $NO_3^- = 38$ and 60% and $14.42 \text{ mg N } \Gamma^{-1}$ of dissolved atmospheric N_2 in the pore water prior to denitrification. The measured overestimation was calculated as the deviation between concentrations calculated according to the approaches of Mulvaney (1984) and Spott and Stange (2007).

- (i) The observed overestimation of denitrified (N_2+N_2O) concentrations due to the use of Eqn. for B given by Mulvaney (1984) could be explained by the fact that this approach assumes that there is only a small fraction of labelled denitrified (N_2+N_2O) (B) in a mixture with atmospheric N_2 (A) (see calculations, Method I) whereas B was relatively high in the water samples of this study. Originally, this approach was derived for the measurement of labelled denitrification gases in soil air samples. Under standard conditions of temperature and pressure (273.15 K and 100 kPa), for example, 1 cm^3 air

contains 34.4 $\mu\text{mol N}_2$ whereas 1 cm^3 pure water includes only 0.816 $\mu\text{mol N}_2$ in equilibrium with a headspace of atmospheric composition, i.e. in water samples the background of natural N_2 is about 42 times smaller than in soil air samples. The overestimation of B_c due to the use of Eqn. for B given by Mulvaney (1984) in the case of high B/A ratios for modelled mixtures of A and B as explained in the Experimental section (see Sect. 2.3.2.1) was calculated (Fig. 2.3) and could also be shown as the divergence from the concentrations of denitrified ($\text{N}_2+\text{N}_2\text{O}$) calculated with the approach of Spott and Stange (2007) (Fig. 2.2(B)). The Eqn. for B given by Mulvaney (1984) resulted in an overestimation of denitrified labelled ($\text{N}_2+\text{N}_2\text{O}$) which increases in parallel with the labelled ($\text{N}_2+\text{N}_2\text{O}$) concentrations. This is similar to observations during this study (Fig. 2.2(B)). The reason is that the fraction of labelled denitrification products ($\text{N}_2+\text{N}_2\text{O}$) (B) is not negligible and increases relative to the amount of natural ($\text{N}_2+\text{N}_2\text{O}$) (A). Hence, the Eqn. for B given by Mulvaney (1984) must lead to an increasing overestimation of B as the B/A ratio increases. The theoretical and measured overestimations are in good agreement (Fig. 2.3). The theoretical calculations show that the overestimation of denitrified ($\text{N}_2+\text{N}_2\text{O}$) concentrations due to the use of this mathematical method is below 5 % if the B/A ratio in the sample is ≤ 0.05 and the ^{15}N abundance in the evolved denitrified ($\text{N}_2+\text{N}_2\text{O}$) is between 40 and 60 atom %.

- (ii) The sensitivity of all approaches to errors in determining the ^{15}N -abundance values of the denitrified NO_3^- (X) was evaluated (Fig. 2.4). During tracer tests, dilution of the tracer solution with ambient groundwater is regularly reported (Istok et al., 1997; Addy et al., 2002; Well et al., 2003; Haggerty et al., 1998). X can thus be variable within a tracer plume and can be difficult to estimate if the ^{15}N -labelled tracer NO_3^- mixes during the tracer test with pore water NO_3^- . For example, X decreased from 60 to 37.4% within the non-sulphidic mesocosms due to dilution of ^{15}N -enriched NO_3^- with pore water NO_3^- . This illustrates the need to determine X and to evaluate error propagation with respect to calculated fractions of labelled denitrified ($\text{N}_2+\text{N}_2\text{O}$) (B). Since the estimation of X is subject to potential errors because $^{30}\text{N}_2$ can be biased by NO^+ formation in the mass spectrometer, it is necessary to check the impact of this error on B , as calculated with the three mathematical approaches. For this purpose, various theoretical mixtures of natural and ^{15}N -labelled ($\text{N}_2+\text{N}_2\text{O}$) with different fractions of B were modelled in the same manner as was used to test the approach given by Mulvaney (1984) described above. B was then calculated from theoretical isotopologue abundances by applying the three mathematical approaches on these theoretical

mixtures and taking into account a defined error in X (between 0 and ± 20 atom %). For the equations given by Spott and Stange (2007) and Nielsen (1992), the error in B_c is independent of X as well as of the ratio of labelled denitrified (N_2+N_2O) to natural background (N_2+N_2O) (i.e. B/A) in the analysed gas mixture (Fig. 2.4). The error in the calculated concentrations of denitrified (N_2+N_2O), obtained by applying Eqn. for B given by Mulvaney (1984), shows a strong dependence on the value of X as well as on the B/A ratio (Fig. 2.4). The equations given by Spott and Stange (2007) are twice as sensitive to errors in X than the calculations by Nielsen (1992). For example, if the ideal and measured ^{15}N abundances of X differ by 5 %, the deviation between calculated and ideal concentrations of denitrified (N_2+N_2O) obtained with the approach given by Spott and Stange (2007) is 10%, whereas this deviation is only 5 % when using the equations given by Nielsen (1992). As reported earlier (Well and Myrold, 1999), the Eqn. for B given by Mulvaney (1984) is quite robust to errors in the calculated ^{15}N abundance of the denitrified NO_3^- (X), if the ^{15}N abundances of X are between 40 and 60 atom %. In this case a 10 % error in X would lead only to an error in the calculated concentrations of denitrified (N_2+N_2O) of below 5 %. For lower or higher ^{15}N abundances in the denitrified NO_3^- this mathematical approach becomes increasingly sensitive to errors (Fig. 2.4).

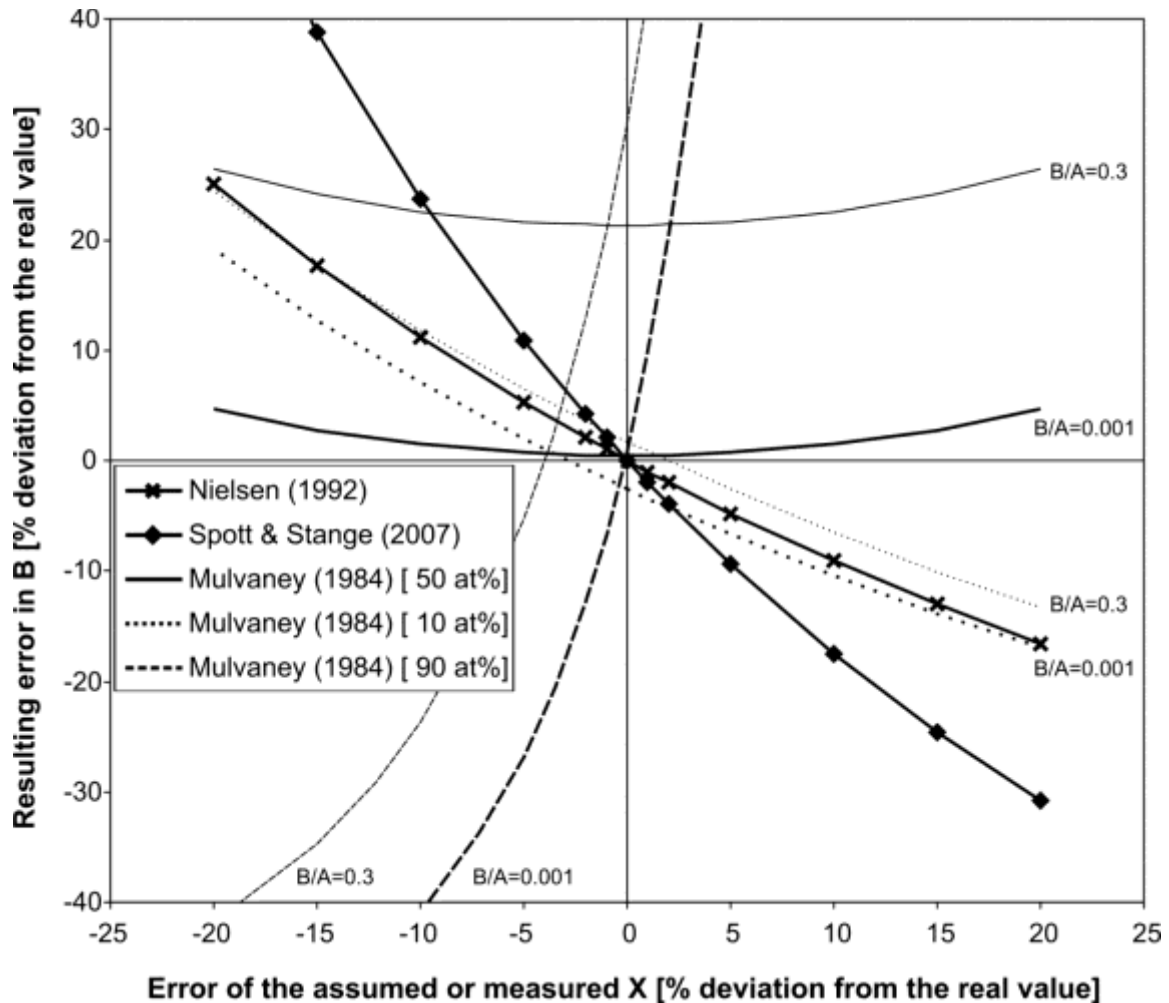


Fig. 2.4: Susceptibility of the three investigated mathematical approaches to errors in ^{15}N abundance of denitrified NO_3^- . X is the ^{15}N fraction in the denitrified NO_3^- and A and B are the fractions of natural and denitrified N_2 within the mixture analysed. Contrary to the approaches of Nielsen (1992) and Spott and Stange (2007), the error in B is dependent on X and the B/A ratio when the Eqn. for B from Mulvaney (1984) is used.

- (iii) Except for the initial period (24 h and 44 h in the sulphidic and non-sulphidic mesocosms, respectively) the calculated concentrations of denitrified ($\text{N}_2+\text{N}_2\text{O}$) are nearly identical for the IPM (Nielsen, 1992) and for the approach given by Spott and Stange (2007). In this period the relative difference between the two methods is between 2 and 53 %. Changing concentrations of natural background ($\text{N}_2+\text{N}_2\text{O}$) in the pore water might have contributed to the observed initial differences between the two methods in addition to the different sensitivities to errors in the ^{15}N -abundance values of X (discussed above). Contrary to the two other approaches the IPM relies on the subtraction of the background concentration of natural N_2 and N_2O – in this case

(N_2+N_2O) (A_c) – from the measured total concentration of N_2 and N_2O (D_c). The A_c in the extracted water samples can change during a tracer test if the tracer solution mixes with the surrounding pore water or as a result of in situ degassing. Changing A_c will affect only the concentrations of denitrified (N_2+N_2O) (B_c) calculated with the IPM, whereas the approaches given by Mulvaney (1984) and by Spott and Stange (2007) directly calculate the fraction of denitrified (N_2+N_2O) in an analysed sample. The sensitivity of the IPM to variations in A_c during a tracer test will decrease with increasing concentrations of B_c . The IPM relies on the measurement of $^{29}N_2$ and $^{30}N_2$ but increasing concentrations of denitrified (N_2+N_2O) will lead to decreasing fractions of $^{29}N_2$ and $^{30}N_2$ coming from natural background (N_2+N_2O) in relation to ^{15}N -labelled $^{29}N_2$ and $^{30}N_2$ evolved during denitrification. This might have contributed to the decrease in the relative difference between the IPM and the approach given by Spott and Stange (2007) during the tracer experiment (Fig. 2.2(B)).

2.4.3 Denitrification rates and influence of the experimental set-up on the measured time pattern of denitrified (N_2+N_2O)

After the start of the production of denitrified (N_2+N_2O) within the incubated aquifer material, both non-sulphidic and sulphidic aquifer material showed a time interval during which there was an almost linear increase in dissolved concentrations of denitrified (N_2+N_2O) (Fig. 2.2(A)). The denitrification rates (D_r) were estimated from this time interval where there was a linear increase of denitrified (N_2+N_2O) . The D_r values of the non-sulphidic and sulphidic material were $55.3 \pm 0.12.5$ and $360.3 \pm 73 \mu\text{g N kg}^{-1} \text{ day}^{-1}$, respectively.

The mean D_r of the sulphidic mesocosms ($360 \mu\text{g N kg}^{-1} \text{ day}^{-1}$) is similar to the mean D_r of $284 \mu\text{g N kg}^{-1} \text{ day}^{-1}$ obtained by GC-IRMS analysis after anaerobic incubations of sulphidic aquifer material from the same aquifer (Weymann et al., 2010). The D_r value of the non-sulphidic material measured during this ^{15}N tracer experiment ($55 \mu\text{g N kg}^{-1}$) is nearly 50% higher than the highest D_r value reported by Weymann et al. (2010) for non-sulphidic material (D_r from 0.2 to $35 \mu\text{g kg}^{-1} \text{ day}^{-1}$). The higher D_r value measured during this laboratory ^{15}N -tracer test might be due to the documented spatial heterogeneity within the aquifer (Weymann et al., 2008; von der Heide et al., 2008). Moreover, the mentioned anaerobic incubations were carried out at $10 \text{ }^\circ\text{C}$, whereas the incubation temperature during the laboratory ^{15}N -tracer test was $20 \text{ }^\circ\text{C}$, leading to a faster reaction.

After 65 h, the concentration of denitrified (N_2+N_2O) (B_c) of the sulphidic material showed no further increase and reached an almost stable level of between 3100 and 3350 $\mu\text{g N } \Gamma^{-1}$, whereas there was a further ongoing increase in B_c in the non-sulphidic material. It is assumed that this was due to experimental artefacts.

Could a decrease of denitrification activity due to the exhaustion of electron donors or acceptors during the experiment be a plausible explanation for the stable B_c values of the sulphidic mesocosms?

At the end of the ^{15}N -tracer experiment, the final NO_3^- concentrations within the pore water of the sulphidic mesocosms were between 5.2 and 5.9 $\text{mg N } \Gamma^{-1}$. Wall et al. (2005) reported a threshold of 0.88 $\text{mg NO}_3^- \text{-N } \Gamma^{-1}$ below which NO_3^- became a limiting factor for denitrification in the case of river sediment denitrification rates. This low threshold suggests that the NO_3^- concentration was not a limiting factor for denitrification in this experiment. Anaerobic incubations conducted by Weymann et al. (2010) with sulphidic aquifer material from the FFA showed a long-lasting denitrification potential of sulphidic aquifer material from this site with almost constant denitrification rates over several weeks. The possibility can thus be excluded that denitrification stopped after approximately 65 h as a result of a limitation in available electron donors, i.e. available sulphides or organic C. Moreover, the mesocosms were not sealed against the atmosphere. Thus, O_2 diffusion through the supernatant solution to the sediment surface might have lowered denitrification activity at the surface to some extent. This might have contributed to the declining slope of the concentration curve at the end of incubation.

The question then arises as to what extent the relative stable level of denitrified (N_2+N_2O) observed in the sulphidic mesocosms can be explained by in situ degassing of N_2 and N_2O (see Calculations, Estimating potential bias from in situ degassing). In situ degassing as a result of denitrification was reported for an aquifer consisting of sand and gravel in Nord Brabant, The Netherlands (Visser et al., 2007; Visser et al., 2009). To estimate the potential effect of in situ degassing during this study, the expected development of concentration courses of labelled dinitrogen with and without simultaneous in situ degassing of dissolved gas was modelled. The concept of the closed system equilibration (CE) model was used for these calculations (Aeschbach-Hertig et al., 2008).

Without in situ degassing, the modelled concentrations of dissolved denitrified (N_2+N_2O) increased linearly with time according to the measured denitrification rate (Fig. 2.5). With in situ degassing, the modelled concentrations of dissolved denitrified (N_2+N_2O) decreased with time, showing that this process could explain some of the observed non-linear time course of

the dissolved denitrified (N_2+N_2O) concentrations (B_c) (Fig. 2.5). In the sulphidic mesocosms, the calculated actual total dissolved gas pressure (aTDGP) exceeded the maximum total dissolved gas pressure (mTDGP) after 35 h, which initiates a divergence between the modelled B_c curves with and without degassing. However, the flattening of the measured B_c curve is not explainable by degassing only since this process would not lead to the observed stabilising of B_c . In the non-sulphidic samples, aTDGP did not exceed mTDGP (data not shown) until 100 h after tracer application, due to the relatively low denitrification rates. In situ degassing lowered the observed concentrations of denitrified (N_2+N_2O) of these samples by a maximum of 5 % at the end of the experiment. The occurrence of degassing can also be evaluated by using the $^{30}N_2/^{28}N_2$ ratio, since the CE model predicts that this ratio is not affected by degassing and thus increases linearly with time (Fig. 2.5). However, the measured $^{30}N_2/^{28}N_2$ ratio of the sulphidic samples exhibited a decreasing slope. This finding thus confirms that, in addition to degassing, further mechanisms must be considered to explain the observed decrease in the denitrified (N_2+N_2O) concentrations.

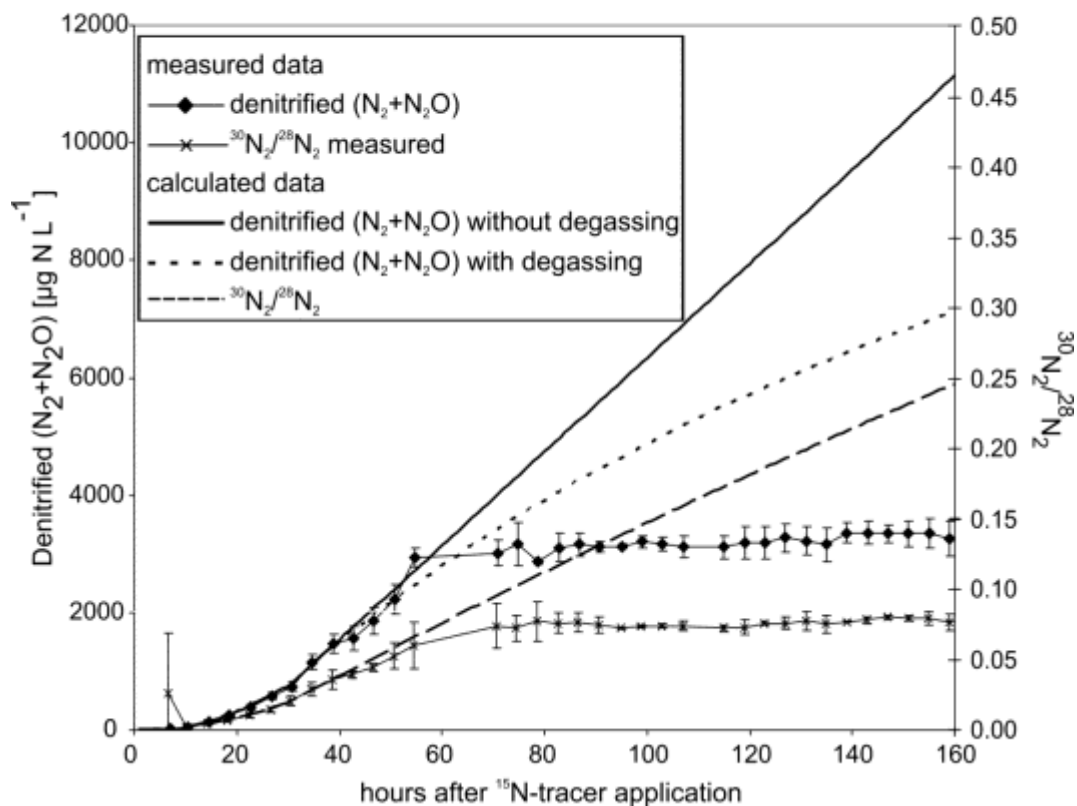


Fig. 2.5: Measured concentration courses of denitrification derived (N_2+N_2O) in the pore water of the sulphidic material compared with calculated concentrations with and without degassing of labelled denitrification gases.

Another explanation for the relative stable concentrations of dissolved denitrified (N_2+N_2O) in the sulphidic mesocosms after 65 h of incubation might be a breakthrough of the supernatant diluted tracer solution which had initially not been in direct contact with the pore space of the sediment. The repeated extraction of samples from the probes caused migration of the supernatant diluted tracer solution through the incubated aquifer material towards the installed filter elements. A breakthrough of the supernatant tracer solution after 65 h could explain the sharply flattened concentration curve of denitrified (N_2+N_2O). During the ^{15}N -tracer test, 0.9 l of pore water per day were sampled out of every mesocosm. After 65 h of incubation this total volume would be 2.5 l. The total pore volume of the incubated aquifer material within the mesocosms was estimated as 5.3 l, calculated from the porosity (0.35) (Franken et al., 2009) and the volume (15 l) of the aquifer material. According to Kollmann (Kollmann, 1986) the hydraulic active pore volume is between 15 and 25 % in fine sands such as the sulphidic aquifer material (fine -, middle -, coarse sand and gravel = 21.8, 54.4, 5.5 and 14.9 %, respectively). In view of this fact and as the diluted tracer solution is not flowing through the aquifer material below the installed filter elements in the lower part of the mesocosms, a hydraulic active pore volume around 2.5 l is plausible. After 65 h of incubation the pore water in the hydraulic active pores would then be exchanged with originally supernatant diluted tracer solution. The constancy after 65 h might reflect steady-state conditions, i.e. the accumulation of N_2 and N_2O gained by denitrification during the residence time of the diluted tracer solution within the denitrifying aquifer material. In the non-sulphidic samples the suspected breakthrough of supernatant diluted tracer solution is not evident since the concentrations of denitrified (N_2+N_2O) continuously increased until the end of the experiment (Fig. 2.2(A)). This could be due to a larger hydraulic active pore volume of this material (fine -, middle -, coarse sand and gravel = 18.4, 74.3, 3.8 and 1.3 %, respectively). The fraction of medium sand was higher than in the sulphidic samples which would explain a higher fraction of hydraulic active pores (Kollmann, 1986).

In essence, the lack of degassing and a larger hydraulic active volume in the non-sulphidic mesocosms might explain why the flattening of the concentration curve of denitrified (N_2+N_2O) was less pronounced for the non-sulphidic mesocosms during the tracer experiment (Fig. 2.2(A)). The modelling of in situ equilibrium degassing with the CE model showed that degassing could reduce the increase of measured denitrified (N_2+N_2O) but could not explain the relative stable concentrations of denitrified (N_2+N_2O) in the water samples of the sulphidic mesocosms after 65 h of incubation.

2.4.4 Comparison of ASCU-MIMS with previous methods

Until now, the measurement of denitrification with MIMS has been limited to water samples from surface waters or samples of the overlying water from flow-through incubation experiments with sediment cores. To measure denitrification in aquifers the sampling and analysis of groundwater are required. MIMS has been previously used in situ to measure N_2/Ar ratios in groundwater (Singleton et al., 2007), but not the isotopic signatures of dissolved gaseous N species. In previous in situ studies using the ^{15}N -tracer technique, the groundwater samples were analysed using offline analysis of dissolved denitrification products by GC-IRMS (Well and Myrold, 2002; Addy et al., 2002; Well et al., 2003; Addy et al., 2005; Konrad, 2007). This new ASCU-MIMS instrumentation combines the mentioned previous methods and will allow the in situ measurement of denitrification in future studies. The results show that the developed method was suitable to derive denitrification rates comparable with the denitrification rates previously measured in the FFA by offline analysis with GC-IRMS.

During the ^{15}N -tracer experiment presented in this study the concentrations of denitrified (N_2+N_2O) were measured automatically every 4 h over 1 week using the ASCU-MIMS system. Only the liquid N_2 trap and the flask containing the standard water had to be refilled – every 8 h and 12 h, respectively. A reduction of the total inner volume of the ASCU would further reduce the needed sampling volume of 150 ml and also shorten the possible sampling intervals.

The advantage of the developed method is that it combines automated sampling with direct measurement of water samples without any sample preparation. It is less laborious than the offline GC-IRMS method because the preparatory degassing step is not needed. Moreover, the measurements are almost in real-time and the success or failure of experiments is thus immediately evident, which will help to optimise in situ experiments. In contrast to offline GC-IRMS measurement, this online ASCU-MIMS procedure enables users to adjust experiments to actual results, e.g. stop measurements in case of undetectable activity or to adjust the sampling intervals to the specific denitrification dynamics. Finally, the relatively low cost of MIMS compared with IRMS will open this technology to a wider group of users.

2.5 Conclusions

For the first time an automated sampling and calibration unit in combination with membrane-inlet mass spectrometry (ASCU-MIMS) was used for the online analysis of ^{15}N -labelled denitrification products in pore water extracted during a ^{15}N -tracer test with aquifer mesocosms in the laboratory. This was done to evaluate MIMS for future in situ measurement of denitrification in aquifers. The ASCU-MIMS approach successfully enabled unattended measurement for 7 days, where only the refilling of the liquid nitrogen trap and the reservoir of standard water had to be conducted manually. By comparing online ASCU-MIMS data with results from established offline isotope analysis by GC-IRMS, it was found that this new method yielded accurate results of produced ($\text{N}_2 + \text{N}_2\text{O}$) within a range of 10 to 3300 $\mu\text{g N l}^{-1}$. Online analysis was even more precise than the GC-IRMS method.

Furthermore, three different mathematical approaches were compared for their suitability to determine the fraction of labelled denitrification gases (B) in water samples from MIMS raw data. All three approaches were in good agreement when the ^{15}N enrichment of the NO_3^- pool undergoing denitrification (X) was known and, in the case of the approach of Mulvaney (1984), the ratio of labelled denitrification gases to natural background N_2 and N_2O (B/A) is small. However, the methods differ in their response to analytical errors and in the necessity to include analysis of $^{30}\text{N}_2$. The new approach given by Spott and Stange (2007) is the most suitable for the determination of denitrification from MIMS raw data. The advantage of the approach given by Mulvaney (1984) is that it only relies on the measurement of the $^{29}\text{N}_2$ to $^{28}\text{N}_2$ ratio and it could be used if the ratio of labelled denitrification gases to natural background N_2 and N_2O (B/A) is small.

During the laboratory tracer test, the linear increase in dissolved denitrification products over approximately 2 days enabled a reliable determination of denitrification rates, where the order of magnitude was in agreement with previous studies. The non-linear behaviour of the concentration curves during the later phase of the experiments could be explained as a combined effect of (i) degassing due to gas production in excess of solubility and (ii) the extracted sample volume exceeding the total volume of the hydraulic active pores in the aquifer material. The presented analysis of these experimental artefacts will help to handle similar effects in future field studies.

Overall, this laboratory experiment show that the tested instrumentation will be suitable for online measurement of ^{15}N -labelled denitrified ($\text{N}_2 + \text{N}_2\text{O}$) dissolved in pore water and it can thus be used as a new tool for push-pull tracer tests for measuring denitrification rates in

Chapter 2

aquifers. Advantages of the new approach include the possibility of conducting measurements almost in real-time, the relatively low cost of the instrumentation and the removal of the laborious sample preparation necessary for offline analysis with GC-IRMS.

3 Predicting the denitrification capacity of sandy aquifers from shorter-term incubation experiments and sediment properties

Abstract

Knowledge about the spatial variability of denitrification rates and the lifetime of denitrification in nitrate contaminated aquifers is crucial to predict the development of groundwater quality. Therefore, regression models were derived to estimate the measured cumulative denitrification of aquifer sediments after one year of incubation from initial denitrification rates and several sediment parameters, namely total sulphur, total organic carbon, extractable sulphate, extractable dissolved organic carbon, hot water soluble organic carbon and potassium permanganate labile organic carbon. For this purpose, aquifer material from two sandy Pleistocene aquifers in Northern Germany was incubated under anaerobic conditions in the laboratory using the ^{15}N tracer technique. The measured amount of denitrification ranged from 0.19 to 56.2 mg N kg⁻¹ yr⁻¹. The laboratory incubations exhibited high differences between non-sulphidic and sulphidic aquifer material in both aquifers with respect to all investigated sediment parameters. Denitrification rates and the estimated lifetime of denitrification were higher in the sulphidic samples. For these samples, the cumulative denitrification measured during one year of incubation ($D_{\text{cum}}(365)$) exhibited distinct linear regressions with the stock of reduced compounds in the investigated aquifer samples. $D_{\text{cum}}(365)$ was predictable from sediment variables within a range of uncertainty of 0.5 to 2 (calculated $D_{\text{cum}}(365)$ /measured $D_{\text{cum}}(365)$) for aquifer material with a $D_{\text{cum}}(365) > 20$ mg N kg⁻¹ yr⁻¹. Predictions were poor for samples with lower $D_{\text{cum}}(365)$, such as samples from the NO_3^- bearing groundwater zone, which includes the non-sulphidic samples, from the upper part of both aquifers where denitrification is not sufficient to protect groundwater from anthropogenic NO_3^- input. Calculation of $D_{\text{cum}}(365)$ from initial denitrification rates was only successful for samples from the NO_3^- -bearing zone, whereas a lag-phase of denitrification in samples from deeper zones of NO_3^- free groundwater caused imprecise predictions.

In this study, $D_{\text{cum}}(365)$ of two sandy Pleistocene aquifers was predictable using a combination of short-term incubations and analysis of sediment parameters. Moreover, the protective lifetime of denitrification sufficient to remove NO_3^- from groundwater in the investigated aquifers is limited, which demonstrates the need to minimise anthropogenic NO_3^- input.

3.1 Introduction

Denitrification, the microbial mediated reduction of nitrate (NO_3^-) and nitrite (NO_2^-) to the nitrogen gasses nitric oxide (NO), nitrous oxide (N_2O) and dinitrogen (N_2) is important to water quality and chemistry at landscape, regional and global scales (Groffman et al., 2006). Since 1860 the inputs of reactive nitrogen (Nr)² to terrestrial ecosystems have increased from 262 to 389 Tg N yr^{-1} (Galloway et al., 2004). The production of reactive nitrogen via the Haber–Bosch process contributed approximately with 100 Tg N yr^{-1} to this tremendous increase. In the European Union diffuse emissions of Nr range from 3 to > 30 kg N ha^{-1} yr^{-1} from which 51 to 85 % are derived from agriculture (Bouraoui et al., 2009). Diffuse Nr emissions from the agricultural sector are therefore the dominant source of NO_3^- fluxes to aquatic systems which leads to the questions, how rates of denitrification will respond to Nr loading (Seitzinger et al., 2006) and where and how long denitrification in aquifers can remediate the anthropogenic NO_3^- pollution of groundwater (Kölle et al., 1985).

NO_3^- pollution of groundwater has become a significant problem due to eutrophication of water bodies (Vitousek et al., 1997) and potential health risks from NO_3^- in drinking water. The latter causes increasing costs for keeping the standard for NO_3^- in drinking water (<50 mg l^{-1} , Drinking Water Directive 98/83/EC) (Dalton and Brand-Hardy, 2003; Defra, 2006). Therefore, knowledge about the denitrification capacity of aquifers is crucial. The term denitrification capacity of aquifers or aquifer material used in this study refers to the amount of NO_3^- that can be denitrified per m^3 aquifer or per kg of aquifer material until significant denitrification activity stops because of exhaustion of electron donors.

Denitrification in groundwater is mainly depending on the amount and microbial availability of reduced compounds in the aquifers, capable to support denitrification and is of a high spatial variability, ranging from 0 to 100 % of the NO_3^- input (Seitzinger et al., 2006). The main constituents of reduced compounds acting as electron donors during denitrification are organic carbon (organotrophic denitrification pathway), reduced iron and reduced sulphur compounds (lithotrophic denitrification pathway). Iron sulphides are known to be an important electron donor for lithotrophic denitrification (Kölle et al., 1985), recently Korom et al. (2012) indicated that non-pyritic ferrous iron might play a more important role for

²The term reactive nitrogen is used in this work in accordance with Galloway et al. (2004) and includes all biologically or chemically active N compounds like reduced forms (e.g. NH_3 , NH_4^+), oxidized forms (e.g. NO_x , HNO_3 , N_2O , NO_3^-) and organic compounds (e.g. urea, amines, proteins...).

denitrification than considered up to now. They assume that ferrous iron from amphiboles contributed to denitrification with 2–43 % in a glaciofluvial shallow aquifer in North Dakota.

Denitrification in groundwater can be a very slow to fast process. Frind et al. (1990) reported that lithotrophic denitrification has a half-life of 1 to 2 yr in the deeper zone (5 to 10 m below soil surface) of the well investigated Fuhrberger Feld aquifer (FFA). Contrary to the high denitrification rates in deeper reduced parts of this aquifer (lithotrophic denitrification zone) Weymann et al. (2010) reported very low denitrification rates with values as low as $4 \mu\text{g N kg}^{-1} \text{ d}^{-1}$ in the surface near groundwater (organotrophic denitrification zone) of the same aquifer. Denitrification rates in the organotrophic zone were one to two orders of magnitude lower than in its deeper parts and altogether too low to remove NO_3^- from groundwater.

While there are numerous laboratory incubation studies evaluating denitrification rates of aquifer sediments, there are only few studies reporting the amount of denitrification measured over several months of incubation and/or the stock of reactive compounds capable to support denitrification in the investigated aquifer sediments (Kölle et al., 1985; Houben, 2000; Mehranfar, 2003; Weymann et al., 2010; Well et al., 2005). Even less investigations tried to develop stochastic models to estimate the measured denitrification from independent sediment variables (Konrad, 2007; Well et al., 2005). Mehranfar (2003) and Konrad (2007) estimated the availability of a given stock of reduced compounds within sediments during incubation experiments that lasted at least one year, showing that approximately 5 to 50 % of sulphides were available for denitrification during incubation. However, in both studies incubation time was insufficient for complete exhaustion of reductants within the experiments.

Since laboratory investigations of denitrification rates in aquifer material are time consuming and expensive, in situ measurements are helpful to increase knowledge about the spatial distribution of denitrification in aquifers. In situ denitrification rates can be derived from concentration gradients (Tesoriero and Puckett, 2011), in situ mesocosms (Korom et al., 2012) and from push-pull type ^{15}N tracer tests (Addy et al., 2002; Well and Myrold, 1999, 2002). Well et al. (Well et al., 2003) compared in situ and laboratory measurements of denitrification rates in water saturated hydromorphic soils and showed that both methods were over all in good agreement. Konrad (2007) proposed to estimate long-term denitrification capacity of aquifers from in situ push-pull tests as an alternative to costly drilling of aquifer samples with subsequent incubations. A good correlation between in situ denitrification rates and the cumulative amount of denitrification during incubation based on a small number of

comparisons was reported (Konrad, 2007), but the data set was too small to derive robust transfer functions.

Since the oxidation of reduced compounds in aquifers is an irreversible process, the question arises, how fast ongoing NO_3^- input will exhaust denitrification capacity of aquifers and to which extent this may lead to increasing NO_3^- concentrations. Two studies attempted to answer this. Kölle et al. (1985) calculated a maximum lifetime of lithotrophic denitrification in the FFA of about 1000 yr by a mass balance approach. Houben (2000) modelled the depth shift of the denitrification front in a sandy aquifer in Western Germany giving a progress rate of approximately 0.03 m yr^{-1} .

Overall, there is very limited information on long-term denitrification capacity of aquifer sediments because there are virtually no direct measurements. Because of this, predictions based on stochastic models are hampered by the lack of suitable data sets. Therefore, knowledge about the spatial distribution of denitrification rates is highly demanded (Rivett et al., 2008).

To progress knowledge in this field, established methods were combined with the testing of new concepts. The goals of this study are (a) to get estimates of the exhaustibility of denitrification capacity in aquifers from incubation experiments, (b) to investigate controlling factors and derive predictive models and (c) to check if laboratory ex situ denitrification rates can be derived from actual in situ rate measurements using push-pull tests at groundwater monitoring wells. Here an approach is presented to tackle (a) and (b). In a second study results to (c) will be presented. The specific objectives are (i) to measure denitrification during one year anaerobic incubation of sediment material from two aquifers; (ii) to estimate the total stock of reactive compounds in these samples and their availability for denitrification as well as influencing sediment parameters; (iii) to develop regression models to estimate the measured cumulative denitrification from initial denitrification rates and from sediment properties; and (iv) to estimate the minimal lifetime of denitrification in the investigated aquifer material.

3.2 Materials and methods

3.2.1 Study sites

Aquifer material was collected in the Fuhrberger Feld aquifer (FFA) and the Großenkneten aquifer (GKA), two drinking water catchment areas in Northern Germany (Fig. S3.1 in the Supplement). The FFA is situated about 30 km NE of the city of Hannover and the GKA about 30 km SW of the city of Bremen. Both aquifers consist of carbonate free, Quaternary sands and the GKA additionally of carbonate free marine sands (Pliocene). The thickness of the FFA and GKA is 20 to 40 m and 60 to 100 m, respectively. Both aquifers are unconfined and contain unevenly distributed amounts of microbial available sulphides and organic carbon. Intense agricultural land use leads to considerable nitrate inputs to the groundwater of both aquifers (Böttcher et al., 1990; van Berk et al., 2005). Groundwater recharge is 250 mm yr⁻¹ in the FFA (Wessolek et al., 1985) and 200 to 300 mm yr⁻¹ in the GKA (Schuchert, 2007).

Evidence for intense ongoing denitrification within the FFA is given by nitrate and redox gradients (Böttcher et al., 1992) as well as excess-N₂ measurements (Weymann et al., 2008). The FFA can be divided into two hydro-geochemical zones: the zone of organotrophic denitrification near the groundwater surface with organic carbon (C_{org}) as electron donor and a deeper zone of predominantly lithotrophic denitrification with pyrite as electron donor (Böttcher et al., 1991; Böttcher et al., 1992). Detailed information about the FFA is given by Strebel et al. (1992), Frind et al. (1990) and von der Heide et al. (2008). Extended zones with oxidizing and reducing conditions in the groundwater are also evident in the GKA (van Berk et al., 2005) but their distribution within this aquifer is more complex as in the FFA. The geological structure of the GKA is described in Howar (2005) and Wirth (1990). Intense denitrification is known to occur in the zone of reduced groundwater (van Berk et al., 2005). This was proven by excess-N₂ measurements at monitoring wells within the GKA (Well et al., 2012). But there are no studies on the type of denitrification in this aquifer.

3.2.2 Sampling procedures

The aquifer material used in this study originated from depths between 3–18 m and 8–68 m below soil surface of the FFA and GKA, respectively.

The aquifer material from the FFA was drilled with a hollow stem auger (OD of 205 mm, ID of 106 mm, WELLCODRILL, WD 500, Beedenbostel, Germany) and the core samples were immediately transferred into 2 l glass bottles. The remaining headspace within these bottles was filled with deionised water until it overflowed. Then the bottles were sealed airtight with rubber covered steel lids. Aquifer material from the GKA was drilled by percussion core drilling. The aquifer samples were collected with a double core barrel with an inner PVC liner (OD 95.8 mm, ID 63.4 mm, HWL (HQ) Wireline core barrel, COMPDRILL Bohrausrüstungen GmbH, Untereisesheim, Germany). After sampling, the liner was removed from the core barrel and sealed airtight at both ends with PVC lids. In the laboratory, the aquifer material from the PVC liner was transferred into glass bottles as described above. The aquifer samples were stored at 10 °C (approximately the mean groundwater temperature in both aquifers) in the dark. After sampling of aquifer material, groundwater monitoring wells and multilevel wells were installed in the borings. FFA aquifer samples from depths between 2 to 5 m below soil surface were sampled in April and Mai 2008 and deeper samples in the FFA in June 2007. GKA samples were drilled in December 2008. GKA samples and samples from depths up to 5 m in the FFA were incubated within 4 week after sampling. Deeper FFA samples were incubated 3 to 6 months after sampling.

3.2.3 Laboratory incubations

3.2.3.1 Standard treatment

Anaerobic incubations were conducted to measure the cumulative denitrification and the denitrification rates of the investigated aquifer material as described by Weymann et al. (2010). In total, 41 samples from both aquifers collected between 2 to 68 m below soil surface were incubated. From each sample, 3 to 4 replicates of 300 g fresh aquifer material were filled in 1125 ml transfusion bottles. ^{15}N labelled KNO_3 with 60 atom % ^{15}N (Chemotrade Chemiehandels-gesellschaft mbH, Düsseldorf, Germany) was dissolved in deionised water (200 mg ^{15}N labelled $\text{NO}_3^- \text{ l}^{-1}$). The natural nitrate concentrations in both aquifers are in the

range of 0 to 250 mg NO₃⁻ Γ⁻¹ (Well et al., 2012) (see also Sect. 3.4.5.2). 300 ml of this solution was added to each transfusion bottle and then the bottles were sealed airtight with natural rubber septa of 2 cm thickness and aluminium screw caps. These septa were used because they kept good sealing after multiple needle penetrations from repeated sampling. The mixture of the labelled KNO₃ solution and pore water of the aquifer samples is referred to as batch solution below. The headspace of each transfusion bottle was evacuated for 5 min and then flushed with pure N₂. This procedure was repeated 5 times to ensure anaerobic conditions within the bottles. Samples were incubated for one year in the dark at 10 °C.

The water content of the investigated aquifer material was determined gravimetrically using parallels of the incubated material. The dry weight, the volume of the incubated sediment (assuming a particle density of 2.65 g cm⁻³), the liquid volume and the headspace volume were calculated for each replicate independently. Samples of the headspace gas and the supernatant batch solution were taken at days 1, 2, 7, 84, 168 and 365 of incubation. The transfusion bottles were shaken on a horizontal shaker at 10 °C for 3 h prior to sampling to equilibrate headspace gasses with the dissolved gasses in the batch solutions. For the gas sampling, 13 ml headspace gas were extracted with a syringe and transferred to evacuated 12 ml sample vials (Exetainer® Labco, High Wycombe, UK). By doing so, the gas sample was slightly pressurised within the vial. Subsequently, 20 ml of the supernatant solution were sampled with a syringe and transferred into a PE bottle and frozen until analysis. To maintain atmospheric pressure within the transfusion bottles, 13 ml pure N₂ und 20 ml of O₂ free ¹⁵N labelled KNO₃ solution were re-injected into every transfusion bottle after sampling. The ¹⁵N-labelled KNO₃ solution was stored in a glass bottle, which was sealed air tight with a rubber stopper. Prior to re-injection of the KNO₃ solution into the transfusion bottles, the solution was purged with pure N₂ through a steel capillary for 1 h to remove dissolved O₂. The headspace in the glass bottle was sampled to check O₂ contamination and was always found to be in the range of O₂ signals of blank samples (N₂ injected into evacuated 12 ml sample vials).

3.2.3.2 Intensive treatment

A modified incubation treatment was conducted for aquifer samples with high content of C_{org} and sulphides, to increase the proportion of reduced compounds that are oxidized during incubation. 30 g aquifer material and 270 g quartz sand were filled in transfusion bottles and prepared for anaerobic incubations as described above for the “standard” treatment. The

quartz sand was added to increase the permeability of fine grained parts of the incubated aquifer material. This was done to increase the reactive surface area, i.e. the contact area between tracer solution and reduced compounds. The incubation temperature was 20 °C and samples were permanently homogenized on a rotary shaker in the dark. (Well et al., (2003) reported that during anaerobic incubations a raise of incubation temperatures from 9 to 25 °C resulted in 1.4 to 3.8 higher denitrification rates.) In total, nine aquifer samples were selected from the FFA and GKA and incubated in four replications. Additionally, four transfusion bottles were filled only with the pure quartz sand to check for possible denitrification activity of this material, which was found to be negligible.

3.2.4 Analytical techniques

The particle sizes distribution of the aquifer sediments was determined by wet sieving. The silt and clay fractions were determined by sedimentation following the Atterberg method (Schlichting et al., 1995). Contents of total sulphur (total-S), total nitrogen (total-N) and total organic carbon (C_{org}) of the carbonate free aquifer sediments were analysed with an elemental analyser (vario EL III, ELEMENTAR ANALYSESYSTEME, Hanau, Germany).

For hot water soluble organic carbon (C_{hws}) 10 g aquifer material and 50 ml deionised water were boiled for 1 h and then filtrated (Behm, 1988). Cold water extracts were used for the determination of extractable dissolved organic carbon (DOC_{extr}) and extractable sulphate (SO_4^{2-} extr). C_{hws} and DOC_{extr} in the extracts were measured with a total carbon analyser (TOC 5050, Shimadzu, Kyoto, Japan). To measure the fraction of $KMnO_4$ labile organic carbon (C_1) 15 g aquifer material and 25 ml 0.06 M $KMnO_4$ solution were shaken on a rotating shaker for 24 h and then centrifuged by 865 RCF (Konrad, 2007). 1 ml of the supernatant was sampled and diluted in 100 ml deionised water. C_1 was then determined as the decolourization of the $KMnO_4$ solution by means of a photometer (SPECORD 40, Analytic Jena, Jena, Germany). NO_3^- , NO_2^- and NH_4^+ concentrations were determined photometrically in a continuous flow analyser (Skalar, Erkelenz, Germany). For the determination of SO_4^{2-} concentrations in the batch solutions and SO_4^{2-} extracts, a defined amount of $BaCl_2$ solution was added in excess to the samples and SO_4^{2-} precipitated as $BaSO_4$. The original SO_4^{2-} concentration was then analysed by potentiometric back-titration of the excess Ba^{2+} -ions remaining in the solution using EDTA as titrant. Possible interfering metal cations were removed from the samples prior to this analysis by cation exchange.

The major cations in the batch solution (Na^+ , K^+ , Ca^{2+} , Mg^{2+} , Mn^{4+} , Fe^{3+} and Al^{3+}) were measured by means of Inductively Coupled Plasma-Atomic Emission Spectrometer (ICP-AES, Spectro Analytical Instruments, Kleve, Germany) after stabilizing an aliquot of the batch solution samples with 10 % HNO_3 .

N_2O was measured using a gas chromatograph (Fisons GC8000, Milan, Italy, equipped with an electronic capture detector as described previously by Weymann et al. (2009). O_2 was analysed with a gas chromatograph equipped with a thermal conductivity detector (Fractovap 400, CARLO ERBA, Milan, Italy) as described in Weymann et al. (2010).

The ^{15}N analysis of denitrification derived ($\text{N}_2+\text{N}_2\text{O}$) was carried out by a gas chromatograph (GC) coupled to an isotope ratio mass spectrometer (IRMS) at the Centre for Stable Isotope Research and Analysis in Göttingen, Germany within two weeks after sampling, following the method described in Well et al. (2003). The concentrations of ^{15}N labelled denitrification derived N_2 and N_2O in the gas samples were calculated in the same way as described in detail by Well and Myrold (1999) and Well et al. (2003). A brief explanation, of how total ($\text{N}_2+\text{N}_2\text{O}$) production was determined, is given in the Supplement.

From the obtained molar concentrations of denitrification derived N_2 and N_2O in the gas samples, which are equal to the molar concentrations in the headspace of the transfusion bottles, the dissolved N_2 and N_2O concentrations in the batch solutions were calculated. This was done according to Henry's law using the solubilities for N_2 and N_2O at 10 °C given by Weiss (1970) and Weiss and Price (1980). The detection limit of ^{15}N analysis was calculated as the minimum amount of ^{15}N labelled denitrification derived ($\text{N}_2+\text{N}_2\text{O}$) mixed with the given background of headspace N_2 of natural ^{15}N abundance necessary to increase the measured $^{29}\text{N}_2/^{28}\text{N}_2$ ratio to fulfil the following equation:

$$r_{sa} - r_{st} \geq 3 \times sdr_{st}, \quad (3.1)$$

where r_{sa} and r_{st} are the $^{29}\text{N}_2/^{28}\text{N}_2$ ratios in sample and standard, respectively and sdr_{st} is the standard deviation of repeated r_{st} measurements. The r_{st} values were analysed with IRMS by measuring repeated air samples. Under the experimental conditions, the detection limit for the amount of denitrification derived ^{15}N labelled ($\text{N}_2+\text{N}_2\text{O}$) was 15 to 25 $\mu\text{g N kg}^{-1}$.

Dissolved oxygen, pH and electrical conductivity (pH/Oxi 340i and pH/Cond 340i, WTW Wissenschaftlich-Technische Werkstätten GmbH, Weilheim, Germany) were measured in the groundwater from the installed groundwater monitoring wells.

3.2.5 Calculated parameters

The following parameters describing the denitrification dynamics during anaerobic incubation were calculated from the measurements described above. Denitrification rates $D_r(X)$ were calculated as the cumulative amount of denitrification products formed until the day of sampling divided by the duration of incubation until sampling ($\text{mg N kg}^{-1} \text{ d}^{-1}$), with X as the day of sampling. Denitrification rates were calculated for day 7, 84, 168 and 365 of incubation, $D_r(7)$, $D_r(84)$, $D_r(168)$ and $D_r(365)$, respectively. $D_r(7)$ is also referred to as the initial denitrification rate. $D_{\text{cum}}(365)$ is the cumulative amount of denitrification products per kg dry weight of incubated aquifer material at the end of one year of incubation ($\text{mg N kg}^{-1} \text{ yr}^{-1}$). $D_r(365)$ multiplied by 365 d equals $D_{\text{cum}}(365)$, so below is only referred to $D_{\text{cum}}(365)$. The sulphate formation capacity (SFC) (Kölle et al., 1985) was derived from the measured increase of SO_4^{2-} concentrations in the batch solution between the first sampling (day 1) and the end of incubation (day 365). To correct the SFC value for dissolution of possible SO_4^{2-} -minerals and/or SO_4^{2-} from the pore water of the incubated aquifer material the SO_4^{2-} concentrations in the batch solution after two days of incubation were subtracted from the final SO_4^{2-} concentration after one year. For the aquifer samples from the NO_3^- free zone of both aquifers and for non-sulphidic samples these initial SO_4^{2-} -S concentrations accounted for 25,4 % and 90 % of the final SO_4^{2-} -S concentrations in the batch solutions, respectively. These initial SO_4^{2-} -S concentrations originated supposedly mainly from pore water SO_4^{2-} . The SO_4^{2-} concentrations of the groundwater at the origin of the samples reached 5 to 60 mg S l^{-1} in both aquifers (data not shown).

The stock of reactive compounds (SRC) was estimated from total-S and C_{org} data. For simplicity it was assumed that C_{org} corresponds to an organic substance with the formula CH_2O (Korom, 1991; Trudell et al., 1986) and that all sulphur was in the form of pyrite (FeS_2) (see Sect. 3.4.3.1). C_{org} and total-S values were converted into N equivalents (mg N kg^{-1}) according to their potential ability to reduce NO_3^- to N_2 . C_{org} was converted according to Eq. (4) (electron donor organic C) given in Korom (1991) and total-S values (in form of pyrite) according to Eqs. (5) (electron donor S^-) and (6) (electron donor Fe^{2+}) given in Kölle et al. (1983). The fraction of SRC which is available for denitrification during incubation (aF_{SRC}) (%) was calculated as the ratio of the measured $D_{\text{cum}}(365)$ to the SRC of the incubated aquifer material. The share of total-S values contributing to the aF_{SRC} was calculated from the measured SFC during incubation. The remaining portion of the aF_{SRC} was assigned to microbial available C_{org} compounds in the aquifer samples.

The estimated minimum lifetime of denitrification (emLoD) was calculated as follows:

$$emLoD = \frac{A_{dw} \times (SRC \times aF_{SRC} \times 0.01)}{\text{nitrate input}} [\text{yr m}^{-1}], \quad (3.2)$$

where the dry weight of 1 m³ aquifer material (A_{dw}) (kg m⁻³) is multiplied with the fraction of its SRC (mg N kg⁻¹) content available for denitrification during one year of incubation. This value is then divided by the nitrate input (mg NO₃⁻-N m⁻² yr⁻¹) giving the estimated minimal lifetime of denitrification for 1 m³ of aquifer material. To calculate A_{dw} a porosity of 35 % and an average density of the solid phase of 2.65 g cm⁻³ of the aquifer material was assumed, giving an A_{dw} of 1722.5 kg m⁻³. Furthermore, an average aF_{SRC} of 5 % was used to calculate emLoD (see Sect. 3.4.4). The NO₃⁻ input to the aquifer coming with the groundwater recharge was assumed from literature data on N leaching. Köhler et al. (2006) measured mean NO₃⁻ concentrations in the groundwater recharge under arable sandy soils between 40 and 200 mg NO₃⁻ Γ⁻¹. For a conservative estimate of emLoD the maximum value of 200 mg NO₃⁻ Γ⁻¹ was used. This value gives a nitrate input of 11.3 g NO₃⁻-N m⁻² yr⁻¹ (= 6.6 mg NO₃⁻-N kg⁻¹ yr⁻¹) to the aquifer under condition of a groundwater recharge rate of about 250 mm yr⁻¹ as reported for the GKA and FFA by Schuchert (2007) and Renger et al. (1986), respectively.

3.2.6 Statistical analysis and modelling

Statistical analysis and modelling was performed with Win-STAT for MS Excel Version 2000.1 (R. Fitch Software, Bad Krozingen, Germany). Differences between partial data sets were considered significant at the $P < 0.05$ level (Kruskal–Wallis test (kw), with the null hypothesis that both partial data sets belong to the same population). Spearman rank correlations (r_s) were used to determine significant correlations between sediment parameters and $D_{cum}(365)$. Simple and multiple linear regression analysis were performed to evaluate quantitative relations between $D_{cum}(365)$ and the sediment parameters and to predict $D_{cum}(365)$ from these parameters. Simple linear regressions and multiple linear regressions are in the following referred to as simple regression and multiple regressions. Normal distribution of the measured parameters within the different data sets was tested with the Kolmogorov–Smirnov Test, normal distribution was assumed at the $P > 0.05$ level, with the null hypothesis that the tested parameter was normal distributed. The uniform distribution of residuals of regressions were checked with scatter plots of residuals vs. independent variables

of the respective regression analysis. This was done to ensure homoscedasticity during regression analysis, to ensure that the least-squares method yielded best linear estimators for the modelled parameter.

Experimental data (x) was converted into Box–Cox transformed data ($f^{\text{B-C}}(x)$) according to Eq. (3.3) using different lambda coefficients (λ) to achieve a normal-like distribution of experimental data within the different data sets.

$$f^{\text{B-C}}(x) = \frac{x^\lambda - 1}{\lambda} \quad (3.3)$$

Box–Cox transformations were conducted with the statistic software STATISTICA 8 (StatSoft, Tulsa, USA). To use the regression functions to model $D_{\text{cum}}(365)$, input data have to be transformed according to Eq. (3.3) with the lambda coefficients given in Table S3.5 (see the Supplement).

3.2.7 Basic assumption and methodical limitations of the presented approach

The underlying assumptions of the presented study are that there are quantitative relations between the measured cumulative denitrification during one year of incubation ($D_{\text{cum}}(365)$) and the stock of reduced compounds (SRC) of aquifer material and between the SRC and the denitrification capacity.

The basic limitations of the presented approach are (i) in situ processes are estimated from ex situ incubations, (ii) one year incubations are used for predicting the lifetime of denitrification in the investigated aquifers over several decades, and (iii) ^{15}N labelling of NO_3^- was used because denitrification was assumed to be the dominant process of NO_3^- reduction, in the two aquifers. The limitations of the presented investigation are further discussed in Sect. 3.4.4 and 4.5. This work focuses on organotrophic and sulphide depended denitrification in both aquifers, this seems appropriate taking into account previous investigations (Kölle et al., 1983; Kölle et al., 1985; Hansen and van Berk, 2004) and the evaluation of Fe, Mn and NH_4^+ concentrations in the batch solutions during incubation and in situ in both aquifers (see the Supplement: other possible electron donors).

3.3 Results

3.3.1 Incubations and independent variables: grouping of aquifer material

For data analysis, the aquifer material was grouped by locality (FFA and GKA aquifer material). Moreover, chemical sediment properties (non-sulphidic and sulphidic samples) and groundwater redox state at the sample origin (samples from NO_3^- free and NO_3^- bearing groundwater zone of both aquifers were assigned to NO_3^- -free and NO_3^- -bearing sub-groups, respectively) were taken into account for further differentiation. $0.4 \text{ mg NO}_3^- \text{-N } \Gamma^{-1}$ was the lowest measured NO_3^- concentration above the limit of detection of $0.2 \text{ mg NO}_3^- \text{-N } \Gamma^{-1}$. Therefore, $0.4 \text{ mg NO}_3^- \text{-N } \Gamma^{-1}$ was the lowest concentration to be considered nitrate bearing in this study. Finally, a transition zone sub-group was defined for samples from the region where sulphides were present, but groundwater still contained NO_3^- . Sulphidic and non-sulphidic samples are distinguished using the sulphate formation capacity (SFC ($\text{mg S kg}^{-1} \text{ yr}^{-1}$)) of the incubated aquifer material. Samples with $\text{SFC} > 1 \text{ mg SO}_4^{2-} \text{-S kg}^{-1} \text{ yr}^{-1}$ were assigned sulphidic. The groundwater at the origin of sulphidic samples had always dissolved O_2 concentrations below $1.5 \text{ mg O}_2 \Gamma^{-1}$ (see Sect. 3.4.1). The groundwater at the origin of NO_3^- -free samples was completely anoxic in both investigated aquifers. In the data set, subgroups of non-sulphidic and NO_3^- -bearing as well as sulphidic and NO_3^- -free samples were almost identical (Tables S3.1 and S3.2 in the Supplement). Moreover, statistically significant differences were only found in $D_{\text{cum}}(365)$ with higher values for NO_3^- -bearing in comparison to non-sulphidic samples. NO_3^- -free and sulphidic samples differed significantly only in their total-S values, with higher total-S contents in NO_3^- -free samples. Therefore, the partial data sets of NO_3^- -free and NO_3^- -bearing samples were only discussed when significant differences to subgroups according to sediment properties occurred.

3.3.2 Time course of denitrification products, denitrification rates and cumulative denitrification at the end of incubations

The denitrification rates of non-sulphidic and NO_3^- -bearing samples were significantly lower than those of sulphidic and NO_3^- -free samples (kw: $P < 0.01$) (Table 3.2 and Fig. 3.1). Almost all of the transition zone samples exhibited a clear flattening of the slopes of denitrification derived ($\text{N}_2 + \text{N}_2\text{O}$) concentration curves, i.e. showed decreasing denitrification

rates over time (Fig. 3.1b). Non-sulphidic samples showed a relative constant production of (N_2+N_2O) (Fig. 3.1a), but denitrification rates were highly significant (kw: $P < 0.001$), lower compared to sulphidic samples (Table 3.2, Fig. 3.1).

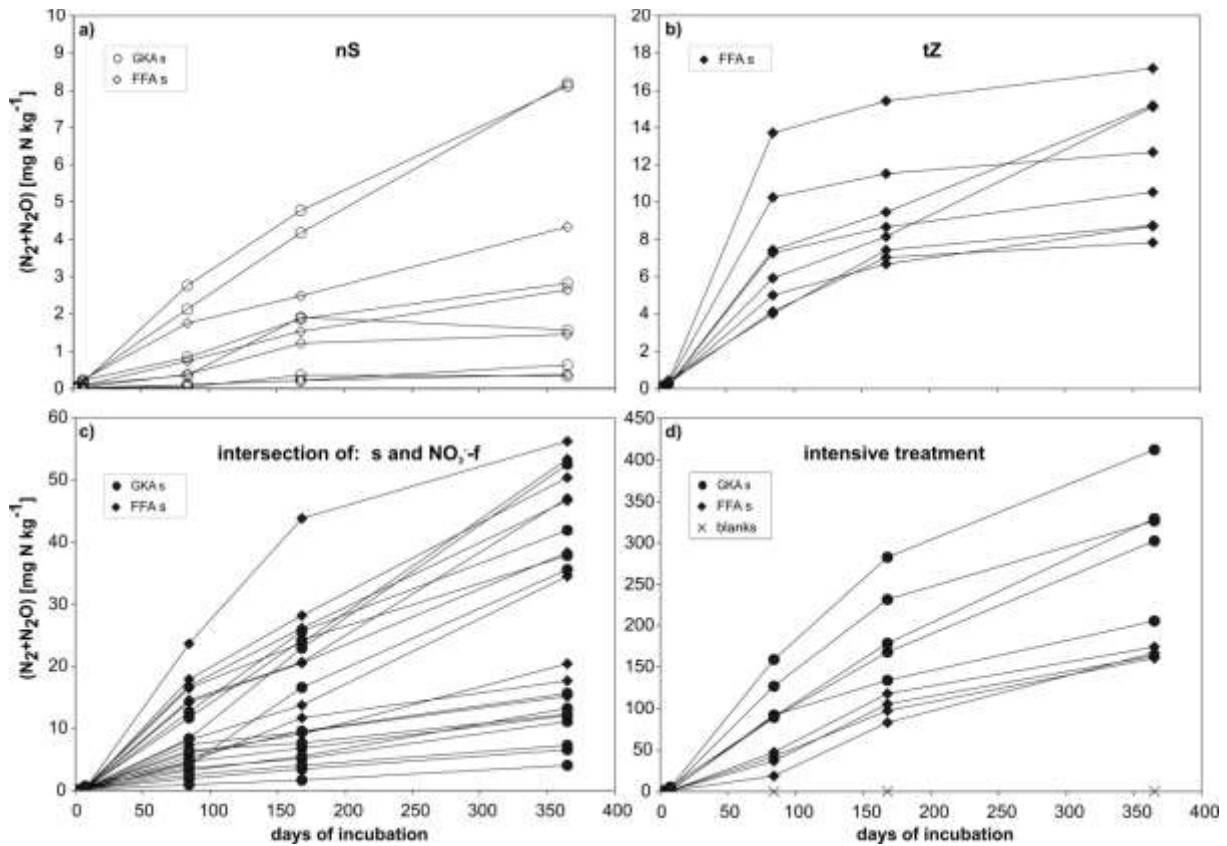


Fig. 3.1: Time courses of denitrification products (N_2+N_2O) (average of 3 to 4 replicas per depth) from different groups of aquifer material during standard (a–c) and intensive treatment (d). Open and closed symbols denote non-sulphidic and sulphidic aquifer material, respectively. Circles and diamonds represent GKA and FFA material, respectively. Crosses indicate blanks of intensive treatment. nS, S, tZ and NO_3^- -f indicate non-sulphidic and sulphidic samples, transition zone material and NO_3^- -free samples, respectively. Error bars were omitted for clarity, but were small in comparison to measured concentrations of denitrification derived (N_2+N_2O).

Both FFA and GKA aquifer material had nearly the same median initial denitrification rates ($D_r(7)$) with values of 33.8 and $31.2\ \mu g\ N\ kg^{-1}\ d^{-1}$, respectively, whereas the maximal $D_r(7)$ of GKA material was over 50 % higher compared to the FFA material (Table 3.2). At the end of incubation, samples from the FFA and GKA had a comparable range of $D_{cum}(365)$ (up to $56\ mg\ N\ kg^{-1}\ yr^{-1}$). Sulphidic samples had significantly higher median $D_r(7)$ and $D_{cum}(365)$ ($35.6\ \mu g\ N\ kg^{-1}\ d^{-1}$ and $15.6\ mg\ N\ kg^{-1}\ yr^{-1}$, respectively) than non-sulphidic samples

(11.5 $\mu\text{g N kg}^{-1} \text{d}^{-1}$ and 1.6 $\text{mg N kg}^{-1} \text{yr}^{-1}$, respectively) (kw: $P < 0.001$) (Table 3.2). Non-sulphidic samples exhibited higher initial denitrification rates ($D_r(7)$) than average denitrification rates ($D_r(365)$), whereas this was vice versa for sulphidic samples. Transition zone samples were similar in $D_r(7)$ compared to sulphidic material, but $D_{\text{cum}}(365)$ was about 25 % lower.

After the intensive treatment incubated aquifer samples were 1 to 17 times higher in $D_r(7)$ (data not shown) and between 3.6 to 17 times higher in $D_{\text{cum}}(365)$ compared to the standard treatment (Table S3.2 in the Supplement, multiplying the aF_{SRC} from intensive treatment by the SRC and 0.01 gives $D_{\text{cum}}(365)$ of intensive treatment), but the intensive treatment did not lead to a complete exhaustion of the stock of reactive compounds during incubations, i.e. samples still exhibited denitrification rates at the end of incubation (Fig. 3.1d).

3.3.3 Sediment parameters

C_{org} exhibited large ranges of similar magnitude in both aquifers (203–5955 and 76–8972 mg C kg^{-1} in the FFA and GKA aquifer samples, respectively) (Table 3.1). The same applied for total-S, (29–603 and 36–989 mg S kg^{-1}) and $\text{SO}_4^{2-}\text{extr}$ (0 to 25 and from 0.3 to 20 mg S kg^{-1}). GKA samples contained significantly lower median DOC_{extr} values than FFA material (9.2 and 6.1 mg C kg^{-1} , respectively). $\text{SO}_4^{2-}\text{extr}$ and DOC_{extr} decreased with depth in the FFA (r_s : $R = -0.83$ and $R = -0.86$, respectively, $P < 0.001$) and in the GKA (r_s : $R = -0.54$ and $R = -0.59$, respectively, $P < 0.05$). The ranges of C_{hws} were comparable for FFA and GKA material (Table 3.1). C_1 values of FFA and GKA samples were not statistically different from each other, but maximum values in GKA samples were almost 3 times higher than in FFA material (Table 3.1). In median, 17 % and 26 % of the C_{org} in the GKA and FFA aquifer material, respectively, belonged to the fraction of C_1 . Statistically significant differences (kw: $P < 0.05$) occurred between the groups of non-sulphidic and sulphidic aquifer material with a ratio of C_1 to C_{org} by 0.17 and 0.24, respectively. Similar differences and ratios applied for the groups of NO_3^- -bearing and NO_3^- -free samples (Table 3.1). Except for values of total-S and DOC_{extr} , the investigated sediment parameters exhibited no significant differences between FFA and GKA aquifer material (Fig. S3.2 in the Supplement). All sediment variables showed significant differences (kw: $P < 0.05$) between the 3 groups of non-sulphidic, sulphidic and transition zone samples (Fig. S3.2 in the Supplement). On average, transition zone samples had lower ranges in all sediment parameters than sulphidic material except in C_{hws} and DOC_{extr} . Non-sulphidic samples exhibited lower average

concentrations in the sediment parameters compared to transition zone samples, except for SO_4^{2-} _{extr} and DOC_{extr} for which the opposite was the case (Table 3.1, Fig. S3.2 in the Supplement).

Table 3.1: Sediment parameters of the incubated aquifer material (medians with ranges in brackets).

Data set	SO_4^{2-} _{extr} ^a	DOC_{extr} ^b	C_{hws} ^c	C_1 ^d	C_{org} ^e	Total-S ^f	C_1/C_{org}
	mg S kg ⁻¹		mg C kg ⁻¹			mg S kg ⁻¹	
FFA	5.36 (0-25.2)	9.21 (5.7-11.6)	29.4 (0.1-42.6)	172.5 (2.7-887)	715.8 (203-5955)	72.3 (28.8-603)	0.165 (0.011-0.42)
GKA	10.52 (0.3-20.2)	6.11 (4.7-9.9)	29.1 (14.9-59)	239.8 (0.9-2505)	802.7 (75.9-8972)	509.6 (36.2-989)	0.264 (0.012-0.60)
non-sulphidic	14.46 (0.3-25.3)	8.96 (5.2-11.6)	21.6 (14.9-59)	91.2 (0.9-260)	236.7 (75.9-1047)	46.1 (28.8-196)	0.165 (0.011-0.42)
sulphidic	4.9 (0-20.2)	6.11 (4.7-10.8)	30.3 (0-42.6)	294.4 (38-2505)	1114.0 (232-8972)	463.7 (44.8-988.8)	0.239 (0.058-0.60)
transition zone	3.55 (0-12.8)	8.21 (6.2-10.8)	32.0 (22-42.5)	138.8 (82.2-463)	664.7 (311-1625)	53.2 (47.1-175.7)	0.226 (0.058-0.36)
NO_3^- -bearing	11.05 (0-25.3)	9.21 (6.2-11.6)	27.6 (14.9-44)	116.9 (0.9-463)	538.3 (75.9-1625)	49.3 (28.8-175.7)	0.191 (0.011-0.42)
NO_3^- -free	4.91 (0.3-20.2)	5.69 (4.7-9.9)	31.1 (0-59)	377.4 (37-2505)	1161.5 (232-8972)	510.4 (44.8-988.8)	0.267 (0.092-0.60)

^a Extractable sulphate-S;

^b extractable dissolved organic carbon;

^c hot-water soluble organic carbon;

^d KMnO_4 labile organic carbon;

^e total organic carbon;

^f total sulphur.

Table 3.2: Initial denitrification rates, cumulative denitrification during one year, stock of reduced compounds, sulphate formation capacity and estimated minimal lifetime of denitrification (medians with ranges in brackets).

Data set	$D_r(7)^a$	$D_{cum}(365)^b$	SRC ^c	SRC _C ^d	SRC _S ^e	aF _{SRC} ^f	SFC ^g	emLoD ^h
	$\mu\text{g N kg}^{-1} \text{d}^{-1}$	$\text{mg N kg}^{-1} \text{yr}^{-1}$	g N kg^{-1}			$\% \text{ yr}^{-1}$	$\text{mg S kg}^{-1} \text{yr}^{-1}$	yr m^{-1}
FFA	33.8 (1.3-69.9)	15.1 (0.19-56.2)	0.70 (0.2-6.0)	0.67 (0.2-5.6)	50.50 (0.0-0.4)	1.5 (0.1-5.4)	5.3 (0-39.4)	5.3 (1.6-45)
GKA	31.16 (0.7-109)	9.6 (0.34-52.5)	1.10 (0.1-8.9)	0.75 (0.1-8.4)	0.36 (0.0-0.7)	0.8 (0.4-1.7)	4.2 (0-30.0)	8.3 (0.7-67)
non-sulphidic	11.5 (0.7-35.3)	1.6 (0.19-8.2)	0.24 (0.1-1.0)	0.22 (0.1-1.0)	0.03 (0.0-0.1)	0.47 (0.1-1.7)	0.3 (0-1.3)	1.8 (0.7-8)
sulphidic	35.6 (12.3-109)	15.6 (4.09-56.2)	1.3 (0.3-8.9)	1.04 (0.2-8.4)	0.32 (0.0-0.7)	1.16 (0.4-5.4)	8.1 (1.2-39)	9.7 (2.4-67)
transitions Zone	36.48 (20.3-61)	11.6 (7.8-17.2)	0.67 (0.3-1.6)	0.62 (0.3-1.5)	0.04 (0.0-0.1)	1.65 (0.6-4.6)	2.9 (1.5-7)	5.05 (2.5-12)
NO ₃ ⁻ -bearing	21.05 (0.7-61)	4.3 (0.19-17.2)	0.54 (0.1-1.6)	0.50 (0.1-1.5)	0.035 (0.0-0.1)	0.80 (0.1-4.6)	1.0 (0-6.9)	4.1 (0.7-12)
NO ₃ ⁻ -free	33.89 (12.3-109)	20.2 (4.1-56.2)	1.44 (0.3-8.9)	1.08 (0.2-8.4)	0.36 (0.0-0.7)	0.94 (0.4-5.4)	9.4 (0.7-39)	10.80 (2.4-67)

^a Initial denitrification rate after day 7;

^b cumulative denitrification during one year;

^c stock of reactive compounds;

^d concentration of reduced compounds derived from measured C_{org} ;

^e concentration of reduced compounds derived from total-S values;

^f fraction of SRC available for denitrification during one year of incubation;

^g sulphate formation capacity;

^h estimated minimal lifetime of denitrification.

3.3.4 The stock of reactive compounds and its availability for denitrification during incubation

3.3.4.1 Standard treatment

The stock of reduced compounds (SRC) of FFA and GKA aquifer material did not differ significantly from each other (0.22–6.0 and 0.97–8.9 g N kg⁻¹, respectively) (Table 3.2 and Fig. 3.2a). In contrast, the median SRC of sulphidic aquifer material (1.3 g N kg⁻¹) was 2 and 5 times higher compared to the non-sulphidic (0.24 g N kg⁻¹) and transition zone material (0.67 g N kg⁻¹). The fraction of SRC available for denitrification during incubation (aF_{SRC}) in the FFA material ranged from 0.08 to 5.44 % and was significantly higher than the range of aF_{SRC} of GKA material (0.36 to 1.74 % aF_{SRC}) (Fig. 3.2b). Transition zone samples exhibited

the highest median aF_{SRC} values (1.65 %), followed by sulphidic (1.16 %) and non-sulphidic aquifer material with the lowest aF_{SRC} values (0.47 %). Statistical significant differences were only found between non-sulphidic samples and the previous two groups (Fig. 3.2b).

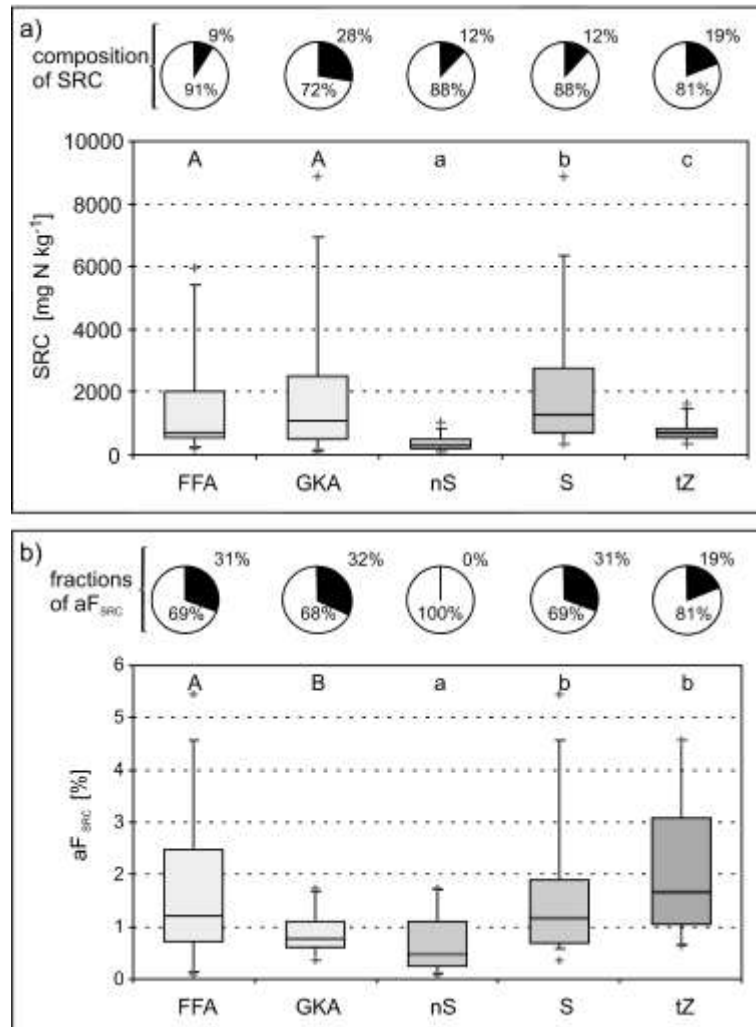


Fig. 3.2: FFA, GKA, nS, S and tZ indicate Fuhrberger Feld, Großenkneten, non-sulphidic, sulphidic and transition zone aquifer material, respectively. White circular segments represent fractions derived from C_{org} and black segments fractions derived from total-S values. Different uppercase letters above the box-plots indicate significant differences of SRC and sF_{SRC} values between FFA and GKA material, different small letters show significant differences between nS, S and tZ (Kruskal–Wallis Test, $P < 0.05$). (a) The stock of reduced compounds (SRC) and its composition in the various groups of aquifer material. The composition of SRC was calculated from C_{org} and total-S values (Sect. 3.2.5). (b) Fraction of SRC available for denitrification during incubation (aF_{SRC}). The aF_{SRC} and its composition was calculated as described in Sect. 3.2.5.

3.3.4.2 Intensive treatment

Since parallel samples for the intensive and standard treatments were used, the SRC was identical for both treatments. Also the intensive treatment was not able to exhaust the denitrification capacity of the incubated aquifer material during incubation (Fig. 3.1). The aF_{SRC} derived from intensive incubations was 3.6 to 17 times higher compared to the standard treatment (Table S3.2 in the Supplement, aF_{SRC} values of the intensive treatment are given in parentheses).

3.3.5 Relationship between the cumulative denitrification and sediment parameters

Correlations between $D_{\text{cum}}(365)$ and sediment parameters showed substantial differences among the various partial data sets (Table 3.3). For the whole data set C_{org} exhibited the closest correlation (r_s : $R = 0.72$, $P < 0.001$) with $D_{\text{cum}}(365)$. In the FFA aquifer material, DOC_{extr} and $\text{SO}_4^{2-}_{\text{extr}}$ showed highly significant negative relations to $D_{\text{cum}}(365)$ (Table 3.3). The relation between these parameters and $D_{\text{cum}}(365)$ was only poor or not significant for the rest of sub data sets. C_{hws} exhibited the highest positive correlations with $D_{\text{cum}}(365)$ in the partial data sets with samples containing relatively low concentrations of sulphides (Table 3.1), i.e. the data sets of non-sulphidic and transition zone samples (r_s : $R = 0.85$ and $R = 0.60$, respectively, $P < 0.001$). C_1 was in closest relation with $D_{\text{cum}}(365)$ in GKA and non-sulphidic samples (r_s : $R = 0.87$ and $R = 0.73$, respectively, $P < 0.01$). C_{hws} and C_1 were more closely related to $D_{\text{cum}}(365)$ compared to C_{org} within sub-groups of aquifer material with no or only low contents of total-S. In contrast to GKA, the FFA aquifer material exhibited good correlations between C_{hws} and $D_{\text{cum}}(365)$ (r_s : $R = 0.58$, $P < 0.01$) (Table 3.3). In all data sets, the silt content was significantly positively correlated with $D_{\text{cum}}(365)$, except for transition zone aquifer material where this relation was not significant. For the whole data set and FFA and GKA data sets, total contents of C_{org} and sulphur were in closest positive correlation with $D_{\text{cum}}(365)$. In the partial data sets which were differentiated according to chemical parameters, these relations were less pronounced or not significant.

Table 3.3: Spearman rank correlation coefficients between $D_{\text{cum}}(365)$ and sediment parameters for the whole data set and partial data sets.

	SO_4^{2-} _{extr}	DOC_{extr}	C_{hws}	C_1	total-N	C_{org}	Total-S	Sand	Silt
Whole data set	-0.63 ^c	-0.59 ^c	0.36 ^a	0.68 ^c	0.55 ^c	0.72 ^c	0.64 ^c	-0.38 ^b	0.63 ^c
FFA	-0.82 ^c	-0.87 ^c	0.58 ^b	0.38n.s.	0.34n.s.	0.64 ^c	0.82 ^c	-0.44 ^a	0.64 ^c
GKA	-0.49 ^a	-0.40n.s.	0.13n.s.	0.87 ^c	0.78 ^c	0.88 ^c	0.88 ^c	-0.40 ^a	0.73 ^c
non-sulphidic	-0.38n.s.	-0.53 ^a	0.85 ^c	0.73 ^b	0.32n.s.	0.43n.s.	0.65 ^a	-0.81 ^b	0.72 ^b
sulphidic	-0.45 ^a	-0.18n.s.	0.24n.s.	0.46 ^a	0.59 ^c	0.61 ^c	0.33 ^a	-0.28n.s.	0.42 ^a
transition zone	-0.52 ^b	-0.59 ^b	0.60 ^c	-0.74 ^c	-0.59 ^c	-0.61 ^c	0.13n.s.	-0.01n.s.	0.52n.s.

^a Correlation significant at the 0.05 probability level;

^b correlation significant at the 0.01 probability level;

^c correlation significant at the 0.001 probability level;

n.s. not significant.

Table 3.4: Simple linear regressions between $D_{\text{cum}}(365)$ and $D_r(t)$, $f^{B-C}(D_{\text{cum}}(365)) = A+B \times f^{B-C}(D_r(t))$.

Data set	N ^a	$D_r(7)$			$D_r(84)$			$D_r(168)$		
		R ^b	A	B	R ^b	A	B	R ^b	A	B
Whole data set	151	0.59	1.075	1.969	0.95	-0.361	0.962	0.96	0.065	1.085
FFA	86	0.57	2.005	2.705	0.94	-0.345	0.984	0.96	-0.015	1.123
GKA	65	0.68	1.613	2.565	0.94	0.452	1.503	0.94	-0.050	1.102
non-sulphidic	44	0.88	-0.391	1.264	0.95	-0.867	0.792	0.85	-0.216	1.160
transition zone	28	0.01	-3.866	-0.025	0.78	-1.556	1.156	0.69	-0.020	1.963
sulphidic	107	0.10	-2.521	0.304	0.82	0.047	1.697	0.91	1.326	2.514
NO_3^- -bearing	64	0.86	0.815	1.818	0.98	-1.446	0.427	0.94	-0.771	0.748
NO_3^- -free	87	0.15	-1.757	0.217	0.91	-0.613	0.750	0.94	0.183	1.394
FFA non-sulphidic	20	0.94	-2.125	0.239	0.97	-2.015	0.205	0.82	-1.527	0.441
FFA sulphidic	66	0.08	-1.928	0.880	0.82	-0.351	1.373	0.90	-0.462	0.785
GKA non-sulphidic	24	0.86	1.608	2.583	0.98	-0.546	0.926	0.87	1.007	1.877
GKA sulphidic	41	0.30	-1.684	1.028	0.86	2.147	2.863	0.91	2.353	3.343
FFA NO_3^- -free	38	0.58	-0.340	0.613	0.95	-0.754	0.675	0.89	0.027	1.279
GKA NO_3^- -free	49	0.31	-1.423	0.454	0.85	-0.462	0.808	0.93	0.125	1.374

^a Sample number;

^b correlation coefficient.

3.3.6 Regression models to predict $D_{\text{cum}}(365)$

3.3.6.1 Predicting $D_{\text{cum}}(365)$ from initial denitrification rates

Initial denitrification rates derived after 7 days of incubation ($D_r(7)$) exhibited only good linear relations with $D_{\text{cum}}(365)$ for non-sulphidic samples (with sub-sets of FFA and GKA non-sulphidic samples) and for the group of NO_3^- -bearing samples with correlation coefficients > 0.86 (Table 3.4). For the other data sets, $D_{\text{cum}}(365)$ was not predictable by $D_r(7)$ (Table 3.4 and Fig. 3.3). Moreover, especially sulphidic and NO_3^- -free samples, exhibited a considerable lag-phase at the beginning of incubation, which resulted in poor predictions of $D_{\text{cum}}(365)$ from $D_r(7)$. In contrast to $D_r(7)$, the average denitrification rate after 84 days of incubation, i.e. at the next sampling time $D_r(84)$, showed good to excellent regressions ($R > 0.78$) with $D_{\text{cum}}(365)$ for the whole and most of the partial data sets. An exception were the transition zones samples which showed declining denitrification rates during incubation (Fig. 3.1).

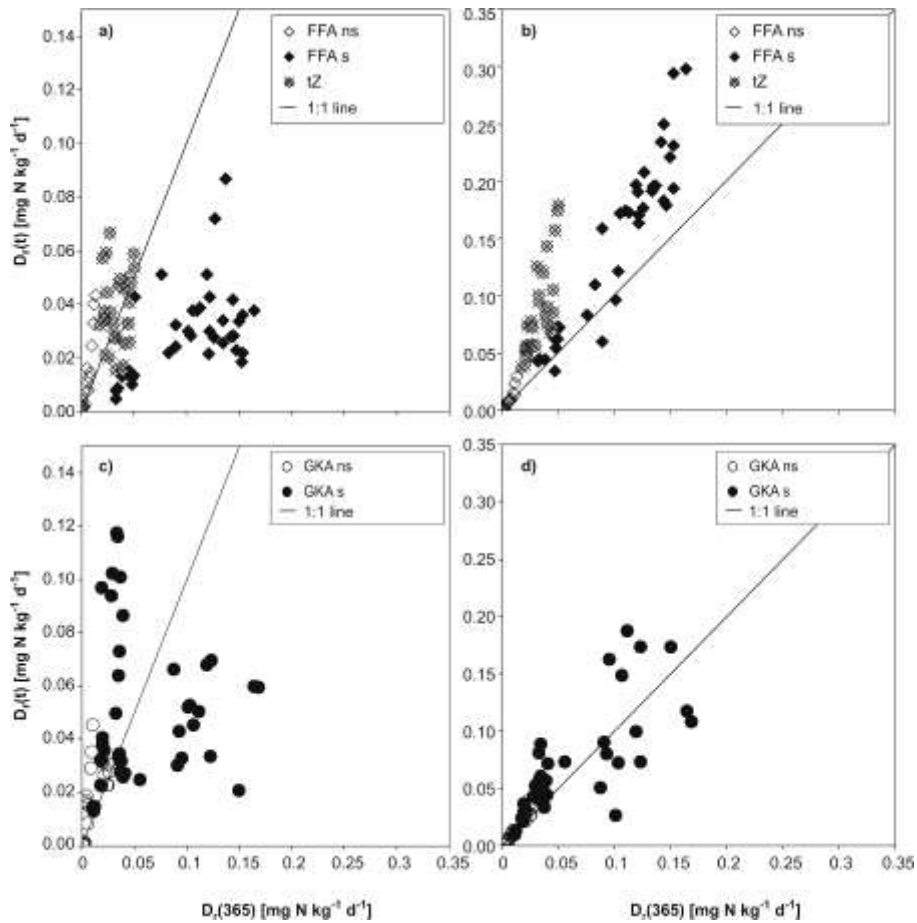


Fig. 3.3: Relation between denitrification rates determined during 7 ($D_r(7)$), 84 ($D_r(84)$) and 365 ($D_r(365)$) days of incubation. (a) $D_r(7)$ vs. $D_r(365)$ of FFA samples. (b) $D_r(84)$ vs. $D_r(365)$ of FFA samples. (c) $D_r(7)$ vs. $D_r(365)$ of GKA samples. (d) $D_r(84)$ vs. $D_r(365)$ of GKA samples.

3.3.6.2 Predicting $D_{\text{cum}}(365)$ from sediment parameters

Simple regression and multiple regression analysis was performed to predict $D_{\text{cum}}(365)$ from independent sediment variables, i.e. the silt content, C_{org} , total-S, SO_4^{2-} -extr, DOC_{extr} , C_{hws} and C_1 . The goodness of fit between modelled and measured $D_{\text{cum}}(365)$ is given by correlation coefficients, the ratio of calculated to measured $D_{\text{cum}}(365)$ ($R_{\text{c/m}}$) and the average deviation of $R_{\text{c/m}}$ from the mean in the various sub data sets.

Simple regression models yielded a significant lower goodness of fit than multiple regressions (Table 3.5, Tables S3.3 and S3.4 in the Supplement). Simple regressions with individual sediment parameters demonstrated that C_{org} and C_1 yielded best predictions of $D_{\text{cum}}(365)$ when the whole data set was analysed (Table S3.3 in the Supplement). Regression analysis of partial data sets grouped according to chemical properties, i.e. groups including samples from both aquifers, resulted in R values below 0.8 for all tested variables. For the sulphidic samples, C_{org} or C_1 values were the best individual sediment parameters to model $D_{\text{cum}}(365)$ when considering partial data sets including samples from both aquifers. For the individual aquifers, some single sediment parameters were very good estimators ($R > 0.8$) for $D_{\text{cum}}(365)$, e.g. total-S and DOC_{extr} in the FFA data set and C_{org} , total-S and C_1 for GKA. C_{org} was clearly less correlated with $D_{\text{cum}}(365)$ in those sub-groups of aquifer material with low contents of SRC, i.e. the non-sulphidic aquifer material.

Combinations of total-S and C_{org} did not substantially increase the goodness of fit of the regression models to predict $D_{\text{cum}}(365)$ in comparison to simple regressions with these two variables (Table 3.5, selection I in comparison to Tables S3.3 and S3.4 in the Supplement), in some cases the goodness of fit even worsened. Only for the partial data sets of non-sulphidic samples a linear combination of these two variables was slightly better than a simple regression with one of the independent variables.

Table 3.5, selection II lists the combinations including C_{org} , total-S, C_1 , and SO_4^{2-} -extr which revealed the highest correlation coefficient with $D_{\text{cum}}(365)$ for the corresponding data sets. Compared to simple regressions these linear combinations improved correlation coefficients of regressions for most partial data sets. Also the range of deviations of calculated from measured $D_{\text{cum}}(365)$ values ($R_{\text{c/m}}$) was smaller (Table S3.4 in the Supplement). For the whole data set and the sulphidic samples for example, the correlation coefficient R increased from 0.80 to 0.86 and from 0.66 to 0.79, respectively, if instead of regressions between C_{org} and $D_{\text{cum}}(365)$ the combination of $C_{\text{org}}-C_1$ was used to model $D_{\text{cum}}(365)$. This combination was also better than regressions with C_1 alone (Table 3.5 in comparison to Table S3.4 in the

Predicting the denitrification capacity from shorter-term incubations

Table 3.5: Results of multiple linear regression analysis between $D_{\text{cum}}(365)$ and various selections of sediment parameters. To achieve normal distribution, all variables in the different data sets were Box–Cox transformed. Regression coefficients are given for the equation $f^{\text{B-C}}(D_{\text{cum}}(365)) = C_1 + C_2 \times f^{\text{B-C}}(\% \text{ silt}) + C_3 \times f^{\text{B-C}}(C_{\text{org}} \text{ mg kg}^{-1}) + C_4 \times f^{\text{B-C}}(\text{total-S mg kg}^{-1}) + C_5 \times f^{\text{B-C}}(\text{SO}_4^{2-}{}_{\text{extr}} \text{ mg S kg}^{-1}) + C_6 \times f^{\text{B-C}}(\text{DOC}_{\text{extr}} \text{ mg C kg}^{-1}) + C_7 \times f^{\text{B-C}}(C_{\text{hws}} \text{ mg C kg}^{-1}) + C_8 \times f^{\text{B-C}}(C_1 \text{ mg C kg}^{-1})$.

Data set	N ^a	R ^b	F ^c	Regression coefficients							
				C ₁	C ₂	C ₃	C ₄	C ₅	C ₆	C ₇	C ₈
Selection I: C_{org} and total-S											
Whole data set	151	0.82	153.1	-9.739	*	2.008	0.302	*	*	*	*
FFA	86	0.83	96.1	-17.950	*	1.366	5.565	*	*	*	*
GKA	65	0.86	85.6	-0.431	*	0.015	0.027	*	*	*	*
non-sulphidic	44	0.80	37.4	-204.2	*	0.586	247.877	*	*	*	*
sulphidic	107	0.66	40.5	-3.229	*	1.328	-5.0E-5	*	*	*	*
NO ₃ ⁻ -bearing	64	0.71	30.3	-205.28	*	0.302	236.599	*	*	*	*
NO ₃ ⁻ -free	87	0.80	76.9	-7.192	*	2.018	-0.003	*	*	*	*
transition zone	28	0.72	15.5	-446.52	*	-5.474	712.716	*	*	*	*
Selection II: Two sediment parameters giving the highest correlation coefficient											
Whole data set	111	0.86	154.1	-8.529	*	1.849	*	*	*	*	0.164
FFA	46	0.89	84.6	-18.935	*	*	7.553	-0.044	*	*	*
GKA	65	0.93	204.7	-5.326	*	1.274	*	*	*	*	0.204
non-sulphidic	44	0.80	37.4	-204.2	*	0.586	247.877	*	*	*	*
sulphidic	67	0.79	53.9	-6.399	*	2.254	*	*	*	*	-0.363
NO ₃ ⁻ -bearing	56	0.80	51.2	-184.96	*	*	216.915	-0.191	*	*	*
NO ₃ ⁻ -free	55	0.89	102.2	-9.437	*	2.963	*	*	*	*	-0.927
transition zone	20	0.74	12.8	193.30	*	-2.692	*	*	*	*	-181.402
Selection III: stepwise multiple regression with all sediment parameters											
Whole data set	111	0.93	172.9	-0.090	*	1.415	*	-0.154	-3.169	*	0.146
FFA	46	0.95	105.9	0.466	-0.350	*	*	*	-0.309	0.299	0.166
GKA	65	0.97	188.4	-4.953	-0.545	*	0.014	-0.191	4.926	*	0.306
non sulphidic	44	0.96	122.7	-85.481	*	-0.525	*	*	-0.479	127.635	0.032
sulphidic	67	0.84	31.5	-6.166	-0.211	2.333	0.001	-0.091	*	*	-0.522
NO ₃ ⁻ -zone	56	0.93	112.0	2.589	*	*	*	-0.167	-0.142	*	0.240
NO ₃ ⁻ -free	55	0.91	68.2	-8.581	*	2.581	0.003	-0.325	*	*	-0.754
transition zone	20	0.91	23.1	72.50	0.756	-18.033	*	-0.299	*	-0.186	*

*: Variable not included in the regression model;

^a number of included samples;

^b correlation coefficient;

^c f -coefficient.

Supplement). The combination of total-S and $\text{SO}_4^{2-}\text{extr}$ improved the correlation coefficient with $D_{\text{cum}}(365)$ in comparison to simple regression with total-S clearly for all sub data sets containing sulphidic aquifer material. For FFA samples this combination raised R of the simple regressions from 0.83 to 0.89.

For all data sets, except the sub data set of sulphidic material, multiple regressions between $D_{\text{cum}}(365)$ and all 7 independent sediment parameters (direct multiple regression) yielded correlation coefficients $R > 0.92$ (data not shown), i.e. over 84 % of the variance of the measured $D_{\text{cum}}(365)$ values could be explained with this regression. For sulphidic aquifer material, R was 0.83. A stepwise multiple regression, which gradually adds the sediment parameters to the regression model according to their significance yielded results which were almost identical to the results of direct multiple regression (Table 3.5, selection III). The stepwise multiple regression model reduced the number of needed regression coefficients (i.e. the number of needed sediment variables) to model $D_{\text{cum}}(365)$ from 7 to 3 or 5. The goodness of fit as indicated by mean $R_{\text{c/m}}$ values close to 1 and small ranges of $R_{\text{c/m}}$ values was usually the best with multiple regression analysis, especially for samples with $D_{\text{cum}}(365)$ values below $20 \text{ mg N kg}^{-1} \text{ yr}^{-1}$ (Table S3.4 in the Supplement).

3.3.7 Predicting the stock of reduced compounds (SRC) from $D_{\text{cum}}(365)$ and estimation of the minimal lifetime of denitrification (emLoD)

The mean $D_{\text{cum}}(365)$ values of the 3 to 4 replications per aquifer sample were used to predict the SRC of the aquifer samples with simple regressions (Table 3.6). For the whole data set the measured $D_{\text{cum}}(365)$ values exhibited good linear relations with the SRC of the incubated aquifer samples ($R = 0.82$). $D_{\text{cum}}(365)$ of GKA samples showed good to excellent and clearly better regressions with the SRC than the $D_{\text{cum}}(365)$ of FFA samples. The prediction of SRC from $D_{\text{cum}}(365)$ was also clearly better for sulphidic and NO_3^- -free samples compared to samples from already oxidized parts of both aquifers (Table 3.6).

The minimal lifetime of denitrification (emLoD) of the incubated aquifer material was estimated for a nitrate input of $11.3 \text{ g NO}_3^- \text{-N m}^{-2} \text{ yr}^{-1}$ as described in Sect. 3.2.5. With this nitrate input and an assumed fraction of the SRC available for denitrification during incubation (aF_{SRC}) of 5 % the calculated emLoD of 1 m^3 of aquifer material ranged between 0.7–8 and 2.4–67 yr m^{-1} for non-sulphidic and sulphidic aquifer material, respectively (Tables 3.2 and S3.2 in the Supplement). The estimated median emLoD of sulphidic material was 5 times higher than the one of non-sulphidic samples. FFA and GKA samples were not

statistically different in their emLoD values (kw: $P < 0.05$) (median emLoD values of NO_3^- -free aquifer samples from the FFA and GKA are 19.8 ± 15 yr and 10.5 ± 20 yr, respectively; see also Table S3.2 in the Supplement).

Table 3.6: Simple regression between $D_{\text{cum}}(365)$ and SRC, $f^{\text{B}-\text{C}}(\text{SRC}) = A + B \times f^{\text{B}-\text{C}}(D_{\text{cum}}(365))$. $D_{\text{cum}}(365)$ is the mean of 3 to 4 replications per aquifer sample.

Data set	N ^a	R ^b	A	B
Whole data set	40	0.82	5.186	0.302
FFA	22	0.76	3.560	0.064
GKA	18	0.95	5.635	0.785
non-sulphidic	11	0.36	4940.4	1618.2
sulphidic	29	0.73	9.006	2.292
NO_3^- -bearing	17	0.49	134.13	26.763
NO_3^- -free	23	0.79	28.971	5.068
transition zone	8	0.58	5.034	-0.415

^a Sample number

^b correlation coefficient.

3.4 Discussion

3.4.1 Groundwater redox state and sample origin

The non-sulphidic aquifer material in this study, which exhibited low denitrification rates, originated generally from aquifer regions with dissolved O_2 concentrations $> 1.5 \text{ mg } \Gamma^{-1}$ ($= 42 \text{ } \mu\text{mol } O_2 \text{ } \Gamma^{-1}$) and is already largely oxidized. These aquifer parts could be referred to as aerobic ($1\text{--}2 \text{ mg } O_2 \text{ } \Gamma^{-1}$ (Rivett et al., 2008)). In laboratory experiments with homogeneous material, the intrinsic O_2 threshold for the onset of denitrification is between 0 and $10 \text{ } \mu\text{mol } O_2 \text{ } \Gamma^{-1}$ (Seitzinger et al., 2006). Reported apparent O_2 thresholds for denitrification in aquifers are between 40 to $60 \text{ } \mu\text{mol } \Gamma^{-1}$ (Green et al., 2008; Green et al., 2010; McMahon et al., 2004; Tesoriero and Puckett, 2011). Green et al. (2010) modelled the apparent O_2 threshold for denitrification in a heterogeneous aquifer and found that an apparent O_2 threshold obtained from groundwater sample analysis of $< 40 \text{ } \mu\text{mol } O_2 \text{ } \Gamma^{-1}$ is consistent with an intrinsic O_2 threshold of $< 10 \text{ } \mu\text{mol } \Gamma^{-1}$. This apparent threshold of $40 \text{ } \mu\text{mol } O_2 \text{ } \Gamma^{-1}$ corresponds well with the threshold of minimal and maximal dissolved O_2 concentrations at the origins of non-sulphidic and sulphidic aquifer material, respectively, in both aquifers. The sulphides that occur in zones where O_2 is still measurable in the groundwater might represent residual sulphides from poorly perfused micro areas within the aquifer material.

3.4.2 Predicting $D_{\text{cum}}(365)$ from initial denitrification rates and time course of denitrification

An important goal of denitrification research is to predict long-term denitrification capacity of aquifers from initial denitrification rates.

The conducted incubations showed that there are significant quantitative relations between $D_{\text{cum}}(365)$ and the SRC of the incubated aquifer samples (Table 3.6) and it can be assumed that the SRC represents a maximum estimate of the long-term denitrification capacity of aquifer material. Taking this into account it was tested if initial denitrification rates can predict $D_{\text{cum}}(365)$. This was done to facilitate determination of $D_{\text{cum}}(365)$ since laboratory measurements of initial denitrification rates ($D_r(7)$) are more rapid and less laborious and expensive compared to one-year incubations to measure $D_{\text{cum}}(365)$. Moreover, initial denitrification rates can also be measured in situ at groundwater monitoring wells (Konrad,

2007; Well et al., 2003) and can thus be determined without expensive drilling for aquifer material. Konrad (2007) tested this approach with a small data set (13 in situ measurements) and 26 pairs for $D_r(7)$ vs. $D_r(\text{in situ})$ and only 5 pairs for $D_r(\text{in situ})$ vs. $D_{\text{cum}}(365)$. One objective of this study is to develop transfer functions to predict $D_{\text{cum}}(365)$ from $D_r(7)$. The next step would be to compare in situ denitrification rates ($D_r(\text{in situ})$) from push-pull experiments at the location of the incubated aquifer samples with their $D_{\text{cum}}(365)$ measured in this study and to check if $D_{\text{cum}}(365)$ can be derived from $D_r(\text{in situ})$.

By and large, the measured range of $D_{\text{cum}}(365)$ values agreed well with previous incubations studies, which investigated the denitrification activity of aquifer material from comparable Pleistocene sandy aquifers. Well et al. (2005) and Konrad (2007) report total ranges for D_{cum} of 9.5 to 133.6 mg N kg⁻¹ yr⁻¹ and 0.99 to 288.1 mg N kg⁻¹ yr⁻¹, respectively. Weymann et al. (2010) conducted incubations with aquifer material from one location within the FFA, reporting ranges of $D_{\text{cum}}(365)$ of organotrophic (\approx non-sulphidic) and lithotrophic (\approx sulphidic) aquifer material between 1–12.8 and 14.5–103.5 mg N kg⁻¹ yr⁻¹, respectively (calculated from reported denitrification rates). All of these denitrification capacities are comparable to results obtained during this study (Table 3.2), indicating that the selection of sites and sampling location represent the typical range of denitrification properties of this kind of Pleistocene sandy aquifers.

Two aspects have to be considered when using $D_r(7)$ as an indicator for $D_{\text{cum}}(365)$: aspect (i): the availability of reactive compounds may change during incubation and aspect (ii): different microbial communities resulting from the availability of different electron donors and acceptors may be evident in samples from different aquifer redox zones (Griebler and Lueders, 2009; Kölblboelke et al., 1988; Santoro et al., 2006) and possible shifts within the microbial community during incubation have thus to be taken into account (Law et al., 2010).

With respect to aspect (i), it is straightforward that the availability of reduced compounds for denitrification in aquifer material directly influences the measured denitrification rates since denitrification is a microbially mediated process and the significant majority of microbes in aquifers are attached to surfaces and thin biofilms (Griebler and Lueders, 2009; Kölblboelke et al., 1988). Therefore, the area of reactive surfaces of reduced compounds within the sediment might control the amount of active denitrifiers in an incubated sample and thus the measured denitrification rates and vice versa. Therefore, denitrification rates are an indirect measure of the availability of reduced compounds for denitrification and the availability of reduced compounds may reduce due to oxidation during incubation. On the contrary, growth of the microbial community may change the apparent

availability of reduced compounds due to the increase of the area of “colonised” reduced compounds within the incubated aquifer material and thus leading to increasing denitrification rates during incubation.

The almost linear time-course of denitrification in non-sulphidic and sulphidic samples (Fig. 3.1a and c) indicate minor changes of the availability of reduced compounds during incubation. The linear time courses also suggest a pseudo zero order kinetic of denitrification where denitrification rates are independent of changes in NO_3^- or reduced compounds during the incubations. NO_3^- concentrations in the batch solution of incubated samples were always above $3.0 \text{ mg NO}_3^- \text{-N } \Gamma^{-1}$ during the whole incubation period and thus above the reported threshold of $1.0 \text{ mg NO}_3^- \text{-N } \Gamma^{-1}$, below which denitrification is reported to become NO_3^- limited (Wall et al., 2005). Results from in situ tracer experiments given by Korom et al. (2005) (Figs. 4 and 6) and Trudell et al. (1986) (Fig. 7 time course of NO_3^- concentrations after an adaptation time of 200 h) indicate that denitrification during this experiments could be described with a zero-order kinetic, i.e. that denitrification was independent of nitrate concentrations over a fast concentration range down to values similar to the threshold reported by Wall et al. (2005).

The small denitrification rates measured in the non-sulphidic samples may then be the result of only small amounts of organic carbon oxidized during denitrification. The consumed fraction of available organic carbon might release fresh surfaces which can further be oxidized during denitrification. The relative stable denitrification rates of non-sulphidic samples may then reflect that the area of microbial available surface of reduced compounds exhibits negligible change during incubation. This is plausible for the case that the surface of the organic matter is relatively small in comparison to its volume, which applies to the lignitic pebbles in the FFA (Frind et al., 1990).

Most of the sulphidic aquifer samples from the zone of NO_3^- -free groundwater in both aquifers showed also a relative constant linear increase of denitrification products during incubation (Fig. 3.1c). This aquifer material was not yet in contact with dissolved O_2 and NO_3^- from the groundwater. Hence, the reduced compounds, if initially present in the solid phase, are supposed to be not yet substantially depleted. The relative constant linear increase of denitrification products of these samples suggests that the denitrifying community had a relative constant activity during incubation, implying a constant amount of denitrifying microbes and thus constant areas of reactive surfaces. In contrast, almost all transition zone samples exhibited clearly declining denitrification rates during incubation (Fig. 3.1b). This group represents aquifer material already depleted in reduced compounds (Table 3.1 and

Fig. 3.2a) but still containing residual contents of reactive sulphides and therefore showing a $SFC > 1 \text{ mg SO}_4^{2-}\text{-S kg}^{-1} \text{ yr}^{-1}$. These residual sulphides might be relatively quickly exhausted during incubation leading to a loss of reactive surfaces and in the following to a flattening of the slope of measured denitrification products ($\text{N}_2 + \text{N}_2\text{O}$).

The intensive incubation experiment gave up to 17 times higher denitrification rates than the standard incubations (Table S3.2 in the Supplement) and differed from the standard incubations only in three points: (i) dilution of aquifer material with pure quartz sand, (ii) higher incubation temperatures (20 °C instead of 10 °C) and (iii) continuous shaking of the incubated sediments on a rotary shaker. The denitrification activity of the added pure quartz was found to be negligible. Well et al. (2003) evaluated the temperature effect on denitrification rates measured during laboratory incubations. An increase of incubation temperature from 9 to 25 °C resulted in 1.4 to 3.8 times higher denitrification rates. In contrast to this the intensive incubation experiment presented in this study gave up to 17 times higher denitrification rates than the standard incubations. This suggests that not only higher temperatures but also the continuous shaking of the incubated aquifer material may have led to higher denitrification rates by the enlargement of the surfaces of reduced compounds within the aquifer material due to physical disruption of pyrite and/or organic carbon particles. The latter was visible as black colouring of the batch solution which was not noticeable at the beginning of intensive incubations and also not during the standard incubations. But in contrast to initial expectations, the intensive treatment did not lead to a faster decline of denitrification rates during incubation (Fig. 3.1d). The reasons for this might be that the loss of reactive surfaces of reduced compounds due to consumption during denitrification was small compared to their amount. Also the shaking might have contributed to the creation of reactive surfaces and thus may have supported denitrification. A possible temperature effect on the suite of active denitrifiers during incubations and from these on the resulting denitrification rates, was not investigated during this study, but should be considered in further studies.

With respect to the importance of changes in the availability of electron acceptors for the communities of active microbes present in aquifer material (aspect ii), it is assumed that in the sulphidic samples from the zone of NO_3^- -free groundwater, the population of denitrifiers had to adapt to the addition of NO_3^- as a new available electron acceptor, e.g. by growth of denitrifying population and changes in the composition of the microbial community (Law et al., 2010). This adaptation processes requires time and might be a reason for the missing correlation between $D_t(7)$ and $D_{\text{cum}}(365)$ during incubation of sulphidic samples in both

aquifers, whereas $D_r(84)$ was a good predictor for $D_{cum}(365)$ (Fig. 3.3 and Table 3.4). This explanation is in line with the fact that spatial heterogeneity of microbial diversity and activity is strongly influenced by several chemical and physical factors including the availability of electron donors and acceptors (Griebler and Lueders, 2009; Kölblboelke et al., 1988; Santoro et al., 2006). Santoro et al. (2006) investigated the denitrifier community composition along a nitrate and salinity gradient in a coastal aquifer. They conclude that for the bacterial assemblage at a certain location, “steep gradients in environmental parameters can result in steep gradients (i.e. shifts) in community composition”.

The observed adaptation phase is in accordance with results given by Konrad (2007) who found also only after 84 days of incubation good relations between mean denitrification rates and $D_{cum}(365)$, whereas the sampling after day 21 of incubation gave poor correlations. From this it is concluded that 7 days of incubation were not sufficient to get reliable estimates of $D_{cum}(365)$ from $D_r(7)$ for aquifer samples from deeper reduced aquifer regions in both investigated aquifers, whereas there are good transfer functions to predict $D_{cum}(365)$ from $D_r(84)$ for all partial data sets.

It can be concluded that prediction of denitrification from initial denitrification rates ($D_r(7)$) during incubation experiments is possible for non-sulphidic samples, which were already in contact with groundwater NO_3^- . The denitrification capacity of these samples must have been exhausted to some extent during previous denitrification or oxidation with O_2 and the laboratory incubations reflect the residual stock of reductants. To the contrary, the denitrification capacity of sulphidic samples was not predictable from $D_r(7)$. These samples were not yet depleted in reduced compounds and therefore these samples exhibited significantly higher denitrification rates during incubation. With respect to in situ measurements of denitrification rates with push-pull tests in the reduced zones of aquifers the required adaptation time of the microbial community to tracer NO_3^- might lead to an underestimation of possible denitrification rates.

3.4.3 Predicting $D_{\text{cum}}(365)$ of aquifer sediments, correlation analysis and regression models

3.4.3.1 Sediment parameters and their relation to $D_{\text{cum}}(365)$

Correlation analysis

C_{org} , SO_4^{2-} _{extr}, C_{hws} and C_1 exhibited no significant differences between both aquifers, whereas the amount of total-S was significantly higher and DOC_{extr} values significantly lower for GKA compared to FFA samples. But in contrast, the opposite groups of non-sulphidic to sulphidic aquifer material differed significantly in all of the analysed independent sediment variables (kw: $P < 0.05$) (Table 3.1 and Fig. S3.2 in the Supplement). The same applies also for the opposite groups of NO_3^- -free and NO_3^- -bearing aquifer material (data not shown).

The measured range of DOC_{extr} (4.7 to 11.6 mg C kg⁻¹) for FFA and GKA aquifer samples are in the range of recently reported values (Weymann et al., 2010) for aquifer samples from the same site at comparable depths. The DOC_{extr} values clearly decreased with depth in both aquifers (Table S3.1 in the Supplement) and exhibited partly significant negative correlations with the $D_{\text{cum}}(365)$ of the incubated aquifer material (Table 3.3) (r_s : $P < 0.05$). Similarly, von der Heide et al. (2010) reported significant negative correlation between DOC and the concentrations of N_2O as an intermediate during reduction of NO_3^- to N_2 in the upper part of the FFA. From these findings it is supposed that the reactive fraction of DOC is increasingly decomposed or immobilised with depth in both aquifers. Moreover, the negative correlation between the DOC_{extr} and the measured $D_{\text{cum}}(365)$ suggests that the contribution of DOC_{extr} to denitrification capacity of the investigated aquifers is relatively small, which is consistent with findings of Tesoriero and Puckett (2011) and Green et al. (2008).

The highest concentrations of SO_4^{2-} _{extr} were measured in samples from the upper parts of both aquifers (Table 3.1). The measured range of SO_4^{2-} _{extr} (Table 3.1) exhibited significant negative correlations with $D_{\text{cum}}(365)$ of FFA and GKA aquifer material (r_s : $R = -0.82$ and $R = -0.49$, respectively, $P < 0.05$) (Table 3.3). SO_4^{2-} _{extr} values decreased with depths in both aquifers (Table S3.1 in the Supplement) and thus exhibited an inverse concentration gradient compared with total-S values. The range of SO_4^{2-} _{extr} of FFA and GKA material is comparable to SO_4^{2-} _{extr} values (20.5 ± 16.7 mg SO_4^{2-} -S kg⁻¹) of aquifer samples from North Bavaria, from a deeply weathered granite with a sandy to loamy texture (Manderscheid et al., 2000). All measured SO_4^{2-} _{extr} values above 10 mg S kg⁻¹ from FFA and GKA samples (except for

the samples from 25.9–26.9 m and 27–28.3 m below surface in the GKA) originated from zones within these two aquifers with pH values of the groundwater between 4.39 and 5.6 (von der Heide unpublished data and own measurements). According to the pH values, the groundwater from these locations is in the buffer zone of aluminium hydroxide and aluminium hydroxysulphates (Hansen, 2005). It is known that hydroxysulphate minerals can store SO_4^{2-} together with aluminium (Al) in acidic soils (Khanna et al., 1987; Nordstrom, 1982; Ulrich, 1986) and aquifers (Hansen, 2005). Therefore, dissolution of aluminium hydroxysulphate minerals may have led to the higher values of SO_4^{2-} in samples from the upper already oxidized parts of both aquifers.

KMnO_4 labile organic carbon (C_1) measured in the aquifer material was closely related to C_{org} (r_s : $R = 0.84$, $P < 0.001$). GKA samples showed a much wider range of C_1 values (0.9 to 2504.7 mg C kg^{-1}) than FFA aquifer material (2.7 to 887 mg C kg^{-1}) (Table 3.1). The total average of C_1 / C_{org} ratios of 0.24 for the whole data set is comparable to the mean ratio of 0.3 reported by Konrad (2007) for 3 comparable sandy aquifers, showing that typically less than half of C_{org} in Pleistocene aquifers is KMnO_4 labile. The higher C_1 / C_{org} ratio in the sulphidic samples might indicate that the C_1 fraction of C_{org} in the upper non-sulphidic parts of both aquifers is already oxidized to a larger extent (Table 3.1). Konrad (2007) assumes that C_1 represents the proportion of C_{org} which might be available for microbial denitrification. A stoichiometric $\text{CH}_2\text{O}(C_{\text{org}})/\text{NO}_3^-$ -N ratio of 1.25 (Korom, 1991) leads to the conclusion that the amount of C_1 was always higher than the measured amount of denitrification after one year of incubation ($D_{\text{cum}}(365)$) of the several aquifer samples. This shows that a significant fraction of C_1 did not support a fast denitrification. It can thus be assumed that C_1 represents rather an upper limit for the bioavailable organic carbon in the incubated sediments. However, among the sediment parameters C_1 was the best predictor of $D_{\text{cum}}(365)$ for GKA samples and non-sulphidic aquifer material and also a comparatively good predictor with respect to the whole data set (Table 3.3).

The values of hot water extracts (C_{hws}) from FFA and GKA aquifer material with the ranges of 0.01–42.6 and 14.9–58.5 mg C kg^{-1} , respectively, are comparable to the range of C_{hws} of 6.2 to 141 mg C kg^{-1} given by Konrad (2007). C_{hws} represents on average a proportion of 6.5 % of the entire C_{org} pool in the aquifer material from FFA and GKA. This value is similar to the proportion of 5 % C_{hws} of the entire C_{org} reported by Konrad (2007), with significantly (kw: $P < 0.05$) higher percentages in the non-sulphidic (12.5 %) compared to the sulphidic samples (3.7 %). Strong and highly significant correlations were found between C_{hws} and $D_{\text{cum}}(365)$ of non-sulphidic material (Table 3.3) and NO_3^- -bearing samples (r_s : $R = 0.85$ and

$R = 0.74$, respectively, $P < 0.001$). Studies on C_{hws} stability in soil organic matter revealed that C_{hws} is not completely bioavailable (Chodak et al., 2003; Sparling et al., 1998). Moreover, these authors conclude that C_{hws} is not a better measure of the available soil organic carbon than total C_{org} values. Balesdent (1996) concluded from natural ^{13}C labelling technique (long-term field experiments with maize) that coldwater extracts contain amounts of slowly mineralizable “old” C_{org} pools and this can also be expected for hot water extracts. The close correlation between C_{hws} and $D_{cum}(365)$ in the non-sulphidic aquifer material and not for deeper sulphidic aquifer material is distinctive but difficult to interpret since C_{hws} represents a non-uniform pool of organic matter. The missing correlation between C_{hws} and $D_{cum}(365)$ might indicate that denitrification in this zone is sulphide dependent.

The measured C_{org} values of FFA and GKA aquifer material (Table 3.1) are comparable to ranges reported by Konrad (2007), Strelbel et al. (1992) and Hartog et al. (2004) (Pleistocene fluvial and fluvio-glacial sandy aquifers in Northern Germany and the eastern part of the Netherlands). The total sulphur contents of FFA and GKA aquifer samples are also comparable to the ranges reported by these authors, except Hartog et al. (2004) who reported 4 to 5 times higher total-S contents. Bergmann (1999) and Konrad (2007) investigated the distribution of S species in aquifer material from sandy aquifers in North Rhine-Westphalia and Lower Saxony, Germany, respectively, and found that 80 to over 95% of the total-S value is represented by sulphide-S.

3.4.3.2 Predicting $D_{cum}(365)$ from sediment variables

Single sediment parameters like C_{org} , C_1 or total-S are partly good to very good estimators for the measured $D_{cum}(365)$ in the data set (Table S3.3 in the Supplement). Grouping of aquifer material according to hydro-geochemical zones strongly increases the predictive power of single independent sediment parameters with respect to the measured denitrification during incubation (Table S3.3 in the Supplement). For example, C_{org} and C_1 values are very good parameters to predict $D_{cum}(365)$ for GKA aquifer material, which almost linearly increased with measured C_{org} and C_1 values. The predictability of $D_{cum}(365)$ with simple regressions, linear combinations of two sediment parameters and multiple regressions was best when these models were applied to partial data sets of one aquifer, whereas predictions were always worse when samples from both aquifers were included (Tables 3.5 and S3.3 in the Supplement). For example, total-S values exhibited good simple regressions ($R > 0.8$) with partial data sets that contain only aquifer material from one aquifer. Conversely, the linear

correlation coefficients between total-S and $D_{\text{cum}}(365)$ of sulphidic aquifer material and NO_3^- -free samples (both groups contain FFA and GKA aquifer material) were relatively low with R of 0.4 and 0.32, respectively. The proportion of total-S in SRC of the GKA samples was 3 times higher than in samples from the FFA, whereas the share of sulphides contributing to the measured denitrification capacity was almost the same in FFA and GKA material during incubation (Fig. 3.2b). This shows that samples from both sites were distinct in the reactivity of sulphides which may be related to the geological properties of the material including the mineralogy of the sulphides and the origin of the organic matter.

C_{org} and total-S can be seen as integral parameters with no primary information about the fraction of reactive and non-reactive compounds (with regard to denitrification) represented by these parameters. As already discussed above, C_1 might be an upper limit for the fraction of microbial degradable organic carbon as part of total organic carbon (C_{org}) in a sample of aquifer material. In the data set, C_1 exhibited better regressions with $D_{\text{cum}}(365)$ than C_{org} for aquifer material with relatively low $D_{\text{cum}}(365)$, i.e. non-sulphidic aquifer material and transition zone samples (Table S3.3 in the Supplement). In these two partial data sets it can be assumed that the reduced compounds available for denitrification are already depleted by oxidation with NO_3^- and dissolved O_2 . The median C_{org} contents of non-sulphidic and transition zone samples were only about 20 % and 60 % of the one of NO_3^- -free samples (Table 3.1). Hence, C_{org} in non-sulphidic and transition zone samples might represent less reactive residual C_{org} compared to aquifer material which was not yet in contact with groundwater NO_3^- or dissolved O_2 . This might be the reason for the comparatively low correlation of C_{org} and $D_{\text{cum}}(365)$ in the depleted aquifer material of non-sulphidic and transition zone samples. Similar to this finding, Well et al. (2005) reported poor correlations between C_{org} and the measured amount of denitrification for hydromorphic soil material with low measured denitrification activity during incubation.

Multiple regression analysis clearly enabled the best prediction of $D_{\text{cum}}(365)$. Except for sulphidic samples, correlation coefficients > 0.91 were achieved for all other partial data sets (Table 3.5). But multiple regression models are of limited practical use because the measurement of several sediment parameters is time consuming and expensive.

The goodness of fit of the regression models was highly variable. Simple regressions, linear combinations of two sediment variables and multiple regression analysis could predict the order of magnitude of $D_{\text{cum}}(365)$. The uncertainty of calculated $D_{\text{cum}}(365)$ as given by the ratio of calculated $D_{\text{cum}}(365)$ vs. measured $D_{\text{cum}}(365)$ ($R_{\text{c/m}}$) was within a range of 0.2 to 2 for aquifer material with a measured $D_{\text{cum}}(365) > 20 \text{ mg N kg}^{-1} \text{ yr}^{-1}$ when simple regression

models and multiple regressions were applied (Table S3.4 in the Supplement). In case of less reactive aquifer material ($D_{\text{cum}}(365) < 20 \text{ mg N kg}^{-1} \text{ yr}^{-1}$), only multiple regressions were able to predict $D_{\text{cum}}(365)$ close to this range of uncertainty, whereas simple regressions models yielded poor fits. Well et al. (2005) performed anaerobic incubations with soil material of the saturated zone of hydromorphic soils from Northern Germany in order to measure and calculate denitrification during incubations. They used multiple regressions models to model cumulative denitrification from independent sediment variables. Similar to the results presented here, they report that prediction of denitrification with regression models was unsatisfactory for samples with low measured denitrification rates ($< 36.5 \text{ mg N kg}^{-1} \text{ yr}^{-1}$, this threshold fits also to the data presented here) and they presumed that a considerable variability in the fraction of reactive organic carbon in the measured C_{org} is the reason for this observation.

3.4.4 From $D_{\text{cum}}(365)$ and SRC to the assessment of the lifetime of denitrification within the investigated aquifers

As already defined above the denitrification capacity can be defined as the part of the SRC capable to support denitrification. The lifetime of denitrification in aquifer material depends on the combination of the denitrification capacity, i.e. the stock of available reduced compounds, the NO_3^- input and the kinetics of denitrification.

Two key assumptions were made for the assessment of the lifetime of denitrification in both aquifers from the conducted incubation experiments. There are relations between (i) the measured $D_{\text{cum}}(365)$ and the stock of reduced compounds (SRC) and (ii) between the SRC and the denitrification capacity.

(i) The measured $D_{\text{cum}}(365)$ was a good predictor for the SRC for the whole data set and GKA samples. The SRC was also predictable for sulphidic and NO_3^- -free samples. To the contrary, $D_{\text{cum}}(365)$ was a poor indicator for the SRC of aquifer material from already oxidized parts of both aquifers with relatively low amounts of SRC (Table 3.6). Since the conducted incubations were not able to exhaust the denitrification capacity of the aquifer samples, the real fractions of the SRC available for denitrification (aF_{SRC}) in the incubated samples and even more so the in situ aF_{SRC} remained unknown.

(ii) The low total-S values in the upper parts of both aquifers (Table S3.1) suggest that most of the sulphides present in both aquifers (see Sect. 3.4.3.1) are not resistant to oxidation. Moreover, sulphides are supposed to be the dominant reduced compound supporting

denitrification in the FFA (Kölle et al., 1983). Both aquifers (FFA and GKA) still contain reduced compounds in form of organic matter in their oxidized upper parts. So obviously, certain fractions of the whole SRC are resistant to oxidation. But it is unknown how the ratio of oxidizable to non-oxidizable C_{org} may change with depth in both aquifers. During this study it was found that the C_I/C_{org} ratio was higher for deeper (sulphidic) aquifer samples compared with non-sulphidic samples from the upper region in both aquifers. This suggests that the proportion of organic C which is recalcitrant is higher in the already oxidized zone (see Sect. 3.4.3.1). A reason for this might be that the proportion of mineral associated organic carbon to total organic carbon is higher in this zone.

(Mineral association of organic matter is assumed to increase the recalcitrance fraction of total organic matter (Eusterhues et al., 2005). Eusterhues et al. (2005) reported for a dystic cambisol and a haplic podzol from northern Bavaria that 80–95 % of the total organic carbon content of the particle size fraction ($< 6.3 \mu\text{m}$) in the C horizon is mineral associated organic matter and Fe oxides were identified as the most relevant mineral phases for the formation of organo-mineral associations. Fe oxides can form during lithotrophic denitrification with pyrite and they are known to exist frequently in oxidized aquifers.)

With regard to assumption (ii) a further assumption for the assessment of the lifetime of denitrification is that the ratio of SRC to $D_{cum}(365)$ during incubations is a rough measure to estimate the aF_{SRC} capable of supporting denitrification in situ.

Since the real value of aF_{SRC} remained unknown, the estimated minimal lifetime of denitrification (emLoD) was calculated with an assumed average aF_{SRC} of 5 %. This value was assumed from intensive incubations with median aF_{SRC} of 6.4 % and the fact that denitrification did not stop during all incubations (Fig. 3.1) and thus the real aF_{SRC} of the incubated aquifer samples were higher than the measured ones (Table S3.2 in the Supplement).

The data set provides spatial distribution of $D_{cum}(365)$ and SRC values in both aquifers. From this data the lifetime of denitrification (Eq. 3.2) as well as the depth shift of the denitrification front in both aquifers were estimated. The simplified approach of calculating emLoD with Eq. (3.2) implicitly assumes that the residence time of groundwater in 1 m^3 aquifer material is sufficient to denitrify the nitrate input coming with groundwater recharge, if the amount of microbial available SRC is big enough to denitrify the nitrate input. If the residence time is too short, NO_3^- would reach the subsequent m^3 of aquifer material with groundwater flow, even if the first m^3 still possess a SRC available for denitrification. This means the denitrification front would have a thickness of more than 1 m and the real lifetime of

denitrification within 1 m³ would be longer than predicted by Eq. (3.2). This was the case at multilevel wells B2 and N10 in the FFA in the depths between 8–10 and 4.5–8.6 m, respectively. At this depths the groundwater still contains NO₃⁻, although the measured $D_{\text{cum}}(365)$ of the aquifer material during incubation was higher than the estimated nitrate input (6.6 mg N kg⁻¹ yr⁻¹). Two reasons might explain this, either the nitrate input is considerably higher than $D_{\text{cum}}(365)$ of these aquifer material or there are flow paths through the aquifer, where reduced compounds are already exhausted.

All non-sulphidic samples originated from the NO₃⁻-bearing zone of both aquifers, i.e. their $D_{\text{cum}}(365)$ values were too low to remove the nitrate input during groundwater passage. Therefore, the protective lifetime of denitrification in the investigated aquifers was estimated from the thickness of the NO₃⁻-free zone in both aquifers and the amount of microbial available SRC (Table S3.1 in the Supplement). The median emLoD of NO₃⁻-free aquifer samples from the FFA and GKA are 19.8 ± 15 and 10.5 ± 20 yr m⁻¹, respectively. The high standard deviation of the calculated emLoD values reflects the high heterogeneity of the SRC distribution in both aquifers. These median values of emLoD are equal to a depth shift of the denitrification front of 5 to 9.5 cm yr⁻¹, respectively, into the sulphidic zone, if groundwater flow would only have a vertical component. Since real groundwater flow has a vertical and horizontal component at a given location, the real depth shift of the oxidation front should be lower, depending on the relation of vertical to horizontal groundwater flow velocity.

With respect to the thickness of the NO₃⁻-free zone at multilevel well N10 in the FFA and at the investigated groundwater wells in the GKA, of 16 and 42 m, respectively, this gives a protective lifetime of denitrification of approximately 315 yr and 440 yr, respectively. These values are conservative estimates, on condition that only 5 % of the SRC are available for denitrification and that the nitrate input is 11.3 g N m⁻² yr⁻¹. According to Eq. (3.2), emLoD is inverse to nitrate input and thus would increase with decreasing nitrate input. From SFC measurements and assuming a nitrate input of 4.5 g N m⁻² yr⁻¹ Kölle et al. (1985) estimated a protective lifetime of denitrification of about 1000 yr summed up over the depth of the FFA aquifer at one location, giving 50 yr lifetime of denitrification per depth meter. Using the same estimated nitrate input as in this study (11.3 g NO₃⁻-N m⁻² yr⁻¹), the data given by Kölle et al. (1985) would give a lifetime of denitrification of about 20 yr per depth meter. With respect to the high spatial heterogeneity of SRC values this value fits well to the data for sulphidic aquifer material (Table S3.2 in the Supplement) presented here.

Taking into account the above stated limitations of the assessment of emLoD within the investigated aquifers from shorter-term incubations, the calculated emLoD should be validated by long-term in situ test as described by Korom et al. (2005).

3.4.5 Are laboratory incubation studies suitable for predicting in situ processes?

In the following a few conclusions from the presented study are given, trying to contribute to this question. Therefore, a couple of sub-problems arising from this question are discussed.

3.4.5.1 Limitations of the $^{15}\text{NO}_3^-$ labelling approach

^{15}N labelling of NO_3^- with subsequent analysis of produced ^{15}N labelled N_2 and N_2O did not exclude the possible contribution of dissimilatory nitrate reduction to ammonium (DNRA) since ^{15}N of NH_4^+ was not checked. Moreover, the approach presented here was not suitable to identify a possible coupling of DNRA with anaerobic ammonium oxidation (anammox) with subsequent formation of ^{15}N labelled N_2 from the labelled NO_3^- during anaerobic incubations. Hence, despite the fact that previous investigations reported denitrification as the dominant process of NO_3^- attenuation in the FFA (Kölle et al., 1983; Kölle et al., 1985), a certain contribution by DNRA-anammox cannot be excluded. DNRA is seldom reported to be the dominant process of NO_3^- reduction in groundwater systems (Rivett et al., 2008). To the best knowledge of the author there are no studies about anaerobic ammonium oxidation (anammox) in fresh water aquifers. The possible contribution of DNRA-anammox to NO_3^- consumption during incubation is discussed in more detail in the supplement.

3.4.5.2 Are the NO_3^- concentrations during incubation comparable to those in situ and what is their influence on the measured denitrification rates?

The NO_3^- concentrations in the FFA range from 0–43 (median 8.5) $\text{mg N } \Gamma^{-1}$ and in the GKA from 0–57.6 (median 7.2) $\text{mg N } \Gamma^{-1}$ (Well et al., 2012). The nitrate concentrations at the beginning of the batch experiments were in the range of 35 to 43 $\text{mg N } \Gamma^{-1}$, depending on the amount of pore water in the incubated sediments diluting the added tracer solution. During the incubation experiments the measured NO_3^- concentrations were always within the ranges of NO_3^- concentrations found in both aquifers.

The almost linear time course of denitrification products (see Sect. 3.4.2) accompanied by a parallel decrease of NO_3^- concentrations in the batch solutions suggests that the NO_3^- concentrations were of no or only minor importance for the measured denitrification rates during the conducted incubation experiments, i.e. the kinetics of denitrification were zero-order. The presented experimental results are in accordance with several workers who reported that the kinetics of denitrification (possibly at NO_3^- concentrations above 1 mg N l^{-1} (see Sect. 3.4.2)) are zero-order, i.e. independent of nitrate concentration, which suggest that the supply of electron donors controls the denitrification rates (Rivett et al., 2008). In a recent publication Korom et al. (2012) stated that denitrification in aquifers appears to be most often reported as zero-order. This statement was based on Green et al. (2008) and Korom (1992) and citations therein. Similarly, Tesoriero and Puckett (2011) found that in most suboxic zones of 12 shallow aquifers across the USA in situ denitrification rates could be described with zero-order rates.

In accordance with the cited studies, the experimental results indicate that the supply of electron donors controlled the measured denitrification rates during the conducted incubation experiments, rather than NO_3^- concentrations. Presumably this can also be expected in situ in both aquifers, if the observation period of rate measurements is short enough, so that the consumption of electron donors does not change the supply of denitrifiers with electron donors significantly. Decreasing concentrations of reduced compounds supporting denitrification would lead to decreasing denitrification rates, i.e. to first-order rates. From these findings it might be concluded that the comparability of laboratory and in situ denitrification rates is less affected by the concentration of NO_3^- as long as denitrification becomes not NO_3^- limited.

3.4.5.3 Is one year incubation suitable to predict the denitrification capacity over many decades in an aquifer?

The presented experiments are an approach to narrow down the real denitrification capacity of the investigated aquifer material. Longer incubation periods would have been better, but there are always practical limits and incubation experiments could not be conducted over several decades.

Linear regressions showed that there are quantitative relations at least between $D_{\text{cum}}(365)$ and the SRC of the incubated aquifer samples from the reduced zone in both aquifers (Table 3.6) and it can be assumed that the SRC in a certain degree determines the long-term

denitrification capacity of aquifer material. From this, one-year incubations may give (minimum) estimates of the denitrification capacity of aquifer samples. Furthermore, one year of incubation seems long enough to overcome microbial adaptation processes encountered at the beginning of the conducted incubations (see Sect. 3.4.2). During the intensive incubation experiment 4.6 to 26.4 % of the stock of reduced compounds (SRC) of the incubated aquifer material was available for denitrification with median values of 6.4 % (Table S3.2 in the Supplement). From the results of standard and intensive incubations it was assumed that 5 % of the SRC is available for denitrification in the investigated sediments. The SRC of aquifer material from the zone of NO_3^- -bearing groundwater was only 40 % compared to the SRC present in aquifer material from the zone of NO_3^- -free groundwater in both aquifers (Table 3.2), suggesting that an availability of 5 % of the SRC did not over estimate the denitrification capacity of the investigated aquifers. Nonetheless, quantitative relations between $D_{\text{cum}}(365)$, SRC and the long-term denitrification capacity of aquifers can only be verified by long-term in situ experiments, for example like those described by Korom et al. (2005).

3.4.5.4 Did laboratory incubation studies really indicate what happens in situ?

They cannot exactly retrace all processes contributing to the reduction of NO_3^- to N_2 and N_2O and their interaction under in situ conditions. But laboratory incubations might allow to get estimates of the amount of reduced compounds present in the incubated aquifer material that are able to support denitrification. And laboratory incubations should be compared with short-term and long-term in situ measurements to check the meaningfulness of laboratory incubations for the in situ process as well as the predictability of long-term in situ processes from short-term measurements. In a second study to follow laboratory incubations and in situ measurements at the origin of the incubated aquifer material will be compared.

3.5 Conclusions

The relationship between the cumulative denitrification after one year of anaerobic incubation ($D_{\text{cum}}(365)$), initial laboratory denitrification rates, different sediment parameters and the stock of reduced compounds (SRC) of incubated aquifer samples from two Pleistocene unconsolidated rock aquifers was investigated. This was done to characterize denitrification capacity of sediment samples from the two aquifers and to further develop approaches to predict exhaustion of denitrification capacity and $D_{\text{cum}}(365)$.

Measured denitrification rates and ranges of the investigated sediment parameters coincided with previous studies in comparable aquifers suggesting that the results derived in this study are transferable to other aquifers.

$D_{\text{cum}}(365)$ appeared to be a good indicator for the long-term denitrification capacity of aquifer material from the reduced zone of both aquifers since it was closely related to the SRC.

$D_{\text{cum}}(365)$ could be estimated from actual denitrification rates in samples that originated from regions within both aquifers that were already in contact with NO_3^- bearing groundwater, i.e. where the microbial community is adapted to NO_3^- as an available electron acceptor for respiratory denitrification. These regions are thus favourable for the determination of $D_{\text{cum}}(365)$ from short-term laboratory experiments. Based on these findings, it can be expected that in situ measurement of actual denitrification rates will be suitable to estimate $D_{\text{cum}}(365)$ in the zone of NO_3^- bearing groundwater, if denitrification is not limited by dissolved O_2 . In the deeper zones that had not yet been in contact with NO_3^- , $D_{\text{cum}}(365)$ was poorly related to initial denitrification rates. Only after prolonged incubation of several weeks denitrification rates could predict $D_{\text{cum}}(365)$ of these samples.

$D_{\text{cum}}(365)$ could also be estimated using transfer functions based on sediment parameters. Total organic carbon (C_{org}) and KMnO_4 -labile organic C (C_1) yielded best transfer functions for data sets containing aquifer material from both sites, suggesting that transfer functions with these sediment parameters are more transferable to other aquifers when compared to regressions based on total-S values. $D_{\text{cum}}(365)$ could be predicted relatively well from sediment parameters for aquifer material with high contents of reductants. Conversely, samples depleted in reductants exhibited poor predictions of $D_{\text{cum}}(365)$, probably due to higher microbial recalcitrance of the residual reductants.

It is concluded that best predictions of $D_{\text{cum}}(365)$ of sandy Pleistocene aquifers result from a combination of short-term incubation for the non-sulphidic, NO_3^- -bearing zones and

analysing the stock of reduced compounds in sulphidic zones which are to date not yet depleted by denitrification processes.

During incubations only samples from the transition zone between the non-sulphidic and NO_3^- -free zones showed clearly declining denitrification rates and therefore it was difficult to predict $D_{\text{cum}}(365)$ of these samples. The declining denitrification rates of these aquifer samples resulted possibly from the small contents of residual reduced compounds that might get available due to physical disruption during sampling and incubation. For non-sulphidic aquifer material and all sulphidic aquifer samples from the zone of NO_3^- -free groundwater denitrification rates could be described with zero-order kinetics, suggesting that denitrification

was independent of NO_3^- concentration during incubation of these samples. For the progressing exhaustion of reductants in denitrifying aquifers, it is suspected that the temporal dynamics is governed by the loss of reactive surfaces leading to reduced microbial habitats in the incubated sediment and to reduced denitrification rates, but this needs to be confirmed.

The protective lifetime of denitrification is limited in the investigated locations of the two aquifers but is expected to last for several generations, where the NO_3^- -free anoxic groundwater zone extends over several meters of depth. But where this zone is thin or contains only small amounts of microbial available reduced compounds it is needed to minimize anthropogenic NO_3^- input.

3.6 Supplement to chapter 3:

Predicting the denitrification capacity of sandy aquifers from shorter-term incubation experiments and sediment properties

Other possible electron donors

During incubations Fe and Mn concentrations in the batch solution were always (mostly far) below 1 mg Fe Γ^{-1} and 0,5 mg Mn Γ^{-1} . Only some transition zone samples showed Fe concentrations between 4 and 7 mg Fe Γ^{-1} at the beginning of incubation. The measured concentrations of Fe(II) and Mn(II) in the groundwater at the origin of the samples are below < 0.5 mg Fe Γ^{-1} and < 0.1 mg Mn Γ^{-1} in the oxidized zone of both aquifers. Only in the reduced NO_3^- free zone of both aquifers concentrations of Fe(II) and Mn(II) are higher (1 to 7 mg Fe Γ^{-1} and < 0,1 mg Mn Γ^{-1} in the GKA and 4 to 16 mg Fe Γ^{-1} and 0.1 to 1 mg Mn Γ^{-1} in the FFA). Therefore, only solids like e.g. pyrite are possible sources for the electron donors for NO_3^- reduction in both aquifers and it is assumed that pyrite is the major source for Fe(II). Recently Korom et al. (2012) indicated that non-pyritic ferrous iron might play a more important role for denitrification than considered up to now. They assume that ferrous iron from amphiboles contributed to denitrification with 2–43 % in a glaciofluvial shallow aquifer in North Dakota.

The NH_4^+ concentrations in the groundwater at the sample origins are below detection limit in the GKA and below 0.5 mg N Γ^{-1} at multilevel well N10 in the FFA, it is assumed that NH_4^+ is not a significant electron donor during NO_3^- reduction in both aquifers (see also section 3.4.5.1 and below).

Limitations of the $^{15}\text{NO}_3^-$ labelling approach

For the quantification of denitrification ^{15}N labelled NO_3^- was used during the conducted anaerobic incubations. ^{15}N labelling of nitrate can not completely exclude the possible contribution of dissimilatory nitrate reduction to ammonium (DNRA) followed by anaerobic ammonium oxidation (anammox) to the formation of ^{15}N labelled N_2 from the labelled NO_3^- during anaerobic incubations.

Under strict anaerobic conditions, DNRA is an alternative pathway for the reduction of NO_3^- . But DNRA is seldom reported to be the dominant process of NO_3^- reduction in groundwater systems (Rivett et al., 2008) and chemical modelling by van de Leemput et al. (2011) suggested that DNRA is rather of importance under low NO_3^- concentrations and high C: NO_3^- ratios. But denitrification was presumably not NO_3^- limited since NO_3^- concentrations were always above 1 mg N Γ^{-1} (Wall et al., 2005) during the incubations. DNRA is presumably not an important process during this investigation because the batch

solutions contained only small amounts of NH_4^+ ($< 0,5 \text{ mg N } \Gamma^{-1}$, samples from B2 in depth 8-10 m $\approx 1 \text{ mg N } \Gamma^{-1}$). Also NH_4^+ accumulation was generally not observed during the conducted experiments. Since the incubations were anaerobic NH_4^+ accumulation should be expected if DNRA was a significant contributing process, except anammox consumed the possibly produced NH_4^+ immediately. If significant N_2 production via anammox occurred, this would have been difficult to observe since NH_4^+ and NO_2^- , the educts of this process, came from the same ^{15}N labelled NO_3^- pool in the batch solution. (At the beginning of incubation NO_2^- concentrations were below detection and NH_4^+ concentrations $< 0,5 \text{ mg N } \Gamma^{-1}$, respectively.) If anammox contributed significantly to N_2 production, then also DNRA must have been a significant process with half the turnover rate of anammox.

Contrary to marine environments, where high rates of anammox are reported (Canfield et al., 2010), in freshwater systems there is not much evidence for anammox (van de Leemput et al., 2011; Burgin and Hamilton, 2007). To the best knowledge of the author, there are no studies about anammox in fresh water aquifers, whereas it is reported to exist in wastewater treatment systems, marine sediments and lakes (Jetten et al., 1998; Schubert et al., 2006; Dalsgaard et al., 2005). To distinguish anammox from denitrification during anaerobic incubation experiments ^{15}N labelled NO_2^- might be used.

NH_4^+ concentrations in the groundwater are mostly below detection limit in the GKA and in the reduced zone at multilevel well N10 in the FFA between 0,3 and 0,5 $\text{mg NH}_4^+ \Gamma^{-1}$ (own measurements). Therefore, the possible occurrence of DNRA or DNRA-anammox can not strictly be excluded in both aquifers.

Quantification of total $\text{N}_2+\text{N}_2\text{O}$ production

The molecular ion masses 28 and 29 ($^{28}\text{N}_2$, $^{29}\text{N}_2$) were recorded for IRMS analysis of denitrification derived ^{15}N labelled N_2 and N_2O . The N_2O in the headspace samples was reduced to N_2 in a reduction column prior to the mass spectrometer entrance. The headspace samples were a mixture of unlabeled N_2 und denitrification denitrified ^{15}N labelled N_2 and N_2O . On condition that (i) the ^{15}N abundance of the denitrified NO_3^- is known, (ii) denitrification is the sole gaseous nitrogen forming process and (iii) the amount of N_2 evolved from the ^{15}N labelled NO_3^- pool is small compared with the unlabelled N_2 in the sample, the fraction of denitrified N_2 in a given mixture can be determined by measuring only $^{29}\text{N}_2/^{28}\text{N}_2$ ratios using the equations provided by Mulvaney (1984) (see also discussion in: (Mulvaney, 1984) and (Eschenbach and Well, 2011)). For the measurement of the ^{15}N abundance of the

denitrified NO_3^- and to check for the conditions mentioned above, replicate samples were measured as described in detail in (Well et al., 1998).

The headspace samples represented a mixture of two binomial N_2 isotopologue distributions according to the ^{15}N abundances of the unlabelled N_2 and the ^{15}N labelled denitrification derived ($\text{N}_2+\text{N}_2\text{O}$), respectively. A high frequency discharge unit was then used for online equilibration of N_2 molecules prior to isotope analyses. After equilibration the measured samples consisted of one binomial distribution of N_2 isotopologues according to the total ^{15}N abundance of the mixture. The ^{15}N abundance of the denitrified NO_3^- can then be calculated from the measurement of the $^{29}\text{N}_2/^{28}\text{N}_2$ ratios of unequilibrated and equilibrated replicate samples (Well et al., 1998).

Fit between NO_3^- consumption and ($\text{N}_2+\text{N}_2\text{O}$) production

The NO_3^- decrease during incubations showed the same pattern as the measured production of ($\text{N}_2+\text{N}_2\text{O}$) by GC-IRMS. The measurement of ($\text{N}_2+\text{N}_2\text{O}$) production by GC-IRMS was more precise and had a lower detection limit compared to the measurement of NO_3^- consumption (compare Fig. 3.1a and Fig. S3.3a).

The N balance between the NO_3^- content at the start of incubations and the sum of NO_3^- and denitrification derived ($\text{N}_2+\text{N}_2\text{O}$) concentrations during incubation was for most of the incubated samples $< 1 \text{ mg N / batch assay}$. The samples with the highest measured production of ($\text{N}_2+\text{N}_2\text{O}$) showed also the highest deviation between the amount of NO_3^- consumed and the measured production of ($\text{N}_2+\text{N}_2\text{O}$) (compare Fig. 3.1c and Fig. S3.3c).

Recommendations for future anaerobic incubations

Control of air contamination during incubation experiments

Canfield et al. (2010) recommended to de-aerate rubber septa by boiling them for 24 hours in water and store them in a He atmosphere before use. An elegant way to check for possible air contamination is the measurement of Ar in the headspace of the transfusion bottles during incubation. Increasing Ar concentrations are an indicator of air contaminations during incubation. Unfortunately it was not possible to measure Ar during the incubations, due to instrumental restrictions.

Predicting the denitrification capacity from shorter-term incubations

Table S3.1: Sediment parameters and basic properties of all incubated samples.

Sample location	Depth interval m	SG ^a	SO ₄ ^{2-b} mg S kg ⁻¹	mg C kg				C _{org}	total-S mg S kg ⁻¹	total-N mg N kg ⁻¹	Sand [%]	Silt [%]
				DOC ^c	C _{hws} ^d	C _l ^e	C _{org}					
FFA B1	6.0-7.0	s ⁿ	3.3	7.2	30.3	82.2	643	86	33	95.0	5.0	
FFA B1	7.0-8.0	s	3.3	5.7	32.3	887.0	5955	603	94	94.8	5.2	
FFA B2	2.0-3.0	n s ⁿ	10.2	11.5	20.0	2.7	237	29	26	98.9	0.2	
FFA B2	3.0-4.0	n s ⁿ	25.3	10.2	17.2	2.7	203	38	23	98.9	0.2	
FFA B2	4.0-5.0	n s ⁿ	19.5	8.9	21.6	228.6	545	46	54	96.4	1.3	
FFA B2	8.0-9.0	s ⁿ	0.0	6.9	33.8	93.9	1625	176	31	40.4	59.6	
FFA B2	9.0-10.0	s ⁿ	0.9	6.2	40.0	116.9	538	156	28	94.7	5.3	
FFA B4	7.0-8.0	s	n.d. ¹	n.d. ¹	n.d. ¹	n.d. ¹	483	220	21	97.3	2.7	
FFA B4	8.0-9.0	s	n.d. ¹	n.d. ¹	n.d. ¹	n.d. ¹	1114	359	39	95.4	4.7	
FFA B6	2.0-3.0	n s ⁿ	17.7	11.6	22.1	259.6	695	56	41	97.8	0.6	
FFA B6	3.0-4.0	n s ⁿ	23.3	10.3	21.6	172.5	1047	59	46	97.8	0.4	
FFA N10	4.5-5.0	s ⁿ	5.4	9.2	22.2	462.7	1291	50	87	94.9	1.0	
FFA N10	5.0-5.5	s ⁿ	3.8	9.6	27.6	206.9	737	49	55	98.0	0.3	
FFA N10	5.5-6.0	s ⁿ	12.8	10.8	28.4	160.6	687	49	36	97.4	0.4	
FFA N10	7.7-8.3	s ⁿ	n.d. ¹	n.d. ¹	41.2	n.d. ¹	311	57	10	96.3	3.8	
FFA N10	8.3-8.6	s ⁿ	n.d. ¹	n.d. ¹	42.5	n.d. ¹	320	47	11	97.9	2.2	
FFA N10	10.0-10.4	s	n.d. ¹	n.d. ¹	n.d. ¹	n.d. ¹	310	45	18	96.3	3.7	
FFA N10	10.4-10.7	s	n.d. ¹	n.d. ¹	n.d. ¹	n.d. ¹	5627	464	113	96.4	3.6	
FFA N10	12.0-13.0	s	n.d. ¹	n.d. ¹	0.0	n.d. ¹	2554	558	64	96.7	3.3	
FFA N10	13.0-14.0	s	n.d. ¹	n.d. ¹	39.7	n.d. ¹	1848	588	53	95.1	4.9	
FFA N10	16.0-17.0	s	1.1	5.7	42.6	241.0	2608	448	51	97.2	2.8	
FFA N10	17.0-18.0	s	n.d. ¹	n.d. ¹	41.1	n.d. ¹	2504	441	48	96.9	3.1	
GKA	8.0-9.0	n s ⁿ	14.5	8.1	18.3	1.8	102	54	9	96.8	1.4	
GKA	9.0-10.0	n s ⁿ	14.5	9.0	14.9	0.9	76	38	6	97.3	0.9	
GKA	22.0-23.0	n s ⁿ	11.1	8.6	43.8	221.3	176	42	15	95.4	1.2	
GKA	23.0-24.0	n s ⁿ	10.8	9.4	33.7	50.3	192	36	23	96.0	0.9	
GKA	25.9-27.0	s	8.2	6.1	31.1	1021.2	2553	682	69	87.6	12.4	
GKA	27.0-28.3	s	4.8	5.8	39.0	1531.1	6373	989	127	79.6	20.4	
GKA	28.3-29.3	s	10.3	8.1	27.4	2504.9	4159	883	114	76.8	21.3	
GKA	29.3-30.3	s	12.7	6.6	26.2	2205.8	4543	760	96	83.9	14.2	
GKA	30.3-31.2	s	13.6	5.2	28.9	347.7	784	509	14	97.6	2.2	
GKA	31.3-32.0	s	18.1	9.9	42.6	192.0	834	494	27	96.5	3.2	
GKA	32.9-33.7	s	20.2	5.1	20.8	377.4	821	630	23	96.9	2.8	
GKA	33.7-34.7	s	15.6	5.3	29.2	150.5	752	510	17	98.5	1.4	
GKA	35.7-36.7	s	2.2	5.4	32.0	2391.1	8972	708	120	96.9	3.1	
GKA	36.7-37.7	s	5.1	5.5	22.4	37.7	232	677	3	98.8	1.2	
GKA	37.7-38.7	s	0.5	4.7	23.2	447.4	1162	379	30	97.8	2.3	
GKA	65.1-65.4	s	1.8	6.2	23.7	239.8	1009	716	39	89.4	10.7	
GKA	67.1-67.5	n s	0.3	6.9	56.5	132.1	358	196	21	92.1	7.9	
GKA	67.5-68.0	n s	3.5	5.2	58.5	n.d. ¹	377	194	44	94.7	5.3	

^a sediment group; ^b extractable sulphate-S; ^c extractable dissolved organic carbon; ^d extractable hot-water soluble carbon; ^e KMnO₄ labile organic carbon; ¹ n.d.: not determined; n s non-sulphidic; s sulphidic aquifer material, n s and s with the subscript n indicates NO₃⁻-bearing samples.

Table S3.2: Denitrification rates, cumulative denitrification, stock of reduced compounds, sulphate formation capacity and estimated minimal lifetime of denitrification of all incubated samples.

Sample location	Depth interval m	SG ^a	$D_r(7)^b$	$D_{cum}(365)^d$	SRC ^e	SRC _C ^f	SRC _S ^g	aF_{SRC}^h	SFC ⁱ	em_{LoD}^j yr
			$\mu\text{g N kg}^{-1} \text{d}^{-1}$	$\text{mg N kg}^{-1} \text{yr}^{-1}$						
FFA B1	6.0-7.0	s ⁿ	51.66	17.18	659.6	599.5	60.1	2.60	6.1	5.0
FFA B1	7.0-8.0	s	33.89	56.24	5974.2	5552.7	421.5	0.94	39.4	44.8
FFA B2	2.0-3.0	n s ⁿ	1.27	0.19	240.8	220.7	20.1	0.08	0.1	1.8
FFA B2	3.0-4.0	n s ⁿ	2.12	0.37	215.4	189.2	26.3	0.17	-0.1	1.6
FFA B2	4.0-5.0	n s ⁿ	35.27	4.34	540.2	508.0	32.2	0.80	1.0	4.1
FFA B2	8.0-9.0	s ⁿ	21.05	10.53	1638.2	1515.5	122.7	0.64 ^(10.0)	3.5	12.3
FFA B2	9.0-10.0	s ⁿ	41.41	12.68	610.7	502.0	108.7	2.08 ^(26.4)	2.2	4.6
FFA B4	7.0-8.0	s	45.67	20.16	603.6	450.2	153.4	3.34	9.6	4.5
FFA B4	8.0-9.0	s	25.24	34.09	1289.5	1038.9	250.7	2.64	22.0	9.7
FFA B6	2.0-3.0	n s ⁿ	11.53	2.64	687.0	648.9	39.1	0.38	0.3	5.2
FFA B6	3.0-4.0	n s ⁿ	6.93	1.46	1017.4	976.5	40.9	0.14	0.1	7.6
FFA N10	4.5-5.0	s ⁿ	35.97	8.69	1239.0	1204.1	34.8	0.70	1.5	9.3
FFA N10	5.0-5.5	s ⁿ	61.03	8.75	721.6	687.1	34.5	1.21	2.1	5.4
FFA N10	5.5-6.0	s ⁿ	36.99	7.82	674.6	640.3	34.3	1.16	5.2	5.1
FFA N10	7.7-8.3	s ⁿ	33.71	15.04	329.5	290.0	39.5	4.56	1.5	2.5
FFA N10	8.3-8.6	s ⁿ	20.25	15.17	331.5	298.7	32.9	4.58	6.9	2.5
FFA N10	10.0-10.4	s	12.34	17.45	320.6	289.3	31.3	5.44	5.4	2.4
FFA N10	10.4-10.7	s	23.75	50.07	5571.6	5247.7	323.9	0.90	9.4	41.8
FFA N10	12.0-13.0	s	26.47	52.84	2771.3	2381.7	389.6	1.91	37.9	20.8
FFA N10	13.0-14.0	s	35.58	38.04	2134.1	1723.3	410.8	1.78	18.2	16.0
FFA N10	16.0-17.0	s	69.90	46.65	2744.7	2431.5	313.2	1.70 ^(6.3)	23.6	20.6
FFA N10	17.0-18.0	s	34.48	46.55	2642.7	2335.0	307.8	1.76 ^(6.3)	36.8	19.8
GKA	8.0-9.0	n s ⁿ	0.81	0.63	132.6	95.0	37.6	0.47	0.9	1.0
GKA	9.0-10.0	n s ⁿ	0.71	0.34	97.1	70.7	26.4	0.35	0.4	0.7
GKA	22.0-23.0	n s ⁿ	14.68	1.57	193.3	164.2	29.1	0.81	0.2	1.5
GKA	23.0-24.0	n s ⁿ	31.77	2.83	204.5	179.2	25.3	1.38	0.0	1.5
GKA	25.9-27.0	s	26.36	15.63	2857.4	2381.0	476.4	0.55	1.2	21.4
GKA	27.0-28.3	s	29.43	41.82	6634.0	5943.2	690.8	0.63 ^(4.9)	8.3	49.8
GKA	28.3-29.3	s	46.38	37.82	4495.6	3878.5	617.2	0.84 ^(7.3)	13.8	33.7
GKA	29.3-30.3	s	57.08	35.49	4766.8	4236.0	530.8	0.74 ^(6.4)	8.1	35.8
GKA	30.3-31.2	s	26.07	6.54	1086.9	731.4	355.4	0.60	3.8	8.2
GKA	31.3-32.0	s	14.06	4.09	1122.4	777.7	344.7	0.36	5.0	8.4
GKA	32.9-33.7	s	38.39	7.28	1206.0	765.6	440.4	0.60	10.2	9.1
GKA	33.7-34.7	s	62.14	12.25	1057.4	700.9	356.6	1.16	17.7	7.9
GKA	35.7-36.7	s	64.30	52.46	8861.3	8366.7	494.6	0.59 ^(4.6)	30.0	66.5
GKA	36.7-37.7	s	87.51	11.07	689.6	216.7	472.8	1.60	9.2	5.2
GKA	37.7-38.7	s	109.2	12.06	1347.7	1083.1	264.7	0.89 ^(15.3)	4.6	10.1
GKA	65.1-65.4	s	33.12	13.22	1441.2	941.3	499.9	0.92	1.3	10.8
GKA	67.1-67.5	n s	30.54	8.18	471.0	333.8	137.2	1.74	1.3	3.5
GKA	67.5-68.0	n s	23.62	8.11	487.1	351.5	135.6	1.67	0.7	3.7

^a sediment group; ^b initial denitrification rate; ^c average denitrification rate after one year; ^d cumulative denitrification after one year; ^e depot of reactive compounds (SRC); ^f concentration of reduced compounds derived from measured C_{org} ; ^g concentration of reduced compounds derived from total-S values; ^h fraction of SRC available for denitrification during one year of incubation, in parenthesis aF_{SRC} from the intensive treatment; ⁱ sulphate formation capacity (SFC); ^j estimated minimal lifetime of denitrification; n s non-sulphidic; s sulphidic aquifer material, n s and s with the subscript n indicates NO_3^- -bearing samples.

Predicting the denitrification capacity from shorter-term incubations

Table S3.3: Simple regression between $D_{\text{cum}}(365)$ and sediment parameters (X), $f^{B-C}(D_{\text{cum}}(365)) = A + B \times f^{B-C}(X)$. Regressions with C_{org} , total-S are listed for each partial data set. Regression with a third independent sediment variable are only given, if correlation coefficient were better compared to correlations with C_{org} or total-S.

Data set	X ^a	N ^b	R ^c	A	B
Whole data set	C_{org}	151	0.80	-11.022	2.654
whole data set	total-S	151	0.71	-2.397	0.805
whole data set	C_1	111	0.83	-1.028	0.492
FFA	C_{org}	86	0.72	-26.950	8.017
FFA	total-S	86	0.83	-14.879	6.312
FFA	DOC_{extr}	46	0.84	10.503	-0.495
GKA	C_{org}	65	0.93	-9.525	2.457
GKA	total-S	65	0.86	-0.252	0.026
GKA	C_1	65	0.93	-0.730	0.416
non-sulphidic	C_{org}	44	0.52	-5.434	1.205
non-sulphidic	total-S	44	0.77	-231.440	284.854
non-sulphidic	C_{hws}	44	0.77	-164.600	233.898
sulphidic	C_{org}	107	0.66	-3.097	1.293
sulphidic	total-S	107	0.40	2.747	0.001
sulphidic	C_1	67	0.60	-0.119	0.638
NO_3^- -bearing	C_{org}	64	0.58	-4.946	0.661
NO_3^- -bearing	total-S	64	0.67	-268.670	312.977
NO_3^- -bearing	C_1	56	0.73	-0.737	0.267
NO_3^- -free	C_{org}	87	0.77	-5.862	1.623
NO_3^- -free	total-S	87	0.32	3.741	0.004
transition zone	C_{org}	28	0.58	18.117	-4.020
transition zone	total-S	28	0.20	-178.180	277.350
transition zone	C_1	20	0.73	192.880	-190.340

^a Independent sediment parameter

^b Sample number

^c Correlation coefficient.

Table S3.4: Ratios of modelled $D_{\text{cum}}(365)$ vs measured $D_{\text{cum}}(365)$ (group means with standard deviation, ranges in parentheses) for samples with high ($> 20 \text{ mg N kg}^{-1}$) and low $D_{\text{cum}}(365)$ ($< 20 \text{ mg N kg}^{-1}$).

Data set	Modelled $D_{\text{cum}}(365)$ /Measured $D_{\text{cum}}(365)$					
	Multiple regressions			Simple regressions		
	Selection I ^a	Selection II ^b	Selection III ^c	C _{org}	Total-S	best ^d
	$D_{\text{cum}}(365) \geq 20 \text{ mg N kg}^{-1} \text{ yr}^{-1}$					
Whole data set	0.88 ±0.33 (0.33 – 1.67)	0.89 ±0.28 (0.39 – 1.26)	0.87 ±0.24 (0.55 – 1.30)	0.86 ±0.32 (0.29 – 1.53)	0.68 ±0.25 (0.42 – 1.54)	0.83 ±0.38 (0.22 – 1.35)
FFA	0.86 ±0.12 (0.71 – 1.26)	0.86 ±0.50 (0.79 – 0.93)	0.84 ±0.07 (0.74 – 0.94)	0.71 ±0.17 (0.30 – 1.08)	0.86 ±0.15 (0.68 – 1.29)	0.57 ±0.06 (0.49 – 0.66)
GKA	0.89 ±0.33 (0.41 – 1.47)	1.14 ±0.18 (0.78 – 1.38)	1.08 ±0.19 (0.79 – 1.34)	1.14 ±0.19 (0.88 – 1.46)	0.84 ±0.30 (0.39 – 1.38)	1.13 ±0.26 (0.67 – 1.51)
sulphidic	0.73 ±0.22 (0.44 – 1.35)	0.78 ±0.16 (0.57 – 1.13)	1.15 ±0.38 (0.81 – 2.05)	0.74 ±0.22 (0.43 – 1.36)	0.33 ±0.09 (0.23 – 0.68)	0.66 ±0.25 (0.28 – 1.19)
	$D_{\text{cum}}(365) < 20 \text{ mg N kg}^{-1} \text{ yr}^{-1}$					
Whole data set	2.29 ±3.06 (0.20 – 18.28)	1.90 ±2.27 (0.17 – 11.08)	1.38 ±1.02 (0.34 – 6.23)	2.69 ±4.40 (0.23 – 26.07)	3.03 ±3.85 (0.20 – 18.32)	1.72 ±1.49 (0.23 – 8.79)
FFA	2.52 ±3.03 (0.23 – 12.41)	1.77 ±1.44 (0.34 – 5.69)	1.14 ±0.66 (0.26 – 3.41)	3.56 ±4.90 (0.24 – 20.27)	2.63 ±3.39 (0.25 – 13.64)	2.19 ±2.53 (0.18 – 11.82)
GKA	1.73 ±1.29 (0.31 – 5.51)	1.35 ±0.71 (0.23 – 3.10)	1.19 ±0.43 (0.30 – 2.16)	1.39 ±0.82 (0.23 – 3.99)	1.76 ±1.38 (0.34 – 6.02)	1.35 ±0.68 (0.23 – 3.02)
non-sulphidic	1.36 ±1.04 (0.18 – 5.23)	1.36 ±1.04 (0.18 – 5.23)	1.09 ±0.45 (0.52 – 0.45)	1.94 ±2.39 (0.21 – 10.45)	1.47 ±1.00 (0.18 – 8.25)	1.55 ±0.94 (0.24 – 7.26)
sulphidic	1.49 ±0.84 (0.51 – 4.33)	1.29 ±0.66 (0.33 – 3.13)	1.39 ±0.60 (0.43 – 3.19)	1.48 ±0.84 (0.50 – 4.36)	1.27 ±0.61 (0.69 – 3.69)	1.46 ±0.76 (0.44 – 3.49)
transition zone	1.03 ±0.22 (0.71 – 1.52)	1.03 ±0.22 (0.67 – 1.56)	1.01 ±0.13 (0.84 – 1.27)	1.05 ±0.27 (0.64 – 1.77)	1.07 ±0.32 (0.67 – 1.73)	1.03 ±0.24 (0.72 – 1.58)

^a C_{org} and total-S;^b two sediment parameters giving highest correlation coefficient;^c stepwise multiple regression;^d simple regression with the sediment parameter giving the best correlations with $D_{\text{cum}}(365)$.**Table S3.5:** Lambda values of the Box-Cox transformed sediment parameters.

Data set	Lambda values											
	$D_t(7)$	$D_t(84)$	$D_t(168)$	$D_{\text{cum}}(365)$	silt	C _{org}	total-S	SO ₄ ²⁻ _{extr}	DOC _{extr}	C _{hws}	C _l	SRC
Whole data set	0.512	0.346	0.341	0.294	0.021	-0.056	0.132	0.700	-0.213	0.040	0.171	-0.024
FFA	0.626	0.441	0.428	0.370	0.007	-0.176	-0.196	0.347	1.426	0.811	0.364	-0.185
GKA	0.503	0.345	0.259	0.208	-0.206	-0.080	0.750	0.670	-0.789	-0.133	0.170	0.039
non-sulphidic	0.220	0.100	0.172	0.106	-0.069	-0.050	-1.217	0.784	0.732	-1.400	0.758	1.492
sulphidic	0.219	0.209	0.305	-0.06	-0.067	-0.111	1.100	0.358	-2.02	0.635	-0.059	0.229
NO ₃ ⁻ -bearing	0.408	0.134	0.221	0.235	-0.210	0.108	-1.145	0.650	1.401	-0.039	0.261	0.797
NO ₃ ⁻ -free	0.160	0.103	0.313	0.144	-0.337	-0.017	0.950	0.214	-2.422	-0.335	0.230	0.492

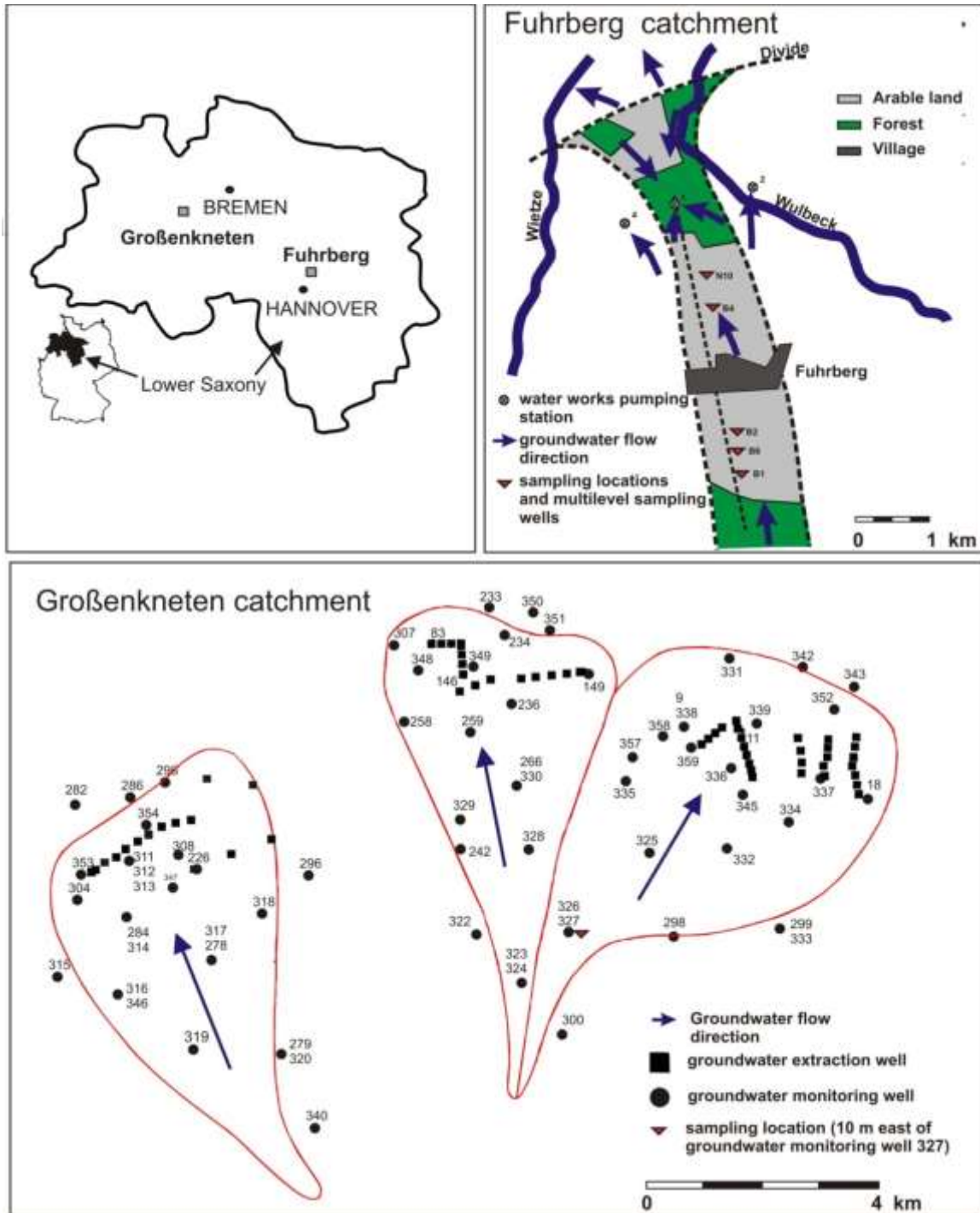


Fig. S3.1: Sampling locations within the Fuhrberger Feld and Großenkneten catchment in Lower Saxony (Germany).

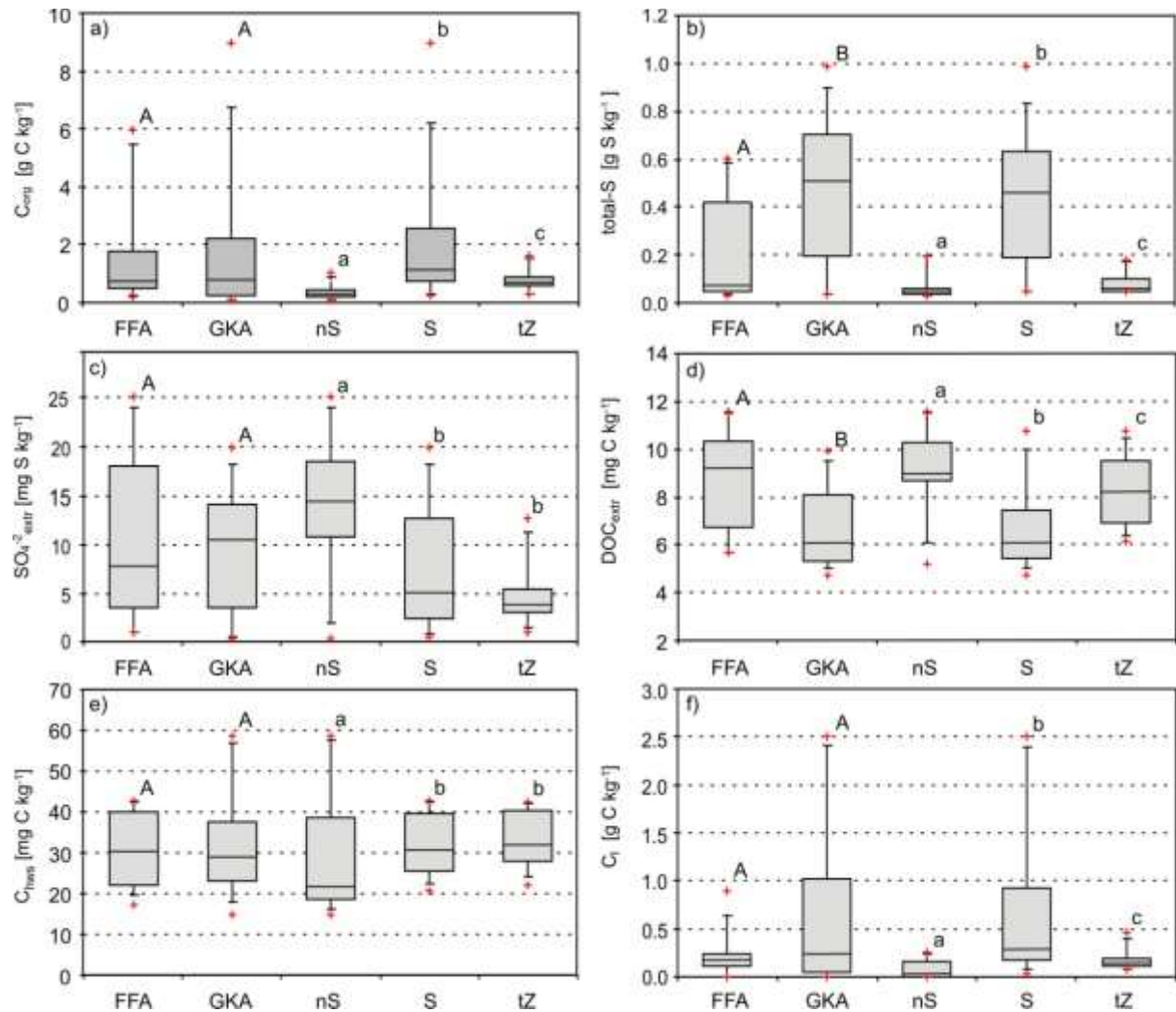


Fig. S3.2: Distribution of different sediment parameters in the aquifer material from the Fuhrberger Feld aquifer (FFA) and the Großenkneten aquifer (GKA) and in the various established groups of aquifer material: a) organic carbon, b) total sulphur, c) extractable sulphate, d) extractable dissolved organic carbon, e) hot water soluble organic carbon, f) potassium permanganate labile organic carbon. n S, S and tZ indicate non-sulphidic -, sulphidic and transition zone aquifer material, respectively. Different uppercase letters above the box-plots indicate significant differences between FFA and GKA material, different small letters show significant differences between n S, S and tZ (Kruskal-Wallis-Test ($P < 0.05$)).

Predicting the denitrification capacity from shorter-term incubations

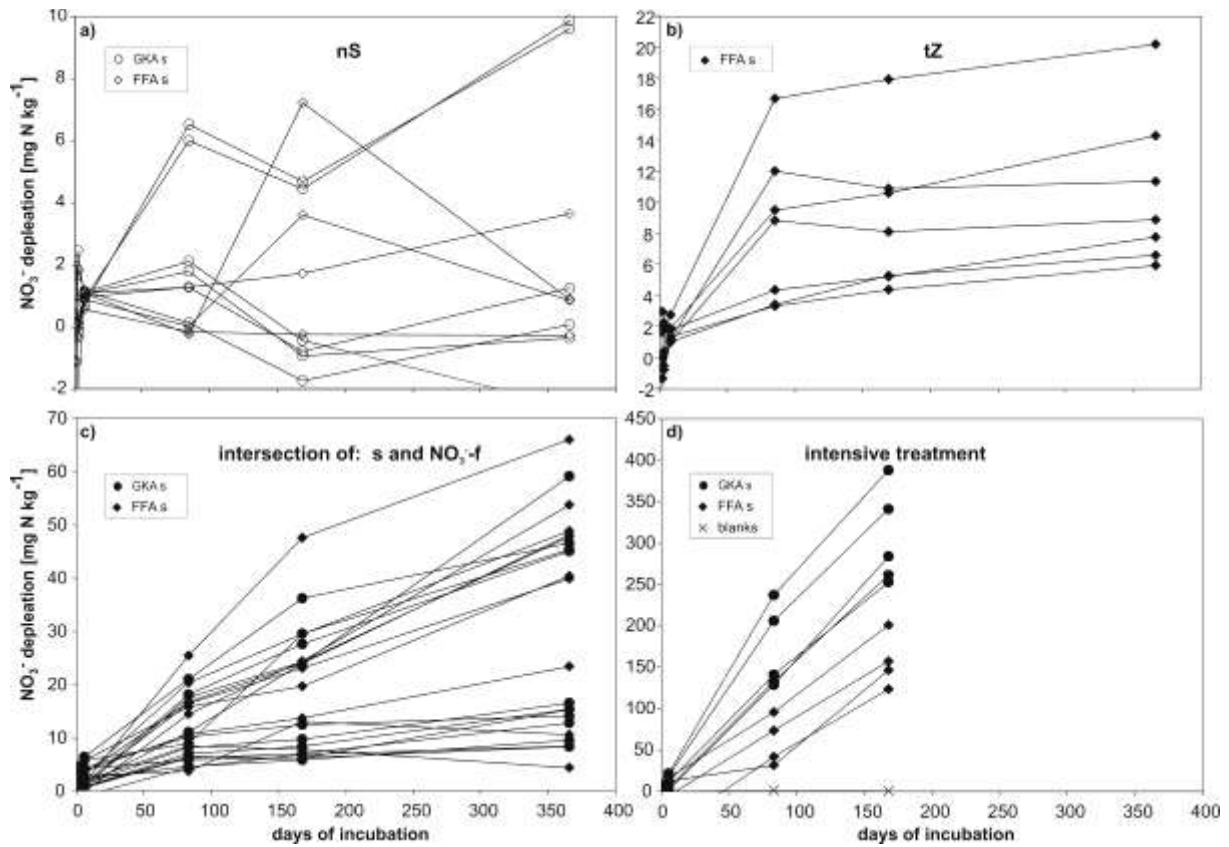


Fig. S3.3: Measured NO_3^- consumption during incubations. (The NO_3^- concentrations at the last sampling date of intensive incubations were not measured.)

4 Predicting the denitrification capacity of sandy aquifers from in situ measurements using push-pull ^{15}N tracer tests

Abstract

Knowledge about the spatial variability of in situ denitrification rates ($D_r(\text{in situ})$) and their relation to the denitrification capacity in nitrate-contaminated aquifers is crucial to predict the development of groundwater quality. Therefore, 28 push-pull ^{15}N tracer tests for the measurement of in situ denitrification rates were conducted in two sandy Pleistocene aquifers in Northern Germany. In situ denitrification rates were compared with laboratory measurements. Therefore, aquifer material from the same locations and depths as the push-pull injection points was incubated and initial and average denitrification rates and the cumulative denitrification after one year of incubation ($D_{\text{cum}}(365)$) of these aquifer samples as well as the stock of reduced compounds (SRC) was compared with in situ measurements of denitrification. This was done to derive transfer functions suitable to predict $D_{\text{cum}}(365)$ and SRC from $D_r(\text{in situ})$.

$D_r(\text{in situ})$ ranged from 0 to $51.5 \mu\text{g N kg}^{-1} \text{d}^{-1}$ and were significantly higher in the sulphidic zone of both aquifers compared to the zone of non-sulphidic aquifer material. Overall regressions between the $D_{\text{cum}}(365)$ and SRC of the tested aquifer material with $D_r(\text{in situ})$ exhibited only a modest linear correlation for the full data set. But the predictability of $D_{\text{cum}}(365)$ and SRC from $D_r(\text{in situ})$ data clearly increased for aquifer samples from the zone of NO_3^- -bearing groundwater.

In the NO_3^- -free aquifer zone a lag phase of denitrification after NO_3^- injections was observed, which confounded the relationship between reactive compounds and in situ denitrification activity. This finding was attributed to adaptation processes in the microbial community after NO_3^- injections, because NO_3^- can then be used as new available electron acceptor. This lag phase resulted in poor prediction of $D_{\text{cum}}(365)$ and SRC. Exemplarily, it was demonstrated that the microbial community in the NO_3^- -free zone close below the NO_3^- -bearing zone can be adapted to denitrification by amending wells with NO_3^- -injections for an extended period. In situ denitrification rates were 30 to 65 % higher after pre-conditioning with NO_3^- . Results from this study suggest that pre-conditioning is crucial for the measurement of $D_r(\text{in situ})$ in deeper aquifer material from the NO_3^- -free groundwater zone and for the predictability of $D_{\text{cum}}(365)$ and SRC from $D_r(\text{in situ})$ of such aquifer material.

Chapter 4

Further research is needed to evaluate transferability of the derived model functions to other aquifers and to confirm the feasibility of pre-conditioning in deeper aquifers that have not been in contact with NO_3^- .

4.1 Introduction

Denitrification, the microbial mediated reduction of nitrate (NO_3^-) and nitrite (NO_2^-) to the nitrogen gasses nitric oxide (NO), nitrous oxide (N_2O) and dinitrogen (N_2) is important to water quality and chemistry at landscape, regional and global scales (Groffman et al., 2006). NO_3^- is quantitatively the most abundant reactive nitrogen species. Diffuse NO_3^- emissions from the agricultural sector are the dominant source of Nr^3 fluxes to aquifers. Denitrification in aquifers, reviewed e.g. by Korom (1992), Hiscock et al. (1991), (Burgin and Hamilton, 2007), Rivett et al. (2008), ranges from 0 to 100% of total NO_3^- input with a high spatial variability (Seitzinger et al., 2006). This leads to the question, how individual aquifers will respond to the anthropogenic NO_3^- pollution of groundwater. Not only the questions how rates of denitrification will respond to Nr loading (Seitzinger et al., 2006) and where and how long denitrification in aquifers can remediate NO_3^- pollution (Kölle et al., 1985) are of importance. Since continuous NO_3^- input via seepage waters leads to ongoing exhaustion of the reductive capacity of aquifers. This can be a problem for keeping the standard for NO_3^- in drinking water ($<50 \text{ mg } \Gamma^{-1}$, Drinking Water Directive 98/83/EC) and due to possible eutrophication of water bodies (Vitousek et al., 1997). But NO_3^- can also mobilise unforeseen species such as uranium (U) which can be mobilised if NO_3^- reaches reduced aquifer zones (Senko et al., 2002; Istok et al., 2004). Therefore, knowledge about the denitrification capacity of aquifers is needed to predict the possible development of ground water quality.

The presented study compares in situ denitrification rates measured in two sandy Pleistocene aquifers in Northern Germany (Fuhrberger Feld aquifer (FFA) and the aquifer of Großenkneten (GKA)) with laboratory measurements of denitrification of aquifer samples from this two aquifers (Eschenbach and Well, 2013). Frind et al. (1990) reported that due to lithotrophic denitrification, NO_3^- has a half-life of 1 to 2 years in the deeper zone (below 5 to 10 m) of the well investigated Fuhrberger Feld aquifer. Weymann et al. (2010) reported very low denitrification rates with values as low as $4 \mu\text{g N kg}^{-1} \text{ d}^{-1}$ in the surface near groundwater, in the organotrophic denitrification zone of the same aquifer. In a recent study Eschenbach and Well (2013) measured median denitrification rates of 15.1 and $9.6 \text{ mg N kg}^{-1} \text{ yr}^{-1}$ during one year anaerobic incubations of FFA and GKA aquifer samples, with significantly higher denitrification rates in the deeper parts of both aquifers. This study and Konrad (2007) showed that the cumulative denitrification after prolonged incubation of

³ The term reactive nitrogen is used in this work in accordance with Galloway et al. (2004) and includes all biologically or chemically active N compounds like reduced forms (e.g. NH_3 , NH_4^+), oxidized forms (e.g. NO_x , HNO_3 , N_2O , NO_3^-) and organic compounds (e.g. urea, amines, proteins...).

aquifer samples is partially highly significant correlated to the stock of reduced compounds (SRC) and this is for a data set of few samples also reported for the correlation of in situ denitrification rates and the SRC (Konrad, 2007). Good correlation between initial laboratory denitrification rates of incubated aquifer material and the SRC was obtained from aquifer zones where NO_3^- is present and the microbial community is hence adapted to NO_3^- as an available electron acceptor. In contrast, samples from NO_3^- -free zone showed a lag time of denitrification of several weeks during incubations (Eschenbach and Well, 2013) possibly due to the initial absence of denitrifying enzymes.

In this study laboratory measurements of denitrification rates and related sediment parameters (Eschenbach and Well, 2013) are compared with in situ measurements of denitrification rates at the origin of the incubated aquifer samples.

In situ denitrification rates can be measured using single well push-pull tests. These tests, perhaps first used for the in situ measurement of denitrification rates by Trudell et al. (1986), have proven to be a relatively low-cost instrument to obtain quantitative information about several aquifer properties. Briefly, during push-pull tests the test solution containing solutes of interest is rapidly injected into a well (push-phase). During a subsequent longer period the test solution-groundwater mixture is sampled (pull-phase). Conservative tracers like Bromide (Br^-) are added to the test solution prior to injection to account for mixing with ambient groundwater. This method was applied in a variety of studies to derive in situ denitrification rates indirectly by the measurement of NO_3^- depletion during push-pull tests (Trudell et al., 1986; Istok et al., 1997; Schroth et al., 2001; McGuire et al., 2002; Harris et al., 2006; Istok et al., 2004). In comparison only a limited number of studies directly measured denitrification rates from the gaseous denitrification products (Sanchez-Perez et al., 2003; Kneeshaw et al., 2007; Well and Myrold, 2002; Addy et al., 2002; Well et al., 2003; Addy et al., 2005; Kellogg et al., 2005; Konrad, 2007; Well and Myrold, 1999). Beside the study of Konrad (2007) these push-pull tests were only conducted in surface near groundwater.

Well et al. (2005) showed that in situ denitrification rates measured with the push-pull ^{15}N tracer method in the saturated zone of hydromorphic soils agreed relatively well with denitrification rates measured in parallel soil samples. Konrad (2007) reported a close correlation between in situ denitrification rates and the cumulative denitrification after at least one year of incubation based on a small number of only 5 comparisons, so the data set was too small to derive robust transfer functions.

Since denitrification is a microbial mediated redox reaction, it is straightforward that the composition, activity and amount of microbes in aquifers should directly influence the

measured denitrification rates during single well push-pull tests. But it is not known to which extent the state of microbial community influences the feasibility of push-pull tests for the measurement of reliable in situ denitrification rates.

Steep gradients in the composition of microbial communities resulting from the distribution and availability of electron donors and acceptors in aquifers are reported to occur in aquifers (Kölbelboelke et al., 1988; Griebler and Lueders, 2009; Santoro et al., 2006). Law et al. (2010) reported substantial changes in the microbial community composition after the begin of denitrification and the transition from denitrification to Fe(III)-reduction within incubated aquifer material. Higher microbial activities after bio stimulation of indigenous microorganisms by the injection of electron donors into aquifers was reported by Istok et al. (2004), Kim et al. (2005) und Kim et al. (2004). Compared with preceding push-pull tests at the same groundwater monitoring wells, the multiple injection of electron donors increased the reduction rates of NO_3^- , pertechnetate (Tc(VII)) and U(VI) measured during subsequent push-pull tests in a shallow unconfined silty-clayey aquifer (Istok et al., 2004). Trudell et al. (1986) found increasing denitrification rates during a 12-day push-pull test in NO_3^- -free groundwater suggesting that the microbial community needed a certain time to adapt to NO_3^- before denitrification could proceed at a rate equivalent to the availability of reduced compounds.

This study is the second part of combined approach (a) to quantify exhaustibility of the denitrification capacity in aquifers, (b) to investigate controlling factors and derive predictive models during incubation experiments, and (c) to check if the cumulative denitrification measured after one year of incubation ($D_{\text{cum}}(365)$) (Eschenbach and Well, 2013) can be derived from in situ denitrification rates measured with push-pull tracer tests. Here a study on (c) is presented. The specific objectives of this study are (i) to measure in situ denitrification rates with push-pull ^{15}N tracer tests at groundwater monitoring wells, (ii) to develop regression models to predict $D_{\text{cum}}(365)$ as well as the stock of reduced compounds from in situ denitrification rates (iii) to test an approach to adapt the microbial community in NO_3^- -free aquifer zones to NO_3^- as a new available electron donor during experiments as a means of conditioning prior to subsequent push-pull ^{15}N tracer tests

4.2 Materials and methods

4.2.1 Study sites

In situ measurements of denitrification were conducted in the Fuhrberger Feld aquifer (FFA) and the Großenkneten aquifer (GKA). Both aquifers are located in drinking water catchment areas in the North of Germany. The FFA is situated about 30 km NE of the city of Hanover and the GKA about 30 km SW of the city of Bremen. Both aquifers consist of carbonate free, Quaternary sands and the deeper parts of the GKA additionally of carbonate free marine sands (Pliocene). The thickness of the FFA and GKA is 20 to 40 m and 60 to 100 m, respectively. Both aquifers are unconfined and contain unevenly distributed amounts of microbial available sulphides and organic carbon. Intense agricultural land use leads to considerable NO_3^- inputs to the groundwater of both aquifers (Böttcher et al., 1989; van Berk et al., 2005; Schuchert, 2007). Groundwater recharge is 250 mm yr^{-1} in the FFA (Wessolek et al., 1985) and 200 to 300 mm yr^{-1} in the GKA (Schuchert, 2007).

Evidence of an intense ongoing denitrification within the FFA is given by NO_3^- and redox gradients (Böttcher et al., 1992) as well as excess- N_2 measurements (Weymann et al., 2008). The FFA can be divided into two hydro-geochemical zones, the zone of organotrophic denitrification near the groundwater surface with organic carbon (C_{org}) as electron donor and a deeper zone of predominantly lithotrophic denitrification with pyrite as electron donor (Böttcher et al., 1991; Böttcher et al., 1992). Detailed information about the FFA is given by Strebel et al. (1992), Frind et al. (1990) and von der Heide et al. (2008). The geological structure of the GKA is described in Howar (2005) and Wirth (1990). Extended zones with oxidizing and reducing conditions in the groundwater are evident in the GKA (van Berk et al., 2005) but their distribution within the aquifer is more complex as in the FFA. But denitrification is known to occur in the zone of reduced groundwater (van Berk et al., 2005). Own excess- N_2 measurements (Well et al., 2012) at monitoring wells prove intense denitrification within the GKA. But there are no studies on the type of denitrification in this aquifer.

4.2.2 Single well push-pull ^{15}N tracer tests

To quantify in situ denitrification rates ($D_r(\text{in situ})$), a total of 28 single well push-pull ^{15}N tracer tests, afterwards referred to as push-pull tests, were performed in the FFA and GKA (Table 4.1) by injecting ^{15}N labelled NO_3^- tracer solution into groundwater monitoring wells. In the FFA, push-pull tests were conducted at multilevel wells consisting of PE tubings (4 mm ID) (Böttcher et al., 1985). Each of these tubings were connected to a filter element at the respective depth. In the GKA, conventional groundwater monitoring wells were used (101 mm ID) with 1 to 4 m long filter screens and multilevel wells (CMT multilevel system, Soilinst, Georgetown, Canada) consisting of PE pipes with 3 individual channels (13 mm ID) with 25 cm long filter screens at the end. Each channel ended in a different depth. To allow a direct comparison with a previous laboratory incubation study (Eschenbach and Well, 2013), wells from the same locations and with filter screens at the same depth where the aquifer samples had been collected were selected in the FFA and GKA. In situ experiments were conducted principally as described in previous studies (Addy et al., 2002; Trudell et al., 1986; Well et al., 2003).

Table 4.1: Overview of the conducted push-pull ^{15}N tracer tests in both aquifers and depth position of their filter screens. Push-pull tests with and without pre-conditioning were conducted at multilevel well B4 in 7, 8, 9 and 10 m below soil surface.

Monitoring well	Fuhrberg (multilevel wells)					Großenkneten (conventional monitoring and multilevel wells)					
	B1	B2	B4	B6	N10	Gro 326	Gro 327	S1	S2	CMT 1	CMT 2
	position of the filter screen in m below soil surface										
Non-sulphidic zone (NO_3^- -bearing zone)		3		3		8-10					8.3
		4.2		6							22.8
Transition zone (NO_3^- -bearing zone)		8			5						
		9									
		10			8						
Sulphidic zone (NO_3^- -free zone)	7	14	7*			35-39	66-67	26-27			26.8
	8		8, 8*								29.3
			9, 9*								31.3
			10*								33.5

* Push-pull tests with pre-conditioning.

Sampling

In case of multilevel wells groundwater and tracer solution were extracted with a peristaltic pump (Masterflex COLE-PARMER, Vernon Hills, USA). A submersible pump (GRUNDFOS MP1, Bjerringbro, Denmark) was used for common groundwater monitoring wells.

During sampling an outflow tubing with the extracted groundwater or tracer solution was placed at the bottom of 26 mL or 120 ml serum bottles (multilevel wells and common groundwater monitoring wells, respectively). After an overflow of at least three times the volume of these bottles, the tubing was removed and the bottles were immediately sealed air tight with grey butyl rubber septa (ALTMANN, Holzkirchen, Germany) and aluminium crimp caps. 4 replications were collected per sampling. Groundwater was sampled from the injection depth prior to each push-pull test.

Push-pull tests

A single well push-pull test consists of the injection of a tracer solution into a monitoring well (push-phase) and the extraction of the mixture of test solution and groundwater from the same well.

push-phase

To prepare the tracer solution, 50 l of groundwater were extracted from multilevel wells (FFA and GKA) or 220 l at common groundwater monitoring wells (GKA) for each push-pull test (Fig. 4.1). The groundwater was pumped to a stainless steel storage container (Type BO 220 l, SPEIDEL, Offerdingen, Germany), which was equipped with a floating lid to avoid gas exchange with the atmosphere and thus maintain the dissolved gas composition of the extracted groundwater. After extraction, a stock solution of deionised water (100 ml) with dissolved ^{15}N labelled potassium nitrate (KNO_3 with 60 atom % ^{15}N) and potassium bromide (KBr) was added to attain a concentration of $10 \text{ mg } ^{15}\text{N} \text{ labelled } \text{NO}_3^- \text{-N } \Gamma^{-1}$ and $10 \text{ mg } \text{Br}^- \Gamma^{-1}$, respectively. The mixture of the stock solution and the extracted groundwater is hereinafter referred to as tracer solution. The tracer solution was mixed for 1 hour with a submersible pump (submersible pump Gigant, Eijkelkamp, Giesbeek, The Netherlands) within the stainless steel storage container. The extracted groundwater at push-pull measuring points located in the NO_3^- -bearing groundwater zone (NO_3^- -bearing zone) contained varying concentrations of NO_3^- (Table 4.2). Consequently, the NO_3^- in the tracer solution of these push-pull tests was a mixture of natural and ^{15}N enriched NO_3^- and NO_3^- concentrations in

these tracer solutions were $> 10 \text{ mg NO}_3^- \text{-N } \Gamma^{-1}$ (see discussion about influence of NO_3^- concentrations on denitrification rates in section 4.4.2 and in Eschenbach and Well (2013)).

During injection, the outflow of the stainless steel storage container was connected with tygon tubings to the selected depths of the multilevel wells. For common groundwater monitoring wells the submersible pump was connected with a pump riser pipe and an inflatable packer (Packer set, UIT Umwelt- und Ingenieurtechnik GmbH, Dresden, Germany). The packer was installed within the groundwater monitoring well to prevent mixing of the injected tracer solution with the water column in the groundwater monitoring well (Fig. 4.1). The packer was inflated with air to a pressure of 1 bar above the pressure of the overlying water column. The inflated packer and the pump riser pipe remained during the entire tracer test within the groundwater monitoring well. The pump riser pipe was connected with a PVC hose (13 mm ID) to the stainless steel container. For both types of monitoring wells, the tracer solution was injected gravimetrically.

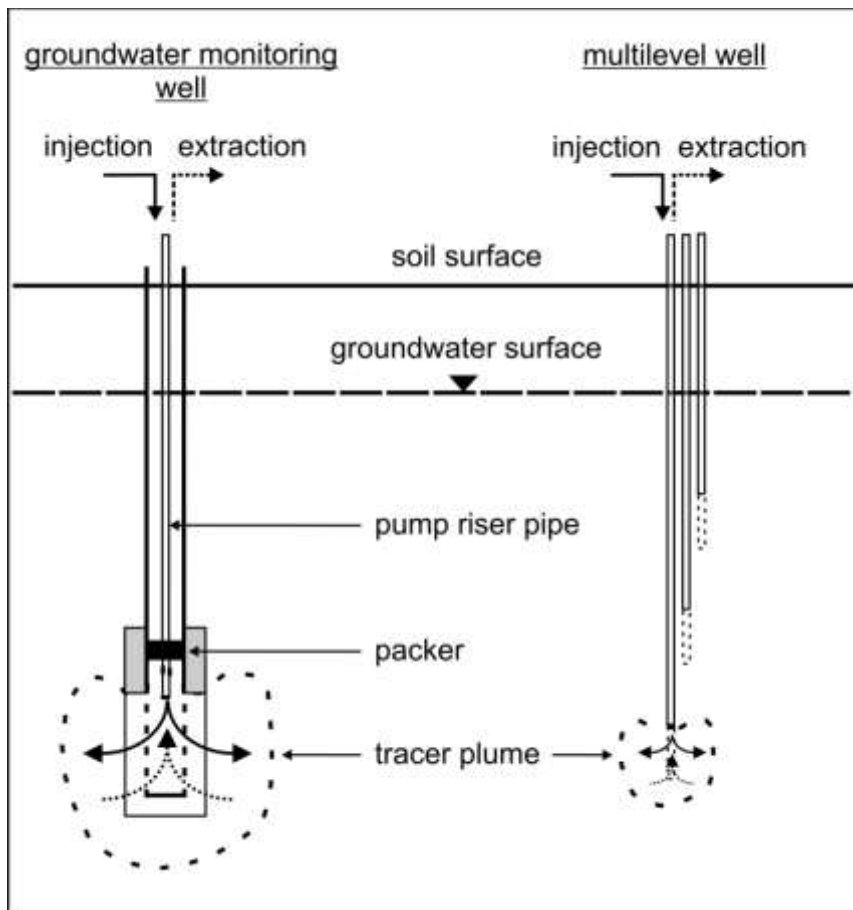


Fig. 4.1: Schematic of push-pull ^{15}N tracer tests at groundwater monitoring and multilevel wells.

pull-phase

The common groundwater monitoring wells in the GKA were constantly sampled at 12 hour intervals. The multilevel wells in the FFA were sampled every 12 hours during night and every 3 to 4 hours during day to investigate temporal patterns more detailed. The multilevel wells were more suitable for this, due to their smaller dead volumes and extraction rates. The pull phase of the conducted tracer test lasted maximal 72 hours. The first sampling was performed immediately after injection. Prior to each sampling, an amount of ground water sufficient to replace the dead volume of the groundwater monitoring well was extracted. In total, 4 l and 30 to 60 l were extracted per sampling from multilevel and groundwater monitoring wells, respectively. For common ground water monitoring wells the sampling volume differed because of different lengths of filter screens and resulting different dead volumes. During extraction, groundwater temperature, dissolved oxygen, pH and electrical conductivity (pH/Oxi 340i and pH/Cond 340i, WTW Wissenschaftlich-Technische Werkstätten GmbH, Weilheim, Germany) were measured in a flow-through chamber.

4.2.4 Pre-conditioning of wells in the NO_3^- -free zone of the FFA

To stimulate denitrification in the NO_3^- -free zone with suspected lack of active denitrifiers (Eschenbach and Well, 2013) groundwater monitoring wells were amended by repeated injections of groundwater with added NO_3^- of natural ^{15}N abundance. Injections were designed to maintain elevated NO_3^- levels in the vicinity of the filter screens during a period of several weeks. This was done to test if in situ denitrification rates measured in these wells after pre-conditioning would reflect the average denitrification rates measured during one year of incubation of corresponding aquifer samples (Eschenbach and Well, 2013).

Pre-conditioning was performed at 4 depths in the NO_3^- -free groundwater zone at multilevel well B4 in the FFA. Therefore 800 l of NO_3^- -free reduced groundwater were extracted from a groundwater monitoring well with filter a screen at 7 to 8m depth below soil surface, which is located 30 m west of multilevel well B4 into a 800 l tank container (IBC Tank Wassertank Container 800 l, Barrel Trading GmbH & Co. KG, Gaidorf, Germany) using a drill pump (Wolfcraft Bohrmaschinenpumpe 8 mm Schaft, Wolfcraft GmbH, Kempenich, Germany). The drill pump was connected with a PVC hose (13 mm ID) to the groundwater monitoring well and to the 800 l tank container. The extracted groundwater was supplemented with KNO_3 of natural ^{15}N abundance to a concentration of $10 \text{ mg NO}_3^- \text{-N l}^{-1}$. Approximately 40 l per depth level of the NO_3^- amended groundwater were injected weekly into the depths 7, 8, 9

and 10 m below soil surface at multilevel well B4. The injection rate was approx. 1 l min^{-1} . For 7 and 8 m depth the peristaltic pump and for 9 and 10 m depth the drill pump were used for injection and both pumps were connected with tygon tubings to the selected depths of the multilevel well. The first injection took place on February 22, 2011 and the last on March 22, 2011. At all 5 pre-conditioning injections were conducted at the 4 depths. From March 29 to April 01, 2011 4 push-pull tests were performed, as described above, in the previously pre-conditioned injection depths.

4.2.3 Incubation of parallels of aquifer material

Laboratory experiments were performed to compare denitrification rates measured during laboratory anaerobic incubations ($D_1(365)$) with in situ denitrification rates. The incubated aquifer material originated from the same location and depths as the filter screens of the push-pull test injection points. The aquifer material was sampled and incubated as described in detail in Eschenbach and Well (2013).

Briefly, parallels of aquifer material from both aquifers were collected between 2 to 68 m below soil surface. The aquifer samples were incubated in transfusion bottles, in 3 to 4 replications. ^{15}N labelled KNO_3 solution was added and the transfusion bottles were sealed airtight. To ensure anaerobic conditions during incubation, the headspaces of the transfusion bottles were evacuated and flushed with pure N_2 . Afterwards, the samples were incubated for one year in the dark at 10°C , which is approximately the groundwater temperature in both aquifers. The transfusion bottles were shaken manually two times a week to mix sediment and batch solution. The headspace and the supernatant batch solution in the transfusion bottles were sampled at days 1, 2, 7, 84, 168 and 365 of incubation.

4.2.5 Analytical techniques

4.2.5.1 Analysis of dissolved ^{15}N labelled denitrified N_2 and N_2O

Water samples sampled during push-pull tests were adjusted to 25°C and a headspace was generated within the serum bottles by the injection of 15 or 40 ml of ambient air into the 26 and 115 ml serum bottles, respectively, replacing the same volume of sample solution. The replaced solution was directly transferred into 20 ml PE vials and frozen for later NO_3^- and

SO₄²⁻ analysis. After headspace generation the serum bottles were agitated for 3 h on a horizontal shaker at constant temperature of 25°C to equilibrate the dissolved gases with the headspace gas. Finally, 13 ml of the headspace gas of each serum bottle were extracted with a plastic syringe and then transferred to an evacuated 12 ml sampling vial (Exetainer® Labco, High Wycombe, U.K.). The sampled nitrogen gases in the 12 ml vials were then a mixture of N₂ and N₂O gained from atmosphere and from denitrification, respectively.

The ¹⁵N analysis of gas samples was performed by isotope ratio mass spectrometry (IRMS) at the Centre for Stable Isotope Research and Analysis in Göttingen, Germany using a Delta V advantage IRMS (Thermo Scientific, Bremen, Germany) following the method described in Well et al. (2003). Analysis included reduction of N₂O to N₂ prior to IRMS. The sum of N₂ and N₂O isotopologues was thus detected as N₂ in the mass spectrometer. Therefore, the phrase (N₂+N₂O) is used when the sum of denitrification derived N₂ and N₂O is meant. The ¹⁵N abundance of (N₂+N₂O) was derived from the measured 29/28 molecular ion mass ratio by equilibrating replicate samples by electrodeless discharge (Well et al., 1998), which allowed calculating the fraction of (N₂+N₂O) from denitrification as well as the ¹⁵N abundance of denitrified (N₂+N₂O) which is equal to the ¹⁵N abundance in NO₃⁻ undergoing denitrification. N₂O was measured using a gas chromatograph (Fisons GC 8000, Milan Italy) equipped with a split-injector and an electron capture detector and a HP-Plot Q column (50 m length × 0.32 mm ID; Agilent Technologies, Santa Clara, USA) kept at 38°C. Gas analysis was completed within two weeks after the respective push-pull tests. The concentrations of denitrification derived ¹⁵N labelled N₂ and N₂O in the gas samples were calculated as described by Well and Myrold (1999) and Well et al. (2003), respectively. The concentration of N₂O in the added atmospheric air was taken into account when calculating denitrified N₂O in the sample. The measured molar concentrations of N₂ and N₂O in the headspace samples were converted into dissolved gas concentrations using gas solubilities given by Weiss (1970) and Weiss and Price (1980) and taking into account the temperature, headspace pressure and the liquid-to-headspace volume ratio during equilibration of dissolved gases with the headspace gases in the serum bottles.

4.2.5.2 Analysis of NO_3^- , SO_4^{2-} and Br^-

NO_3^- concentrations in the water samples were determined photometrically in a continuous flow analyser (Skalar, Erkelenz, Germany). SO_4^{2-} concentrations were analysed by potentiometric back-titration of excess Ba_2^+ ions remaining in the solution after addition of a defined amount of BaCl_2 in excess to SO_4^{2-} . SO_4^{2-} precipitated as BaSO_4^{2-} . The original SO_4^{2-} concentration was then analysed by potentiometric back-titration of the excess Ba_2^+ ions remaining in the solution using EDTA as titrant. Possible interfering metal cations were removed from the samples prior to this analysis by cation exchange. Bromide (Br^-) was analysed with an Inductively Coupled Plasma-Atomic Emission Spectrometer (ICP-AES, Spectro Analytical Instruments, Kleve, Germany) after stabilizing the aliquot of the analysed water samples with 10% HNO_3 .

4.2.6 Calculations of denitrification rates

Measured concentrations of denitrification derived ($\text{N}_2+\text{N}_2\text{O}$) were converted from the unit ($\mu\text{g N l}^{-1}$) to ($\mu\text{g N kg}^{-1}$) under the following assumptions: (i) the average density of the solid aquifer material is 2.65 g cm^{-3} and (ii) the effective porosity of the aquifer material was estimated to be 0.3 from literature values for sediments of similar grain size distribution (Kollmann, 1986), with a range of uncertainty of 0.2 to 0.4, respectively.

The concentrations of denitrification derived ($\text{N}_2+\text{N}_2\text{O}$) measured during the push-pull tests were corrected for dilution caused by dispersion, diffusion and the tortuosity of the pores. To do this the dilution factor ($F_{dil}(ti)$) (Eqn. 4.1) was derived from the concentration changes of the conservative tracer Br^- during the push-pull tests as proposed by Sanchez-Perez et al. (2003):

$$F_{dil}(ti) = \frac{[\text{Br}^-]_{t_0}}{[\text{Br}^-]_{ti}} \quad (4.1)$$

where $\text{Br}^-_{t_0}$ and Br^-_{ti} are the Br^- concentrations of the injected tracer solution and the sampled tracer solution at sampling time ti , respectively. The corrected concentrations of denitrification derived ($\text{N}_2+\text{N}_2\text{O}$) are then obtained by multiplying the uncorrected concentrations of ($\text{N}_2+\text{N}_2\text{O}$) at time ti with $F_{dil}(ti)$. Denitrification rates were calculated from the tangent of dilution corrected time courses of denitrification derived ($\text{N}_2+\text{N}_2\text{O}$) concentrations at time intervals with the steepest increase during the respective push-pull test (Sanchez-Perez et al., 2003; Istok et al., 2004).

4.2.7 Detection limit and precision of denitrification derived (N₂+N₂O) measurements

The detection limit of ¹⁵N analysis was calculated as the minimum amount of ¹⁵N labelled denitrification derived (N₂+N₂O) mixed with the given background of headspace N₂ of natural ¹⁵N abundance necessary to increase the measured ²⁹N₂/²⁸N₂ ratio to fulfil the following equation:

$$r_{sa} - r_{st} \geq 3 \times sdr_{st} \quad (4.2)$$

where r_{sa} and r_{st} are the ²⁹N₂/²⁸N₂ ratios in sample and standard, respectively and sdr_{st} is the standard deviation of repeated r_{st} measurements. The r_{st} values were analysed with IRMS by measuring repeated air samples. Under the experimental conditions, the detection limit for the amount of denitrified ¹⁵N labelled (N₂+N₂O) was 5 and 1 µg N Γ⁻¹ for samples in 26 and 115 ml serum bottles, respectively, depending on the different ratio of liquid sample to headspace in the respective serum bottles.

The mean coefficient of variation (CV) of concentration measurements of denitrification derived (N₂+N₂O) (µg N Γ⁻¹) in 3 replicates per sampling event during all push-pull tests was 0.18. The conversion of concentration data from the unit (µg N Γ⁻¹) to (µg N kg⁻¹) increased the mean CV significantly to 0.49. (The mean CV after conversion to (µg N kg⁻¹) was calculated from the 3 concentrations resulting from the range of effective porosity values (see Sect. 4.4.4).

4.2.8 Statistical analysis and modelling

Statistical analysis and regression modelling was conducted with WinSTAT for MS Excel Version 2000.1 (R. Fitch Software, Bad Krozingen, Germany). Experimental data (x) was converted into Box-Cox transformed data ($f^{B-C}(x)$) according to Eqn. (4.3) using different lambda coefficients (λ) to achieve a normal like distribution of experimental data within the different data sets.

$$f^{B-C}(x) = \frac{(x^\lambda - 1)}{\lambda} \quad (4.3)$$

Box-Cox transformations were performed with the statistic software STATISTICA 8 (StatSoft, Tulsa, USA). Simple linear regression analysis was conducted to evaluate quantitative relations between in situ denitrification rates (D_r (in situ)) and various sediment parameters of corresponding aquifer material measured in the laboratory (Eschenbach and Well, 2013). Normal distribution of the measured parameters within the different data sets

and the residuals of linear regressions were tested with the Kolmogorov-Smirnov-Test, normal distribution was assumed at the $P > 0.05$ level, with the null hypothesis that the tested parameter was normal distributed. The uniform distribution of residuals of regressions were checked with scatter plots of residuals vs. independent variables of the respective regression analysis. This was done to ensure homoscedasticity during regression analysis, i.e. to ensure that the least-squares method yielded best linear estimators for the modelled parameter. To use the regression functions given in the result section with own data the experimental values have to be transformed according to Eqn. 4.3 with the lambda coefficients given in Table S4.2 supplementary material).

Differences between partial data sets were considered significant at the $P < 0.05$ level (Kruskal-Wallis test (kw) with the null hypothesis that both partial data sets belong to the same population).

4.2.9 Estimating sediment properties using regression functions with D_r (in situ)

In situ denitrification rates (D_r (in situ)) measured during push-pull tests were used to model parameters of the investigated aquifer samples measured in the laboratory. These parameters were: (i) the cumulative denitrification after one year of incubation ($D_{cum}(365)$), (ii) the stock of reduced compounds (SRC) and (iii) several sediment parameters like water soluble organic carbon (C_{hws}), the fraction of $KMnO_4$ labile organic carbon (C_1), total sulphur (total-S) and total organic carbon (C_{org}). $D_{cum}(365)$ is the cumulative amount of denitrification products per kg dry weight of incubated aquifer material at the end of one year of anaerobic incubation ($mg\ N\ kg^{-1}$). The SRC is the amount of sulphides and C_{org} converted into N equivalents ($mg\ N\ k^{-1}$) according to their potential ability to reduce NO_3^- to N_2 . These sediment parameters and denitrification rates were analysed during a laboratory incubation study with aquifer samples from the FFA and GKA (Eschenbach and Well, 2013).

This aquifer samples were collected from drilled material obtained during well construction of groundwater monitoring and multilevel wells in the FFA and GKA. The analysed aquifer samples originated from depth intervals of approximately 1 m above to 1 m below filter screens or filter element of respective groundwater monitoring or multilevel wells, used for push-pull tests (Table 4.1).

4.3 Results

4.3.1 Grouping of push-pull test measuring points

Wells were grouped according to the redox state of groundwater and aquifer properties into sub data sets of in situ denitrification rates ($D_r(\text{in situ})$) measured in the NO_3^- -bearing and NO_3^- -free groundwater zone (NO_3^- -bearing and NO_3^- -free zone, respectively) and into $D_r(\text{in situ})$ measured in the zone of non-sulphidic, sulphidic and transition zone aquifer material (Table 4.1 and 4.2). Sulphidic and non-sulphidic aquifer material was distinguished using the sulphate formation capacity (SFC ($\text{mg S kg}^{-1} \text{ yr}^{-1}$)) of incubated parallels of aquifer material (Eschenbach and Well, 2013). Samples with a SFC $> 1 \text{ mg SO}_4^{2-}\text{-S kg}^{-1} \text{ yr}^{-1}$ were assigned sulphidic. The transition zone was defined as aquifer material from the region where sulphides were present, but groundwater still contained NO_3^- . For a detailed description of the classification of aquifer material see Eschenbach and Well (2013).

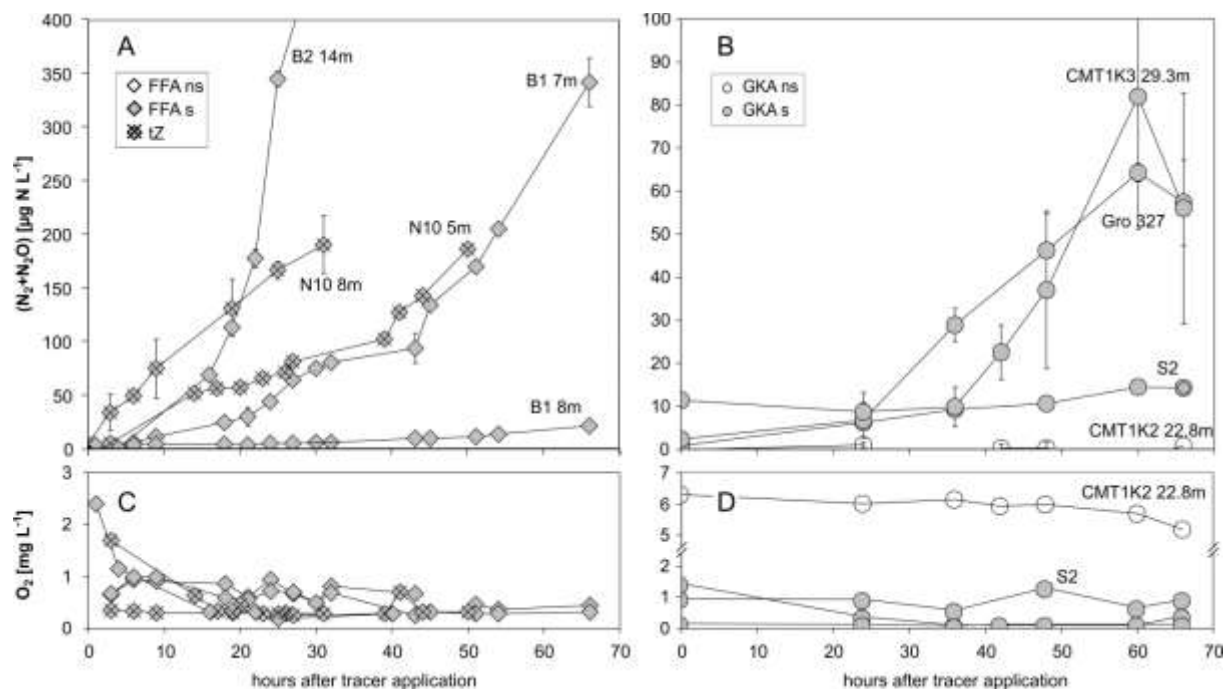


Fig. 4.2: Time courses of denitrification derived ($\text{N}_2 + \text{N}_2\text{O}$) and dissolved O_2 during ^{15}N push-pull tests in the FFA (A and C) and GKA (B and D). FFA Fuhrberger Feld aquifer; GKA Großenkneten aquifer; ns non-sulphidic; s sulphidic and tZ transition zone aquifer material.

Table 4.2: Background conditions of groundwater at the locations of push-pull ^{15}N tracer tests.

Location	inj. depth ^a m	aquifer zone	O ₂	NO ₃ ⁻	N ₂ O	SO ₄ ²⁻	pH	redox	con ^b
			mg l ⁻¹	mg N l ⁻¹	µg N l ⁻¹	mg S l ⁻¹		mV	µS cm ⁻¹
FFA B1	7.0	sulphidic	0.67	< 0.25	n.d.	27.64	6.00	-171	473
FFA B1	8.0	sulphidic	0.76	< 0.25	n.d.	24.73	6.04	-175	440
FFA B2	3.0	non-sulphidic	3.66	41.47	1.59	15.07	4.66	273	563
FFA B2	4.2	non-sulphidic	0.96	27.59	68.31	36.94	4.83	209	564
FFA B2	8.0	transition zone	0.16	12.58	0.03	32.52	4.48	341	553
FFA B2	9.0	transition zone	0.13	7.09	0.05	38.41	4.65	367	488
FFA B2	10.0	transition zone	0.06	1.0	n.d.	43.30	4.75	374	458
FFA B2	14.0	sulphidic	0.40	0.63	n.d.	42.51	6.75	117	453
FFA B4	8.0	sulphidic	0.22	< 0.25	1.14	42.30	5.28	-38	432
FFA B4	9.0	sulphidic	0.12	< 0.25	0.70	51.19	5.43	-	-
FFA B6	3.0	non-sulphidic	9.51	6.10	0.02	13.95	5.70	365	255
FFA B6	6.0	non-sulphidic	1.28	19.55	10.66	22.45	5.18	349	441
FFA N10	5.0	transition zone	0.12	13.12	184.8	59.87	4.61	341	660
FFA N10	8.0	transition zone	0.16	0.4	1.03	52.03	5.60	3	463
GKA 326	8-10	non-sulphidic	6.30	3.06	0.12	4.67	4.10	374	105
GKA CMT2	8.3	non-sulphidic	6.10	3.14	0.12	5.06	4.40	387	100
GKA CMT2	22.8	non-sulphidic	5.70	3.98	0.56	12.09	5.10	276	163
GKA CMT2	26.8	sulphidic	0.10	< 0.25	0.01	18.57	5.40	30	221
GKA S2	26-27	sulphidic	0.30	< 0.25	n.d.	17.85	5.30	161	217
GKA CMT1	29.3	sulphidic	0.20	< 0.25	n.d.	18.16	5.50	-24	240
GKA CMT1	31.3	sulphidic	0.14	< 0.25	n.d.	17.91	5.20	134	195
GKA CMT1	33.5	sulphidic	0.20	< 0.25	n.d.	18.60	5.10	122	272
GKA 327	35-39	sulphidic	0.10	< 0.25	0.13	10.85	5.30	26	275
GKA S1	66-67	non-sulphidic	0.13	< 0.25	0.02	5.10	5.72	-54	103

FFA Fuhrberger Feld aquifer;

GKA Großenkneten aquifer;

^a injection depth;

^b conductivity.

4.3.2 In situ denitrification rates and time courses of denitrification products

D_r (in situ) ranged from 0.0 to 51.5 $\mu\text{g N kg}^{-1} \text{d}^{-1}$. Mean D_r (in situ) in the FFA (9.1 $\mu\text{g N kg}^{-1} \text{d}^{-1}$) were almost 4 to 5 times higher than in the GKA, but differed statistical not significant from the ones in the GKA (Fig. 4.2 and 4.3, Tables 4.3 and 4.4).

The non-sulphidic zone of both aquifers exhibited the lowest mean D_r (in situ) (1.04 $\mu\text{g N kg}^{-1} \text{d}^{-1}$) of all partial data sets (Table 4.4) and statistical significant differences

(kw: $P < 0.05$) occurred with the full and all partial data sets except D_r (in situ) measured in the GKA and in the NO_3^- -bearing zone of both aquifers. The other partial data sets exhibited no significant differences between one another. Mean D_r (in situ) of the transition zone ($9.32 \mu\text{g N kg}^{-1} \text{d}^{-1}$) was slightly higher than in the sulphidic zone of both aquifers.

Except for the multilevel well B6 in 6 m depth all push-pull injection points with O_2 concentration above $1 \text{ mg O}_2 \text{ l}^{-1}$ in the groundwater exhibited D_r (in situ) below $0.75 \mu\text{g N kg}^{-1} \text{d}^{-1}$ (Tables 4.2 and 4.3) and parallels of aquifer material from this locations were assigned to non-sulphidic aquifer material during laboratory incubations (Eschenbach and Well, 2012, 2013).

D_r (in situ) measured after pre-conditioning of push-pull injection points at multiple well B4 (FFA) (67.83 to $152.70 \mu\text{g N kg}^{-1} \text{d}^{-1}$) were 30 to 65 times higher than D_r (in situ) measured one year before without pre-conditioning (2.76 and $2.28 \mu\text{g N kg}^{-1} \text{d}^{-1}$) (Table 4.3).

Among the total of 28 push-pull tests, 24 were conducted without pre-conditioning from which twelve were located in the NO_3^- -bearing and twelve in the NO_3^- -free zone of both aquifers, respectively. Among the 12 push-pull tests in the NO_3^- -free zone all of the 5 FFA locations showed an exponential increase of denitrification derived ($\text{N}_2 + \text{N}_2\text{O}$) during push-pull tests, whereas in the GKA this was only the case in two to three of the 7 GKA locations. In contrast to this, only 2 out of 12 push-pull tests in the NO_3^- -bearing zone of both aquifers exhibited exponential increases and these push-pull tests were located in the transition zone of multilevel well B2. The two push-pull tests at multilevel well B4 (NO_3^- -free zone of the FFA) showed an exponential increase of denitrification derived ($\text{N}_2 + \text{N}_2\text{O}$). After pre-conditioning at the same depths of multilevel well B4 the time course of denitrification products showed no exponential increase during the first two days (Fig. 4.4).

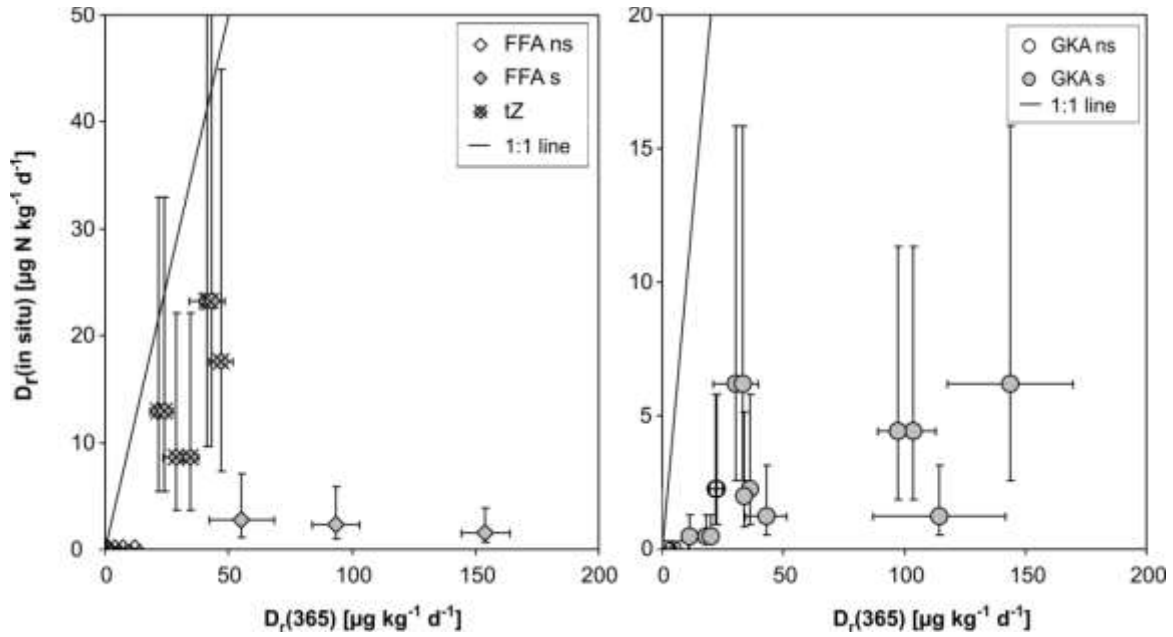


Fig. 4.3: Relation between in situ denitrification rates determined by ^{15}N push-pull tracer tests and average denitrification rates during one year of incubation (Eschenbach and Well, 2013). FFA Fuhrberger Feld aquifer; GKA Großenkneten aquifer; ns non-sulphidic; s sulphidic and tZ transition zone aquifer material.

4.3.3 Relationship between $D_r(\text{in situ})$, $D_{\text{cum}}(365)$ and aquifer parameters

4.3.3.1 Comparison of $D_r(\text{in situ})$ and $D_{\text{cum}}(365)$

$D_r(\text{in situ})$ was compared with mean denitrification rates during 365 days of laboratory incubation ($D_r(365)$) (Eschenbach and Well, 2013) with aquifer material collected from the locations of the monitoring wells (see Sect. 4.2.3). $D_r(365)$ was obtained by dividing cumulative denitrification derived ($\text{N}_2 + \text{N}_2\text{O}$) production ($D_{\text{cum}}(365)$) by incubation time (365 d). $D_r(\text{in situ})$ was generally lower than $D_r(365)$ (Fig. 4.3 and Table S4.1 supplementary material). The means of the $D_r(\text{in situ})$ -to- $D_r(365)$ ratio were calculated for the different partial data sets giving a range of 0 to 0.47, with the lowest and highest ratios for the data sets of GKA and transition zone push-pull tests, respectively (Table 4.4). In the transition zone, $D_r(\text{in situ})$ -to- $D_r(365)$ ratios were significantly higher compared to the other data sets (kw: $P < 0.05$). $D_r(\text{in situ})$ of FFA aquifer material was statistical significant closer related to $D_r(365)$ than $D_r(\text{in situ})$ measured in the GKA. The mean $D_r(\text{in situ})$ -to- $D_r(365)$ ratio from the

NO_3^- -bearing zone of both aquifers (0.23) was significantly larger than in the NO_3^- -free zone of both aquifers (0.1) (Table 4.4).

$D_r(\text{in situ})$ after pre-conditioning (well B4, FFA) was comparable or higher than $D_r(365)$ with $D_r(\text{in situ})$ -to- $D_r(365)$ ratios of 0.73 to 2.6 (Fig. 4.3 and Table 4.4). $D_r(\text{in situ})$ was 30 to 65 times higher compared to values obtained without pre-conditioning at the same wells (Fig. 4.5 and Table 4.3).

Table 4.3: In situ denitrification rates ($D_r(\text{in situ})$) and minimum and maximum values of $D_r(\text{in situ})$ in dependence of the range of estimated effective porosities (0.2 to 0.4). $D_r(\text{in situ})$ were calculated from a regression line through the $(\text{N}_2+\text{N}_2\text{O})_{\text{den}}$ concentrations at time intervals with the steepest increase of $(\text{N}_2+\text{N}_2\text{O})_{\text{den}}$ during the respective push-pull test. Tracer tests after pre-conditioning are marked with *.

Location	Injection depth m	Aquifer zone	$D_r(\text{in situ})$	$D_r(\text{in situ})$	$D_r(\text{in situ})$	R^a
				max	min	
$\mu\text{g N kg}^{-1} \text{d}^{-1}$						
FFA B1	7.0	sulphidic ^c	17.59	27.361	10.261	0.94
FFA B1	8.0	sulphidic ^c	1.512	2.352	0.882	0.92
FFA B2	3.0	non-sulphidic ^b	0.120	0.186	0.070	0.14
FFA B2	4.2	non-sulphidic ^b	0.065	0.102	0.038	0.01
FFA B2	8.0	transition zone ^b	0.429	0.667	0.250	0.95
FFA B2	9.0	transition zone ^b	1.415	2.201	0.825	0.90
FFA B2	10.0	transition zone ^b	8.650	13.456	5.046	0.99
FFA B2	14.0	sulphidic ^c	51.47	80.078	30.029	0.82
FFA B4	8.0	sulphidic ^c	2.755	4.286	1.607	0.98
FFA B4	9.0	sulphidic ^c	2.278	3.544	1.329	0.86
FFA B6	3.0	non-sulphidic ^b	0.057	0.089	0.033	0.02
FFA B6	6.0	non-sulphidic ^b	4.998	7.774	2.915	0.96
FFA N10	5.0	transition zone ^b	12.89	20.052	7.520	0.95
FFA N10	8.0	transition zone ^b	23.19	36.074	13.528	0.99
FFA B4*	7.0	sulphidic ^c	152.6	237.527	89.073	0.94
FFA B4*	8.0	sulphidic ^c	67.83	105.514	39.568	0.99
FFA B4*	9.0	sulphidic ^c	145.5	226.481	84.930	0.98
FFA B4*	10.0	sulphidic ^c	150.7	234.530	87.949	1.00
GKA 326	8-10	non-sulphidic ^b	0.747	1.162	0.436	0.96
GKA CMT2	8.3	non-sulphidic ^b	0.051	0.079	0.030	0.02
GKA CMT2	22.8	non-sulphidic ^b	0.009	0.013	0.005	0.00
GKA CMT2	26.8	sulphidic ^c	1.233	1.918	0.719	0.70
GKA S2	26-27	sulphidic ^c	0.860	1.338	0.502	0.99
GKA CMT1	29.3	sulphidic ^c	4.427	6.886	2.582	0.78
GKA CMT1	31.3	sulphidic ^c	0.504	0.784	0.294	0.63
GKA CMT1	33.5	sulphidic ^c	2.002	3.114	1.168	0.77
GKA 327	35-39	sulphidic ^c	6.192	9.632	3.612	0.99
GKA S1	66-67	non-sulphidic ^c	2.271	3.533	1.325	1.00

FFA Fuhrberger Feld aquifer; GKA Großenkneten aquifer; ^a correlation coefficient of the regression line;

^b NO_3^- -bearing zone; ^c NO_3^- -free zone.

4.3.3.2 Regression models to predict $D_{\text{cum}}(365)$, SRC and denitrification relevant aquifer parameters from $D_r(\text{in situ})$

Simple linear regression analysis was applied to obtain regression models for the prediction of $D_{\text{cum}}(365)$ from $D_r(\text{in situ})$ for the full and partial data sets. The goodness of fit of the regression models given by the correlation coefficient (R) and the average ratio of calculated $D_{\text{cum}}(365)$ to measured $D_{\text{cum}}(365)$ ($R_{c/m}$) for the full and partial data sets.

The goodness of fit of regression models to predict $D_{\text{cum}}(365)$ by $D_r(\text{in situ})$ varied for the various sub data sets from no fit in the sulphidic zone and a good approximation of $D_{\text{cum}}(365)$ by $D_r(\text{in situ})$ in the NO_3^- -bearing zone ($R = 0.04$ and $R = 0.84$, respectively, Table 4.5). For the full data set, the goodness of fit was modest ($R = 0.62$) resulting in a wide range of deviations between calculated and measured $D_{\text{cum}}(365)$ from -49.1 to $18.1 \text{ mg N kg}^{-1}$ in the different sub data sets. Linear relationships between $D_r(\text{in situ})$ and $D_{\text{cum}}(365)$ were better for GKA in comparison to FFA aquifer material. Aquifer material which was not jet in contact with NO_3^- bearing groundwater (NO_3^- -free zone and most of sulphidic zone material) exhibited $D_r(\text{in situ})$ values which were clearly less correlated with $D_{\text{cum}}(365)$ than aquifer material which was already in contact with NO_3^- -bearing groundwater (non-sulphidic zone, transition zone and NO_3^- -bearing zone) (Table 4.5).

The goodness of fit of regression models to calculate the SRC from $D_r(\text{in situ})$ was on average slightly worse than the one of regression models to predict $D_{\text{cum}}(365)$ from $D_r(\text{in situ})$. As for the prediction of $D_{\text{cum}}(365)$ the best goodness of fit of regression models was obtained for the sub data sets of GKA, the transition zone and the NO_3^- -bearing zone with coefficients of determination of $R = 0.75$, 0.77 and 0.50 (Table 4.5). Like $D_{\text{cum}}(365)$ also for SRC the prediction was best for zones of both aquifers were the aquifer material was already in contact with NO_3^- -bearing groundwater. Contrary to other partial data sets, the sub-set of $D_r(\text{in situ})$ measured in sulphidic aquifer material exhibited a clearly better goodness of fit between $D_r(\text{in situ})$ and SRC than between $D_{\text{cum}}(365)$ and $D_r(\text{in situ})$, $R = 0.41$ and $R = 0.04$, respectively.

As already mentioned above pre-conditioning strongly increased the measured $D_r(\text{in situ})$ rates. Regressions between $D_r(\text{in situ})$ and $D_{\text{cum}}(365)$ as well as the SRC of corresponding aquifer samples exhibited a modest goodness of fit ($R = 0.54$ and $R = 0.53$, respectively) (Table 4.5).

Table 4.4: Means, standard deviation and ranges of $D_r(\text{in situ})$ of the data sets. Statistical significant differences (kw: $P < 0.05$) between $D_r(\text{in situ})$ values measured in the various sub data sets occurred only between $D_r(\text{in situ})$ measured in the non-sulphidic zone and some of other partial data sets.

Data set	N ^c	$D_r(\text{in situ})^a$ ($\mu\text{g kg}^{-1} \text{ N d}^{-1}$)			non-sulphidic ^d	N ^e	$D_r(\text{in situ}) / D_r(365)^b$	
		means	range				means	
Whole data set	24	6.07±11.36	0.00 – 51.48	s ¹	34	0.15±0.20	0.00 – 0.60	
FFA	14	9.10±14.20	0.06 – 51.48	s ¹	16	0.26±0.24	0.01 – 0.60	
GKA	10	1.83±2.02	0.00 – 6.19	ns	18	0.06±0.06	0.00 – 0.20	
non-sulphidic zone	8	1.04± 1.78	0.00 – 5.00	-	11	0.05±0.08	0.00 – 0.23	
sulphidic zone	14	8.59±13.67	0.43 – 51.48	s ²	23	0.20±0.22	0.01 – 0.60	
transition zone	5	9.32±9.32	0.43 – 23.19	s ¹	8	0.47±0.14	0.25 – 0.60	
NO ₃ ⁻ -bearing zone	12	4.38±7.24	0.00 – 23.19	ns	17	0.23±0.24	0.00 – 0.60	
NO ₃ ⁻ -free zone	16	7.76±14.53	0.50 – 51.48	s ¹	17	0.10±0.10	0.01 – 0.37	
pre-conditioned	4	128.1±43.4	63.1 – 152.7	-	4	1.77±0.70	1.14 – 2.76	

^a all $D_r(\text{in situ})$ measurements, ^b only $D_r(\text{in situ})$ measurements with corresponding incubated parallels of incubated aquifer samples ^c number of $D_r(\text{in situ})$ measurements; ^d statistical differences between non-sulphidic and other data sets (s significant differences; ns not significant differences; ¹ differences significant at the 0.05 probability level; ² differences significant at the probability level; ³ differences significant at the 0.001 probability level); ^e number of comparisons between $D_r(\text{in situ})$ and corresponding incubated aquifer samples.

Regression analysis between several denitrification relevant parameters of parallels of aquifer material (Eschenbach and Well, 2013) and $D_r(\text{in situ})$ revealed that for some partial data sets, the linear regressions between some of these parameters and $D_r(\text{in situ})$ were even better than between $D_r(\text{in situ})$ and $D_{\text{cum}}(365)$ (Table S4.3 supplementary material in comparison to Table 4.5). For GKA aquifer material $D_{\text{cum}}(365)$ was in closest linear correlation with $D_r(\text{in situ})$. Contrary to this for FFA aquifer material $D_r(\text{in situ})$ was closer related to $\text{SO}_4^{2-}_{\text{extr}}$ and C_{hws} than to $D_{\text{cum}}(365)$ or SRC. For sub data sets grouped according to the SFC of the incubated aquifer material several parameters were in better or the same linear correlation to $D_r(\text{in situ})$ than $D_{\text{cum}}(365)$. For non-sulphidic aquifer material these were C_{org} and total-S, in case of sulphidic aquifer material $\text{SO}_4^{2-}_{\text{extr}}$ and total-S and for transition zone aquifer material C_{org} and total-S. In case of NO₃⁻-bearing zone aquifer material the C_{org} and $\text{SO}_4^{2-}_{\text{extr}}$ and for NO₃⁻-free zone $\text{SO}_4^{2-}_{\text{extr}}$ and C_1 exhibited better or the same correlation coefficients with $D_r(\text{in situ})$ as with $D_{\text{cum}}(365)$ or SRC.

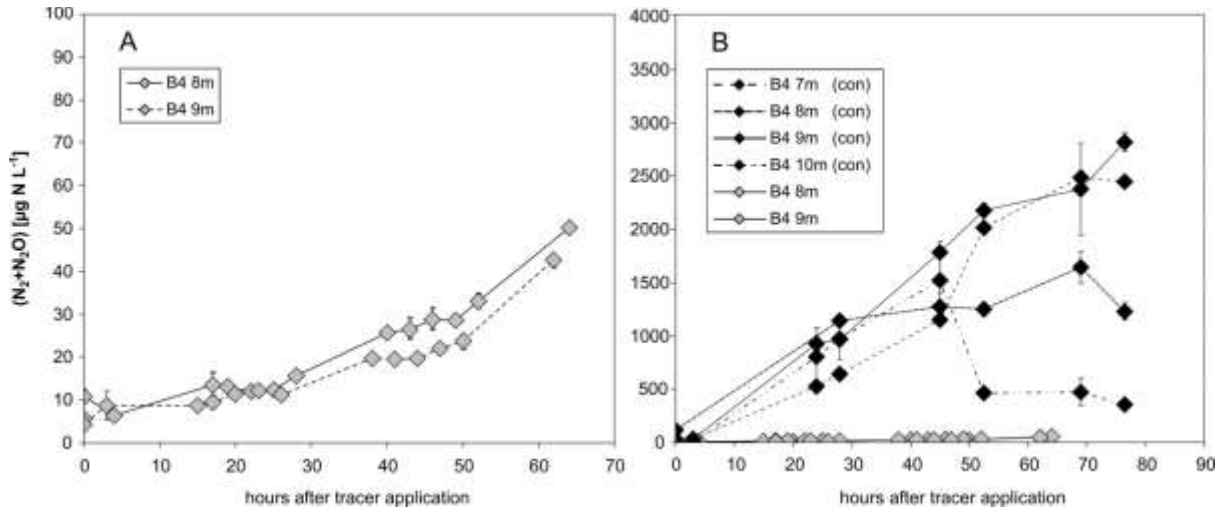


Fig. 4.4: Time courses of denitrification derived (N_2+N_2O) during push-pull tests without pre-conditioning (A) (grey diamonds) and with pre-conditioning B (black diamonds) at multilevel well B4 in the FFA. The push-pull tests without pre-conditioning at B4 was conducted in April 2010. One year later in April 2011 the aquifer material of the respective depths was conditioned over 5 weeks with NO_3^- amended groundwater of natural ^{15}N abundance prior to the ^{15}N push-pull tests.

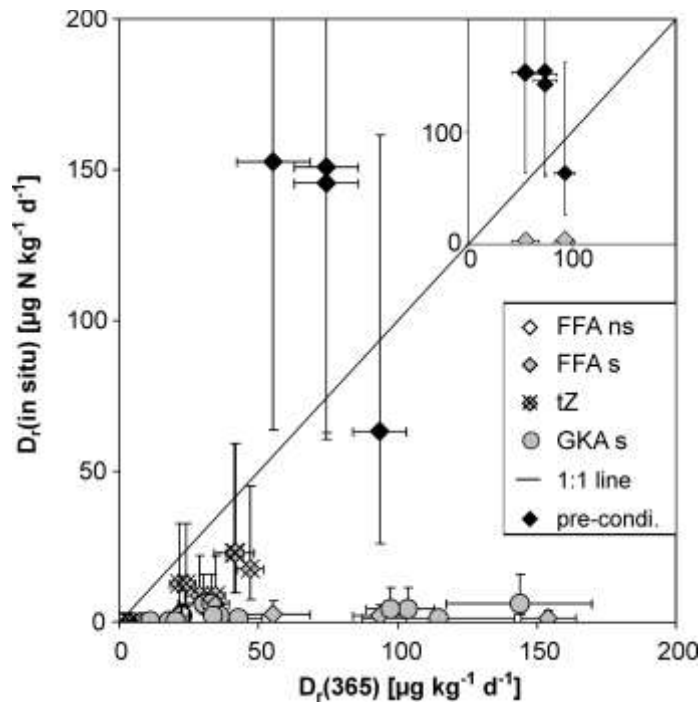


Fig. 4.5: $D_r(\text{in situ})$ after 5 weeks of pre-conditioning of aquifer material (black diamonds) in comparison to $D_r(\text{in situ})$ without pre-conditioning. The small diagram shows the difference between $D_r(\text{in situ})$ after pre-conditioning and unconditioned $D_r(\text{in situ})$ at multilevel well B4 in the FFA.

Table 4.5: Simple regressions between D_r (in situ) and $D_{cum}(365)$ and SRC from anaerobic incubations with corresponding aquifer material. $f^{B-C}(X) = A + B \times f^{B-C}(D_r(\text{in situ}))$.

Data set	X^a	N^b	A	B	R^c	calculated/measured		Deviation ($\text{mg kg}^{-1} \text{ yr}^{-1}$)	
						mean	range	mean	range
Whole data set	$D_{cum}(365)$	34	2.878	0.603	0.62	2.29±4.19	0.16 – 22.96	-3.07±14.67	-47.2 – 12.8
Whole data set	SRC	34	6.123	0.152	0.40	1.51±1.31	0.12 – 5.19	-671.2±2091	-7734 – 1379
FFA	$D_{cum}(365)$	16	2.640	0.578	0.52	2.83±4.90	0.13 – 19.18	-3.08±14.71	-49.1 – 7.0
FFA	SRC	16	3.772	0.006	0.07	1.22±0.82	0.11 – 2.92	-377.8±1375	-5317 – 413.7
GKA	$D_{cum}(365)$	18	3.046	0.818	0.82	1.34±0.92	0.26 – 3.85	-2.25±12.28	-30.8 – 15.5
GKA	SRC	18	8.024	0.613	0.75	1.43±1.23	0.178 – 4.47	-617.0±2179	-5780 – 2390
non-sulphidic	$D_{cum}(365)$	11	1.050	0.156	0.40	2.25±3.20	0.26 – 10.65	-0.10±2.41	-5.2 – 1.8
non-sulphidic	SRC	11	8407	752.8	0.43	1.50±0.84	0.46 – 3.19	31.54±240.7	-553 – 272.6
sulphidic	$D_{cum}(365)$	23	4.185	-0.033	0.04	1.33±0.90	0.30 – 4.19	-3.32±15.13	-39.4 – 13.1
sulphidic	SRC	23	21.40	-1.372	0.41	0.30±0.18	0.03 – 0.61	-1823±2313	-8564 – -144
transition zone	$D_{cum}(365)$	8	1.109	0.581	0.53	1.03±0.26	0.74 – 1.43	-0.36±2.84	-4.5 – 3.3
transition zone	SRC	8	5.349	-0.602	0.77	1.05±0.41	0.58 – 1.92	-50.11±340.6	-518.7 – 561
NO_3^- -bearing	$D_{cum}(365)$	17	2.132	0.454	0.84	2.21±3.76	0.13 – 15.17	-0.67±2.52	-6.3 – 2.7
NO_3^- -bearing	SRC	17	193.3	16.32	0.55	1.36±0.75	0.41 – 2.76	-19.35±365.2	-929 – 462.6
NO_3^- -free	$D_{cum}(365)$	17	7.774	2.036	0.36	1.47±0.88	0.31 – 3.00	-1.69±16.23	-38.7 – 18.1
NO_3^- -free	SRC	17	77.61	8.421	0.21	1.78±1.46	0.27 – 4.47	-485.4±2494	-6077 – 2095
pre-conditioned ¹	$D_{cum}(365)$	4	14.402	0.099	0.54	1.06±0.35	0.62 – 1.47	0.12±9.49	-5.22 – 9.41
pre-conditioned ¹	SRC	4	319.5	4.895	0.53	1.12±0.52	0.51 – 1.77	5.5±462	-638.0 – 464

¹ experimental data of pre-conditioned push-pull tracer tests was not Box-Cox transformed before regression analysis, because of the small number of data pairs. For these data pairs the following equation applies: $X = A + B \times D_r(\text{in situ})$.

^a Independent sediment parameter

^b number of samples

^c correlation coefficient.

4.4 Discussion

4.4.1 Time courses of denitrification products and $D_r(\text{in situ})$ compared with $D_r(365)$

The main objective of this study is to predict the cumulative denitrification measured during one year of laboratory incubation of aquifer samples ($D_{\text{cum}}(365)$) from in situ denitrification rates ($D_r(\text{in situ})$). In comparison to costly drilling of aquifer material and laboratory measurement of $D_{\text{cum}}(365)$, $D_r(\text{in situ})$ can be measured with relatively low cost push-pull tests at existing groundwater monitoring wells, which would also allow spatial mapping of denitrification activity within aquifers.

There are only scarce data comparing the stock of reduced compounds (SRC) or longer-term denitrification rates (e.g. $D_r(365)$) with $D_r(\text{in situ})$. Well et al. (2003) showed for denitrification in the saturated zone of hydromorphic soils that laboratory derived denitrification rates after 24 h of anaerobic incubation are in good agreement with in situ denitrification rates, but the study was limited to near-surface groundwater. Konrad (2007) tested this approach in deeper aquifer zones with a small data set of pairs of $D_r(\text{in situ})$ vs D_{cum} (4 push-pull ^{15}N tracer tests and incubations of corresponding aquifer material) and found partly good spearman rank correlation coefficients of $R \geq 0.8$.

In this study, transfer functions were developed to predict $D_{\text{cum}}(365)$ from $D_r(\text{in situ})$ measurements with a larger data set to test the influence of the different redox zones typically present in aquifers on the transferability of $D_r(\text{in situ})$ to $D_{\text{cum}}(365)$. Moreover pre-conditioning was evaluated by addition of NO_3^- to aquifer material and the subsequent measurement of in situ denitrification rates. To compare previous $D_r(\text{in situ})$ data with presented measurements, all data was converted to the dimension $\mu\text{g N kg}^{-1} \text{d}^{-1}$ assuming an effective pore space of 0.3 and an average density of dry aquifer solids of 2.65 g cm^{-3} .

$D_r(\text{in situ})$ values measured in the FFA and GKA (Table 4.3) are comparable with $D_r(\text{in situ})$ ($2.3 - 27.1 \mu\text{g N kg}^{-1} \text{d}^{-1}$) measured by Konrad (2007) in two Pleistocene sandy aquifers in Northern Germany (aquifers of Thülsfelde and Sulingen, about 40 km west and 30 km south of the city of Bremen, respectively). Also $D_r(\text{in situ})$ reported by (Addy et al., 2002) and (Addy et al., 2005) show a similar range of denitrification rates with $2.1 - 121.2$ and $0.5 - 87.9 \mu\text{g N kg}^{-1} \text{d}^{-1}$, respectively. Those values were measured in two riparian sites and a site with marsh sediments on Rhode Island USA. Somewhat larger spans of $D_r(\text{in situ})$ were reported by Well et al. (2003) for water-saturated mineral sub-soils from various locations in Northern Germany and by Konrad (2007) for the sandy to silty aquifer of Wehnsen (about 30

km southeast of the FFA) with $D_r(\text{in situ})$ from 0 – 300 and 45 – 339 $\mu\text{g N kg}^{-1} \text{d}^{-1}$, respectively. These larger spans cover also the magnitude of $D_r(\text{in situ})$ values measured at multilevel well B4 in the FFA after pre-conditioning (Table 4.3). Sanches-Perez (2003) measured $D_r(\text{in situ})$ from 22.1 to 7646.4 $\mu\text{g N kg}^{-1} \text{d}^{-1}$ with the acetylene inhibition method in 2 shallow sandy aquifers in France and Spain. Overall, there is a wide range of reported $D_r(\text{in situ})$ in aquifers.

But there is not only a strong local variability in $D_r(\text{in situ})$ of aquifers also $D_r(\text{in situ})$ can change substantially during push-pull tests itself. During a push-pull test conducted by Trudell et al. (1986) in situ denitrification rates increased strongly. During the 12 day lasting pull-phase of this tracer test in the O_2 and NO_3^- -free groundwater zone of a shallow sandy aquifer in south western Ontario Canada $D_r(\text{in situ})$ increased from 30.3 to 504.6 $\mu\text{g N kg}^{-1} \text{d}^{-1}$ (Trudell et al., 1986).

In the NO_3^- -free zone, an exponential increase of denitrified ($\text{N}_2+\text{N}_2\text{O}$) was observed during most of the push-pull tests. Sections of exponential time courses of dilution corrected denitrification products observed during tracer tests were also previously reported (Eschenbach and Well, 2011; Konrad, 2007). In the study of Konrad (2007) 5 out of 13 push-pull tests showed an exponential increase of dilution corrected denitrification products. 4 of these 5 push-pull tests were located in the NO_3^- -free groundwater zone. As a result, it is concluded, that the exponential increase of denitrification products observed during push-pull tests in this study and preceding studies can probably be attributed to growth and stimulation of denitrifiers by the injection of NO_3^- into aquifer zones that had previously not been in contact with NO_3^- . Trudell et al. (1986) found an increase of denitrifying bacteria species during a 12 day lasting tracer test. Although Trudell et al. (1986) stated that the absolute accuracy of these values might be questionable, these results are nevertheless indicative for an increase in the population of denitrifiers. This increase in the denitrifying population was accompanied by a 17-fold increase of measured denitrification rates. Several other investigations showed increasing microbial activity after bio stimulation of aquifer sediments by the injection of electron donors to monitoring wells (Istok et al., 2004; Kim et al., 2004; Kim et al., 2005). Istok et al. (2004) reported that the viable biomass on solid samplers installed in monitoring wells more than doubled compared with samplers installed in monitoring wells without electron donor addition.

To the authors knowledge, pre-conditioning of aquifer material prior to a push-pull ^{15}N tracer test by the injection of only NO_3^- as new available electron acceptor was firstly used in the

present study to establish a denitrifying microbial community in the strict anaerobic zone of an aquifer.

Pre-conditioning at multilevel well B4 (see Sect. 4.2.4) in the FFA resulted in a 30- to 65-fold increase in measured in situ denitrification rates compared with push-pull tests without pre-conditioning at the same depths of multilevel well B4 (Table 4.3 and Fig. 4.5). From the results of the cited previous studies it is concluded that pre-conditioning in the NO_3^- -free zone of the FFA has led to growth of the community of active denitrifiers in the aquifer material in the vicinity of the respective injection points. The degree of increase of $D_r(\text{in situ})$ due to pre-conditioning might be rather an upper limit for the increase of active denitrifiers in the investigated aquifer material because pre-conditioning might not only lead to bacterial growth but also to a higher denitrification rate per microbial cell due to synthesis of enzymes for denitrification during pre-conditioning. In this study, pre-conditioning resulted not only in higher denitrification rates but also the time course of denitrification derived ($\text{N}_2+\text{N}_2\text{O}$) did not show a section of a distinct exponential increase compared with the prior measurements without pre-conditioning (Fig. 4.4). This fact is interpreted in the way that denitrifiers in the tested aquifer material after pre-conditioning were ready to denitrify and that the size of the denitrifying community were in a kind of equilibrium to the surface area of reduced compounds capable to support denitrification (saRC) present in the aquifer material (see also Sect. 4.4.2 discussion on reaction kinetics).

The groups of $D_r(\text{in situ})$ measuring points located in the GKA and the ones in the non-sulphidic and NO_3^- -free zone of both aquifers showed worst agreement between $D_r(\text{in situ})$ and $D_r(365)$ (lowest mean ratios of $D_r(\text{in situ})$ to $D_r(365)$ of all data sets (Table 4.4)). Non-sulphidic aquifer material exhibited low denitrification rates during the push-pull tests also because dissolved O_2 inhibited NO_3^- reduction. Dissolved O_2 concentrations in the ambient groundwater and therefore also in the injected test solutions were $> 1 \text{ mg O}_2 \text{ l}^{-1}$ at 6 out of 8 injection points in the non-sulphidic zone of both aquifers (Table 4.2). $D_r(365)$ of non-sulphidic aquifer material measured during anaerobic incubation in the laboratory (Eschenbach and Well, 2013) can therefore be seen as a potential activity which is only partly effective under in situ conditions due to low consumption of dissolved O_2 in groundwater. This is also reflected by the low $D_r(\text{in situ})$ to $D_r(365)$ ratio in the non-sulphidic wells (Table 4.4).

The mean $D_r(\text{in situ})$ -to- $D_r(365)$ ratio of $D_r(\text{in situ})$ measurements in the NO_3^- -bearing zone were twice as high compared to the NO_3^- -free zone (Table 4.4 and Fig. 4.3). It is hypothesized that the reason is that in the NO_3^- -free zone the microbial community had to

adapt to the “new” electron acceptor NO_3^- transported with the test solution to microbes attached at sediment surfaces. Denitrifiers, if initially present, had to grow and to start to denitrify, which results in an increase of denitrification rates during push-pull tests. Mean $D_r(\text{in situ})$ and the ratio of $D_r(\text{in situ})$ -to- $D_r(365)$ of 0.47 were highest in the transition zone, showing that in the transition zone $D_r(\text{in situ})$ and $D_r(365)$ were in closer agreement compared with other zones in both aquifers. During the push-pull tests in the transition zone the ambient concentration of dissolved O_2 were always below $0.13 \text{ mg } \Gamma^{-1}$ and NO_3^- was always detectable in the ambient groundwater at the 5 injection points in the transition zone (Table 4.2). Denitrification was therefore presumably not inhibited by dissolved O_2 and the microbial population already adapted to NO_3^- as an available electron acceptor.

4.4.2 Interpretation of observed time courses of produced ($\text{N}_2+\text{N}_2\text{O}$)

Kübeck et al. (2010) described the turnover rate of electron acceptors like NO_3^- or O_2 in aquifers with a multiplicative Michaelis-Menten kinetic consisting of two Monod-terms. Using their approach one can describe denitrification in aquifers as follows:

$$\mu(\text{NO}_3^-) = \mu_{\max}(\text{NO}_3^-) \cdot \frac{C(\text{NO}_3^-)}{K_S(\text{NO}_3^-) + C(\text{NO}_3^-)} \cdot \frac{C(\text{mdRC})}{K_S(\text{mdRC}) + C(\text{mdRC})} \quad (4.4)$$

$\mu(\text{NO}_3^-)$ and $\mu_{\max}(\text{NO}_3^-)$ are the observed and the maximal denitrification rate, respectively with the dimension ($\text{mmol } \Gamma^{-1} \text{ s}^{-1}$). $C(\text{NO}_3^-)$ ($\text{mmol } \Gamma^{-1}$) is the concentration of NO_3^- and $C(\text{mdRC})$ the concentration of the microbial degradable reduced compounds ($\text{mmol } \Gamma^{-1}$) capable to support denitrification like organic carbon or sulphides etc.. The two unknown half-saturation constants $K_S(\text{NO}_3^-)$, $K_S(\text{mdRC})$ and in result $\mu_{\max}(\text{NO}_3^-)$ are characteristic properties of the investigated aquifer material with respect to possible denitrification rates and $K_S(\text{NO}_3^-) \cdot 2$ is the concentration of NO_3^- below which denitrification becomes NO_3^- limited.

Now we use Eqn. (4.4) to interpret the observed time courses of denitrification rates, i.e. turnover rates of NO_3^- . The concentration of NO_3^- in the sampled test solutions during the pull-phase of the conducted push-pull tests were always clearly above $1.0 \text{ mg } \text{NO}_3^- \text{-N } \Gamma^{-1}$, which is assumed to be the threshold of NO_3^- concentrations limiting denitrification rates reported by Wall et al. (2005). Therefore, we assume that NO_3^- concentrations were in excess to denitrification during the conducted push-pull tests, which means that the first Monod-term in Eqn. (4.4) approaches 1 since $C(\text{NO}_3^-) \gg K_S(\text{NO}_3^-)$. Thus, denitrification rates should be independent of NO_3^- concentrations during the conducted push-pull tests and denitrification rates should depend only on the second Monod-term in Eqn (4.4), i.e. on $C(\text{mdRC})$. In the two

investigated aquifers the majority of reduced compounds are not dissolved but solid organic carbon and sulphides. These amounts of organic carbon and sulphides represent the stock of reduced compounds (*SRC*) in both aquifers (Eschenbach and Well, 2013). We define now that the *mdRC* is the proportion of *SRC* used by microbes during denitrification and *saRC* is the surface area of reactive surfaces potentially capable to support denitrification. Since the significant majority of microbes in aquifers are attached to surfaces and thin biofilms (Griebler and Lueders, 2009; Kölblboelke et al., 1988) the actual $C(mdRC)$ might represent microbially colonized surface areas of reduced compounds in reaction contact to 1 l groundwater. If the total *saRC* is used by actively denitrifying microbes, then the measured denitrification rate $\mu(NO_3^-)$ should be equal to $\mu_{max}(NO_3^-)$ and the activity and amount of denitrifiers present in the investigated aquifer sediments are in a state of equilibrium to these reactive surfaces. But as discussed above, it can be assumed that the amount of denitrifying microbes in aquifer material of the NO_3^- -free zone is not in an equilibrium to NO_3^- and we suppose this also applies also to the *saRC*. The exponential increase of denitrified (N_2+N_2O) during the conducted push-pull tests (Fig. 4.2 and 4.4) is supposedly based on the stimulation of growth (Trudell et al., 1986) and activity of denitrifiers in the investigated aquifer material by the injected NO_3^- . It is assumed that this microbial stimulation leads also to an increase of $C(mdRC)$ (Eqn. 4.4) during push-pull tests because the proportion of *saRC* supporting denitrification should increase, if parts of the *saRC* are populated by active denitrifiers. If the denitrifying community is adapted to NO_3^- and changes not substantially during a push-pull test, one can suppose that then also $C(mdRC)$ is relatively constant. In this case also denitrification rates should be relatively constant and a zero order reaction model should fit the measured data during the relatively short duration of a push-pull test. It is suspected that these conditions apply for the NO_3^- -bearing zone. After pre-conditioning at multilevel well B4 no exponential increase of denitrified (N_2+N_2O) was observed in comparison to previous tests at the same well without pre-conditioning (Fig. 4.4). This is interpreted as a more constant activity of denitrifiers during the push-pull tests after pre-conditioning. After bio stimulation by injecting electron donors like ethanol, glucose, propane or fumarate it is reported that the zero-order reaction model could be used to describe reduction rates during push-pull tests (Istok et al., 2004; Kim et al., 2004; Kim et al., 2005). These previous findings might support the interpretation presented here that pre-conditioning leads to a kind of equilibrium between the denitrifying community and the injected NO_3^- and the *saRC* present in the aquifer material, which supposedly results in relatively constant $C(mdRC)$ during the

short time of a push-pull test, which would result according to Eqn. (4.4) in constant reaction rates.

4.4.3 Predicting $D_{\text{cum}}(365)$ and SRC of aquifer sediments from $D_r(\text{in situ})$

Only a modest goodness of fit ($R = 0.62$) was found using linear regression between $D_r(\text{in situ})$ and $D_{\text{cum}}(365)$ for the full data set (Table 4.5). Without Box-Cox transformations of input data the correlation coefficient was even lower ($R = 0.1$). This shows that it was necessary to transform the input data to approach normal distribution and homoscedasticity for regression analysis. Otherwise the ordinary least squares method did not find the best or efficient linear estimators for regression coefficients.

Like in the previous laboratory study (Eschenbach and Well, 2013) (Chapter 3) grouping of $D_r(\text{in situ})$ measuring points by locality or according to hydro-geochemical zones increased the predictive power of $D_r(\text{in situ})$ with respect to the measured $D_{\text{cum}}(365)$ and SRC of aquifer parallels for some partial data sets. Altogether, $D_r(\text{in situ})$ was the best predictor for $D_{\text{cum}}(365)$ and SRC of the partial data set of GKA aquifer material with correlation coefficients of 0.82 and 0.75, respectively. For the FFA the predictive power of $D_r(\text{in situ})$ for $D_{\text{cum}}(365)$ and SRC was significantly lower compared to the GKA (Table 4.5). This finding mirrors results of laboratory incubations with FFA and GKA material reported by Eschenbach and Well (2013) (Table 4.4 of the cited study) (see chapter 3), in which initial denitrification rates ($D_r(7)$) of GKA material were a better predictor of $D_{\text{cum}}(365)$ than in case of FFA material. Contrary to GKA aquifer samples, the SRC of the FFA samples was not predictable by $D_r(\text{in situ})$. One reason might be a different microbial availability of organic carbon (C_{org}), which is one major constituent of SRC in the FFA and GKA (Eschenbach and Well, 2013), in both aquifers. The ratio of KMnO_4 labile organic carbon (C_1) to C_{org} was almost twice as high in GKA material compared to FFA material (Eschenbach and Well, 2013), suggesting that the proportion of C_{org} available for microbes is higher in GKA aquifer material and on the other hand that a significant proportion of C_{org} is unavailable for denitrification in the FFA.

Grouping of aquifer material according to hydro-geochemical zones or sediment parameters resulted in better regressions between $D_r(\text{in situ})$ and $D_{\text{cum}}(365)$ and SRC for partial data sets where NO_3^- is still present in the groundwater (transition and NO_3^- -bearing zone). Relatively weak fits were obtained for data sets with push-pull measuring points located completely or mostly in the zone of NO_3^- free groundwater (NO_3^- -free zone and sulphidic aquifer material, respectively) and in the non-sulphidic zone (Table 4.5). For the

NO_3^- -free zones this is attributed to a missing adaptation of the microbial community to NO_3^- as electron acceptor as discussed above. In the study of Trudell et al. (1986) it took at least 8 days until measured denitrification rates stopped to increase during the push-pull test. During this study, such long pull-periods were not possible because of comparatively higher groundwater velocities in both aquifers. At some injection points in the FFA, the tracer plume moved away with groundwater already within 35 h after injection.

Konrad (2007) reported similar correlation coefficients of linear relations between D_r (in situ) and $D_{\text{cum}}(365)$ of $R = 0.60$ and even better linear relations between D_r (in situ) and C_{org} and sulphide-S with $R = 0.67$ and 0.90 (Spearman rank correlation coefficient). But these relationships were based on the comparison of laboratory data and in situ data from only 5 push-pull ^{15}N tracer tests. NO_3^- was detectable in the groundwater at all 5 of these injection points.

Overall, modelled $D_{\text{cum}}(365)$ and modelled SRC were in the same order of magnitude as the measured values. The mean ratios of calculated $D_{\text{cum}}(365)$ to measured $D_{\text{cum}}(365)$ and calculated SRC and measured SRC were best for the transition zone with ratios near 1 and worst for the sulphidic and NO_3^- -free zone (Table 4.5). D_r (in situ) underestimated especially $D_{\text{cum}}(365)$ and SRC of deeper aquifer samples with high values of $D_{\text{cum}}(365)$ and SRC to a large extent (Table 4.5) as already discussed above probably because of the lack of adaptation of the microbial community to NO_3^- . Only 20 % of the incubated aquifer samples, for which parallel in situ measurements exists (Table S4.1), exhibited $D_{\text{cum}}(365)$ and SRC values $> 20 \text{ mg N kg}^{-1} \text{ yr}^{-1}$ (the threshold of better predictions of $D_{\text{cum}}(365)$ from simple regressions with sediment variables reported by Eschenbach and Well (2013) Sect. 4.3.2) and $> 2000 \text{ mg N kg}^{-1}$, respectively. Strikingly, all these aquifer samples originated from D_r (in situ) measuring points in the zone of NO_3^- -free groundwater were D_r (in situ) rates are relatively low in comparison to $D_{\text{cum}}(365)$ or SRC of these aquifer parallels (Table S4.1 and Fig 4.3). Consequently, these comparatively low D_r (in situ) values in relation to $D_{\text{cum}}(365)$ and SRC result in an underestimation of these parameters using the regression models. This is reflected in the negative means of absolute deviations between calculated and measured $D_{\text{cum}}(365)$ and SRC values (Table 4.5) meaning that there are few but considerable deviations from measured values.

Pre-conditioning at multilevel well B4 led to a ratio closer to 1 of D_r (in situ) to $D_r(365)$ (Table 4.4). The ratios of calculated to measured values of $D_{\text{cum}}(365)$ and SRC were 0.85 and 1.11, respectively, after pre-conditioning and thus clearly better than for the sub data sets of push-pull tests without pre-conditioning in comparable aquifer zones (sulphidic and NO_3^- -

free zone) (Table 4.5). From this, although only 4 push-pull test with pre-conditioning were conducted, it is assumed that pre-conditioning might increase the predictability $D_{cum}(365)$ and SRC from D_r (in situ) measurements for of the tested aquifer material.

4.4.4 Possible confounding factors and uncertainties

Addy et al. (2002) discussed 3 potential confounding factors for the quantification of ^{15}N gas formation during push-pull tests: (i) dilution of denitrification gases, (ii) degassing of ^{15}N labelled denitrification gasses during the pull-phase of ^{15}N tracer tests (see therefore also discussion in Eschenbach and Well (2011)) and (iii) a lag phase between ^{15}N tracer injection and microbial response. In the following it is briefly referred to (iii).

Microbial adaptation processes after ^{15}N tracer injection might require time especially in the NO_3^- -free zone of aquifers (see Sect. 4.4.2), where aquifer material is brought into contact with NO_3^- for the first time. After pre-conditioning a clear lag phase was not observed during push-pull tests in the NO_3^- -free zone at multilevel well B4 in the FFA, therefore it is believed that this is attributed to the stimulation of denitrifiers due to the repeated injections of NO_3^- enriched groundwater at this multilevel well. Therefore, pre-conditioning might be a way to shorten or eliminate the observed lag phases between tracer injections and microbial response.

An additional uncertainty during push-pull tests (iv) is the effective porosity of investigated aquifer sediments. The effective porosity determines the volume of aquifer solids in reaction contact with 1 l test solution. Therefore, this value is needed to relate concentration data of evolved ($\text{N}_2+\text{N}_2\text{O}$) from ($\mu\text{g N l}^{-1}$) to ($\mu\text{g N kg}^{-1}$). This conversion strongly increases the coefficient of variation (CV) of concentration measurements of denitrified ($\text{N}_2+\text{N}_2\text{O}$) and thus increases the uncertainty of measured D_r (in situ) because of the uncertainty of the real effective porosity of the tested aquifer material (see Sect. 4.2.7). The effective porosity at the injection point can be measured with pumping tests prior or after the push-pull ^{15}N tracer test to reduce this source of uncertainty.

4.5 Conclusions

The relationship between in situ denitrification rates ($D_r(\text{in situ})$) was evaluated in two Pleistocene aquifers in Northern Germany and the cumulative denitrification measured during one year of incubation ($D_{\text{cum}}(365)$) and the stock of reduced compounds (SRC) of aquifer samples. Direct comparison of in situ push-pull tests and laboratory incubation of aquifer material collected from the location of push-pull wells proved to be a suitable approach to collect the necessary data set.

$D_r(\text{in situ})$ without pre-conditioning were generally lower than average denitrification rates after one year of incubation ($D_r(365)$) in the laboratory. This was especially the case for $D_r(\text{in situ})$ measurements in the NO_3^- free groundwater zone.

Prediction of $D_{\text{cum}}(365)$ and SRC from $D_r(\text{in situ})$ for data sets containing data from both aquifers was only satisfactory in the aquifer zones where NO_3^- was present. This type of in situ tests might thus be suitable for mapping $D_{\text{cum}}(365)$ and SRC in NO_3^- bearing zones of Pleistocene sandy aquifers using existing monitoring wells. It is thus a promising and low-cost method to estimate $D_{\text{cum}}(365)$ of aquifer material from aquifer zones where NO_3^- is still present in the groundwater.

In the NO_3^- -free aquifer zone increasing denitrification rates were observed during the conducted push-pull tests, which was interpreted as the result of adaptation processes of the denitrifying communities following NO_3^- injections. This confounded the relationship between reactive compounds and $D_r(\text{in situ})$ measured during push-pull tests, which resulted in poor prediction of $D_{\text{cum}}(365)$ and SRC.

In this study it was demonstrated exemplarily that the microbial community in the NO_3^- -free zone close below the NO_3^- -bearing zone can be adapted to denitrification by amending wells with NO_3^- injections for an extended period. In situ denitrification rates measured after this pre-conditioning reflected the $D_{\text{cum}}(365)$ and SRC satisfactorily. Therefore it is assumed that pre-conditioning is a prerequisite for the measurement of in situ denitrification rates using push-pull tracer tests in NO_3^- -free zones. Further research is needed to check if this microbial adaptation would also work in deeper layers far below the NO_3^- -bearing zone.

4.6 Supplement to chapter 4:

Predicting the denitrification capacity of sandy aquifers from in situ measurements using push-pull ^{15}N tracer tests

Table S4.1: Denitrification rates, cumulative denitrification, stock of reduced compounds, sulphate formation capacity and estimated minimal lifetime of denitrification of incubated samples from both aquifers (Eschenbach and Well, 2013) and corresponding in situ denitrification rates.

Sample location	Depth interval m	Aquifer zone ^a	$D_{cum}(365)^b$ mg N kg ⁻¹ yr ⁻¹	mg N kg ⁻¹			SFC ^f mg S kg ⁻¹ yr ⁻¹	D_r (in situ) µg N kg ⁻¹ d ⁻¹
				SRC ^c	SRC _C ^d	SRC _S ^e		
FFA B1	6.0-7.0	transition zone	17.18	659.6	599.5	60.1	6.1	17.59
FFA B1	7.0-8.0	sulphidic	56.24	5974.2	5552.7	421.5	39.4	1.51
FFA B2	2.0-3.0	non-sulphidic	0.19	240.8	220.7	20.1	0.1	0.12
FFA B2	3.0-4.0	non-sulphidic	0.37	215.4	189.2	26.3	-0.1	0.12
FFA B2	4.0-5.0	non-sulphidic	4.34	540.2	508.0	32.2	1.0	0.07
FFA B2	8.0-9.0	transition zone	10.53	1638.2	1515.5	122.7	3.5	8.65
FFA B2	9.0-10.0	transition zone	12.68	610.7	502.0	108.7	2.2	8.65
FFA B4	7.0-8.0	sulphidic	20.16	603.6	450.2	153.4	9.6	2.76
FFA B4	8.0-9.0	sulphidic	34.09	1289.5	1038.9	250.7	22.0	2.28
FFA B6	2.0-3.0	non-sulphidic	2.64	687.0	648.9	39.1	0.3	0.06
FFA B6	3.0-4.0	non-sulphidic	1.46	1017.4	976.5	40.9	0.1	0.06
FFA N10	4.5-5.0	transition zone	8.69	1239.0	1204.1	34.8	1.5	12.89
FFA N10	5.0-5.5	transition zone	8.75	721.6	687.1	34.5	2.1	12.89
FFA N10	5.5-6.0	transition zone	7.82	674.6	640.3	34.3	5.2	12.89
FFA N10	7.7-8.3	transition zone	15.04	329.5	290.0	39.5	1.5	23.19
FFA N10	8.3-8.6	transition zone	15.17	331.5	298.7	32.9	6.9	23.19
FFA N10	10.0-10.4	sulphidic	17.45	320.6	289.3	31.3	5.4	-
FFA N10	10.4-10.7	sulphidic	50.07	5571.6	5247.7	323.9	9.4	-
FFA N10	12.0-13.0	sulphidic	52.84	2771.3	2381.7	389.6	37.9	-
FFA N10	13.0-14.0	sulphidic	38.04	2134.1	1723.3	410.8	18.2	-
FFA N10	16.0-17.0	sulphidic	46.65	2744.7	2431.5	313.2	23.6	-
FFA N10	17.0-18.0	sulphidic	46.55	2642.7	2335.0	307.8	36.8	-
GKA	8.0-9.0	non-sulphidic	0.63	132.6	95.0	37.6	0.9	0.00
GKA	9.0-10.0	non-sulphidic	0.34	97.1	70.7	26.4	0.4	0.00
GKA	22.0-23.0	non-sulphidic	1.57	193.3	164.2	29.1	0.2	0.00
GKA	23.0-24.0	non-sulphidic	2.83	204.5	179.2	25.3	-0.0	0.00
GKA	25.9-27.0	sulphidic	15.63	2857.4	2381.0	476.4	1.2	1.23
GKA	27.0-28.3	sulphidic	41.82	6634.0	5943.2	690.8	8.3	1.23
GKA	28.3-29.3	sulphidic	37.82	4495.6	3878.5	617.2	13.8	4.43
GKA	29.3-30.3	sulphidic	35.49	4766.8	4236.0	530.8	8.1	4.43
GKA	30.3-31.2	sulphidic	6.54	1086.9	731.4	355.4	3.8	0.50
GKA	31.3-32.0	sulphidic	4.09	1122.4	777.7	344.7	5.0	0.50
GKA	32.9-33.7	sulphidic	7.28	1206.0	765.6	440.4	10.2	0.50
GKA	33.7-34.7	sulphidic	12.25	1057.4	700.9	356.6	17.7	2.00
GKA	35.7-36.7	sulphidic	52.46	8861.3	8366.7	494.6	30.0	6.19
GKA	36.7-37.7	sulphidic	11.07	689.6	216.7	472.8	9.2	6.19
GKA	37.7-38.7	sulphidic	12.06	1347.7	1083.1	264.7	4.6	6.19
GKA	65.1-65.4	sulphidic	13.22	1441.2	941.3	499.9	1.3	2.27
GKA	67.1-67.5	non-sulphidic	8.18	471.0	333.8	137.2	1.3	2.27
GKA	67.5-68.0	non-sulphidic	8.11	487.1	351.5	135.6	0.7	2.27

FFA Fuhrberger Feld aquifer; GKA Großenkneten aquifer; ^a sediment characteristic; ^b cumulative denitrification after one year of incubation; ^c stock of reactive compounds (SRC); ^d fraction of organic carbon in the SRC; ^e fraction of total-S in the SRC; ^f sulphate formation capacity (SFC).

Table S4.2: Lambda values of the Box-Cox transformed D_r (in situ) and variables measured during anaerobic incubation.

Data set	Lamda values		
	D_r (in situ)	$D_{cum}(365)$	SRC
Whole data set	0.216	0.303	-0.024
FFA	0.214	0.369	-0.185
GKA	0.257	0.236	0.039
non-sulphidic zone	0.041	0.122	1.493
Sulphidic zone	0.190	0.260	0.229
transition zone	-0.150	-0.029	-0.159
NO ₃ ⁻ -bearing	0.099	0.337	0.797
NO ₃ ⁻ -free	0.319	0.670	0.492

Table S4.3: Simple regressions between D_r (in situ) and individual sediment parameters from aquifer parallels. $f^{B-C}(X) = A + B \times f^{B-C}(D_r(\text{in situ}))$. For each sub data set the two sediment parameters with the best correlation coefficient with D_r (in situ) are listed.

Data set	X ^a	N ^b	A	B	R ^c	R ²
Whole data set	SO ₄ ²⁻	29	3.697	-0.564	0.58	0.33
Whole data set	C _{org}	34	5.516	0.134	0.40	0.16
FFA	C _{hws}	14	19.74	1.754	0.75	0.56
FFA	SO ₄ ²⁻	11	3.263	-0.472	0.72	0.52
GKA	total-S	18	92.88	17.51	0.75	0.56
GKA	C _{org}	18	5.612	0.324	0.69	0.48
non-sulphidic	total-S	11	5.128	0.150	0.62	0.38
non-sulphidic	C _{org}	11	680.1	51.58	0.42	0.18
sulphidic	total-S	23	543.2	-109.7	0.69	0.48
sulphidic	SO ₄ ²⁻	18	3.540	-0.614	0.49	0.24
transition zone	total-S	8	0.608	-0.001	0.60	0.36
transition zone	C _{org}	8	5.341	-0.601	0.73	0.53
NO ₃ ⁻ -bearing	C _{org}	17	151.0	12.75	0.55	0.30
NO ₃ ⁻ -bearing	SO ₄ ²⁻	14	5.612	-0.501	0.53	0.28
NO ₃ ⁻ -free	SO ₄ ²⁻	15	3.085	-0.844	0.51	0.26
NO ₃ ⁻ -free	C ₁	14	34.51	5.418	0.29	0.08

^a Independent sediment parameter; ^b Sample number; ^c Correlation coefficient; SO₄²⁻ extractable sulphate-S; C_{hws} hot-water soluble organic carbon; C₁ KMnO₄ labile organic carbon; C_{org} total organic carbon; total-S total sulphur.

Table S4.4: Lambda values of the Box-Cox transformed sediment parameters.

Data set	Lamda values								
	$D_r(7)$	$D_{cum}(365)$	$D_r(\text{in situ})$	C_{org}	total-S	$SO_4^{2-}_{extr}$	DOC_{extr}	C_{hws}	C_l
Whole data set	0.487	0.303	0.216	-0.050	0.132	0.457	0.946	0.825	0.199
FFA	0.583	0.369	0.214	-0.191	-0.292	0.254	-	0.915	0.513
GKA	0.445	0.236	0.257	-0.052	0.685	0.628	-1.307	-0.203	0.291
non-sulphidic	-0.168	0.122	0.041	1.060	0.062	1.161	-	1.434	0.183
sulphidic	0.375	0.260	0.190	0.162	0.965	0.368	-1.931	1.314	-0.081
transition zone	0.397	-0.029	-0.150	-0.158	-1.649	0.642	-0.012	0.783	-0.834
NO_3^- -bearing	0.121	0.337	0.099	0.752	-0.228	0.679	-	2.949	0.492
NO_3^- -free	0.364	0.670	0.319	0.378	1.998	0.297	-3.158	0.970	0.452

Table S4.5: Lambda values of the Box-Cox transformed variables.

Data set	Lamda values				
	SRC	SRC_C	SRC_S	aF_{SRC}	SFC
Whole data set	-0.024	-0.050	0.132	0.155	0.176
FFA	-0.185	-0.191	-0.291	0.326	0.187
GKA	0.039	-0.052	0.685	-0.139	0.193
non-sulphidic	1.493	1.043	-0.054	0.095	-0.014
sulphidic	0.229	0.159	0.941	-0.313	0.117
transition zone	-0.159	-0.158	-1.650	-0.089	-0.152
NO_3^- -bearing	0.797	0.745	-0.307	0.069	0.120
NO_3^- -free	0.492	0.375	1.914	-0.266	0.344

5 Synthesis and general conclusions

The primary source of reactive nitrogen in aquifers is leaching from agro-ecosystems and nitrate (NO_3^-) is the most common reactive nitrogen species in groundwater (Galloway et al., 2003). Denitrification is the key process for the attenuation of anthropogenic NO_3^- pollution of groundwater and riparian buffer zones (Korom, 1992; Burt et al., 1999).

Therefore, the estimation of denitrification rates and the life-time of denitrification in aquifers had been addressed since long (Rivett et al., 2008) but lately these questions was again given more attention due to the European Union Water Framework (European Parliament and Council of the European Union, 2000). According to this directive, a good chemical status of groundwater requires NO_3^- concentrations below the limit of $50 \text{ mg } \Gamma^{-1}$. This limit is regularly exceeded in the groundwater recharge below agricultural fields.

Denitrification is a miserable process to measure (Groffman et al., 2006) and hard to predict with regard to its intensity, its life-time and its spatial distribution in aquifers. This work tries to contribute to these questions at the scale of aquifers as an important part of terrestrial ecosystems and methodically in the field of denitrification measurement methods.

5.1 Methodical Part

Sensitive and time-saving measuring methods for denitrification are still required (Groffman et al., 2006), therefore one objective of this thesis was to develop an automated sampling and calibration unit coupled to a membrane inlet mass spectrometry system (ASCU-MIMS) for online analysis of denitrification during ^{15}N tracer experiments.

Main objective of this part of this thesis was *the development of an automated online system for the mass spectrometric measurement denitrification in aquifer samples after ^{15}N -tracer application*. Therefore, a laboratory ^{15}N tracer experiment was conducted, with incubation of aquifer material from the Fuhrberger Feld aquifer in aquifer mesocosms to test the developed automatic sampling and calibration unit coupled to a membrane inlet mass spectrometer (ASCU-MIMS) (chapter 2, Fig. 2.1). Furthermore, 3 different ^{15}N aided mathematical approaches were evaluated for their suitability to calculate denitrification from MIMS raw data.

Development of an automated online system for the measurement of denitrification in aquifer samples after ^{15}N -tracer application

Online analysis of denitrification rates measured after ^{15}N tracer application with ASCU-MIMS was in good agreement with the well established offline isotope analysis by GC-IRMS. The ASCU-MIMS approach successfully enabled nearly unattended online-measurement for 7 days with sampling intervals of 4 h, where only the refilling of the liquid nitrogen trap and the reservoir of standard water had to be conducted manually every 8 h and 12 h, respectively. Instrumental precision of ASCU-MIMS, estimated from the coefficient of variation (CV) of the 29/28 molecular ion mass ratio, was found to be 0.13 % and therefore lower compared to GC-IRMS (0.02 %). The limit of detection of ^{15}N labelled denitrified ($\text{N}_2+\text{N}_2\text{O}$) with the ASCU-MIMS system was $1.5 \mu\text{g N } \Gamma^{-1}$ and thus slightly better than offline GC-IRMS analysis ($2.5 \mu\text{g N } \Gamma^{-1}$) (Table 2.1).

The advantage of the developed ASCU-MIMS, in comparison to common GC-IRMS methods used in previous denitrification studies (Well and Myrold, 2002; Addy et al., 2002; Addy et al., 2005), is that it combines MIMS analysis without sample preparation (An et al., 2001; Kana et al., 1994; Tortell, 2005; Jensen et al., 1996) with an automated sampling and calibration unit (ASCU). Moreover, the almost real-time measurement of denitrification in water samples immediately reveals failure or success of experiments. This is because a laborious degassing step prior to analysis is not required with this online method. Furthermore, sampling intervals can be adjusted to the specific denitrification dynamics during an experiment. This improves the assessment of microbial adaptation processes at the beginning of a ^{15}N tracer experiments (chapter 4, Sect. 4.4.1). Finally, the change of denitrification dynamics resulting from the exhaustion of substrates can be investigated in more detail.

What ^{15}N -aided mathematical approach is most suitable to analyse MIMS raw data obtained from dissolved gas analysis?

From the investigated 3 ^{15}N aided mathematical approaches (approaches given by Mulvaney (1984), Nielsen (1992) and Spott and Stange (2007)) the approach given by Spott and Stange (2007) was found to be most suitable for the determination of denitrification from MIMS raw data. In contrast to Nielsen (1992) and Spott and Stange (2007), the approach given by Mulvaney (1984) requires only the measurement of the molecular ion masses 29 and 28. This is advantageous since the molecular ion mass 30 is often biased by spectral interferences (see

appendix). The approach given by Mulvaney (1984) can be used if the ratio of ^{15}N labelled denitrification products to the dissolved atmospheric N_2 in the sample is small (≤ 0.05 , if ^{15}N abundance in the evolved ($\text{N}_2+\text{N}_2\text{O}$) is 40 to 60 atom %) (Sect. 2.4.2).

Investigation of confounding factors, like in situ degassing, on the measured ($\text{N}_2+\text{N}_2\text{O}$) production during incubation

After 65 h, the increase of ^{15}N -labelled denitrification derived ($\text{N}_2+\text{N}_2\text{O}$) stopped (Fig 2.2) which could be explained by a combination of in situ degassing of denitrification products and dilution of the samples with new ^{15}N tracer solution during the experiment caused by excessive pumping of pore water (Sect. 2.4.3).

Modelling showed that in situ degassing can significantly lower the measured concentrations of ^{15}N labelled denitrification products in analysed pore water samples during incubation and accordingly measured denitrification rates (chapter 2, Sect. 2.4.3). But in situ degassing could not explain the constant concentrations of denitrification derived ($\text{N}_2+\text{N}_2\text{O}$) observed after 65 h of incubation (Fig. 2.5).

Modelling indicated also that the ratio of $^{30}\text{N}_2/^{28}\text{N}_2$ should be almost not affected by degassing, i.e. should further increase during ongoing reduction of ^{15}N labelled NO_3^- . This is because gas bubbles formed during degassing are trapped in the sediment pores and the entrapped N_2 in these bubbles is still in diffusive exchange with new evolved ^{15}N labelled N_2 dissolved in the pore water. Contrary to this, the measured $^{30}\text{N}_2/^{28}\text{N}_2$ ratio during incubation did not increased further after 65 h of incubation, indicating that in situ degassing was not the reason for constant concentrations of denitrification products after 65 h. The ratio $^{30}\text{N}_2/^{28}\text{N}_2$ can be used to evaluate if or if not in situ degassing might be a reason for a slowdown of measured denitrification rates during ^{15}N tracer experiments.

5.2 Experimental part

There is still urgent research need concerning the upscaling of laboratory measurements of denitrification to the field scale and improved field methods are required (Rivett et al., 2008). The experimental part of this thesis tries to contribute to this challenging task. Therefore, laboratory incubation experiments and ^{15}N push-pull tracer tests were conducted with emphasis on the prediction of denitrification activity in two Pleistocene sandy aquifers in the North of Germany.

Previous work by Kölle et al. (1983), Kölle et al. (1985), Böttcher et al. (1985), Böttcher et al. (1989) and Böttcher et al., (1991) identified lithotrophic denitrification with pyrite as the most important process of NO_3^- reduction in the well investigated Fuhrberger Feld aquifer. Intense ongoing denitrification within the Großenkneten aquifer was proven by excess- N_2 measurements (Well et al., 2012). But there are no studies on the type of denitrification in this aquifer.

Wendland and Kunkel (1999) report that besides particular organic matter especially denitrification via pyrite is supposed to play an important role for NO_3^- attenuation in North American and European aquifers. Kölle et al. (1985) estimated the life-time of denitrification in the Fuhrberger Feld aquifer from pyrite content of aquifer material. But information about the pyrite content in aquifers is generally scarce. This applies also on the amount and microbial availability of C_{org} and other possible electron donors for denitrification in aquifers. Up to now costly drilling with subsequent sampling and analysis of aquifer material is required to obtain these important information, but this is not an option for the prediction of denitrification on aquifer or river catchment scale.

This thesis tries to provide an initial framework for the prediction of denitrification capacity of aquifers with relatively small effort. Therefore, regression models were tested to predict the denitrification capacity and content of reduced compounds of aquifer material from initial denitrification rates measured during anaerobic incubation of aquifer samples and from several sediment parameters. In a second step results from these laboratory measurements were compared with in situ measurements of denitrification at groundwater monitoring wells using push-pull ^{15}N tracer tests.

In this thesis, the term denitrification capacity is defined as the amount of NO_3^- that can be denitrified per volume (m^3) or mass (kg) of aquifer material until significant denitrification activity stops because of exhaustion of electron donors. One of the central assumptions made in this work is that there are quantitative relations between the stock of reduced compounds (SRC) present in aquifer material and its denitrification capacity.

5.2.1 Prediction of the denitrification capacity of sandy aquifers from shorter-term incubations

Predicting the denitrification capacity of aquifer material from incubation experiments is a very challenging task since this means predicting a process that can in certain circumstances last several decades from comparatively short-term measurements.

Therefore, the main objective of the laboratory study introduced in chapter 3 was to estimate the stock of reduced compounds (SRC) of aquifer samples from the measured denitrification during one year of anaerobic incubation ($D_{\text{cum}}(365)$). Additionally it was tested if $D_{\text{cum}}(365)$ could be predicted from initial denitrification rates at the beginning of incubation as well as from sediment parameters using different regression models. The minimal life-time of denitrification in the investigated aquifer material was estimated from experimental data. It is assumed that the denitrification capacity depends on the amount of available electron donors in the sediment, therefore an intensive incubation experiment was conducted to test the exhaustibility of electron donors supporting denitrification in the investigated aquifer samples.

Hypotheses:

The cumulative denitrification after one year of incubation ($D_{\text{cum}}(365)$) is a feasible predictor of the stock of reduced compounds (SRC) in aquifer material.

The $D_{\text{cum}}(365)$ can be predicted from initial denitrification rates at the beginning of incubation as well as from several sediment parameters like organic carbon, total sulphur and others.

The intensive incubation experiment is able to exhaust the denitrification capacity of incubated aquifer material.

Predicting the stock of reduced compounds (SRC) in aquifer material from $D_{cum}(365)$

The investigated aquifer material showed comparable denitrification rates during incubation and similar ranges of the investigated sediment parameters as previous studies on denitrification in comparable aquifers (Weymann et al., 2010; Konrad, 2007) suggesting that the results derived in this study might be transferable to other Pleistocene sandy aquifers in Northern Germany.

Denitrification rates during the incubation experiments could be described with zero-order kinetics except for transition zone samples (chapter 3, Sect. 3.4.2), which showed declining denitrification rates during incubation. This was attributed to small amounts of residual reductants present in this zone that were reduced during the incubations. Beside the samples from the transition zone, these relatively constant denitrification rates suggested that denitrification was more dependent on the stock of reduced compounds (SRC) in the sediment compared to NO_3^- concentrations during incubations.

Overall $D_{cum}(365)$ appeared to be a good indicator for the denitrification capacity of aquifer material from the reduced zone of both aquifers since it was closely related to the SRC (Table 3.6). Contrary, the $D_{cum}(365)$ was less related to the SRC for aquifer samples from already oxidized parts in both aquifers, i.e. for aquifer material supposed to be already depleted in its SRC. In this work it is assumed that a higher recalcitrance of C_{org} is the reason for the lower predictive power of $D_{cum}(365)$ for the SRC of these samples (see also Sect. 5.3.2).

From the measured $D_{cum}(365)$ during standard and intensive incubations and from the fact that denitrification did not stop during standard incubation and intensive incubation experiments it is assumed that 5 % of the SRC of the investigated samples are available for denitrification (chapter 3, Sect. 3.4.4). From this estimation the lifetime of denitrification in the both aquifers was estimated to last for several generations, if the reduced zone is over several meters thick.

Predicting $D_{cum}(365)$ from initial denitrification rates at the beginning of incubation and from sediment parameters

Initial denitrification rates were not able to predict $D_{cum}(365)$ of aquifer samples from the deeper parts of both aquifers which were not yet in contact with NO_3^- bearing groundwater. This fact was attributed to time consuming microbial adaptation processes after the addition of NO_3^- as a new available electron donor to samples from the reduced groundwater zone of both aquifers. In contrast, the average denitrification until day 84 of incubation was a good predictor for $D_{cum}(365)$. Indicating that prolonged incubation is needed to get reliable estimates of the $D_{cum}(365)$.

The $D_{cum}(365)$ could also be estimated using transfer functions based on several sediment parameters. Total organic carbon (C_{org}) and $KMnO_4$ -labile organic carbon (C_1) yielded the best predictions for the whole data-set with aquifer material from both aquifers, all other parameters (total-sulphur, extractable sulphate, hot water extractable carbon, extractable dissolved organic carbon) were less suitable to predict $D_{cum}(365)$ for the whole data-set. Total sulphur (total-S) was only a good predictor for the denitrification capacity for partial data-sets with aquifer material from only one site, suggesting that this sediment parameter gives regressions which were less transferable from one aquifer to another. Transfer functions to predict $D_{cum}(365)$ from sediment parameters exhibited poor fits for aquifer samples already depleted in reductants. This was attributed to higher microbial recalcitrance of residual reductants in these samples.

Exhaustibility of the denitrification capacity of incubated aquifer material

Measuring the denitrification capacity of aquifer material is challenging, since normal incubations are mostly too short to quantify the amount of reduced compounds available to support denitrification. Therefore, experiments capable to exhaust the stock of electron donors are needed to quantify the denitrification capacity of aquifer material. Thus an intensive incubation experiment, at higher incubation temperatures and with continuous shaking during incubation was conducted to exhaust reduced compounds in the investigated aquifer samples (chapter 3, Sect. 3.2.3.2).

The intensive incubation experiment was not able to exhaust the denitrification capacity. From the conducted experiment it is assumed that continuous shaking during incubation increased the stock of microbial available reduced compounds in the incubated aquifer material due to creation of new surfaces or due to physical stress during incubation (chapter 3, Sect. 3.4.2).

Open questions

During the conducted incubations experiments denitrification was reasonably well describable with a zero-order kinetic. This finding is in accordance with Korom et al. (2012) who stated that most published denitrification rates in aquifers are reported as zero-order denitrification rates (chapter 3, Sect. 3.4.5.2). But nonetheless, further research is needed if this is transferable to in situ conditions?

The linear denitrification rates during incubations might be interpreted as the result of a constant amount of active denitrifiers during incubations. Possibly the amount of denitrifiers

is restricted by the area of reactive reduced surfaces (see chapter 4, Sect. 4.4.2) within the incubated sediments and constant denitrification rates are a result of relatively constant areas of reactive surfaces, but this has to be investigated in future studies.

Low concentrations of NH_4^+ in the groundwater can be found in the reduced zone of both aquifers, which leads to the question: Is there a reductive turnover of NO_3^- in the investigated sediments by DNRA coupled to anammox (chapter 3, Sect. 3.6)?

The bioavailability of organic carbon is still not sufficiently clarified (Weymann, 2009). Especially it is of interest if bioavailability of organic carbon changes in different depths within one aquifer, i.e. in different redox zones of one aquifer.

5.2.2 Predicting the denitrification capacity of sandy aquifers from in situ measurements using push-pull ^{15}N tracer tests

The main objective of the conducted push-pull ^{15}N tracer tests introduced in chapter 4 was to measure in situ denitrification rates ($D_r(\text{in situ})$) and to evaluate if $D_{\text{cum}}(365)$ and the stock of reduced compounds (SRC) can be predicted from $D_r(\text{in situ})$. Another aim was to evaluate the influence of pre-conditioning of aquifer material in the zone of NO_3^- free groundwater prior to ^{15}N tracer push-pull experiments.

Hypotheses:

The cumulative denitrification after one year of incubation ($D_{\text{cum}}(365)$) and the stock of reduced compounds (SRC) of incubated aquifer parallels can be predicted from initial in situ denitrification rates ($D_r(\text{in situ})$) measured with ^{15}N push-pull experiments in the field.

Pre-conditioning of aquifer material prior to ^{15}N tracer push-pull tests in the zone of NO_3^- free groundwater increases the measured $D_r(\text{in situ})$ denitrification rates.

Predicting $D_{\text{cum}}(365)$ and SRC from $D_r(\text{in situ})$

The push-pull ^{15}N tracer tests were carried out in groundwater monitoring wells at the same position and with filter screens in the same depths as the origin of aquifer samples, that had been collected for laboratory measurements. In situ denitrification rates measured with these 3 days lasting push-pull tests showed a similar range of $D_r(\text{in situ})$ (0.0 to $51.5 \mu\text{g N kg}^{-1} \text{d}^{-1}$) as previous push-pull tests in aquifers (Konrad, 2007; Addy et al., 2002; Addy et al., 2005). The mean ratio of $D_r(\text{in situ})$ to $D_r(365)$ was lower for aquifer material from the GKA (0.06) than from the FFA (0.26). ($D_{\text{cum}}(365)$ divided by 365 gives $D_r(365)$.) For partial data-sets with aquifer material from both aquifers, this ratio was lowest for material from the zone of NO_3^-

free groundwater (0.1) and highest for material from the transition zone (0.47) (Table 4.4). The in situ measurements showed that $D_r(\text{in situ})$ without pre-conditioning generally underestimated longer term denitrification rates ($D_r(365)$) measured in the laboratory (Fig. 4.2).

Similar to the laboratory study (chapter 3), grouping of $D_r(\text{in situ})$ measuring points by locality or according to hydro-geochemical zones in both aquifers improved the predictive power of $D_r(\text{in situ})$ with respect to $D_r(365)$ and SRC (Table. 4.5). Additionally regression analysis showed that the predictive power of $D_r(\text{in situ})$ is depended on the redox state of the evaluated system, i.e. the occurrence of NO_3^- in groundwater. Regressions revealed closer linear relations between $D_r(\text{in situ})$ data from push-pull tests and laboratory measurements of $D_r(365)$ and SRC if ambient groundwater still contained NO_3^- (Table 4.5). *The poor regressions between $D_r(\text{in situ})$ and laboratory data ($D_{cum}(365)$ and SRC) in the zone of NO_3^- free groundwater were attributed to adaptation processes of the microbial community after injection of tracer NO_3^-* (chapter 4, Sect. 4.4). These adaptation processes of the microbial community might extend over several weeks (chapter 3, Sect. 3.4.2), which can explain the underestimation of longer-term laboratory denitrification rates ($D_r(365)$) by short term in situ measurements ($D_r(\text{in situ})$) (Fig. 4.3).

Effect of pre-conditioning

As already mentioned, in situ denitrification rates, especially in the NO_3^- free groundwater zone of both aquifers, underestimated longer-term laboratory denitrification rates. Therefore, it was evaluated if pre-conditioning can increase in situ denitrification substantially.

During most of the push-pull tests in the NO_3^- free groundwater zone exponential increases of denitrification over time were observable (Fig. 4.2 and 4.4) (chapter 4, Sect. 4.4.1). These observed exponential increases of denitrification products might be interpreted as a result of the stimulation of growth and activity of denitrifiers after NO_3^- injection in previous NO_3^- free aquifer regions. This is in line with observations by Trudel et al. (1986). They measured increasing denitrification rates and an increasing number of denitrifiers in aquifer material during a push-pull test in the NO_3^- free groundwater zone of a shallow sandy aquifer in Ontario USA.

To evaluate pre-conditioning push-pull tests with and without pre-conditioning were conducted at one multilevel well in the FFA. Pre-conditioning was performed by the repeated injection of NO_3^- in the zone of NO_3^- free groundwater at multilevel well B4. Pre-conditioning resulted in a strong increase of measured in situ denitrification rates (30 to 65

times higher than without pre-conditioning) and the ratio of $D_r(\text{in situ})$ to $D_r(365)$ were close to 1 or above (Fig. 4.5 and Table 4.4). After pre-conditioning, denitrification derived N_2 and N_2O showed no exponential increase, whereas exponential increases were observable during previous push-pull tests without pre-conditioning at the same depths of multilevel well B4 (Fig. 4.4).

From the results of the ^{15}N tracer push-pull tests it follows that *pre-conditioning prior to $D_r(\text{in situ})$ measurements is expected to be crucial in deeper NO_3^- -free groundwater zones of aquifers* to get reliable estimates of $D_{\text{cum}}(365)$ and SRC of aquifer material. Pre-conditioning would therefore help to improve field methods, which is strongly required for quantification of field scale denitrification (Rivett et al., 2008).

Interpretation of the time courses of denitrification derived ($\text{N}_2+\text{N}_2\text{O}$)

To interpret the experimental results of in situ measurements a multiplicative Michaelis-Menten kinetics (Eq. 4.4) was assumed to describe the relationship of NO_3^- and the amount of reductants on measured time courses of denitrification derived ($\text{N}_2+\text{N}_2\text{O}$) (chapter 4, Sect 4.4.2).

From these theoretical considerations, with the prerequisite that denitrification during experiments was not NO_3^- limited (see chapter 3, Sect. 3.4.5), *it is hypothesized that pre-conditioning helps to establish a kind of equilibrium between the amount and activity of denitrifiers in the sediments and the surface area of reduced compounds present in the aquifer material. From these theoretical considerations it is also hypothesized that such kind of temporary equilibrium should result in more or less constant denitrification rates during push-pull tests.* But, further studies are required to confirm or disconfirm these theoretical considerations.

Overall Conclusions

The conducted incubation experiments were not able to measure the denitrification capacity of the investigated aquifer sediments because denitrification did not stop during incubations. Nonetheless, $D_{\text{cum}}(365)$ showed good linear regressions with the SRC of the investigated sediments and therefore, it is assumed that $D_{\text{cum}}(365)$ is an estimate of the real denitrification capacity of the investigated aquifer material. But further research is needed to evaluate the influence of type of electron donors and their reactive surface on the relation between $D_{\text{cum}}(365)$ and the denitrification capacity.

Pre-conditioning prior to $D_r(\text{in situ})$ measurements is assumed to be crucial to get reliable estimates of $D_{\text{cum}}(365)$ and SRC of aquifer material from ^{15}N tracer push-pull tests in the deeper NO_3^- -free groundwater zone of aquifers.

5.3 Future research and perspectives and methodical improvements

In the following, some methodical perspectives concerning the measurement of denitrification as well as recommendations for further research in the field of denitrification in aquifers are given.

5.3.1 Methodical improvements

Measuring denitrification with ASCU-MIMS

The possibility of online measurement of denitrification rates by means of an automated sampling and calibration unit in combination with membrane-inlet mass spectrometry (ASCU-MIMS) was studied in chapter (2). Further developments of the described measurement system should test if the liquid nitrogen trap could be omitted (chapter 2 Fig. 1) and then whether the online measurement of carbon dioxide (CO₂) is possible. The parallel measurement of CO₂, beside N₂ one reaction product of organotrophic denitrification, might help to distinguish the share of organotrophic and lithotrophic denitrification to the measured denitrification rates during online analysis. In case of common MIMS analysis, CO₂ was for example measured by Tortell (2005) in oceanic water samples. To calibrate the ASCU-MIMS system for CO₂ measurements they used temperature-controlled standard water sparged with gas mixtures containing different concentrations of CO₂ (Tortell, 2005).

Sparging of temperature-controlled standard waters with different gases of known concentration would help to simplify the calibration of an ASCU-MIMS system. With this procedure it is easy to attain standard water with different dissolved gas concentrations. This would enable calibrating the ASCU-MIMS systems for dissolved gas concentrations according to DIN 32645 published by the German Institute for Standardization (Deutsches Institut für Normung (DIN)).

The developed ASCU-MIMS could be improved by reducing its total inner volumes (Fig. 2.1). This would reduce the needed sampling volume of 150 ml and also shorten the possible sampling intervals. Possible applications of the ASCU-MIMS system are laboratory incubation experiments with the need of a high temporal resolution measurement and high sensitivity of denitrification activity.

Measurement of denitrification with anaerobic incubation experiments

One key point of anaerobic incubations is batch vessels must be closed air tight during incubation to avoid air contamination. Small amounts of air contamination can be difficult to detect during the conducted incubations, since the headspace consisted of pure N₂ (to ensure a sufficient N₂ concentration in the samples during GC-RMS analysis) and O₂ from the air might be consumed in the batch vessel. Therefore, the measurement of Argon (Ar) in the headspace samples might be a relatively easy way to control batch vessels regarding air contaminations which would be accompanied by increasing Ar concentrations in the headspace.

Furthermore, pre-incubation for several weeks is advisable when incubating samples from the zone of NO₃⁻-free groundwater to predict longer term denitrification rates from short-term incubations (chapter 3, section 3.4.2). This follows from the required time needed to adapt the microbial community to NO₃⁻ as an available electron acceptor.

In situ measurement of denitrification in aquifers

Pre-conditioning by the repeated injection of NO₃⁻ amended groundwater resulted in a strong increase of denitrification rates measured during a subsequent ¹⁵N push pull tracer test in the zone of NO₃⁻-free groundwater, compared with a tracer test without pre-conditioning (chapter 4). These results show that pre-conditioning is important to get reliable denitrification rates in the zone of NO₃⁻-free groundwater in aquifers. It is strongly advisable that future studies should evaluate how long aquifer material has to be pre-conditioned until no further increase in measured denitrification rates is observed due to even longer pre-conditioning.

5.3.2 Future research perspectives

Bioavailability of organic carbon

Previous studies showed that almost the total stock of pyrite in Pleistocene aquifers in northern Germany is bioavailable. But the bioavailability of organic carbon is still not sufficiently clarified (Weymann, 2009). Correlation analysis revealed a significant relationship between the C_{org} content of incubated sulphidic aquifer material from deeper parts of both aquifers and denitrification capacity after one year of incubation (Chapter 3, Table 3.3). This relationship was not observed for non-sulphidic aquifer material from upper parts of both aquifers. Weymann et al. (2010) reported similar results from incubation of aquifer material from the FFA. From this finding, it is supposed that bioavailability of organic

matter was larger below the nitrate front in both aquifers, suggesting that the chemical composition and/or bioavailability of organic carbon depended on its position within different redox zones in the investigated aquifers.

To constrain the real reactivity of organic matter in aquifers, more sophisticated methods have to be applied, e.g. as done by Hartog et al. (2004) who investigated the chemical composition of sedimentary organic matter (SOM) on a molecular level (low- and high-weight-molecular compounds) in a sandy aquifer in The Netherlands. No study had done this in the FFA or GKA. The analysis of the composition of organic matter in this aquifer consisting of Pleistocene and Pliocene sandy sediments, revealed that high-molecular-weight compounds were more resistant towards oxygen during incubations than low-molecular-weight-compounds. Hartog et al. (2004) concluded: *“Not the age of SOM, but the extent of oxygen exposure during syn- and postdepositional conditions seems most important in affecting the degradation status of SOM in aquifer sediments and thus their ability to reduce oxidants.”* Taking this into account the influence of the molecular structure (ratio of low- to high-molecular-weight compounds) of the organic matter on the reactivity of organic matter should also be investigated in both aquifers.

Furthermore, Eusterhues et al. (2005) reported that 80-95 % of total organic matter in the C horizons of two soils in northern Bavaria is represented by mineral-associated organic carbon and Fe oxides were identified as the most relevant mineral phases for the formation of organo-mineral associations. In the upper oxidised parts of both aquifers, where Fe oxides are present, the fraction of mineral-associated organic matter and therefore possibly relatively recalcitrant organic matter might be higher compared to deeper reduced parts of both aquifers. But the role of mineral-associated organic matter has not been addressed with respect to the bioavailability of organic carbon for denitrification in both aquifers and thus should be investigated in future research.

Recently, Korom et al. (2012) reported that in a glaciofluvial shallow aquifer in North Dakota non-pyritic ferrous iron from amphiboles might also considerably contribute to denitrification and that this might also apply to other aquifers. There are no investigations about a possible contribution of non-pyritic ferrous iron to the denitrification capacity of aquifer material in the in the FFA and GKA.

In summary, the role and availability of different electron donors for denitrification in aquifers are not sufficiently understood. Therefore, beside a closer examination of the molecular structure of organic matter in aquifers, its status (mineral-associated, particular) and the resulting consequences for the reactivity of organic matter in aquifers as well as the

contribution of other electron donors as for example ferrous iron from amphiboles have to be investigated further.

Nitrate limitation of denitrification

During the conducted incubation experiments it appeared that denitrification could be reasonably well described with zero-order kinetics and it was assumed that the concentration of NO_3^- was of minor importance for the measured denitrification rates during the conducted experiments (see Sect. 3.4.5.2), i.e. denitrification was independent of NO_3^- concentration in the batch solution. Zero-order kinetics of denitrification was also reported from several workers (Korom et al., 2012; Green et al., 2008; Tesoriero and Puckett, 2011). From this the question arises below which concentration denitrification becomes NO_3^- limited? There is only scarce data about NO_3^- limitation of denitrification in aquifers. The concentration below denitrification becomes NO_3^- limited itself might be depend on the stock of reduced compounds capable to support denitrification. Possibly, higher amounts of microbial available SRC result in higher NO_3^- limits of denitrification. But there are virtually no information about a possible connection between SRC and a NO_3^- limit in aquifers.

Influence of the area of reactive surfaces on the measured denitrification rates

In chapter 3 and 4 the possible influence of the area of reactive surfaces on measured denitrification rates is discussed, but this needs to be confirmed experimentally in further research. Kölle et al. 1983 reported the occurrence of pyrite framboids in the FFA aquifer material. Pyrite framboids have a large surface and are therefore highly reactive. It would be interesting to evaluate the distribution of these framboids with depth in the FFA. Are they uniformly distributed with depth or concentrated right below or in the denitrification front?

Other possible reaction paths from NO_3^- to N_2

As discussed in section 3.6 ^{15}N labelling of nitrate can not completely exclude the possible contribution of dissimilatory nitrate reduction to ammonium (DNRA) followed by anaerobic ammonium oxidation (anammox) to the formation of ^{15}N labelled N_2 from the labelled NO_3^- during anaerobic incubations or in situ. Contrary to marine environments, there is not much evidence for anammox in freshwater systems (van de Leemput et al., 2011; Burgin and Hamilton, 2008). To the best knowledge of the author, there are no studies about anammox in fresh water aquifers, whereas it is reported to exist in wastewater treatment systems, marine sediments and lakes (Jetten et al., 1998; Schubert et al., 2006; Dalsgaard et al., 2005).

In situ measurement of denitrification in aquifers

The comparison of in situ denitrification rates ($D_r(\text{in situ})$) measured with ^{15}N tracer push-pull tests (chapter 4) and results from laboratory incubations of corresponding aquifer samples (chapter 3) exhibited poor predictions of the cumulative denitrification after one year of incubation ($D_{\text{cum}}(365)$) and the stock of reduced compounds (SRC) from in situ data for aquifer material from the zone of NO_3^- free groundwater of both aquifers. The reason for this are presumably adaptation processes of the denitrifying community within the aquifer after the injection of the NO_3^- tracer as a new available electron acceptor.

Effect of pre-conditioning on measured in situ denitrification rates

Pre-conditioning of aquifer material with NO_3^- of natural ^{15}N abundance (chapter 4) prior to ^{15}N -tracer push-pull tests in the zone of NO_3^- free groundwater was conducted at 4 different depths of one multilevel well in the FFA (chapter 4.2.4). After pre-conditioning in situ denitrification rates were 27 to 60 times higher and more comparable to $D_r(365)$ compared to in situ rates measured without pre-conditioning at the same locality one year before (Fig. 4.5). To assess the influence of pre-conditioning on the measured in situ denitrification rates, push-pull test with pre-conditioning should be conducted at the remaining push-pull measuring points. In situ denitrification rates after pre-conditioning might allow better predictions of $D_{\text{cum}}(365)$ and SRC of aquifer material from in situ data. Further investigations are crucial to assess the influence of pre-conditioning in more detail. The minimal time needed for pre-conditioning aquifer material in the zone of NO_3^- free groundwater to adept microorganisms to NO_3^- as new available electron acceptor, i.e. the time after which further pre-conditioning have no additional effect on in situ denitrification rates, is of particular interest. But to the authors knowledge there are no studies available dealing with this question.

References

- Addy, K., Kellogg, D. Q., Gold, A. J., Groffman, P. M., Ferendo, G., and Sawyer, C.: In situ push-pull method to determine ground water denitrification in riparian zones, *J. Environ. Qual.*, 31, 1017-1024, 2002.
- Addy, K., Gold, A., Nowicki, B., McKenna, J., Stolt, M., and Groffman, P.: Denitrification capacity in a subterranean estuary below a Rhode Island fringing salt marsh, *Estuaries*, 28, 896-908, 2005.
- Aeschbach-Hertig, W., El-Gamal, H., Wieser, M., and Palcsu, L.: Modeling excess air and degassing in groundwater by equilibrium partitioning with a gas phase, *Water Resources Research*, 44, 12, W08449 10.1029/2007wr006454, 2008.
- An, S. M., Gardner, W. S., and Kana, T.: Simultaneous measurement of denitrification and nitrogen fixation using isotope pairing with membrane inlet mass spectrometry analysis, *Appl. Environ. Microbiol.*, 67, 1171-1178, 2001.
- Balesdent, J.: The significance of organic separates to carbon dynamics and its modelling in some cultivated soils, *Eur. J. Soil Sci.*, 47, 485-493, 10.1111/j.1365-2389.1996.tb01848.x, 1996.
- Behm, R.: Untersuchung zur Bestimmung der leicht umsetzbaren N- und C-Anteile im Heißwasserextrakt des Bodens-Kurzmitteilung, *Archiv für Acker- und Pflanzenbau und Bodenkunde*, 32, 333-335, 1988.
- Bergmann, A.: Hydrogeochemische Untersuchungen anoxischer Redoxprozesse in tiefen Porengrundwasserleitern der Niederrheinischen Bucht - Im Umfeld des Tagebaus Garzweiler I, *Bochumer geol. geotechn. Arb.* 51, 59. Abb., 27. Tab.; Bochum, Germany, 167, 1999.
- Bohlke, J. K., Harvey, J. W., and Voytek, M. A.: Reach-scale isotope tracer experiment to quantify denitrification and related processes in a nitrate-rich stream, midcontinent United States, *Limnol. Oceanogr.*, 49, 821-838, 2004.
- Böttcher, J., Strebel, O., and Duijnsveld, W. H. M.: Vertikale Stoffkonzentrationsprofile im Grundwasser eines Lockergesteins-Aquifers und deren Interpretation (Beispiel Fuhrberger Feld), *Z. dt. Geol. Ges.*, 136, 543-552, 1985.
- Böttcher, J., Strebel, O., and Duijnsveld, W. H. M.: Kinetik und Modellierung gekoppelter Stoffumsetzungen im Grundwasser eines Lockergesteins-Aquifers., *Geoll Jahrb Reihe C* 51, 3-40, 1989.

References

- Böttcher, J., Strebel, O., Voerkelius, S., and Schmidt, H. L.: Using isotope fractionation of nitrate nitrogen and nitrate oxygen for evaluation of microbial denitrification in a sandy aquifer, *J. Hydrol.*, 114, 413-424, 1990.
- Böttcher, J., Strebel, O., and Duijnsveld, W. H. M.: Reply (to a comment of Scott F. Korom), *Water Resources Research*, 27, 3275-3278, 1991.
- Böttcher, J., Strebel, O., and Kölle, W.: Redox conditions and microbial sulfur reactions in the Fuhrberger Feld sandy aquifer., *Progress in Hydrogeochemistry*, 219-226, 1992.
- Boukhenfouf, W., and Boucenna, A.: Uranium content and dose assessment for phosphate fertiliser and soil samples: comparison of uranium concentration between virgin soil and fertilised soil, *Radiation protection dosimetry*, 148, 263-267, 2011.
- Bouraoui, F., Grizzetti, B., and Aloe, A.: Nutrient Discharge from Rivers to Seas for Year 2000, Joint Research Centre Scientific and technical Reports, 77, 2009.
- Burgin, A. J., and Hamilton, S. K.: Have we overemphasized the role of denitrification in aquatic ecosystems? A review of nitrate removal pathways, *Front. Ecol. Environ.*, 5, 89-96, 10.1890/1540-9295(2007)5[89:hwotro]2.0.co;2, 2007.
- Burgin, A. J., and Hamilton, S. K.: NO₃⁻-driven SO₄²⁻ production in freshwater ecosystems: Implications for N and S cycling, *Ecosystems*, 11, 908-922, 10.1007/s10021-008-9169-5, 2008.
- Burt, T. P., Matchett, L. S., Goulding, K. W. T., Webster, C. P., and Haycock, N. E.: Denitrification in riparian buffer zones: the role of floodplain hydrology, *Hydrol. Process.*, 13, 1451-1463, 10.1002/(sici)1099-1085(199907)13:10<1451::aid-hyp822>3.3.co;2-n, 1999.
- Canfield, D. E., Stewart, F. J., Thamdrup, B., De Brabandere, L., Dalsgaard, T., Delong, E. F., Revsbech, N. P., and Ulloa, O.: A Cryptic Sulfur Cycle in Oxygen-Minimum-Zone Waters off the Chilean Coast, *Science*, 330, 1375-1378, 10.1126/science.1196889, 2010.
- Chodak, M., Khanna, P., and Beese, F.: Hot water extractable C and N in relation to microbiological properties of soils under beech forests, *Biol. Fertil. Soils*, 39, 123-130, 10.1007/s00374-003-0688-0, 2003.
- Dalsgaard, T., Thamdrup, B., and Canfield, D. E.: Anaerobic ammonium oxidation (anammox) in the marine environment, *Res. Microbiol.*, 156, 457-464, 10.1016/j.resmic.2005.01.011, 2005.
- Dalton, H., and Brand-Hardy, R.: Nitrogen: the essential public enemy, *J. Appl. Ecol.*, 40, 771-781, 2003.

- Davidson, E. A., and Seitzinger, S.: The enigma of progress in denitrification research, *Ecol. Appl.*, 16, 2057-2063, 2006.
- Defra: Post-conciliation partial regulatory impact assessment - Groundwater proposals under Article 17 of the Water Framework Directive. Draft final report., Department for Environment, Food and Rural Affairs, London, 2006.
- Eschenbach, W., and Well, R.: Online measurement of denitrification rates in aquifer samples by an approach coupling an automated sampling and calibration unit to a membrane inlet mass spectrometry system, *Rapid Commun. Mass Spectrom.*, 25, 1993-2006, 10.1002/rcm.5066, 2011.
- Eschenbach, W., and Well, R.: Predicting the denitrification capacity of sandy aquifers from shorter-term incubation experiments and sediment properties, *Biogeosciences*, 10, 1013-1035, 10.5194/bg-10-1013-2013, 2013.
- European Commission: Report From The Commission To The Council And The European Parliament - On implementation of Council Directive 91/676/EEC concerning the protection of waters against pollution caused by nitrates from agricultural sources based on Member State reports for the period 2004-2007, Corrigendum, 2011.
- European Parliament and Council of the European Union: Directive 2000/60/EC of the European Parliament and the Council of the European Union of 23 October 2000 establishing a framework for Community action in the field of water policy, L 327/1, 2000.
- Eusterhues, K., Rumpel, C., and Kogel-Knabner, I.: Organo-mineral associations in sandy acid forest soils: importance of specific surface area, iron oxides and micropores, *Eur. J. Soil Sci.*, 56, 753-763, 10.1111/j.1365-2389.2005.00710.x, 2005.
- Eyre, B. D., Rysgaard, S., Dalsgaard, T., and Christensen, P. B.: Comparison of isotope pairing and $N_2 : Ar$ methods for measuring sediment-denitrification-assumptions, modifications, and implications, *Estuaries*, 25, 1077-1087, 2002.
- Firestone, M. K.: Biological Denitrification, in: *Nitrogen in Agriculture soils*, edited by: Stevenson, F. J., American Society of Agronomy, Madison, Wis., 289-326, 1982.
- Francis, A. J., Slater, J. M., and Dodge, C. J.: Denitrification in deep subsurface sediments, *Geomicrobiol. J.*, 7, 103-116, 1989.
- Franken, G., Postma, D., Duijnsveld, W. H. M., Böttcher, J., and Molson, J.: Acid groundwater in an anoxic aquifer: Reactive transport modelling of buffering processes, *Applied Geochemistry*, 24, 890-899, 2009.

References

- Frind, E. O., Duynisveld, W. H. M., Strebel, O., and Boettcher, J.: Modeling of multicomponent transport with microbial transformation in groundwater - The Fuhrberg case, *Water Resources Research*, 26, 1707-1719, 1990.
- Galloway, J. N., Aber, J. D., Erisman, J. W., Seitzinger, S. P., Howarth, R. W., Cowling, E. B., and Cosby, B. J.: The nitrogen cascade, *Bioscience*, 53, 341-356, 10.1641/0006-3568(2003)053[0341:tnc]2.0.co;2, 2003.
- Galloway, J. N., Dentener, F. J., Capone, D. G., Boyer, E. W., Howarth, R. W., Seitzinger, S. P., Asner, G. P., Cleveland, C. C., Green, P. A., Holland, E. A., Karl, D. M., Michaels, A. F., Porter, J. H., Townsend, A. R., and Vorosmarty, C. J.: Nitrogen cycles: past, present, and future, *Biogeochemistry*, 70, 153-226, 2004.
- Green, C. T., Puckett, L. J., Bohlke, J. K., Bekins, B. A., Phillips, S. P., Kauffman, L. J., Denver, J. M., and Johnson, H. M.: Limited occurrence of denitrification in four shallow aquifers in agricultural areas of the United States, *J. Environ. Qual.*, 37, 994-1009, 10.2134/jeq2006.0419, 2008.
- Green, C. T., Bohlke, J. K., Bekins, B. A., and Phillips, S. P.: Mixing effects on apparent reaction rates and isotope fractionation during denitrification in a heterogeneous aquifer, *Water Resources Research*, 46, 19, W08525 10.1029/2009wr008903, 2010.
- Griebler, C., and Lueders, T.: Microbial biodiversity in groundwater ecosystems, *Freshw. Biol.*, 54, 649-677, 10.1111/j.1365-2427.2008.02013.x, 2009.
- Groffman, P. M., Altabet, M. A., Bohlke, J. K., Butterbach-Bahl, K., David, M. B., Firestone, M. K., Giblin, A. E., Kana, T. M., Nielsen, L. P., and Voytek, M. A.: Methods for measuring denitrification: Diverse approaches to a difficult problem, *Ecol. Appl.*, 16, 2091-2122, 2006.
- Haggerty, R., Schroth, M. H., and Istok, J. D.: Simplified method of "push-pull" test data analysis for determining in situ reaction rate coefficients, *Ground Water*, 36, 314-324, 1998.
- Hansen, C., and van Berk, W.: Retracing the development of raw water quality in water works applying reactive controlled material flux analyses, *Aquat. Sci.*, 66, 60-77, 10.1007/s00027-003-0686-1, 2004.
- Hansen, C.: Entwicklung und Anwendung hydrogeochemischer Stoffflussmodelle zur Modellierung der Grund- und Rohwasserqualität in Gewinnungsanlagen - Fallbeispiel Fuhrberger Feld, *Clausthaler Geowissenschaften*, 4: XII, PhD Thesis, Univ. of Clausthal, Clausthal-Zellerfeld, Germany, 246 pp., 2005.

- Harris, S. H., Istok, J. D., and Sufita, J. M.: Changes in organic matter biodegradability influencing sulfate reduction in an aquifer contaminated by landfill leachate, *Microb. Ecol.*, 51, 535-542, 10.1007/s00248-006-9043-y, 2006.
- Hartog, N., Van Bergen, P. F., De Leeuw, J. W., and Griffioen, J.: Reactivity of organic matter in aquifer sediments: Geological and geochemical controls, *Geochim. Cosmochim. Acta*, 68, 1281-1292, 10.1016/j.gca.2003.09.004, 2004.
- Hauck, R. D., and Bouldin, D. R.: Distribution of isotopic nitrogen in nitrogen gas during denitrification, *Nature*, 191, 871-&, 1961.
- Hayatsu, M., Tago, K., and Saito, M.: Various players in the nitrogen cycle: Diversity and functions of the microorganisms involved in nitrification and denitrification, *Soil Sci. Plant Nutr.*, 54, 33-45, 10.1111/j.1747-0765.2007.00195.x, 2008.
- Hiscock, K. M., Lloyd, J. W., and Lerner, D. N.: Review of natural and artificial denitrification of groundwater, *Water Res.*, 25, 1099-1111, 1991.
- Houben, G.: Modellansätze zur Prognose der langfristigen Entwicklung der Grundwasserqualität - Fallbeispiel Bourtanger Moor (Emsland), *Aachener Geowissenschaftliche Beiträge* 36, Aachen, Germany, 36, 213, 2000.
- Howar, M.: Geologische 3D-Untergrundmodellierung im Bereich Großenkneten/Ahlhorn., unpubl. Expertise: INSIGHT. Geologische Softwaresysteme GmbH. Köln., Germany, 11 S., 2005.
- Istok, J. D., Humphrey, M. D., Schroth, M. H., Hyman, M. R., and O'Reilly, K. T.: Single-well, "push-pull" test for in situ determination of microbial activities, *Ground Water*, 35, 619-631, 1997.
- Istok, J. D., Senko, J. M., Krumholz, L. R., Watson, D., Bogle, M. A., Peacock, A., Chang, Y. J., and White, D. C.: In situ bioreduction of technetium and uranium in a nitrate-contaminated aquifer, *Environ. Sci. Technol.*, 38, 468-475, 10.1021/es034639p, 2004.
- Jensen, K. M., Jensen, M. H., and Cox, R. P.: Membrane inlet mass spectrometric analysis of N-isotope labelling for aquatic denitrification studies, *FEMS Microbiol. Ecol.*, 20, 101-109, 1996.
- Jetten, M. S. M., Strous, M., van de Pas-Schoonen, K. T., Schalk, J., van Dongen, U., van de Graaf, A. A., Logemann, S., Muyzer, G., van Loosdrecht, M. C. M., and Kuenen, J. G.: The anaerobic oxidation of ammonium, *Fems Microbiol. Rev.*, 22, 421-437, 10.1111/j.1574-6976.1998.tb00379.x, 1998.

References

- Jorgensen, P. R., Urup, J., Helstrup, T., Jensen, M. B., Eiland, F., and Vinther, F. P.: Transport and reduction of nitrate in clayey till underneath forest and arable land, *J. Contam. Hydrol.*, 73, 207-226, 10.1016/j.jconhyd.2004.01.005, 2004.
- Kana, T. M., Darkangelo, C., Hunt, M. D., Oldham, J. B., Bennett, G. E., and Cornwell, J. C.: Membrane inlet mass-spectrometer for rapid high-precision determination of N₂, O₂, and Ar in environmental water samples, *Anal. Chem.*, 66, 4166-4170, 1994.
- Kellogg, D. Q., Gold, A. J., Groffman, P. M., Addy, K., Stolt, M. H., and Blazejewski, G.: In situ ground water denitrification in stratified, permeable soils underlying riparian wetlands, *J. Environ. Qual.*, 34, 524-533, 2005.
- Khalil, K., Mary, B., and Renault, P.: Nitrous oxide production by nitrification and denitrification in soil aggregates as affected by O₂ concentration, *Soil Biology & Biochemistry*, 36, 687-699, 10.1016/j.soilbio.2004.01.004, 2004.
- Khanna, P. K., Prenzel, J., Meiwes, K. J., Ulrich, B., and Matzner, E.: Dynamics of sulfate retention by acid forest soils in an acidic deposition environment, *Soil Sci. Soc. Am. J.*, 51, 446-452, 1987.
- Kim, Y., Istok, J. D., and Semprini, L.: Push-pull tests for assessing in situ aerobic cometabolism, *Ground Water*, 42, 329-337, 10.1111/j.1745-6584.2004.tb02681.x, 2004.
- Kim, Y., Kim, J. H., Son, B. H., and Oa, S. W.: A single well push-pull test method for in situ determination of denitrification rates in a nitrate-contaminated groundwater aquifer, *Water Sci. Technol.*, 52, 77-86, 2005.
- Kneeshaw, T. A., McGuire, J. T., Smith, E. W., and Cozzarelli, I. M.: Evaluation of sulfate reduction at experimentally induced mixing interfaces using small-scale push-pull tests in an aquifer-wetland system, *Applied Geochemistry*, 22, 2618-2629, 10.1016/j.apgeochem.2007.06.006, 2007.
- Köhler, K., Duynisveld, W. H. M., and Bottcher, J.: Nitrogen fertilization and nitrate leaching into groundwater on arable sandy soils, *J. Plant Nutr. Soil Sci.-Z. Pflanzenernahr. Bodenkd.*, 169, 185-195, 10.1002/jpln.200521765, 2006.
- Kölbelboelke, J., Anders, E. M., and Nehr Korn, A.: Microbial communities in the saturated groundwater environment .2. Diversity of bacterial communities in a Pleistocene sand aquifer and their invitro activities, *Microb. Ecol.*, 16, 31-48, 10.1007/bf02097403, 1988.
- Kölle, W., Werner, P., Strebel, O., and Bottcher, J.: Denitrification by pyrite in a reducing aquifer, *Vom Wasser*, 61, 125-147, 1983.

- Köle, W., Strebel, O., and Böttcher, J.: Formation of sulfate by microbial denitrification in a reducing aquifer, *Water Supply*, 3, 35-40, 1985.
- Kollmann, W.: Die Bestimmung des durchflußwirksamen Porenvolumens von Sedimenten und seine Bedeutung für den Grundwasserschutz, *Mitt. österr. geol. Ges.*, 79, 14, 1986.
- Konrad, C.: Methoden zur Bestimmung des Umsatzes von Stickstoff für drei pleistozäne Grundwasserleiter Norddeutschlands, PhD Thesis, Univ. of Tech. Dresden, Dresden, Germany, 161 pp., 2007.
- Korom, S. F.: Modeling of multicomponent transport with microbial transformation in groundwater - The Fuhrberg case - Comment, *Water Resources Research*, 27, 3271-3274, 1991.
- Korom, S. F.: Natural denitrification in the saturated zone - a review, *Water Resources Research*, 28, 1657-1668, 1992.
- Korom, S. F., Schlag, A. J., Schuh, W. M., and Schlag, A. K.: In situ mesocosms: Denitrification in the Elk Valley aquifer, *Ground Water Monit. Remediat.*, 25, 79-89, 2005.
- Korom, S. F., Schuh, W. M., Tesfay, T., and Spencer, E. J.: Aquifer denitrification and in situ mesocosms: modeling electron donor contributions and measuring rates, *Journal of Hydrology (Amsterdam)*, 432/433, 112-126, 10.1016/j.jhydrol.2012.02.023, 2012.
- Kubeck, C., Hansen, C., König, C., van Berk, W., Zervas, A., and Bergmann, A.: Derivation of organic carbon reactivity in a redox-stratified aquifer-hydrogeochemical modelling of kinetically driven reaction systems, *Grundwasser*, 15, 103-112, 10.1007/s00767-009-0136-7, 2010.
- Kumon, Y., Sasaki, Y., Kato, I., Takaya, N., Shoun, H., and Beppu, T.: Codenitrification and denitrification are dual metabolic pathways through which dinitrogen evolves from nitrate in *Streptomyces antibioticus*, *J. Bacteriol.*, 184, 2963-2968, 10.1128/jb.184.11.2963-2968.2002, 2002.
- Lapack, M. A., Tou, J. C., and Enke, C. G.: Membrane extraction mass-spectrometry for the online analysis of gas and liquid process streams, *Anal. Chem.*, 63, 1631-1637, 1991.
- Law, G. T. W., Geissler, A., Boothman, C., Burke, I. T., Livens, F. R., Lloyd, J. R., and Morris, K.: Role of Nitrate in Conditioning Aquifer Sediments for Technetium Bioreduction, *Environ. Sci. Technol.*, 44, 150-155, 10.1021/es9010866, 2010.

References

- Manderscheid, B., Schweisser, T., Lischeid, G., Alewell, C., and Matzner, E.: Sulfate pools in the weathered substrata of a forested catchment, *Soil Sci. Soc. Am. J.*, 64, 1078-1082, 2000.
- Martin, T. L., Kaushik, N. K., Trevors, J. T., and Whiteley, H. R.: Review: Denitrification in temperate climate riparian zones, *Water Air Soil Pollut.*, 111, 171-186, 1999.
- McGuire, J. T., Long, D. T., Klug, M. J., Haack, S. K., and Hyndman, D. W.: Evaluating behavior of oxygen, nitrate, and sulfate during recharge and quantifying reduction rates in a contaminated aquifer, *Environ. Sci. Technol.*, 36, 2693-2700, 10.1021/es015615q, 2002.
- McMahon, P. B., Bohlke, J. K., and Christenson, S. C.: Geochemistry, radiocarbon ages, and paleorecharge conditions along a transect in the central High Plains aquifer, southwestern Kansas, USA, *Applied Geochemistry*, 19, 1655-1686, 10.1016/j.apgeochem.2004.05.003, 2004.
- Mehranfar, O.: Laboruntersuchungen zum langfristigen Denitrifikationspotential im oberflächennahen Grundwasser hydromorpher Mineralböden Nordwestdeutschlands, 128, 2003.
- Morris, J. T., Whiting, G. J., and Chapelle, F. H.: Potential denitrification rates in deep sediments from the southeastern coastal-plain, *Environ. Sci. Technol.*, 22, 832-836, 10.1021/es00172a014, 1988.
- Mulvaney, R. L.: Determination of N¹⁵-labeled dinitrogen and nitrous-oxide with triple-collector mass spectrometers, *Soil Sci. Soc. Am. J.*, 48, 690-692, 1984.
- Nielsen, L. P.: Denitrification in sediment determined from nitrogen isotope pairing, *FEMS Microbiol. Ecol.*, 86, 357-362, 1992.
- Nielsen, M. E., Fisk, M. R., Istok, J. D., and Pedersen, K.: Microbial nitrate respiration of lactate at in situ conditions in ground water from a granitic aquifer situated 450 m underground, *Geobiology*, 4, 43-52, 10.1111/j.1472-4669.2006.00068.x, 2006.
- Nordstrom, D. K.: The effect of sulfate on aluminum concentrations in natural-waters - some stability relations in the system Al₂O₃-SO₃-H₂O AT 298-K, *Geochim. Cosmochim. Acta*, 46, 681-692, 10.1016/0016-7037(82)90168-5, 1982.
- Ostrom, N. E., Russ, M. E., Popp, B., Rust, T. M., and Karl, D. M.: Mechanisms of nitrous oxide production in the subtropical North Pacific based on determinations of the isotopic abundance of nitrous oxide and di-oxygen, *Chemosphere - Global Change Science*, 2, 281-290, 2000.

- Paramasivam, S., Alva, A. K., Prakash, O., and Cui, S. L.: Denitrification in the vadose zone and in surficial groundwater of a sandy entisol with citrus production, *Plant Soil*, 208, 307-319, 1999.
- Poth, M., and Focht, D. D.: N^{15} Kinetic-analysis of N_2O production by *Nitrosomonas-Europaea* - an examination of nitrifier denitrification, *Appl. Environ. Microbiol.*, 49, 1134-1141, 1985.
- Renger, M., Strebel, O., Wessolek, G., and Duynisveld, W. H. M.: Evapotranspiration and groundwater recharge - a case-study for different climate, crop patterns, soil properties and groundwater depth conditions, *Z. Pflanzen. Bodenk.*, 149, 371-381, 10.1002/jpln.19861490403, 1986.
- Riley, R. G., Zachara, J. M., and Wobber, F. J.: DOE/ER-0547T: Chemical Contaminants on DOE Lands and Selection of Contaminant MIXtures for Subsurface Science Reserach. U.S. Department of Energy: Washington, DC., 1992.
- Rivett, M. O., Smith, J. W. N., Buss, S. R., and Morgan, P.: Nitrate occurrence and attenuation in the major aquifers of England and Wales, *Q. J. Eng. Geol. Hydrogeol.*, 40, 335-352, 2007.
- Rivett, M. O., Buss, S. R., Morgan, P., Smith, J. W. N., and Bemment, C. D.: Nitrate attenuation in groundwater: A review of biogeochemical controlling processes, *Water Res.*, 42, 4215-4232, 10.1016/j.watres.2008.07.020, 2008.
- Robertson, W. D., Russell, B. M., and Cherry, J. A.: Attenuation of nitrate in aquitard sediments of southern Ontario, *J. Hydrol.*, 180, 267-281, 10.1016/0022-1694(95)02885-4, 1996.
- Roy, R. N., Misra, R. V., and Montanez, A.: Decreasing reliance on mineral nitrogen - Yet more food, *Ambio*, 31, 177-183, 2002.
- Rysgaard, S., Risgaardpetersen, N., Sloth, N. P., Jensen, K., and Nielsen, L. P.: Oxygen regulation of nitrification and denitrification in sediments, *Limnol. Oceanogr.*, 39, 1643-1652, 1994.
- Sanchez-Perez, J. M., Bouey, C., Sauvage, S., Teissier, S., Antiguada, I., and Vervier, P.: A standardised method for measuring in situ denitrification in shallow aquifers: numerical validation and measurements in riparian wetlands, *Hydrol. Earth Syst. Sci.*, 7, 87-96, 2003.
- Santoro, A. E., Boehm, A. B., and Francis, C. A.: Denitrifier community composition along a nitrate and salinity gradient in a coastal aquifer, *Appl. Environ. Microbiol.*, 72, 2102-2109, 10.1128/aem.72.3.2102-2109.2006, 2006.

References

- Schlichting, E., Blume, H. P., and Stahr, K.: *Bodenkundliches Praktikum*, Blackwell Wissenschaft, Berlin, Germany, 295 S., 1995.
- Schroth, M. H., Kleikemper, J., Bolliger, C., Bernasconi, S. M., and Zeyer, J.: In situ assessment of microbial sulfate reduction in a petroleum-contaminated aquifer using push-pull tests and stable sulfur isotope analyses, *J. Contam. Hydrol.*, 51, 179-195, 2001.
- Schubert, C. J., Durisch-Kaiser, E., Wehrli, B., Thamdrup, B., Lam, P., and Kuypers, M. M. M.: Anaerobic ammonium oxidation in a tropical freshwater system (Lake Tanganyika), *Environ. Microbiol.*, 8, 1857-1863, 10.1111/j.1462-2920.2006.001074.x, 2006.
- Schuchert, A.: Zielflächenidentifikation für Grundwasserschutzmaßnahmen. Eine GIS-Datenanalyse im Wasserschutzgebiet Großenkneten, Landkreis Oldenburg, Diploma thesis, Institute for Geography, University of Bremen, Germany, 2007.
- Seitzinger, S., Harrison, J. A., Bohlke, J. K., Bouwman, A. F., Lowrance, R., Peterson, B., Tobias, C., and Van Drecht, G.: Denitrification across landscapes and waterscapes: A synthesis, *Ecol. Appl.*, 16, 2064-2090, 2006.
- Senko, J. M., Istok, J. D., Suffita, J. M., and Krumholz, L. R.: In-situ evidence for uranium immobilization and remobilization, *Environ. Sci. Technol.*, 36, 1491-1496, 10.1021/es011240x, 2002.
- Siegel, R. S., Hauck, R. D., and Kurtz, L. T.: Determination of (N₂)-N-30 and application to measurement of N₂ evolution during denitrification, *Soil Sci. Soc. Am. J.*, 46, 68-74, 1982.
- Singleton, M. J., Esser, B. K., Moran, J. E., Hudson, G. B., McNab, W. W., and Harter, T.: Saturated zone denitrification: Potential for natural attenuation of nitrate contamination in shallow groundwater under dairy operations, *Environ. Sci. Technol.*, 41, 759-765, 10.1021/es061253g, 2007.
- Smith, L. K., Voytek, M. A., Bohlke, J. K., and Harvey, J. W.: Denitrification in nitrate-rich streams: Application of N₂ : Ar and N¹⁵-tracer methods in intact cores, *Ecol. Appl.*, 16, 2191-2207, 2006.
- Smith, R. L., and Duff, J. H.: Denitrification in a sand and gravel aquifer, *Appl. Environ. Microbiol.*, 54, 1071-1078, 1988.
- Smith, S. J., and Davis, R. J.: Relative movement of bromide and nitrate through soils, *J. Environ. Qual.*, 3, 152-155, 1974.

- Sparling, G., Vojvodic-Vukovic, M., and Schipper, L. A.: Hot-water-soluble C as a simple measure of labile soil organic matter: the relationship with microbial biomass C, *Soil Biology & Biochemistry*, 30, 1469-1472, 10.1016/s0038-0717(98)00040-6, 1998.
- Spott, O., and Stange, C. F.: A new mathematical approach for calculating the contribution of anammox, denitrification and atmosphere to an N₂ mixture based on a N¹⁵ tracer technique, *Rapid Commun. Mass Spectrom.*, 21, 2398-2406, 10.1002/rcm.3098, 2007.
- Spott, O., Russow, R., and Stange, C. F.: Formation of hybrid N₂O and hybrid N₂ due to codenitrification: First review of a barely considered process of microbially mediated N-nitrosation, *Soil Biology & Biochemistry*, 43, 1995-2011, 10.1016/j.soilbio.2011.06.014, 2011.
- Strebel, O., Böttcher, J., and Duijnsveld, W. H. M.: Identifizierung und Quantifizierung von Stoffumsetzungen in einem Sand-Aquifer (Beispiel Fuhrberger Feld). *DVGW Schriftenreihe Wasser*, 73, 55-73, 1992.
- Tanimoto, T., Hatano, K., Kim, D. H., Uchiyama, H., and Shoun, H.: Co-denitrification by the denitrifying system of the fungus *Fusarium-Oxysporum*, *FEMS Microbiol. Lett.*, 93, 177-180, 10.1111/j.1574-6968.1992.tb05086.x, 1992.
- Tesoriero, A. J., and Puckett, L. J.: O₂ reduction and denitrification rates in shallow aquifers, *Water Resources Research*, 47, 10.1029/2011wr010471, 2011.
- Tortell, P. D.: Dissolved gas measurements in oceanic waters made by membrane inlet mass spectrometry, *Limnol. Oceanogr. Meth.*, 3, 24-37, 2005.
- Trudell, M. R., Gillham, R. W., and Cherry, J. A.: An insitu study of the occurrence and rate of denitrification in a shallow unconfined sand aquifer, *J. Hydrol.*, 83, 251-268, 1986.
- Ulrich, B.: Natural and anthropogenic components of soil acidification, *Z. Pflanzen. Bodenk.*, 149, 702-717, 10.1002/jpln.19861490607, 1986.
- van Berk, W., Kübeck, C., Steding, T., van Straaten, L., and Wilde, S.: Vorstudie zur Hydrogeologie im Wassergewinnungsgebiet Großenkneten., 55 S., 2005.
- van de Leemput, I. A., Veraart, A. J., Dakos, V., de Klein, J. J. M., Strous, M., and Scheffer, M.: Predicting microbial nitrogen pathways from basic principles, *Environ. Microbiol.*, 13, 1477-1487, 10.1111/j.1462-2920.2011.02450.x, 2011.
- Visser, A., Broers, H. P., and Bierkens, M. F. P.: Dating degassed groundwater with H-3/He-3, *Water Resources Research*, 43, 14, W10434 10.1029/2006wr005847, 2007.
- Visser, A., Schaap, J. D., Broers, H. P., and Bierkens, M. F. P.: Degassing of H-3/He-3, CFCs and SF₆ by denitrification: Measurements and two-phase transport simulations, *J. Contam. Hydrol.*, 103, 206-218, 10.1016/j.jconhyd.2008.10.013, 2009.

References

- Vitousek, P. M., Aber, J. D., Howarth, R. W., Likens, G. E., Matson, P. A., Schindler, D. W., Schlesinger, W. H., and Tilman, G. D.: Human alteration of the global nitrogen cycle: Sources and consequences, *Ecol. Appl.*, 7, 737-750, 1997.
- von der Heide, C., Bottcher, J., Deurer, M., Weymann, D., Well, R., and Duijnsveld, W. H. M.: Spatial variability of N₂O concentrations and of denitrification-related factors in the surficial groundwater of a catchment in Northern Germany, *J. Hydrol.*, 360, 230-241, 10.1016/j.jhydrol.2008.07.034, 2008.
- von der Heide, C., Bottcher, J., Deurer, M., Duijnsveld, W. H. M., Weymann, D., and Well, R.: Spatial and temporal variability of N₂O in the surface groundwater: a detailed analysis from a sandy aquifer in northern Germany, *Nutr. Cycl. Agroecosyst.*, 87, 33-47, 10.1007/s10705-009-9310-7, 2010.
- Wall, L. G., Tank, J. L., Royer, T. V., and Bernot, M. J.: Spatial and temporal variability in sediment denitrification within an agriculturally influenced reservoir, *Biogeochemistry*, 76, 85-111, 10.1007/s10533-005-2199-6, 2005.
- Weegaerssens, E., Tiedje, J. M., and Averill, B. A.: Evidence from isotope labeling studies for a sequential mechanism for dissimilatory nitrite reduction, *J. Am. Chem. Soc.*, 110, 6851-6856, 10.1021/ja00228a039, 1988.
- Weiss, R. F.: Solubility of nitrogen, oxygen and argon in water and seawater, *Deep-Sea Research*, 17, 721-&, 1970.
- Weiss, R. F., and Price, B. A.: Nitrous-oxide solubility in water and seawater, *Mar. Chem.*, 8, 347-359, 1980.
- Well, R., Becker, K. W., Langel, R., Meyer, B., and Reineking, A.: Continuous flow equilibration for mass spectrometric analysis of dinitrogen emissions, *Soil Sci. Soc. Am. J.*, 62, 906-910, 1998.
- Well, R., and Myrold, D. D.: Laboratory evaluation of a new method for in situ measurement of denitrification in water-saturated soils, *Soil Biology & Biochemistry*, 31, 1109-1119, 1999.
- Well, R., and Myrold, D. D.: A proposed method for measuring subsoil denitrification in situ, *Soil Sci. Soc. Am. J.*, 66, 507-518, 2002.
- Well, R., Augustin, J., Meyer, K., and Myrold, D. D.: Comparison of field and laboratory measurement of denitrification and N₂O production in the saturated zone of hydromorphic soils, *Soil Biology & Biochemistry*, 35, 783-799, 10.1016/s0038-0717(03)00106-8, 2003.

- Well, R., Hoper, H., Mehranfar, O., and Meyer, K.: Denitrification in the saturated zone of hydromorphic soils-laboratory measurement, regulating factors and stochastic modeling, *Soil Biology & Biochemistry*, 37, 1822-1836, 10.1016/j.soilbio.2005.02.014, 2005.
- Well, R., Eschenbach, W., Flessa, H., von der Heide, C., and Weymann, D.: Are dual isotope and isotopomer ratios of N₂O useful indicators for N₂O turnover during denitrification in nitrate-contaminated aquifers?, *Geochim. Cosmochim. Acta*, 90, 265-282, 10.1016/j.gca.2012.04.045, 2012.
- Wendland, F., and Kunkel, R.: Das Nitratabbauvermögen im Grundwasser des Elbeeinzugsgebietes, Forschungszentrum Jülich, 166, 1999.
- Wessolek, G., Renger, M., Strebel, O., and Sponagel, H.: Einfluß von Boden und Grundwasserflurabstand auf die jährliche Grundwasserneubildung unter Acker, Grünland und Nadelwald., *Z. f. Kulturtechnik und Flurbereinigung*, 26, 130-137, 1985.
- Weymann, D., Well, R., Flessa, H., von der Heide, C., Deurer, M., Meyer, K., Konrad, C., and Walther, W.: Groundwater N₂O emission factors of nitrate-contaminated aquifers as derived from denitrification progress and N₂O accumulation, *Biogeosciences*, 5, 1215-1226, 2008.
- Weymann, D.: Nitrous Oxide in denitrifying Aquifers: Reaction Kinetics, Significance of Groundwater-derived Emission and an improved Concept for the Groundwater Emission Factor Phd Thesis, Univ. of Göttingen, Göttingen, Germany, 91 pp., 2009.
- Weymann, D., Well, R., von der Heide, C., Bottcher, J., Flessa, H., and Duijnisveld, W. H. M.: Recovery of groundwater N₂O at the soil surface and its contribution to total N₂O emissions, *Nutr. Cycl. Agroecosyst.*, 85, 299-312, 10.1007/s10705-009-9269-4, 2009.
- Weymann, D., Geistlinger, H., Well, R., von der Heide, C., and Flessa, H.: Kinetics of N₂O production and reduction in a nitrate-contaminated aquifer inferred from laboratory incubation experiments, *Biogeosciences*, 7, 1953-1972, 10.5194/bg-7-1953-2010, 2010.
- Wirth, K.: Hydrogeologisches Gutachten zur Bemessung und Gliederung der Trinkwasserschutzgebiete für die Fassungen Hagel, Sage und Baumweg, Wasserwerk Großenkneten (OOWV). Beratungsbüro für Hydrogeologie (Hrsg.), Göttingen, Germany, 18 S., 1990.

References

Wrage, N., Velthof, G. L., van Beusichem, M. L., and Oenema, O.: Role of nitrifier denitrification in the production of nitrous oxide, *Soil Biology & Biochemistry*, 33, 1723-1732, 10.1016/s0038-0717(01)00096-7, 2001.

Appendix

From the mathematics of isotope dilution mass spectrometry to formulas calculating the contribution of denitrification to N₂ mixtures – a systematization with respect to MIMS

W. Eschenbach and J. Prenzel

Abstract

The currently used formulas in denitrification research based on the ¹⁵N tracer technique did not reveal the close mathematical similarities with formulas used in isotope dilution mass spectrometry (IDSM). The basic difference between IDSM and the ¹⁵N tracer technique is that for the first the sample is modified by adding a spike to it and for the second the system of interest is changed by “spiking” it with a ¹⁵N tracer. The presented formulas clearly show this close relationship of both techniques and differ in their mathematical structure from previous approaches used in denitrification research. It is also shown that with the presented approach the equations of the isotope pairing method (IPM) can be reformulated and that this reformulation is advantageous since it simplifies calculation of denitrification derived N₂. From the presented formulas also equations to calculate instrumental response factors have been derived.

Introduction

What is the purpose of this work? The formulas presented in the following reveal the close mathematical relationship between the ^{15}N tracer technique used in denitrification research (Hauck et al. (1958), Hauck and Bouldin (1961), Siegel et al. (1982), Mulvaney and Kurtz (1982), Mulvaney (1984), Mulvaney and Boast (1986), Nielsen (1992), Arah (1992) and Spott and Stange (2007)) and the formulas used in isotope dilution mass spectrometry (IDMS) which is not obvious from the equations given in the cited papers above or mentioned in these works and “It is certainly a task of scientific analysis to highlight the similarity of things that separates a first consideration, the various phenomena to pursue in foothills, which are apparently different nature” (Schumpeter, 1912). So, one object of this work is to highlight the close mathematical similarities between IDMS and ^{15}N tracer technique caused by conceptual similarities.

The use of the isotope dilution technique goes back to the late 1940s (Gest et al., 1947; Bloch and Anker, 1948). Today IDMS, reviewed by Fassett and Paulsen (1989), Heumann (1992), Rodriguez-Gonzalez et al. (2005) etc., is widely used for concentration measurements of highest accuracy and precision. In this technique a spike containing a substance with a well known isotope distribution and amount is added to a sample. The basic equation (Eq. 1 given in Fassett and Paulsen (1989)) for calculating concentrations with IDMS is:

$$C_x = \left(\frac{C_s W_s}{W_x} \right) \left(\frac{A_s - R_m B_s}{R_m B_x - A_x} \right) \quad (1)$$

The subscripts x and s denote the mole fractions of the isotopes A and B in the sample and spike, respectively. R_m is the measured ratio of isotope A to B after addition of the spike to the sample. C_x and C_s are the concentrations of the analysed element in the sample and the spike and W_x and W_s are the weights of sample and spike.

The measurement of N fluxes from denitrification is complicated by the high background of atmospheric dinitrogen (N_2) in the soil atmosphere (Groffman et al., 2006) or of dissolved atmospheric N_2 in water samples. The pioneering works of Hauck et al. (1958) and Hauck and Bouldin (1961) introduced the ^{15}N tracer technique for the quantification of denitrification to overcome this problem. They provided equations to calculate the fraction of N_2 coming from denitrification of ^{15}N enriched nitrate (NO_3^-) and the determination of the ^{15}N abundance of denitrified NO_3^- from the measured ratios of N_2 isotopologues $^{28}\text{N}_2$, $^{29}\text{N}_2$ and $^{30}\text{N}_2$ on the molecular ion masses 29 to 28 and the molecular ion mass 30 to the sum of the molecular ion masses 28 and 29. The assumptions made for the formulas of Hauck et al. (1958) and Hauck

and Bouldin (1961) are: (i) the pool of denitrified NO_3^- is of uniform ^{15}N labelling, (ii) the initial N_2 , present before mixing with evolved ^{15}N labelled N_2 , has the same isotopologue distribution as atmospheric N_2 , in the investigated system and (iii) that no substantial fractionation between N isotopes occurred during N_2 formation. Years later several papers published by Siegel et al. (1982), Mulvaney and Kurtz (1982) and Mulvaney (1984) presented simplified equations adapted to the use of double or triple collector mass spectrometers equipped with a dual-inlet system. These equations are valid under the additional assumption (iv) that the amount of N_2 in a sample coming from denitrification is negligible in comparison to the amount of background N_2 of natural ^{15}N abundance, which is normally fulfilled if a soil air sample is measured or labelled denitrification derived N_2 dissolved in water is measured after stripping into a headspace of unlabelled N_2 . This additional prerequisite is not necessarily fulfilled during direct measurement of water samples by means of membrane inlet mass spectroscopy (MIMS) (Eschenbach and Well, 2011). Mulvaney and Boast (1986) derived refined formulas which are more complex as the equations before (Siegel et al., 1982; Mulvaney and Kurtz, 1982; Mulvaney, 1984) but valid for any ratio of N_2 coming from denitrification and background N_2 in a sample. These equations are derived for double and triple-collector mass spectrometers with a dual-inlet system which are especially designed for the measurement of ratio differences.

Nielsen (1992) derived new formulas to calculate the concentration of denitrification derived N_2 within samples. The mathematical and conceptual approach of Nielsen (1992) is known as the isotope pairing method (IPM). Mostly, NO_3^- with a very high ^{15}N abundance ($> 95\%$ ^{15}N) is used for IPM and the pairing of ^{14}N from unlabelled NO_3^- of natural ^{15}N abundance and tracer derived ^{15}N enriched NO_3^- is evaluated. The formulas presented by Nielsen (1992) rely on the measurement of excess values of the three N_2 isotopologues in comparison to initial (background) concentrations of $^{28}\text{N}_2$, $^{29}\text{N}_2$ and $^{30}\text{N}_2$ before ^{15}N labelled N_2 has been evolved. In this paper this is done by subtracting the measured intensities on m/z 28, m/z 29 and m/z 30 ($^{28}\text{N}_2$, $^{29}\text{N}_2$ and $^{30}\text{N}_2$, respectively) of an air standard with the same total N_2 amount as in the sample from the measured intensities on m/z 28, m/z 29 and m/z 30 during sample analysis. In case of flow-thru incubation experiments, for which this formulas are often applied, the measured intensities on m/z 28, m/z 29 and m/z 30 of the “inflow” N_2 sample are subtracted from the “outflow” N_2 sample (An et al., 2001). The formulas given by Nielsen (1992) implicitly assume that the distribution of N_2 isotopologues of initial N_2 in the sample before ^{15}N labelled N_2 is produced is the same as the one in the measured N_2 standard.

The equations given by Hauck and Bouldin (1961), Mulvaney and Boast (1986) as well as the ones provided by Arah (1992) require the measurement of two N_2 isotopologue ratios to determine the ^{15}N abundance of N_2 evolved during denitrification of ^{15}N enriched NO_3^- whereas it is sufficient to measure one ratio if the formulas given by Mulvaney and Boast (1986) and the formulas presented here are applied.

All previously mentioned approaches assume (ii) that the initial N_2 , i.e. atmospheric derived N_2 , in the sample has the same distribution of N_2 isotopologues ($^{28}N_2$, $^{29}N_2$ and $^{30}N_2$) as atmospheric N_2 , i.e. the three N_2 isotopologues follow a binomial distribution. Arah (1992) presented a mathematical approach, which provides additional equations that are also valid when the initial background N_2 in the sample has not the same distribution of N_2 isotopologues ($^{28}N_2$, $^{29}N_2$ and $^{30}N_2$) as atmospheric N_2 .

The assumption (i) that the pool of NO_3^- undergoing denitrification is of uniform ^{15}N abundance might not always be an appropriate simplification to the investigated system. The effects of multiple pools of denitrified NO_3^- with different ^{15}N labelling on the calculated denitrification rates are evaluated in the works of Boast et al. (1988) and Arah (1992) and they are not a topic of this work.

Spott and Stange (2007) provided a new mathematical approach calculating the contribution of ^{15}N -labelled N_2 coming from denitrification and from anammox in a mixture with atmospheric N_2 in a sample. Such a sample consists of a mixture of three N_2 sources (atmospheric N_2 , anammox derived N_2 and denitrification derived N_2), which is beyond the scope of this work. Here are only formulas presented that are applicable on N_2 mixtures consisting of two N_2 sources.

The formulas based on the ^{15}N tracer technique and currently used in denitrification research did not reveal the close mathematical similarities with formulas used in isotope dilution mass spectrometry (IDSM). The basic difference between IDSM and the ^{15}N tracer technique is that for the first the sample is modified by adding a spike to it and for the second the system of interest is changed by “spiking” it with a ^{15}N tracer. The presented formulas clearly show this close relationship of both techniques and differ in their mathematical structure from previous approaches.

In the following equations are derived to calculate the fraction of denitrification derived N_2 in a mixture with initial (atmospheric) N_2 based on the ^{15}N tracer technique, showing that there is only slight difference between the mathematics of IDMS and the equations of the ^{15}N tracer technique used in denitrification research. If Eqn. (1) is divided by the term $(C_s W_s / W_x)$ one gets an equation usable to calculate the contribution of N_2 derived from denitrified ^{15}N

labelled NO_3^- in a mixture with initial atmospheric N_2 . The here presented 3 quadric solutions to calculate the ^{15}N abundance in the denitrified N pool, are similar to the one presented by (Hauck and Bouldin, 1961) but not the same, since they used different isotopologues ratios ($^{29}\text{N}_2$ to $^{28}\text{N}_2$ and $^{30}\text{N}_2$ to the sum of $^{28}\text{N}_2$ and $^{29}\text{N}_2$) compared to this work.

First an abstract, strict mathematical way to describe samples and derived formulas is given. This is done in order to give the formulas the greatest generality and to show clearly that the structure of solution depends only on the structure of the sample. This means a sample consisting of a mixture of two sources of the analysed substance with different isotope distributions in each source, e.g. a mixture of atmospheric N_2 with ^{15}N labelled denitrification derived N_2 .

Derivations

General formulation

We consider a molecule X that exists in form of n different Isotopologues X_i with $i = 1$ to n . For example, if $X = N_2$ the set of N_2 isotopologues would consist of $X = \{^{28}N_2, ^{29}N_2, ^{30}N_2\}$. Now we assume a sample C consisting of exactly two subsets A and B . These subsets A and B represent two different sources of molecules of X united in the mixture C . Let N_C , N_A , and N_B be the number of X molecules in the sample C and in A and B , respectively and N_{XiA} , N_{XiB} and N_{XiC} be the number of the isotopologues X_i in A , B and C respectively.

$$N_A = \sum_{i=1}^n N_{XiA} \quad (2)$$

$$N_B = \sum_{i=1}^n N_{XiB} \quad (3)$$

Dividing N_A and N_B by N_C gives n_A and n_B the fraction of X molecules in the sample C coming from A and B , respectively. α_i and β_i should be the mole fractions of the isotopologue X_i in A and B .

$$N_C = N_A + N_B \quad (4)$$

$$1 = n_A + n_B \quad (5)$$

$$\alpha_i = \frac{N_{XiA}}{N_A} \quad (6)$$

$$\beta_i = \frac{N_{XiB}}{N_B} \quad (7)$$

Now we want to calculate the ratio n_B/n_A in the mixture (sample) C . Let α_i and β_i be the mole fractions of isotopologue X_i in the subsets A and B , respectively, and α_j and β_j be the mole fractions of isotopologue X_j in the subsets A and B , respectively. For i and j is that $i \neq j$ and that i and j are natural numbers between 1 and n . The ratio R_{ij} of the isotopologues X_i and X_j in the mixture C is

$$R_{ij} = \frac{N_A \alpha_i + N_B \beta_i}{N_A \alpha_j + N_B \beta_j} \quad (8)$$

Reducing by N_C gives:

$$R_{ij} = \frac{n_A \alpha_i + n_B \beta_i}{n_A \alpha_j + n_B \beta_j} \quad (9)$$

It is assumed that the ratio R_{ij} represent an unbiased (corrected) isotopologue ratio. We solve for n_B/n_A .

$$R_{ij} = \frac{\alpha_i}{\alpha_j + \frac{n_B}{n_A} \beta_j} + \frac{n_B}{n_A} \cdot \frac{\beta_i}{\alpha_j + \frac{n_B}{n_A} \beta_j} \quad (10)$$

$$\frac{n_B}{n_A} = \left(R_{ij} - \frac{\alpha_i}{\alpha_j + \frac{n_B}{n_A} \beta_j} \right) \cdot \frac{\alpha_j + \frac{n_B}{n_A} \beta_j}{\beta_i} \quad (11)$$

$$\frac{n_B}{n_A} = R_{ij} \frac{\alpha_j}{\beta_i} + R_{ij} \frac{n_B}{n_A} \frac{\beta_j}{\beta_i} - \frac{\alpha_i}{\beta_i} \quad (12)$$

$$\frac{n_B}{n_A} = \frac{R_{ij} \frac{\alpha_j}{\beta_i} - \frac{\alpha_i}{\beta_i}}{1 - R_{ij} \frac{\beta_j}{\beta_i}} \quad (13)$$

$$\frac{n_B}{n_A} = \frac{R_{ij} \alpha_j - \alpha_i}{\beta_i - R_{ij} \beta_j} \quad (14)$$

Eqn. (14) differs from the IDMS formula (Eqn. 1) above only in the fact that for IDMS the value of either n_A or n_B is known. If the ratio (n_B/n_A) is calculated with Eqn. (14), n_A can obviously be expressed as follows:

$$n_A = \frac{n_B}{\left(\frac{n_B}{n_A} \right)} \quad (15)$$

Substituting Eqn. (15) into Eqn. (5) and solving for n_B generates:

$$n_B = \frac{1}{\frac{1}{\left(\frac{n_B}{n_A} \right)} + 1} \quad (16)$$

$[X_C]$ is the concentration of X in the mixture C and $[X_B]$ the concentration of X in the mixture coming from source B , $[X_B]$ is then:

$$[X_B] = [X_C] \cdot n_B \quad (17)$$

Three conditions must be met for these formulas to be valid: (i) the sample contains only two sources (A and B) of X , (ii) the sampled substance does not undergo any chemical reaction after sampling and (iii) the two subsets of X must have different and known distributions of isotopes or isotopologues of X . With the use of Eqn. (14) specialized formulas can easily be

derived for the calculation of n_B/n_A ratios in samples under condition that Eqns. (2) and (7) describe the sample with respect to the substance X , which is to be analysed, correctly. In contrast to the IDMS the concentration of substance X is here measured directly for the whole sample and not from changing the sample by adding a well known spike to it. But the mathematical structure of Eqn. (14) and Eqn. (1) is equivalent if Eqn. (1) is divided by the term $(C_s W_s / W_x)$.

Application of the derived formulas to N_2 isotopologues mixtures of two sources based on the ^{15}N tracer method

In the following we use Eqn. (14) to get formulas to calculate the fraction of ^{15}N labelled N_2 derived by denitrification in a mixture with initial N_2 , for example atmospheric N_2 , of different N_2 isotopologue distribution.

The sample C should contain two subsets of N_2 , subset A and B . Subset A should consist of initial N_2 present before ^{15}N labelled N_2 is formed during denitrification in the investigated system. The initial N_2 should have the ^{15}N abundance a . The subset B should contain ^{15}N enriched N_2 derived from denitrified NO_3^- with the ^{15}N abundance of b . The subscripts 28, 29 and 30 indicate $^{28}N_2$, $^{29}N_2$ and $^{30}N_2$. The symbols α_{28} , α_{29} , α_{30} and β_{28} , β_{29} , β_{30} denote mole fractions of $^{28}N_2$, $^{29}N_2$ and $^{30}N_2$ in the subsets A and B , respectively (initial and denitrification derived N_2 isotopologues). The number of N_2 molecules in A , B and C are N_A , N_B and N_C and the fractions of initial N_2 and denitrification derived N_2 in the sample C are n_A and n_B , respectively. The concentration of N_2 in the mixture C coming from subset A and B is $[N_{2A}]$ and $[N_{2B}]$, respectively. The sample C can then be described with the Eqns. (2) to (7). In both subsets A and B the distribution of the three N_2 isotopologues should follow binomial distribution according to the ^{15}N abundances a and b . Under these conditions the mole fractions of N_2 isotopologues of initial and denitrification derived N_2 can be expressed as follows:

The molecular fractions of initial N_2 isotopologues in the subset A are

$$\alpha_{28} = (1-a)^2 \quad (18a)$$

$$\alpha_{29} = 2a(1-a) \quad (18b)$$

$$\alpha_{30} = a^2 \quad (18c)$$

If the isotopologues distribution of the three N₂ isotopologues in the initial N₂ is equal to the one of atmospheric N₂, then $\alpha_{28}=\alpha_{28atm}$, $\alpha_{29}=\alpha_{29atm}$ and $\alpha_{30}=\alpha_{30atm}$, in which the subscript atm denotes mole fractions of atmospheric N₂ isotopologues.

In subset *B* the mole fractions of β_{28} , β_{29} and β_{30} can be defined as:

$$\beta_{28} = (1 - b)^2 \quad (19a)$$

$$\beta_{29} = 2b(1 - b) \quad (19b)$$

$$\beta_{30} = b^2 \quad (19c)$$

N_{C28} , N_{C29} and N_{C30} are the numbers of ²⁸N₂, ²⁹N₂ and ³⁰N₂ isotopologues in the mixture *C*.

The number of the different N₂ isotopologues in the mixture can be calculated as follows:

$$N_{C28} = N_A \alpha_{28} + N_B \beta_{28} \quad (20a)$$

$$N_{C29} = N_A \alpha_{29} + N_B \beta_{29} \quad (20b)$$

$$N_{C30} = N_A \alpha_{30} + N_B \beta_{30} \quad (20c)$$

From the Eqns. (20a) and (20b) the ratio $R_1=N_{C29}/N_{C28}$ in the sample *C* can be formulated, giving:

$$R_1 = \frac{N_{C29}}{N_{C28}} = \frac{N_A \alpha_{29} + N_B \beta_{29}}{N_A \alpha_{28} + N_B \beta_{28}} = \frac{n_A \alpha_{29} + n_B \beta_{29}}{n_A \alpha_{28} + n_B \beta_{28}} \quad (21)$$

We define that $\alpha_{29}=\alpha_i$, $\alpha_{28}=\alpha_j$, $\beta_{29}=\beta_i$ and $\beta_{28}=\beta_j$, now it is obvious that Eqn. (21) is equivalent to Eqn. (9) and we can rewrite Eqn. (14) to:

$$\frac{n_B}{n_A} = \frac{R_1 \alpha_{28} - \alpha_{29}}{\beta_{29} - R_1 \beta_{28}} \quad (22)$$

and immediately get a solution of the sought ratio of n_B/n_A .

The isotopologues ratios R_2 and R_3 can be formulated with Eqns. (20a) to (20c) as follows:

$$R_2 = \frac{N_{C30}}{N_{C28}} = \frac{N_A \alpha_{30} + N_B \beta_{30}}{N_A \alpha_{28} + N_B \beta_{28}} = \frac{n_A \alpha_{30} + n_B \beta_{30}}{n_A \alpha_{28} + n_B \beta_{28}} \quad (23)$$

$$R_3 = \frac{N_{C30}}{N_{C29}} = \frac{N_A \alpha_{30} + N_B \beta_{30}}{N_A \alpha_{29} + N_B \beta_{29}} = \frac{n_A \alpha_{30} + n_B \beta_{30}}{n_A \alpha_{29} + n_B \beta_{29}} \quad (24)$$

Solutions for the n_B/n_A ratio using R_2 and R_3 can be derived in exactly the same manner. For R_2 we define $\alpha_{30}=\alpha_i$, $\alpha_{28}=\alpha_j$, $\beta_{30}=\beta_i$ and $\beta_{28}=\beta_j$ and for R_3 we set $\alpha_{30}=\alpha_i$, $\alpha_{29}=\alpha_j$, $\beta_{30}=\beta_i$ and $\beta_{29}=\beta_j$ with Eqn. (14) we get immediately the solutions for these two isotopologues ratios with respect to the sought n_B/n_A ratio:

$$\frac{n_B}{n_A} = \frac{R_2 \alpha_{28} - \alpha_{30}}{\beta_{30} - R_2 \beta_{28}} \quad (25)$$

$$\frac{n_B}{n_A} = \frac{R_3\alpha_{29} - \alpha_{30}}{\beta_{30} - R_3\beta_{29}} \quad (26)$$

Assuming binomial distribution of N₂ isotopologues in denitrified and initial N₂ we can substitute Eqns. (18a) to (18c) and (19a) to (19c) into Eqns. (22), (25) and (26) giving:

$$\frac{n_B}{n_A} = \frac{R_1(1-a)^2 - 2a(1-a)^2}{2b(1-b) - R_1(1-b)^2} \quad (27)$$

$$\frac{n_B}{n_A} = \frac{R_2(1-a)^2 - a^2}{b^2 - R_2(1-b)^2} \quad (28)$$

$$\frac{n_B}{n_A} = \frac{R_3 2a(1-a) - a^2}{b^2 - R_3 2b(1-b)} \quad (29)$$

If the initial N₂ exhibits no binomial distribution of N₂ isotopologues, assuming random pairing during any N₂ formation, this means that the initial N₂ itself consists of different subsets of N₂ with different N₂ isotopologue distributions or that the initial N₂ consists of synthetic N₂, where the different N₂ isotopologues might be discriminated in relation to each other during industrial purification processes. In these cases the mole fractions α_{28} , α_{29} and α_{30} of initial N₂ can not be calculated with the Eqns. (18a) to (18c) and the N₂ isotopologue mole fractions of initial N₂ must be measured before denitrification derived ¹⁵N labelled N₂ has been evolved. In this case the Eqns. (21a) to (21c) provided in the paper given by Arah (1992) can be applied.

The ratios R_1 , R_2 and R_3 represent unbiased and / or corrected mass spectrometric data. From the calculated ratio of n_B/n_A the concentration of denitrification derived N₂ in the mixture C ($[N_{2B}]$) can be calculated using Eqns. (16) and (17). The Eqns. (22), (25) and (26) to (29), have the same mathematical structure as Eqn. (1) after dividing it by $(C_s W_s / W_x)$, revealing the close mathematical relationship between IDMS and the calculation of ¹⁵N labelled N₂ derived from denitrification with the ¹⁵N tracer technique.

Previous works provide equations for double-collector mass spectrometers to calculate the ¹⁵N abundance of denitrified NO₃⁻ (b) for the measurement of absolute N₂ isotopologue ratios of $^{29}N_{2mix}/^{28}N_{2mix}$ and $^{30}N_{2mix}/(^{28}N_{2mix} + ^{29}N_{2mix})$ (Hauck and Bouldin, 1961). For the measurement of ratio differences with a dual-inlet mass spectrometer Mulvaney and Boast (1986) derived equations using the ratios $^{29}N_{2mix}/(^{28}N_{2mix} + ^{30}N_{2mix})$, $^{29}N_{2mix}/(^{28}N_{2atm} + ^{30}N_{2atm})$, $^{30}N_{2mix}/(^{28}N_{2mix} + ^{29}N_{2mix})$ and $^{30}N_{2atm}/(^{28}N_{2atm} + ^{29}N_{2atm})$ (double-collector instruments) and the ratios $^{29}N_{2mix}/^{28}N_{2mix}$, $^{29}N_{2atm}/^{28}N_{2atm}$, $^{30}N_{2mix}/^{28}N_{2mix}$ and $^{30}N_{2atm}/^{28}N_{2atm}$ (triple-collector instruments). Since the given formulas are derived for the absolute ratios $^{29}N_{2mix}/^{28}N_{2mix}$,

$^{30}\text{N}_{2\text{mix}}/^{28}\text{N}_{2\text{mix}}$ and $^{30}\text{N}_{2\text{mix}}/^{29}\text{N}_{2\text{mix}}$ and for completeness 3 quadratic equations to calculate b for all combinations of the three N_2 isotopologue ratios are derived, which was not done in the cited papers (Eqn. (33) and Table 1). Beside b , each of the equations (27) to (29) contains the two unknowns n_A and n_B . Equating these equations with each other gives:

$$\frac{R_1(1-a)^2 - 2a(1-a)}{2b(1-b) - R_1(1-b)^2} = \frac{R_2(1-a)^2 - a^2}{b^2 - R_2(1-b)^2} \quad (30)$$

$$\frac{R_1(1-a)^2 - 2a(1-a)}{2b(1-b) - R_1(1-b)^2} = \frac{R_3 2a(1-a) - a^2}{b^2 - R_3 2b(1-b)} \quad (31)$$

$$\frac{R_2(1-a)^2 - a^2}{b^2 - R_2(1-b)^2} = \frac{R_3 2a(1-a) - a^2}{b^2 - R_3 2b(1-b)} \quad (32)$$

The Eqns. (30), (31) and (32) contain only b as unknown and can be rearranged to the quadratic equations (T_I), (T_{II}) and (T_{III}), respectively (Table 1). With Eqn. (33) Quadratic equations (TI), (TII) and (TIII) can be solved for the unknown ^{15}N abundance of denitrified NO_3^- (b).

$$b = \frac{-D \pm \sqrt{D^2 - 4CE}}{2C} \quad (33)$$

The constants D , C and E of the quadratic equations are given in Table 1, R_I , R_2 and R_3 are the measured and corrected N_2 isotopologue ratios. If the N_2 isotopologues in the initial N_2 follow binomial distribution, then the mole fractions of initial N_2 α_{28} , α_{29} and α_{30} in the term F (Table 1) can be calculated with Eqns. (18a), (18b) and (18c), respectively, with a as the ^{15}N abundance of the initial N_2 .

Table 1. Quadratic equations (T_I), (T_{II}) and (T_{III}) and values of the constants.

quadratic equations	Variables			
	C	D	E	F
(T _I) $0 = b^2 C_I + b D_I + E_I$	$F_I (R_2 - 1) - 2 - R_1$	$2(-F_I R_2 + 1 + R_1)$	$F_I R_2 - R_1$	$\frac{R_1 \alpha_{28} - \alpha_{29}}{R_2 \alpha_{28} - \alpha_{30}}$
(T _{II}) $0 = b^2 C_{II} + b D_{II} + E_{II}$	$F_{II} (-1 - 2R_3) - 2 - R_1$	$2(1 + R_1 + F_{II} R_3)$	$-R_1$	$\frac{R_1 \alpha_{28} - \alpha_{29}}{R_3 \alpha_{29} - \alpha_{30}}$
(T _{III}) $0 = b^2 C_{III} + b D_{III} + E_{III}$	$1 - R_2 - F_{III} (1 + 2R_3)$	$2(R_2 + F_{III} R_3)$	$-R_2$	$\frac{R_2 \alpha_{28} - \alpha_{30}}{R_3 \alpha_{29} - \alpha_{30}}$

In the most common special case a is equal to the ^{15}N abundance of atmospheric N_2 . If the N_2 isotopologues in the initial N_2 follow no binomial distribution the mole fractions of $^{28}\text{N}_2$, $^{29}\text{N}_2$ and $^{30}\text{N}_2$ of initial N_2 (α_{28} , α_{29} and α_{30} , respectively) have to be measured before ^{15}N labelled

N₂ is formed. Arah (1992) firstly derived equations to calculate b in this case, but he used a different procedure of solution. In the derivations of Hauck and Bouldin (1961) and Mulvaney and Boast (1986) it is assumed that the initial N₂ is always equal to atmospheric N₂.

Discussion

Contrary to the previous approaches the presented mathematical expressions clearly reveal the close mathematical relation between isotope dilution mass spectrometry (IDMS) and the ¹⁵N tracer approach used in denitrification research. For IDMS the sample is altered by adding a spike with a well known isotope distribution and amount to it, for the ¹⁵N tracer approach the system of interest is altered by “spiking” it with a ¹⁵N tracer. These conceptual similarities are mirrored in the similarities of the equations. Different to the derivation of previous approaches Eqns. (2) to (14) are formulated in an abstract way, which makes it easier to see similarities in related tasks and to transfer them to similar questions, e.g. the evaluation of ¹³C/¹²C ratios measured in soil organic matter originating from two pools with different ¹³C abundances. (Appendix 2).

The presented equations are simpler and shorter than the ones given by Hauck and Bouldin (1961), Mulvaney and Boast (1986) or Arah (1992) and based on the same prerequisites as those approaches, i.e. discrimination between the N isotopes is negligible during N₂ formation and the denitrified NO₃⁻ originates from one pool of uniform ¹⁵N abundance, which is equal to the requirement that the sample has to contain only two subsets of N₂ isotopologues with different isotopologue distributions (initial N₂ and evolved ¹⁵N labelled N₂). Contrary to the formulas presented by (Hauck and Bouldin, 1961) and (Mulvaney and Boast, 1986) the presented equations are able to calculate the fraction of ¹⁵N labelled N₂ in mixture with initial N₂ that has not the same N₂ isotopologue (²⁸N₂, ²⁹N₂, ³⁰N₂) distribution as atmospheric N₂ and also for every of the three N₂ isotopologue ratios ²⁹N₂/²⁸N₂, ³⁰N₂/²⁸N₂ and ³⁰N₂/²⁹N₂.

The equations given by Mulvaney and Boast (1986) are especially designed for the use of dual-inlet mass spectrometers and the very precise measurement of ratio differences. The presented formulas as the one given by Hauck and Bouldin (1961) require the measurement of absolute ratios and therefore suitable for membrane inlet mass spectrometers (MIMS), which have no dual-inlets systems.

The Eqns. (22) and (25) to (29) derived in this paper have the same solution, which is useful to immediately check the calculated results from experimental data. Numerical modelling

shows that the Eqns. (27), (28) and (29) react differently to false b values used for calculating the ratio of ^{15}N labelled N_2 derived from denitrification and initial N_2 (n_B/n_A). If the assumed or measured ^{15}N abundance of the denitrified NO_3^- (b) is overestimated then the calculated (n_B/n_A) ratio of Eqn. (27) > Eqn. (28) > Eqn. (29) and if b is underestimated then the result of Eqn. (27) < Eqn. (28) < Eqn. (29). These inequalities hold irrespective of the n_B/n_A ratio and the real ^{15}N enrichment of denitrified NO_3^- in the sample as long as no implausible negative n_B/n_A ratios are calculated from the given data, which also implies that the used value of b is false. If the prerequisites for the validity of the derived equations are met and one is sure that the used value of b is right and the results of the Eqns. (27), (28) and (29) are unequal, then (i) supposedly the mass spectrometer is not properly calibrated for the detection of $^{28}\text{N}_2$, $^{29}\text{N}_2$ and $^{30}\text{N}_2$ on the molecular ion masses m/z 28, m/z 29 and m/z 30, respectively, (ii) the N_2 isotopologue distribution of initial N_2 was not the one assumed, e.g. not equal to atmospheric N_2 , or (iii) the assumption regarding a uniform labelled pool during denitrification does not hold (substantial shifts in the ^{15}N abundance of denitrified NO_3^- or substantial isotopic fractionation processed occurred during the experiment). If (ii) is the reason for different results obtained with Eqns. (27) to (29) the N_2 isotopologue distribution of initial N_2 has to be measured before ^{15}N labelled N_2 is formed.

The quadric formulas to calculate the ^{15}N abundance (b) in the pool of denitrified NO_3^- presented here (Table 1) are similar to the one provided by Hauck and Bouldin (1961), but they used the ratios ($^{29}\text{N}_2/^{28}\text{N}_2$ and $^{30}\text{N}_2/(^{28}\text{N}_2+^{29}\text{N}_2)$) to calculate b . Here solutions are provided for all simple ratios of $^{29}\text{N}_2/^{28}\text{N}_2$, $^{30}\text{N}_2/^{28}\text{N}_2$ and $^{29}\text{N}_2/^{28}\text{N}_2$.

From the presented formulas instrumental response factors are derived to correct the measured $^{29}\text{N}_2/^{28}\text{N}_2$, $^{30}\text{N}_2/^{28}\text{N}_2$ and $^{30}\text{N}_2/^{29}\text{N}_2$ (Appendix 3).

Acknowledgements

This research was made possible by financial support from the Deutsche Bundesstiftung Umwelt (DBU).

References

- An, S. M., Gardner, W. S., and Kana, T.: Simultaneous measurement of denitrification and nitrogen fixation using isotope pairing with membrane inlet mass spectrometry analysis, *Appl. Environ. Microbiol.*, 67, 1171-1178, 2001.
- Arah, J. R. M.: New formulas for mass-spectrometric analysis of nitrous-oxide and dinitrogen emissions, *Soil Sci. Soc. Am. J.*, 56, 795-800, 1992.
- Bloch, K., and Anker, H. S.: An extension of the isotope dilution method, *Science*, 107, 228-228, 10.1126/science.107.2774.228, 1948.
- Boast, C. W., Mulvaney, R. L., and Baveye, P.: Evaluation of N¹⁵ tracer techniques for direct measurement of denitrification in soil. 1. Theory, *Soil Sci. Soc. Am. J.*, 52, 1317-1322, 1988.
- Eschenbach, W., and Well, R.: Online measurement of denitrification rates in aquifer samples by an approach coupling an automated sampling and calibration unit to a membrane inlet mass spectrometry system, *Rapid Commun. Mass Spectrom.*, 25, 1993-2006, 10.1002/rcm.5066, 2011.
- Fassett, J. D., and Paulsen, P. J.: Isotope-dilution mass-spectrometry for accurate elemental analysis, *Anal. Chem.*, 61, A643-&, 10.1021/ac00185a001, 1989.
- Gest, H., Kamen, M. D., and Reiner, J. M.: The theory of isotope dilution, *Archives of Biochemistry*, 12, 273-281, 1947.
- Groffman, P. M., Altabet, M. A., Bohlke, J. K., Butterbach-Bahl, K., David, M. B., Firestone, M. K., Giblin, A. E., Kana, T. M., Nielsen, L. P., and Voytek, M. A.: Methods for measuring denitrification: Diverse approaches to a difficult problem, *Ecol. Appl.*, 16, 2091-2122, 2006.
- Hauck, R. D., Melsted, S. W., and Yanlwitch, P. E.: Use of N-isotope distribution in nitrogen gas in the study of denitrification., *Soil Sci.*, 86, 287-291, 1958.
- Hauck, R. D., and Bouldin, D. R.: Distribution of isotopic nitrogen in nitrogen gas during denitrification, *Nature*, 191, 871-&, 1961.
- Heumann, K. G.: Isotope-dilution mass-spectrometry (IDMS) of the elements, *Mass Spectrom. Rev.*, 11, 41-67, 10.1002/mas.1280110104, 1992.
- Jensen, K. M., Jensen, M. H., and Cox, R. P.: Membrane inlet mass spectrometric analysis of N-isotope labelling for aquatic denitrification studies, *FEMS Microbiol. Ecol.*, 20, 101-109, 1996.

- Kana, T. M., Darkangelo, C., Hunt, M. D., Oldham, J. B., Bennett, G. E., and Cornwell, J. C.: Membrane inlet mass-spectrometer for rapid high-precision determination of N₂, O₂, and Ar in environmental water samples, *Anal. Chem.*, 66, 4166-4170, 1994.
- Mulvaney, R. L., and Kurtz, L. T.: A new method for determination of N¹⁵-labeled nitrous-oxide, *Soil Sci. Soc. Am. J.*, 46, 1178-1184, 1982.
- Mulvaney, R. L.: Determination of N¹⁵-labeled dinitrogen and nitrous-oxide with triple-collector mass spectrometers, *Soil Sci. Soc. Am. J.*, 48, 690-692, 1984.
- Mulvaney, R. L., and Boast, C. W.: Equations for determination of N¹⁵ labeled dinitrogen and nitrous-oxide by mass-spectrometry, *Soil Sci. Soc. Am. J.*, 50, 360-363, 1986.
- Nielsen, L. P.: Denitrification in sediment determined from nitrogen isotope pairing, *FEMS Microbiol. Ecol.*, 86, 357-362, 1992.
- Rodriguez-Gonzalez, P., Marchante-Gayon, J. M., Alonso, J. I. G., and Sanz-Medel, A.: Isotope dilution analysis for elemental speciation: A tutorial review, *Spectroc. Acta Pt. B-Atom. Spectr.*, 60, 151-207, 10.1016/j.sab.2005.01.005, 2005.
- Schumpeter, J. A.: Kredit und Kapital, Theorie der wirtschaftlichen Entwicklung, Kapitel III., in: *The Essence of J. A. Schumpeter Die wesentlichen Texte (1996)*, edited by: Leube, K. R., Wien, 334, 1912.
- Siegel, R. S., Hauck, R. D., and Kurtz, L. T.: Determination of (N₂)-N-30 and application to measurement of N₂ evolution during denitrification, *Soil Sci. Soc. Am. J.*, 46, 68-74, 1982.
- Spott, O., and Stange, C. F.: A new mathematical approach for calculating the contribution of anammox, denitrification and atmosphere to an N₂ mixture based on a N-15 tracer technique, *Rapid Commun. Mass Spectrom.*, 21, 2398-2406, 10.1002/rcm.3098, 2007.

Appendix 1

The isotope pairing method (IPM) developed by Nielsen (1992) relies on the measurement of excess values of N₂ isotopologues (²⁸N₂, ²⁹N₂ and ³⁰N₂) derived from denitrification. To analyse these excess values of N₂ isotopologues dissolved gas concentrations can be measured at the in- and outflow of flow-chambers. The outflow sample contains then a mixture of initial unlabelled N₂ and the evolved labelled N₂ formed during residence time in the chamber. The measured intensities of the N₂ isotopologues at the inflow are then subtracted from the intensities measured at the outflow (An et al., 2001). Nielsen (1992) subtracted an air standard with the same amount of N₂ from the measured intensities of N₂ isotopologues of a sample to evaluate excess values of N₂ isotopologues. This requires that the initial N₂ in the sample, before denitrification derived ¹⁵N labelled N₂ evolves, has the same N₂ isotopologue distribution as atmospheric N₂.

With the notation used in this work Eqn. (1) given by Nielsen (1992) can be formulated as follows:

$$D_{15} = (N_{C29} - N_A \alpha_{29}) + 2(N_{C30} - N_A \alpha_{30}) \quad (\text{A1.1})$$

Where D_{15} is the rate of denitrification of ¹⁵NO₃⁻ and the terms $(N_{C29} - N_A \alpha_{29})$ and $(N_{C30} - N_A \alpha_{30})$ are the amounts of excess ²⁹N₂ and ³⁰N₂, respectively, coming from denitrification after ¹⁵NO₃⁻ addition. $N_A \alpha_{29}$ and $N_A \alpha_{30}$ are the amounts of initial ²⁹N₂ and ³⁰N₂ in the sample before denitrification derived N₂ has evolved. If the initial N₂ shows a binomial distribution of N₂ isotopologues and has the ¹⁵N abundance a (maybe equal to atmospheric N₂) Eqn. (A1.1) can be simplified using the Eqns. (18b) and (18c) to:

$$D_{15} = N_{C29} + 2N_{C30} - N_A (2a(1-a) + a^2) \quad (\text{A1.2})$$

The denitrification rate of ¹⁴NO₃⁻ (D_{14}) is then expressed in accordance to Eqn. (2) given by Nielsen (1992):

$$D_{14} = D_{15} \cdot \frac{(1-b)}{b} \quad (\text{A1.3})$$

Where b is the ¹⁵N abundance in the denitrified NO₃⁻. The value of N_A can be calculated after solving Eqn. (4) for N_A . N_C and N_B are the number of total N₂ and denitrification derived N₂ in the analysed sample, if the volume or weight of the analysed sample is known this gives concentration data. Therefore N_C is measured as the concentration of N₂ in the sample and N_B can be calculated using Eqns. (27) or (28) or (29) and Eqns. (16) and (17). The ¹⁵N abundance (b) in the denitrified N₂ can be calculated after solving one of the quadric Eqns. (T_I) to (T_{III}) (Table 1) with Eqn. (33). The way to calculate D_{15} and D_{14} presented here has the advantage that all needed parameters can be obtained by one measurement instead of two, as is required

by the approach given by Nielsen (1992) who measured the production of evolved labelled N₂ in a batch mode assay or An et al. (2001) who uses a flow through system. This is on condition that the N₂ isotopologue distribution of initial N₂ in the batch assay is known, what is the case if initial N₂ is derived from atmospheric N₂. Using Eqn. (33) the ¹⁵N abundance of the actual denitrified NO₃⁻ during the experiment can be measured for every sampling time during incubation experiments. If initial N₂ in the sample has not the same N₂ isotopologue distribution as atmospheric N₂ than it is not correct to subtract an air standard with the same N₂ amount as the sample from measured N₂ isotopologues intensities of a sample as proposed by Nielsen (1992). In this case the presented formulation of D₁₅ and D₁₄ is also advantageous.

Appendix 2

As another example we imagine a soil containing only organic material derived from C₃-plants. This soil was then fertilized over a certain time period with C₄-plant material. From the analysed soil sample we want to know the fraction of soil organic carbon after fertilization that is derived from C₄-plants. The fraction of ¹³C and ¹²C of the soil organic material before fertilization should be α_{13} and α_{12} , respectively. In the C₄-plant material ¹³C and ¹²C should have the fractions of β_{13} and β_{12} , respectively. The value of α_{13} and β_{13} is between 0 and 1, furthermore α_{13} is not equal β_{13} . The soil organic material in the soil sample after fertilization can be divided in two sets A and B, for organic material derived from C₃- and C₄-plants. N_A and N_B should be the numbers of C atoms of both sets in the sample. With this description of the sample the ratio R of ¹³C/¹²C in the soil sample after fertilization can be described with the following equation:

$$R = \frac{N_A \alpha_{13} + N_B \beta_{13}}{N_A \alpha_{12} + N_B \beta_{12}} \quad (\text{A2.1})$$

With $\alpha_{13}=\alpha_i$, $\alpha_{12}=\alpha_j$, $\beta_{13}=\beta_i$ and $\beta_{12}=\beta_j$ Eqn. (A2.1) can be transformed to Eqn. (8) and the solution to the desired ratio of n_A/n_B can easily be derived from Eqn. (14) giving:

$$\frac{n_B}{n_A} \frac{R \alpha_{12} - \alpha_{13}}{\beta_{13} - R \beta_{12}} \quad (\text{A2.2})$$

(The carbon isotopes are measured as CO₂ isotopologues after combustion on the ion masses 44 (= ¹²C¹⁶O¹⁶O) and 45 (= ¹³C¹⁶O¹⁶O). If not negligible the contribution of ¹²C¹⁶O¹⁷O to ion mass 45 must be corrected when analysing the ion mass ratio m/z 45/ m/z 44.)

Appendix 3

The equations derived in this chapter are based on theoretical considerations and the above derived formulas. The formulas in this section (Appendix 3) have still to be evaluated experimentally.

Equations to correct the spectral interferences during the measurement of N₂ isotopologues

Spectral interferences can seriously affect the accuracy of mass spectrometric analysis of N₂ isotopologues, especially of ³⁰N₂ on the molecular ion mass 30. From the presented equations (Eqn. 2 to 29) formulas to correct this spectral interferences are derived. This presented approach relies on theoretical consideration and has still to be tested with experimental data.

Parameters which can affect the accuracy of isotope ratio measurement are mass discrimination, the dead time of the detector and spectral interferences (Rodriguez-Gonzalez et al., 2005). Mass discrimination within a mass spectrometer leads to a discrimination of lighter isotopes relative to heavier isotopes. If an electron multiplier is used for detection, the dead time of the detector might become a problem at high counting rates, leading to lower numbers of recorded isotopes compared to the number of isotopes that really reach the detector. Spectral interferences, caused by molecular ions with the same mass to charge ratio (m/z) as the ones to be measured, can seriously affect the correct measurement of isotope ratios. For a detailed discussion on all of these three topics see Rodriguez-Gonzales et al. (2005). They provide also equations for the correction of detector dead time and mass discrimination effects. Since the detector dead time and mass discrimination are not or less dependent from sample matrix compared to spectral interferences, these both parameters should be corrected before applying equations to correct the spectral interferences.

N₂ isotopologue ratios can be biased by spectral interferences with CO⁺ and NO⁺ within the mass spectrometer. Especially the measurement of ³⁰N₂ on the molecular ion mass m/z 30 is often disturbed by the formation of ¹⁴NO⁺ within the mass spectrometer. (O in the ion formulas below is for ¹⁶O.) Also ²⁸N₂ and ²⁹N₂ on m/z 28 and m/z 29 can be affected by ¹²CO⁺ and ¹³CO⁺ possible molecular ion fragments of CO₂ (Jensen et al., 1996). To correct different instrumental sensitivities for N₂ isotopologues detected on the molecular ion masses m/z 29 and m/z 30 during MIMS analysis of dissolved gases Jensen et al. (1996) introduced a linear

instrumental response factor for $^{30}\text{N}_2$ in relation to $^{29}\text{N}_2$. (They used a Dataquad DQ100 quadrupole mass spectrometer (Spectramass; Congleton UK)). Their response factor presupposed a linear deviation of the measured $^{29}\text{N}_2$ to $^{30}\text{N}_2$ intensities from the true ratio in the sample in dependence of signal intensities on the respective molecular ion masses during analysis. In the following we call their instrumental response factors sample response factors. From Eqns. (27), (28) and (29) we derive formulas to calculate sample response factors for all three N_2 isotopologue ratios, whereas Jensen et al. (1996) provided only a response factor for the $^{29}\text{N}_2/^{30}\text{N}_2$ ratio.

First of all we assume that the detected ion currents on m/z 28, m/z 29 and m/z 30 are the sums of $^{28}\text{N}_2^+ + ^{12}\text{CO}^+$, $^{29}\text{N}_2^+ + ^{13}\text{CO}^+$ and $^{30}\text{N}_2^+ + ^{14}\text{NO}^+$, respectively, than applies.

$$(i\ m/z28) = (i\ ^{28}\text{N}_2^+) + (i\ ^{12}\text{CO}^+) \quad (\text{A3.1})$$

$$(i\ m/z29) = (i\ ^{29}\text{N}_2^+) + (i\ ^{13}\text{CO}^+) \quad (\text{A3.2})$$

$$(i\ m/z30) = (i\ ^{30}\text{N}_2^+) + (i\ ^{14}\text{NO}^+) \quad (\text{A3.3})$$

Where $(i\ m/z28)$, $(i\ m/z29)$ and $(i\ m/z30)$ are the recorded sums of the ion currents on molecular ion masses m/z 28, m/z 29 and m/z 30. $(i\ ^{28}\text{N}_2^+)$, $(i\ ^{29}\text{N}_2^+)$ and $(i\ ^{30}\text{N}_2^+)$ are the ion currents coming from molecular nitrogen (N_2) and $(i\ ^{12}\text{CO}^+)$, $(i\ ^{13}\text{CO}^+)$ and $(i\ ^{14}\text{NO}^+)$ are the ion currents of $^{12}\text{CO}^+$, $^{13}\text{CO}^+$ and $^{14}\text{NO}^+$.

Now we introduce the following sample response factors f' , f'' and f''' to correct the measured N_2 isotopologue ratios:

$$R_1 = r_1 f' = \frac{(i\ m/z29) f'}{(i\ m/z28)} = \frac{(i\ ^{29}\text{N}_2)}{(i\ ^{28}\text{N}_2)} = \frac{^{29}\text{N}_2}{^{28}\text{N}_2} \quad (\text{A3.4})$$

$$R_2 = r_2 f'' = \frac{(i\ m/z30) f''}{(i\ m/z28)} = \frac{(i\ ^{30}\text{N}_2)}{(i\ ^{28}\text{N}_2)} = \frac{^{30}\text{N}_2}{^{28}\text{N}_2} \quad (\text{A3.5})$$

$$R_3 = r_3 f''' = \frac{(i\ m/z30) f'''}{(i\ m/z29)} = \frac{(i\ ^{30}\text{N}_2)}{(i\ ^{29}\text{N}_2)} = \frac{^{30}\text{N}_2}{^{29}\text{N}_2} \quad (\text{A3.6})$$

Where r_1 , r_2 and r_3 are uncorrected (in terms of spectral interferences) N_2 isotopologue ratios $^{29}\text{N}_2/^{28}\text{N}_2$ ($= (i\ m/z29)/(i\ m/z28)$), $^{30}\text{N}_2/^{28}\text{N}_2$ ($= (i\ m/z30)/(i\ m/z28)$) and $^{30}\text{N}_2/^{29}\text{N}_2$ ($= (i\ m/z30)/(i\ m/z29)$), respectively. From Eqn. (A3.1) to (A3.3) it can be assumed that f' , f'' and f''' are not independent from the abundance of CO_2 , N_2 and O_2 in the mass spectrometer and/or in the sample. Therefore f' , f'' and f''' might only be valid for measurements with the same/similar concentration of CO_2 , O_2 and N_2 within the mass spectrometer (i.e. with the same concentrations in the sample). Consequently these response factors have to be connected with the concentrations of the respective gases in the mass spectrometer.

Now we will derive these sample response factors. The sample response factor f' could easily be derived from air equilibrated standard water, which for example can be used to calibrate a MIMS system (Kana et al., 1994). Air equilibrated standard water can be interpreted as a sample containing just one set of dissolved atmospheric N_2 with a known ratio of $^{29}N_2/^{28}N_2$. Using Eqn. (A3.4) the sample response factor f' is then:

$$f' = \frac{^{29}N_2}{^{28}N_2} \cdot \frac{(i\ m/z\ 28)}{(i\ m/z\ 29)} \quad (A3.7)$$

To check, if f' is dependent from the concentration of dissolved atmospheric N_2 or other dissolved gases in the measured air equilibrated water, air equilibrated water of different N_2 concentrations should be analysed.

Since $^{30}N_2$ in atmospheric N_2 corresponds only to a fraction below $1.34 \cdot 10^{-10}$ of total N_2 this small amount of $^{30}N_2$ dissolved in air equilibrated water may be not sufficient to calibrate molecular ion mass $m/z\ 30$ for this N_2 isotopologue. Standards containing a mixture of dissolved atmospheric N_2 and ^{15}N labelled N_2 derived from denitrification could be prepared as described in Jensen et al. (1996). The Eqns. (27), (28) and (29) can then be used to derive the sample response factors f' , f'' and f''' from the measurement of such standards. The prerequisites to do this are: (i) the ^{15}N abundance (b) of the subset of ^{15}N enriched N_2 in the standard is well known, (ii) discrimination between N isotopes during formation of ^{15}N labelled N_2 can be neglected and (iii) the initial (atmospheric) N_2 exhibits a binomial distribution of N_2 isotopologues, with the ^{15}N abundance a . With Eqn. (A3.4) we can rewrite Eqn. (27) giving:

$$\frac{n_B}{n_A} = \frac{r_1 f' (1-a)^2 - 2a(1-a)}{2b(1-b) - r_1 f' (1-b)^2} \quad (A3.8)$$

Solving Eqn. (A3.8) for f' yields:

$$f' = \frac{\left(\frac{n_B}{n_A}\right) 2b(1-b) + 2a(1-a)}{r_1(1-a)^2 + \left(\frac{n_B}{n_A}\right) r_1(1-b)^2} \quad (A3.9)$$

If the amount of ^{15}N labelled N_2 in the sample is negligible, Eqn. (A3.9) reduces to Eqn. (A3.7). The sample response factor for $^{30}N_2$ in relation to $^{28}N_2$ (f'') can be derived as follows:

Using Eqn. (A3.5) we can rewrite Eqn. (28) to:

$$\frac{n_B}{n_A} = \frac{r_2 f'' (1-a)^2 - a^2}{b^2 - r_2 f'' (1-b)^2} \quad (A3.10)$$

Solving Eqn. (A3.10) for f'' yields:

$$f'' = \frac{\left(\frac{n_B}{n_A}\right)b^2 + a^2}{r_2(1-a)^2 + \left(\frac{n_B}{n_A}\right)r_2(1-b)^2} \quad (\text{A3.11})$$

Substituting Eqn. (A3.8) into Eqn. (A3.11) gives f'' :

$$f'' = \frac{\left(\frac{r_1 f'(1-a)^2 - 2a(1-a)}{2b(1-b) - r_1 f'(1-b)^2}\right)b^2 + a^2}{r_2(1-a)^2 + \left(\frac{r_1 f'(1-b)^2 - 2a(1-a)}{2b(1-b) - r_1 f'(1-b)^2}\right)r_2(1-b)^2} \quad (\text{A3.12})$$

To calculate f''' we rewrite Eqn. (29) using Eqn. (A3.6) to:

$$\frac{n_B}{n_A} = \frac{r_3 f''' 2a(1-a) - a^2}{b^2 - r_3 f''' 2b(1-b)} \quad (\text{A3.13})$$

solving Eqn. (A3.13) for f''' gives:

$$f''' = \frac{\left(\frac{n_B}{n_A}\right)b^2 + a^2}{r_3 2a(1-a) + \left(\frac{n_B}{n_A}\right)r_3 2b(1-b)} \quad (\text{A3.14})$$

Substituting Eqn. (A3.8) into Eqn. (A3.14) yields f''' :

$$f''' = \frac{\left(\frac{r_1 f'(1-a)^2 - 2a(1-a)}{2b(1-b) - r_1 f'(1-b)^2}\right)b^2 + a^2}{r_3 2a(1-a) + \left(\frac{r_1 f'(1-b)^2 - 2a(1-a)}{2b(1-b) - r_1 f'(1-b)^2}\right)r_3 2b(1-b)} \quad (\text{A3.15})$$

To calculate the sample response factors f' , f'' and f''' only a and b , the ^{15}N abundances of initial and evolved labelled N_2 , have to be known and the N_2 isotopologue ratios r_1 , r_2 and r_3 have to be measured.

The sample response factors f' , f'' and f''' could possibly be altered by the formation of CO^+ and $^{14}\text{NO}^+$ within the mass spectrometer. $^{12}\text{CO}^+$ and $^{13}\text{CO}^+$ are possible fragments of CO_2 and might interfere on the molecular ion masses m/z 28 and m/z 29 (An et al., 2001). $^{14}\text{NO}^+$ can be formed by the combination of N_2 and O_2 molecules within the ion source in dependence of the amount of N_2 and O_2 within the mass spectrometer (An et al., 2001; Jensen et al., 1996).

Therefore, the formation of CO^+ and NO^+ is a function of the amount of CO_2 , N_2 and O_2 within the ion source of the mass spectrometer. Since the recorded ion currents on molecular ion masses m/z 44 and m/z 28 and m/z 32 are proportional to the amount of CO_2 , N_2

and O₂ within the ion source, the formation of CO⁺ and NO⁺ can be assumed to be also a function of the ion currents on these molecular ion masses. The formation of ¹²CO⁺, ¹³CO⁺ and ¹⁴NO⁺ can then be formulated as follows:

$$(i^{12}\text{CO}^+) = k1_{m/z28} \circ (i^{12}\text{CO}_2) \quad (\text{A3.16})$$

$$(i^{13}\text{CO}^+) = k2_{m/z29} \circ (i^{13}\text{CO}_2) \quad (\text{A3.17})$$

$$(i^{14}\text{NO}^+) = k3_{m/z30} \circ (i \text{O}_2) \circ (i \text{N}_2) \quad (\text{A3.18})$$

Where (i ¹²CO₂), (i ¹³CO₂), (i O₂) and (i N₂) are the ion currents of the educts and (i ¹²CO⁺), (i ¹³CO⁺) and (i NO⁺) are the ion currents of the resulting ions. The factors of proportionality $k1_{m/z28}$, $k2_{m/z29}$ and $k3_{m/z30}$ have to be determined experimentally and \circ is an operator representing a mathematical operation like multiplication or addition etc.. Which kind of mathematical operation applies to the Eqn. (A3.16) to (A3.18) has to be determined from experimental data. Now we introduce the sample ion correction factors F^{28} , F^{29} and F^{30} and define that:

$$f' = \frac{F^{29}}{F^{28}} \quad (\text{A3.19})$$

$$f'' = \frac{F^{30}}{F^{28}} \quad (\text{A3.20})$$

$$f''' = \frac{F^{30}}{F^{29}} \quad (\text{A3.21})$$

With Eqn. (A3.19) to (A3.21) we can rewrite Eqn. (A3.4) to (A3.6) to:

$$R_1 = r_1 f' = \frac{(i \text{mz}29)}{(i \text{mz}28)} \cdot \frac{F^{29}}{F^{28}} = \frac{(i^{29}\text{N}_2)}{(i^{28}\text{N}_2)} = \frac{^{29}\text{N}_2}{^{28}\text{N}_2} \quad (\text{A3.22})$$

$$R_2 = r_2 f'' = \frac{(i \text{mz}30)}{(i \text{mz}28)} \cdot \frac{F^{30}}{F^{28}} = \frac{(i^{30}\text{N}_2)}{(i^{28}\text{N}_2)} = \frac{^{30}\text{N}_2}{^{28}\text{N}_2} \quad (\text{A3.23})$$

$$R_3 = r_3 f''' = \frac{(i \text{mz}30)}{(i \text{mz}29)} \cdot \frac{F^{30}}{F^{29}} = \frac{(i^{30}\text{N}_2)}{(i^{29}\text{N}_2)} = \frac{^{30}\text{N}_2}{^{29}\text{N}_2} \quad (\text{A3.24})$$

Now it is obvious that F^{28} , F^{29} and F^{30} represent the factors needed to correct the measured ion currents on the molecular masses m/z 28, m/z 29 and m/z 30 to obtain the ion currents of ²⁸N = (i ²⁸N₂), ²⁹N₂ = (i ²⁹N₂) and ³⁰N₂ = (i ³⁰N₂), i.e. correct (i mz28), (i mz29) and (i mz30) for CO⁺ and NO⁺. From Eqn. (A3.22) to (A3.24) we obtain:

$$(i \text{mz}28) \cdot F^{28} = (i^{28}\text{N}_2) \quad (\text{A3.25})$$

$$(i \text{mz}29) \cdot F^{29} = (i^{29}\text{N}_2) \quad (\text{A3.26})$$

$$(i \text{mz}30) \cdot F^{30} = (i^{30}\text{N}_2) \quad (\text{A3.27})$$

Insert the assumed rules of formation of CO^+ and NO^+ Eqn. (A3.16) to (A3.18) into the assumed composition of the measured ion currents Eqn. (A3.1) to (A3.3) and we obtain:

$$(i\ m/z28) = (i\ ^{28}\text{N}_2) + (k1_{m/z28} \circ (i\ ^{12}\text{CO}_2)) \quad (\text{A3.28})$$

$$(i\ m/z29) = (i\ ^{29}\text{N}_2) + (k2_{m/z29} \circ (i\ ^{13}\text{CO}_2)) \quad (\text{A3.29})$$

$$(i\ m/z30) = (i\ ^{30}\text{N}_2) + (k3_{m/z30} \circ (i\ \text{O}_2) \circ (i\ \text{N}_2)) \quad (\text{A3.30})$$

Insertion of Eqn. (A3.28) to (A3.30) into Eqn. (A3.25) to (A3.27) and solving for F^{28} , F^{29} and F^{30} gives:

$$F^{28} = 1 - \frac{k1_{m/z28} \circ (i\ ^{12}\text{CO}_2)}{(i\ m/z28)} \quad (\text{A3.31})$$

$$F^{29} = 1 - \frac{k2_{m/z29} \circ (i\ ^{13}\text{CO}_2)}{(i\ m/z29)} \quad (\text{A3.32})$$

$$F^{30} = 1 - \frac{k3_{m/z30} \circ (i\ \text{O}_2) \circ (i\ \text{N}_2)}{(i\ m/z30)} \quad (\text{A3.33})$$

Contrary to the equations for the sample response factors f' , f'' and f''' the sample ion correction factors F^{28} , F^{29} and F^{30} are formulated in response to the measured ion currents of the educts of the interfering ions CO^+ and NO^+ .

Assuming the formation of $^{13}\text{CO}^+$ is negligible compared to $^{29}\text{N}_2$ ($(i\ ^{29}\text{N}_2) \gg (i\ ^{13}\text{CO}^+)$), then Eqn. (A3.32) reduces to:

$$F^{29} = 1 \quad (\text{A3.34})$$

With Eqn. (A3.34) and Eqn. (A3.21) we can express F^{30} now as follows:

$$F^{30} = f''' \quad (\text{A3.35})$$

Eqn. (A3.35) holds as long as the formation of $^{13}\text{CO}^+$ can be neglected during measurement, this should especially be the case at high ion currents of $^{29}\text{N}_2$ in the mass spectrometer, i.e. at high concentrations of $^{29}\text{N}_2$ in the measured sample. With this prerequisite we can solve Eqn. (A3.33) for $k3_{m/z30}$ using Eqn. (A3.35). If $k3_{m/z30}$ in Eqn. (A3.33) is linked multiplicatively with the ion currents $(i\ \text{O}_2)$ and $(i\ \text{N}_2)$, then we can solve Eqn. (A3.33) with the calculated value of F^{30} for $k3_{m/z30}$ as follows:

$$k3_{m/z30} = \frac{1 - F^{30}}{(i\ m/z30)} \cdot \frac{1}{(i\ \text{O}_2)(i\ \text{N}_2)} \quad (\text{A3.36})$$

Accordingly we can solve Eqn. (A3.31).

The formation factors $k1_{m/z28}$, $k2_{m/z29}$ and $k3_{m/z30}$ should be calculated for different O_2 , N_2 and CO_2 concentrations within the mass spectrometer, to correct samples in dependence of the amount of these gases. Contrary to previous instrumental response factors F^{28} , F^{29} and F^{30} are

formulated in dependence of the intensity of ion currents that are assumed to be in relation to CO^+ and NO^+ formation in the mass spectrometer.